

UNIVERSITÄTSKLINIKUM HAMBURG-EPPENDORF

Transplantation und Stammzell Immunbiologie Labor (TSI)

Klinik und Poliklinik für Herz- und Gefäßchirurgie

Universitäres Herzzentrum Hamburg (UHZ)

Prof. Dr. med. Sonja Schrepfer

Identifying New Targets, Developing Novel Models, and Investigating Innovative Strategies for the Treatment of Rejection in Thoracic Transplantation

Dissertation

zur Erlangung des Grades eines Doktors der Medizin

an der Medizinischen Fakultät der Universität Hamburg

vorgelegt von:

Xiaoqin Hua

aus Wuxi, China

Hamburg 2012

Angenommen von der

Medizinischen Fakultät der Universität Hamburg am: 01.11.2012

Veröffentlicht mit Genehmigung der

Medizinischen Fakultät der Universität Hamburg.

Prüfungsausschuss, der/die Vorsitzende: Prof. Dr. Sonja Schrepfer

Prüfungsausschuss, zweite/r Gutachter/in: Prof. Dr. Udo Schumacher

CONTENTS

| | |
|--|-----------|
| 1. Background..... | 4 |
| 2. Purpose..... | 7 |
| 3. Acute cellular rejection..... | 8 |
| 4. Chronic rejection..... | 11 |
| 4.1 Obliterative bronchiolitis in lung transplant..... | 11 |
| 4.2 Transplant vasculopathy in heart transplant..... | 14 |
| 5. Stem cell therapy..... | 17 |
| 5.1 Self-repair by stem cells <i>in situ</i> | 17 |
| 5.2 Injection therapy of stem cells..... | 19 |
| 6. Summary..... | 23 |
| 7. Reference..... | 24 |
| 8. Appendix..... | 34 |
| 8.1 Abbreviations..... | 34 |
| 8.2 Manuscripts..... | 36 |
| 8.3 CV..... | 37 |
| 9. Acknowledgement..... | 43 |
| 10. Confirmation..... | 44 |

1. Background

Transplantation has been considered as the last hope for patients with end-stage organ failure, and innumerable efforts have been made in the last century. According to the records in the modern medical history, Austrian surgeon Emmerrich Ullmann made the kidney transplant in dog technically feasible in 1902 (1). Russian doctor Voronoy performed the first case of human kidney transplant in 1936 (2, 3), and the recipient survived for four days. All of the early trials of organ transplants ended with failure except autografts. In 1940s, the Cambridge immunologist Peter Medawar revealed the mechanism of rejection as a specific immune response to foreign antigen using a skin transplant model, further discovered the acquired immune tolerance (4), and was awarded the 1960 Nobel Prize in Physiology or Medicine together with Sir Burnet. Their findings were fundamental to the modern transplant immunology and the practice of organ transplant, and were milestones in the medical history. The first case of human kidney transplant was performed by surgeon Joseph Murray in 1954 in between identical twins and achieved long-term survival (5). Later on, French immunologist Jean Dausset discovered human leukocyte antigen (HLA) in 1958 (6). The American immunologist Baruj Benacerraf observed different extents of immune response were mounted in a population of outbred guinea pigs, and discovered the major histocompatibility complex (MHC) genes which encode cell surface molecules crucial for the immune system to recognize self and non-self (7). Based on all the previous findings, immunosuppressants started a brand new era of transplantation.

Today many pathways in the immune system are targets for immunosuppressive agents. Plenty of immunosuppressants were invented, widely used in the clinic, and improved graft survival. The mortality of the recipients was extremely high in the 1950s when radiation was the only method to suppress the recipient's immune system (8). The regimen composed of azathioprine was proposed and elevated the 1-year survival of kidney transplants (9). However, it led to an overall weakened immune system, resulting in high incidence of infection after operation (10). In 1978, Cyclosporine was introduced to the clinic by Dr. Calne, helped the first year survival of renal graft reach to 80% (11), and was then widely applied in a combined regimen with glucocorticoids. This regimen greatly facilitated the development of the clinical organ transplant, but its renal toxicity also became a major problem (12). Tacrolimus, the first macrolide immunosuppressant, was discovered by Kino in 1987 (13), and successfully translated into the clinic of liver and kidney transplantation by the transplant pioneer Dr. Starzl in 1989 (14). It has saved innumerable grafts by reversing acute rejection which no routine regimen of immunosuppressants at that time was able to stop (15-18). In 1995, the antiproliferative medication, Mycophenolate Mofetil (MMF) (19) and in 1999, the mammalian target of rapamycin (mTOR) inhibitor sirolimus (20) were introduced and

dramatically reduced the incidence of acute renal rejection. Besides, there was also a large progress in biological induction therapies, such as thymoglobulin (21) and anti-IL-2-receptor monoclonal antibody (22, 23).

However, rejection still remains as the largest obstacle to graft survival in allogeneic transplantation (24-28). Since the routinely used immunosuppressants are not specific, patients suffer from side effects (29), such as nephrotoxicity (30, 31), neurotoxicity (32, 33), or diabetes (34-37). Most of the immunosuppressants impair the recipient's immune defense and surveillance while inhibiting rejection, leading to higher risk for infection and malignancy. Furthermore, immunosuppressants that inhibit metabolism may result in hematopoietic system damage. Indeed, glucocorticoids may induce gastrointestinal ulcer, hemorrhage, and perforation and the disturbance on metabolism may also trigger hypertension, hyperlipidemia, hyperglycemia, osteoporosis, etc. These side effects may even worsen the former diseases and complicate the situation.

Heart Transplantation

In the field of heart transplantation, Norman Shumway and Richard Lower established the model of orthotopic canine heart transplantation at Stanford University and tried to translate it to the clinic around 1960. The first human heart transplant, performed by Christiaan Barnard in 1967, was revolutionary and broke the silence (38). Followed one month later, Norman Shumway performed the first case in the United States (39). Afterwards, many centers all over the world started to perform heart transplantations. However, survival rates were disappointing and by the end of 1968, the mean survival was 29 days according to the data from 102 cases worldwide (40). The poor results were critically due to the inadequate understanding of complications and the appropriate strategy to treat them leading to a decrease of heart transplantations. The introduction of cyclosporine as immunosuppressant in the early 1980s (41), together with the endomyocardial biopsy as the diagnostic tool for acute allograft rejection in the 1970s (42), led to the resurgence of this field. Nowadays, the median survival is 11 years for the complete cohort of both adult and pediatric recipients (24). Graft failure, infection, and rejection are the main causes of death within the first postoperative year, but one year after transplantation, the causes of graft failure are most likely cardiac allograft vasculopathy (CAV), which leads to 20%, 30%, and 45% of morbidity at 3, 5, and 8 years, respectively, and 10% of the mortality between 1 and 3 year after transplant (24). Most immunosuppressive regimens include a calcineurin inhibitor, an anti-metabolite, and glucocorticoid in the early postoperative period. mTOR inhibitors have been more emphasized to lower the calcineurin inhibitor level and hence the nephrotoxicity, and also to prevent CAV. However, side effects of immunosuppressants, such as nephrotoxicity,

hyperlipidemia, and hypertension, are strongly related to the short- and long-term morbidity after transplantation (24). In addition, nearly half of the recipients are diagnosed with malignancy by 15 years after transplant (24).

Lung Transplantation

Lung transplantation has been established as the last hope for the patients with end-stage pulmonary diseases. James Hardy did the first case of allogeneic single lung transplantation in 1963. Due to graft dysfunction, infection, rejection, and airway complications, lung transplantation progressed slowly in the next two decades. In 1982, Bruce Reitz at Stanford University first performed successfully the heart-lung transplantation for a patient with idiopathic pulmonary hypertension (43). One year later, David K. Cooper performed a right lung transplant, and the patient had survived for 6.5 years (44). Five years later, the Washington University lung transplantation group proposed the bilateral sequential lung transplantation, and succeeded in clinical procedure (45). Currently, the most common regimen incorporates tacrolimus, mycophenolate, and prednisone. The ISHLT registry in 2011 showed that the overall median survival was 5.5 years, and it was great improvement on the overall half-life compared with the data (4.8 years) in 1988 (25). Within the first year after transplantation, the major causes of death are graft failure and non-CMV infections. One year after transplantation, the primary causes of mortality switch to bronchiolitis obliterans syndrome (BOS) and non-CMV infections. With the high morbidity of 49% and 75% by 5 and 10 years after transplantation (25, 46), BOS remains the major hurdle to long-term survival. However, the etiology and pathogenesis are still not so well understood, and the current immunosuppressants are able to delay but not to prevent or reverse the development of BOS (47, 48).

2. Purpose

Achieving long-term graft survival without unspecific systemic side-effects is the aim of transplant surgeons, cardiologists and pulmonologists, and patients, and it's also the ultimate goal of transplant immunology. Since immunology is progressing and immunological and molecular biological techniques are improving, increasingly more strategies have been established and further developed. On one hand, novel targets have been discovered and identified to block or inhibit immune response in recipients. On the other hand, the donated organ, tissue, or cells could also be modified to induce low or none immunogenicity to escape the immune recognition and attack. The latter might meanwhile solve the problem of organ shortage. Animal models that can mimic the pathogenesis of acute and, even more important, chronic rejection are needed for basic mechanism studies. Indeed, there is a special need in establishing humanized models, which are much closer to the human pathogenesis, to minimize the translational gap to the clinic.

3. Acute Cellular Rejection

Approximately 20% to 30% recipients after heart transplantation present moderate or severe acute cellular rejection in the first postoperative year, most commonly in the first 6 months (49, 50). Acute graft dysfunction may directly lead to severe situations of hemodynamic compromise, such as insufficient cardiac output and remarkably high pulmonary capillary wedge pressure (PCWP). The number and severity of acute rejection episodes are found to be correlated with development of CAV and mortality (51). It also significantly increases short and long term morbidity and mortality, and often results in irreversible myocardial damage (52-54).

Histologically, the acute cardiac rejection (ACR) is manifested as different extents of inflammatory cell infiltration, and consequent myocardial injury (55, 56). In addition to maintaining sufficient cardiac output and adequate blood pressure, and employing the high dose corticosteroid intravenously as the first-line therapy, other immunosuppressants are also required to resolve the symptoms and prevent long-term complications.

ACR is mediated predominantly by T lymphocytes. After allogeneic antigen recognition by both direct and indirect ways (57), recipient's T cells are activated through multi-signal pathways. "Signal 1" is triggered by the binding of alloantigen-MHC complex to T cell receptor (TCR), and further enhanced by "Signal 2", namely, co-stimulatory signal. This will activate three downstream pathways such as calcium-calcineurin pathway, nuclear factor kappa B (NF- κ B) pathway, and mitogen-activated protein kinase (MAPK) pathway, and further lead to up-regulated expression of many crucial molecules in T cells, such as IL-2 and IL-15, which will initiate cell proliferation by activating mTOR. This trigger for cell proliferation is called Signal 3 (58). Traditional immunosuppressants inhibit or mitigate rejection with pleiotropic side effects. Novel immunosuppressants are being continuously invented and tested aiming at more efficacy and higher selectivity to inhibit allogeneic rejection and minimized occurrence of side effects. Selective inhibition of signal 3 has now emerged as new strategy for immunosuppression (59-61). Our study is the first report on two novel Janus kinase 1/3 (JAK1/3) inhibitors, R507 and R545, in experimental cardiac allograft survival, showing its efficacy of inhibiting on cellular immune response, preventing of acute allograft rejection, and assessing interaction with tacrolimus.

Deuse T, Hua X, Taylor V, Stubbendorff M, Baluom M, Chen Y, Park G, Velden J, Streichert J, Reichensperner H, Robbins RC, Schrepfer S. Significant reduction of acute cardiac allograft rejection by selective JAK1/3-inhibition using R507 and R545. Transplantation 2012 (in press):

Pharmacokinetics and pharmacodynamics of R507 and R545 were first evaluated. The plasma levels reached peak two to three hours after administration. Both of them were found to be potent inhibitors of JAK1 and JAK3 with 20-fold or greater selectivity over JAK2 and tyrosine kinase 2 (Tyk2) in cells. Non-volume loaded heterotopic heart transplantations (62) were performed from donor Brown Norway rats to Lewis rats, a strain combination with high immune response. Recipients were randomly assigned to groups treated with different medications, namely R507 HD (high dose, 60mg/kg, b.i.d.), R507 LD (low dose, 15mg/kg b.i.d.), R545 HD (20mg/kg, b.i.d.), R545 LD (5mg/kg b.i.d.), Tac HD (tacrolimus, 4mg/kg q.d.) and Tac LD (1mg/kg q.d.), or left untreated (no medication group). The doses of R507 and R545 were chosen according to the previous studies in the rat collagen-induced arthritis model, where high dose of both medications succeeded in suppressing the disease in all the cases (unpublished data). Transplantation of Lewis-to-Lewis was performed to serve as syngeneic control. The efficacies of R507 and R545 were investigated by a 5-day study for acute cellular rejection, and the graft survival study for assessment of graft survival rates.

With respect to cellular immune response, Enzyme-linked immunosorbent spot (Elispot) assays on post-operation day (POD) 5 showed a significantly more IFN- γ and IL-4 release as response of TH1- and TH2-cells to the allogeneic grafts in the no medication group compared with the syngeneic group ($p < 0.001$ for each cytokine). The R507 HD and R545 HD were highly effective to reduce the IFN- γ and IL-4 spot frequencies ($p < 0.001$ for each vs. no medication), which had comparable value as Tac HD. R507 LD and R545 LD showed surprisingly low IFN- γ release, and the reduction on IL-4 release was even stronger than Tac LD ($p < 0.001$). Intra-graft cytokine levels were also measured, which revealed significantly less IFN- γ and IL-10 in both R507 HD and R545 HD groups ($p < 0.05$ vs. no medication). Histopathological assessment captured a typical picture of acute cardiac allograft rejection in no medication group, showing destroyed myocardium, massive mononuclear cell infiltration, hemorrhages, edema, and vasculitis. The pathological ISHLT scoring (56) revealed reduced immune response in the treated group and showed dose dependent effects. The CD3+ T cells and CD68+ macrophages were quantified and demonstrated a massive infiltration pattern in no medication group. Only three HD groups yielded remarkable decreased CD3+ cell infiltration compared with no medication group ($p < 0.001$). The high dose groups of two JAK1/3 inhibitors performed better in suppressing infiltration than Tac HD did ($p < 0.001$). For the humoral immune response, significant decrease of IgM antibodies were detected in all HD and LD groups ($p < 0.001$ vs. no medication), and no dose-dependent effect was observed in donor-specific antibody suppression. Meanwhile, blood chemistry showed increased high-density lipoprotein (HDL) and decreased low-density lipoprotein (LDL) levels in the JAK1/3

inhibitor groups, which might be caused by normalized LDL receptor and increased LDL uptake due to inhibition of JAK1 in the oncostatin M pathway (63).

In the survival study, heart beating was palpated and scored until it stopped. Both sub-therapeutic and therapeutic R507 and R545 prolonged mean graft survival with similar effect as Tac LD and HD, respectively. In combination regimens, however, only R507 LD combined with Tac LD showed highly beneficial synergistic drug interactions, which reached similar effect as R507 HD alone (CI=0.584).

In summary, this study proved both R507 and R545 are potent novel immunosuppressants with high JAK1/3 selectivity and favorable pharmacokinetics. Interruption of signal 3 transduction is able to render a powerful immunosuppression. R507 is a very promising candidate to make its way into clinical trials. The up-to-date data show that the phase 1 clinical trial has been successfully concluded (unpublished data).

4. Chronic rejection

4.1 Obliterative bronchiolitis (OB) in lung transplantation

OB remains the most common chronic complication and major obstacle to long-term survival in lung transplant patients (25, 64). No specific and effective treatment has been established yet and the detailed pathogenesis of OB remains poorly understood. Nevertheless, accumulating evidence suggests an immunological trigger for epithelial injury, inflammatory cell infiltration, and consequent development of fibroproliferative lesions (65-69).

To better understand the mechanism, pathogenesis, prevention, and treatment of OB, different animal models have been developed. Inbred small rodents, like rats and mice, are largely used in the basic research of transplantation field, because each individual has identical genetic information within the same inbred strain. Mice are preferred because genetically manipulation is feasible and the different transgenic and knock out models may be helpful for the OB-related mechanistic questions. There are various transplantation models to imitate the development of OB in small rodents, such as the orthotopic or heterotopic trachea transplantation model (70). The transplantation of whole lungs in rodents is time-consuming, technically demanding, and animals show considerably high variability within one group (71-73).

Hua X, Deuse T, Tang-Quan KR, Robbins RC, Reichenspurner H, Schrepfer S. Heterotopic and orthotopic tracheal transplantation in mice used as models to study the development of obliterative airway disease. J. Vis. Exp. (35), e1437, DOI: 10.3791/1437 (2010):

In our publication, we performed heterotopic and orthotopic tracheal transplantation models in mice, both of which are reliable models to mimic human OB pathogenesis. Tracheal grafts are fixed and wrapped in the greater omentum in the heterotopic tracheal transplant model, which is technically easy to perform (70, 74) and less time consuming. Complete occlusion of the graft lumen will occur in 28 days after transplant (70, 75, 76). Since the transplantations are heterotopic, recipients don't suffer from the OB symptoms. However, there is no ventilation of tracheal grafts, and therefore, it's not adequate to observe the functional role of epithelium in the pathogenesis of OB, and inhaled formulation cannot be tested in this model. Besides, the peritoneal microenvironment is different from the thoracic milieu (70). On the other hand, the orthotopic model provides a ventilating airway that is more physiological, and makes inhaled medication administration possible (70). A previous study from our lab also showed a much stronger IgM donor-specific alloreactive humoral response in the orthotopic model than that in heterotopic model (70). However, the development of OB lesion is prolonged in the orthotopic model. Our data showed that the luminal obliteration reached its peak, which was approximately 35%~45% (70, 77), on POD60 compared with POD30 and

POD90 in the same strain combination. Recipients may develop symptoms such as stridor and dyspnea.

Therefore, each of these two models has its own pros and cons. The heterotopic model might be appropriate for studies focusing on the development of luminal obliteration and the efficacy of certain medication in preventing fibroproliferation. The orthotopic model might be more suitable for studies dealing with the preservation of epithelium and its physiological function, and to investigate inhaled drug delivery. Currently, there is no ideal animal model to investigate human OB. Researchers should choose the model depending on the basic question of their study.

After the animal models for OB were investigated and compared, we choose the heterotopic tracheal transplantation in mice as animal model to identify the role of the intermediate-conductance calcium-activated potassium channel (KCa3.1) in the pathogenesis of OB, and its possibility as a novel target to prevent the OB after lung transplant.

Hua X, Deuse T, Chen YJ, Wulff H, Köhler R, Stubbendorff M, Reichenspurner H, Robbins RC, Schrepfer S. The potassium channel KCa3.1 as new therapeutic target for preventing obliterative airway disease after lung transplant. Transplantation 2012 (in press).

Recent studies have shown that the KCa3.1 channel plays an important role in Ca²⁺ signaling and T cell activation (78, 79). Opening of this channel restores the driving force for store-operated Ca²⁺-entry through the calcium-release activated calcium (CRAC) channel (80), and sustains the increment in cytosolic calcium level required for the activation of calcineurin pathway. Therefore, T cell activation is enhanced. The KCa3.1 channel is up-regulated on activated T cells compared to naïve and memory T cells (81), suggesting that activated T cells might be more sensitive to channel blockers, which may be used as a therapeutic strategy.

Previous studies showed that pharmacological KCa3.1 blockade is capable of inhibiting T cell proliferation and cytokine production *in vitro* (82-84). *In vivo* studies have also demonstrated that KCa3.1 blockers can prevent autoimmune diseases in animal models and contribute to the prevention of kidney graft rejection in rats (85, 86). As shown by the efficacy of the KCa3.1 blocker TRAM-34 in models of restenosis (87, 88), atherosclerosis (89), and kidney fibrosis (90), additional involvement of this channel has been revealed in smooth muscle cell and fibroblast proliferation. Since the OB after lung transplant takes place due to the allogeneic immune response mainly mediated by T cells and the consequent fibroproliferative changes, the KCa3.1 channel blockade might be considered as a novel therapeutic target for the prevention of airway allograft rejection. In the present study we hypothesized that KCa3.1 blockade could attenuate airway allograft rejection by inhibiting both T cell activation and fibrotic airway obliteration.

Tracheas from CBA donors were heterotopically transplanted into the greater omentum of fully mismatched C57Bl/6J mice. Recipients were either left untreated or received TRAM-34 (120mg/kg/d, i.p.) for 5 days or 28 days. KCa3.1^{-/-} mice with C57Bl/6J background receiving grafts from CBA donors and C57Bl/6J receiving syngeneic grafts were used as control. Histopathology and immunological assays were performed after graft recovery.

In the 5-day study, the acute cellular allogeneic rejection was suppressed by both channel blockade and knock out. In untreated grafts, the subepithelial area was intensively infiltrated by CD3⁺ T cells and F4/80⁺ macrophages, both of which participate in the OAD development as pivotal mediators (91-93). In contrast, the KCa3.1^{-/-} and TRAM-34 groups showed significantly reduced infiltration ($p < 0.001$). Elispots also revealed reduced IFN- γ spot frequencies in the KCa3.1^{-/-} and TRAM-34 groups compared to the untreated group ($p \leq 0.015$ vs. no medication), indicating an attenuated Th1 response. *In vitro* proliferation assays showed dose-dependent reduced proliferation in wild-type cells, but not KCa3.1^{-/-} splenocytes, confirming the specificity of TRAM-34.

In the 28-day chronic study, both the genetic knock out and the pharmacological blockade of KCa3.1 by TRAM-34, reduced luminal obliteration of tracheal grafts from $89 \pm 21\%$ to $53 \pm 26\%$ and $59 \pm 33\%$, respectively ($p = 0.010$ and $p = 0.032$ vs. no medication). Semi-quantitative RT-PCR and immunohistochemistry demonstrated significantly lower amounts of KCa3.1 mRNA and channel expression after TRAM-34 treatment compared to the untreated group ($p = 0.008$), in accordance with the hypothesis of KCa3.1 channel up-regulation in activated T cells in allogeneic rejection. Clinical data showed a significant higher risk for early graft dysfunction and poor prognosis in those lung transplant recipients with pre-existing anti-HLA antibodies (93, 94), implying an important role of humoral response in allogeneic lung graft rejection. To evaluate the humoral rejection, donor reactive antibody assays were performed in our study. The donor specific IgG production in the KCa3.1^{-/-} group was largely reduced compared to the no medication group ($p = 0.018$).

Besides not being able to preserve epithelium, no side effect due to TRAM-34 treatment was observed. The KCa3.1^{-/-} mouse strain was viable and fertile, and no difference in KCa3.1^{-/-} mice was noted compared to wild-type animals before and after transplant.

In summary, this study demonstrated that the KCa3.1 channel plays a critical role in T cell activation in the tracheal transplant model, and pharmacological blockade or genetic knockout of the channel could significantly decrease T cell activation and inhibit the development of OAD. Therefore, specific KCa3.1 blockade may be an additional strategy for patients after lung transplantation.

4.2 Transplant vasculopathy and intimal hyperplasia in heart transplant

As a major chronic complication of heart transplantation, the development of cardiac allograft vasculopathy remains as big hurdle in this field (24, 95-98). It's initiated early after transplantation and progresses over time, causing the neointimal formation and the narrowing and obliteration of the coronary artery lumen. Despite the administration of the current immunosuppressants, the incidence of CAV with clinical evidences is about 20% in 3 years after transplant and 30% by 5 years (24), reflecting the lack of knowledge of the underlying mechanism in the pathogenesis of intimal hyperplasia. Meanwhile, identifying new therapeutic targets becomes one of the most important goals in this field.

Previous studies of our collaborators have already showed that sustained epsilon protein kinase C (ϵ PKC) inhibition starting three days after transplantation was able to suppress chronic allograft rejection, inhibit the development of CAV, and improve cardiac graft survival using a murine heterotopic transplantation model (99). Based on the knowledge that the ϵ PKC is involved in vascular smooth muscle cell (VSMC) activation, to better understand the mechanism of the intimal hyperplasia, we performed our study on a restenosis model after balloon injury and stenting.

Deuse T, Koyanagi T, Erben RG, Hua X, Velden J, Ikeno F, Reichensperner H, Robbins RC, Mochly-Rosen D, Schrepfer S. Sustained inhibition of epsilon protein kinase C inhibits vascular restenosis after balloon injury and stenting. Circulation. 2010 Sep 14; 122(11 S):S170-8.:

Endothelium lining on the abdominal aortic wall in Sprague-Dawley rats was denuded using aortic balloon injury with or without subsequent stenting (Yukon Plus, Translumina, 2.5mm in diameter, and 12mm in length); this technique was developed in our lab (100). Rats were then treated with the selective ϵ PKC activator $\psi\epsilon$ receptor for activated protein kinase C ($\psi\epsilon$ RACK) (101), the selective ϵ PKC inhibitor ϵ V1-2 (102), the cell-penetrating TAT carrier peptide vehicle (TAT₄₇₋₅₇), or saline, in a sustained fashion via implanted osmotic pumps. After 28 days, intimal hyperplasia had developed in saline-treated balloon-injured rat aortas (20.3±8.0%), and was markedly promoted in $\psi\epsilon$ RACK group (32.4±4.9%, p=0.033 vs saline group), but notably inhibited by ϵ V1-2 treatment (9.2±4.3%, p=0.039 vs saline group). The carrier peptide TAT₄₇₋₅₇ neither accelerated nor slowed down the development of lumen obliteration. Proliferating cell nuclear antigen (PCNA) immunohistochemistry revealed that 19±6%, 20±4%, and 25±4% of neointimal cells were undergoing proliferation in the section of saline, TAT₄₇₋₅₇ vehicle, and $\psi\epsilon$ RACK groups, respectively, but the percentage was reduced to 9±3% by the ϵ PKC inhibitor ϵ V1-2 (p=0.003 vs saline group). To explain the phenomena of different sizes of intimal hyperplasia, both the down-stream cascades of the

platelet-derived growth factor (PDGF) receptor via extracellular signal-regulated kinase (ERK) and Akt, postulated to participate in VSMCs proliferation (103), were evaluated *in vivo*. The protein amount in the aortic tissue was quantified by western blot, which rendered a significantly reduction in ERK phosphorylation, but not Akt phosphorylation, by ϵ PKC inhibition. Further investigation on VSMC *in vitro* was performed to understand the detailed mechanism. PKC translocation method found that PDGF stimulation is able to significantly activate ϵ PKC in cultured VSMCs, and the activation can be inhibited by ϵ V1-2 pretreatment. *In vitro* proliferation assay also showed proliferation by PDGF stimulation can be moderately promoted by ϵ PKC activator $\psi\epsilon$ RACK ($p=0.108$ vs. normal saline group), but significantly reduced by ϵ PKC inhibitor ϵ V1-2 ($p<0.001$ vs. normal saline group). Modulation on ϵ PKC had similar effect on *in vitro* VSMCs migration ($p<0.001$ for $\psi\epsilon$ RACK, $p=0.001$ for ϵ V1-2, vs. normal saline). Western blots showed a significant increase in amount of the phosphorylated ERK and Akt 5 minutes after PDGF stimulation, but the treatment of ϵ V1-2 did not have an obvious effect at this time point yet ($p<0.05$). After 6 hours sustained inhibition by ϵ V1-2, there was a great decrease in phosphorylated ERK and Akt ($p<0.05$). That means the ϵ PKC inhibition of PDGF-induced VSMC proliferation is likely due to the inhibition of the ERK and Akt pathways.

To investigate whether there is also an inhibition in restenosis after stenting by ϵ V1-2, stents were implanted into the denuded rat aorta *in vivo* as previously described by our group (100). Six weeks later, the intimal hyperplasia in stented aortas were well developed, and the development of luminal obliteration was significantly reduced by sustained treatment of ϵ V1-2 ($p=0.028$).

In summary, our data indicate a central role of ϵ PKC in the pathogenesis of intimal hyperplasia. Suppressed VSMCs proliferation by ϵ PKC inhibition may be mediated via inhibition of ERK and Akt activation. Therefore, modulation of ϵ PKC could be considered as a new therapeutic target to prevent vascular restenosis.

The balloon injury models in rat abdominal aorta with or without subsequent stent implantation, mentioned in our previous study, are well established and widely used in vascular restenosis research. Other commonly used restenosis models include mice, rabbits, and pigs (100, 104, 105). However, limitations still exist due to the translational gap, and problems might occur by translating these findings into the clinic (106, 107). Therefore, humanized models need to be established.

Hua X, Deuse T, Michelakis ED, Tsao PS, Maegdefessel L, Erben R, Behnisch BB, Reichenspurner H, Robbins RC, Schrepfer S. Human IMA transplantation and stenting: A

humanized model to study the development of intimal hyperplasia. J. Vis. Exp. (63), e3663. DOI: 10.3791/3663 (2012):

We invented a novel humanized rat model to study the restenosis after stent implantation. Human internal mammary artery (IMA, or internal thoracic artery) segment about 10mm in length is used in this model as human material, of which the endothelium is denuded by the passage of a 2-french Forgarty arterial embolectomy catheter. The balloon injury is performed twice to ensure the complete endothelial damage. Human stent with 8mm in length and 2.5-3.0mm in diameter is then implanted into the IMA lumen. The stented IMA segment is temporarily stored in RPMI medium with heparin (500 IU/10ml) on ice in fridge. The recipient rat is prepared. The abdominal aorta is dissected from the infrarenal region to the iliac bifurcation. An aortic segment approximately 5-7 mm in length is replaced with the stented IMA. End-to-end anastomosis is performed by running sutures with 8-0 prolene. Blood flow through the IMA and pulse should be seen. Grafts were harvested after 28 days in our case, and intimal hyperplasia, composed of proliferating vascular smooth muscle cells and fibrotic tissue, was shown in Masson-Goldner trichrome and proved by immunofluorescent staining. To identify the origin of the proliferating cells in restenosis, IMA grafts were stably transduced with the reporter gene Green Fluorescent Protein (GFP) using lentiviral particles. All the daughter cells of human IMA origin will be GFP positive. By staining of either GFP or rat MHC-I, co-localized with smooth muscle α -actin (SMA), the smooth muscle cells within the restenosis area were identified as GFP positive but rat MHC-I negative, demonstrating the human origin. Therefore, the model itself is proved as humanized model. It constitutes a bridge between preclinical research and clinical settings, and can be considered as a translational approach to study the stent restenosis *in vivo*.

5. Stem cell therapy

Myocardial damage due to ischemic heart diseases reduces the amount of working cardiomyocytes, weakens the contractility, and leads to heart failure. Improved revascularization therapies lowered the mortality after myocardial infarction, but consequently, the incidence of heart failure is increasing (108). Thus we need to think about the situation in which myocardium has already been damaged, and heart failure has already occurred. Heart transplantation can be considered as one choice if indications are fulfilled. However, due to the shortage of organ donation as well as the complications of immunosuppressants, researchers are keeping on seeking other therapeutic strategies, such as tissue regeneration by stem cell therapy. However, as is the case for organ transplantation, immune rejection after stem cell transplantation is a potential problem with this type of therapy (109). We believe that systemic immunosuppression, in analogy to allogeneic organ transplantation, is not justifiable and feasible for cell therapy. Therefore, we are aiming to understand the immunobiology of stem cells and decrease their immunogenic potential. In the following studies, we investigated various stem cell types for their regenerative potential.

5.1 Self repair by stem or progenitor cells *in situ*

Weinberger F, Mehrkens D, Friedrich FW, Stubbendorff M, Hua X, Müller JC, Schrepfer S, Evans S, Carrier L, Eschenhagen T. Localization of Islet-1-Positive Cells in the Healthy and Infarcted Adult Murine Heart. Circ Res. 2012 May 11;110(10):1303-10. Epub 2012 Mar 15:

It's well known that the transcription factor Islet-1 is a cardiovascular progenitor marker during early murine development (110). Therefore, cells expressing Islet-1 are very attractive candidates as resident cardiac progenitors and might be helpful for regeneration. Previous studies have shown that the murine Islet-1+ cells maintained the capability to differentiate into cardiomyocytes, and contribute to the formation of sinoatrial node (SAN), atrioventricular node (AVN), and smooth muscle cells (SMCs) in coronary arteries (111-113). Recently, the phenomena have also been observed that few Islet-1+ cells exist in adult murine hearts (114) and young adult rats (115). This fact suggested that the islet-1+ cells as resident cardiac progenitors might be of therapeutic value. As the first step, the three-dimensional distribution and the identity of Islet-1+ cells in adult murine heart needed to be investigated and the changes in amount or location with age or after myocardial infarction also needed to be evaluated.

To identify the Islet-1+ cells, Isl-1-nLacZ-mice (LacZ: β -galactosidase gene) were generated by targeted insertion of a DNA cassette containing nLacZ in the Islet-1 locus (116). Thus, by Bromo-Chloro-Indolyl-Galactopyranoside (X-Gal) staining, Islet-1+ cells could be visualized

in blue color in nuclei. The distribution of Islet-1+ cells was tracked in 30 Islet-1-LacZ mice at different time-points (10 weeks to 18 months after birth). Recognized by eyes or microscopy on the X-Gal stained heart gross specimens or serial heart sections, the location of Islet-1+ cells or clusters was defined by the positive nuclear nLacZ signal, which was also compared to the those from 6 non-transgenic wild-type littermates.

The location of nLacZ+ cells was strictly confined to 3 regions of the adult murine heart. The first kind of clusters locates in the interatrial septum and around the pulmonary veins, on the posterior side of the heart. These round large cells were further characterized as parasympathetic neurons in cardiac ganglia, as shown by the co-localization with acetylcholinesterase (AChE), β -galactosidase (β -gal) and choline acetyltransferase (ChAT). The second group of nLacZ+ cells was scattered distributed within muscular layer of the great vessels, especially in the proximal part of ascending aorta and the trunk of pulmonary artery above aortic and pulmonary valve. They not only expressed β -gal but also smooth muscle actin and smooth muscle myosin heavy chain. The third type of nLacZ+ cells locates in a strictly delimited cluster between the right atrium and superior vena cava. They not only expressed the cardiomyocyte marker α -actinin, but coexpressed the SAN pacemaker cell marker hyperpolarization-activated cyclic nucleotide-gated channel 4 (HCN4). Interestingly, only 50% of the HCN4+ cells are nLacZ+. All of these cell types retained the cell amount and localization between 1 to 18 months after birth. Islet-1 mRNA was also detectable by RT-PCR in the wild-type C57Bl/6J murine heart tissue with SAN at different time-points (12 to 44 weeks after birth, n=31). Consistently Islet-1 mRNA was detectable in postmortem human SAN (n=4). However, neither nLacZ+ signal nor Islet-1 mRNA could be detected in the working cardiomyocytes in left and right ventricles. On 2, 14, and 28 days after left anterior descending (LAD) coronary artery ligation in Islet-1-nLacZ-mice, Islet-1+ cells could not be found in the infarct zone, except for 10 questionable cells in 1/13 hearts.

As the data showed, we found different types of cells that expressed Islet-1 consistently at specific areas, but all of them were differentiated. Together with the fact that Islet-1+ cells are absent in the working cardiomyocytes of the ventricles, this study questions the potential regenerative role of Islet-1+ cells as cardiac progenitors.

5.2 Transplantation of pluripotent stem cells

Compared with the inadequate pluripotency of tissue-specific progenitor cells and their ambiguous anatomical location and differentiation capacity, human embryonic stem cells (hESCs) are promising pluripotent cells able to be differentiated into any cell line (117). Therefore, hESC-based therapy is considered as a promising strategy for regenerative medicine. For instance, in case of myocardial damage, transplantation of ESC-derived cardiomyocytes or cardiac progenitor cells could be a future solution to regain heart function. However, due to the HLA disparity between the donor hESC-derived cells and the recipient's immune system, immune rejection will inevitably occur as previously shown by our group and others (118, 119). It remains as one of the major impediments of this therapy. Generating patient-specific pluripotent stem cells using induced pluripotent stem (iPS) cells from patients-own cells might be a way to avoid allogeneic immune rejection. But up till now, it seems impractical because of the complexity of pluripotent cell induction, the possibility of the genetic abnormality of donor cells, and the uncertainty of time consumption (120). In the clinic, derivatives of these pluripotent stem cells probably have to be used in an allogeneic setting. Though stem cell banks (121, 122) have been being established to match HLA as close as possible, immunosuppression might still be needed. As a result, we sought to change the immunogenicity of the hESCs by generating hypoimmunogenic hESC lines that lack HLA and escape the immune rejection.

Deuse T, Seifert M, Phillips N, Fire A, Tyan D, Kay M, Tsao PS, Hua X, Velden J, Eiermann T, Volk HD, Reichenspurner H, Robbins RC, Schrepfer S. Human leukocyte antigen I knockdown human embryonic stem cells induce host ignorance and achieve prolonged xenogeneic survival. Circulation. 2011 Sep 13;124(11 S):S3-9.

Deuse T, Seifert M, Tyan D, Tsao PS, Hua X, Velden J, Eiermann T, Volk HD, Reichenspurner H, Robbins RC, Schrepfer S. Immunobiology of naïve and genetically modified HLA-class-I-knockdown human embryonic stem cells. J Cell Sci. 2011 Sep 1;124(Pt 17):3029-37.:

First, we identified the lymphocytes that play the central role in mediating hESC rejection. A total of 1×10^6 hESCs were transplanted into the gastrocnemius muscle in either immunocompetent Balb/c mice or other murine strains carrying various kinds of immune defects. Cell survival was recorded by bioluminescence imaging (BLI). An early decrease in cell number occurred in all strains within the first 5 days, which seemed immune-irrelevant and probably due to shear stress and injury from needle injection. Later on, the survival of transplanted cells showed different patterns. All the cells got rejected in immunocompetent Balb/c mice by day 5. Whereas in immunodeficient SCID-beige (SCID: severe combined

immunodeficiency) mice, lacking both T, B lymphocytes and natural killer (NK) cell function, the BLI signal reached back to the initial level on day 21, and increased approximately 50 times by day 80. Teratoma was found at the site of injection in each recipient, demonstrating long-term survival of transplanted cells. In 7 of 9 nude mice with only T cell deficient, the transplanted cells survived and also formed teratoma by day 80. However, both the beige and perforin^{-/-} mice, which lack NK activity, rejected hESCs in a similar time window as Balb/c. Besides, SCID-beige mice adoptively transferred with splenocytes from beige mice can actively reject injected hESCs. To further investigate the immunogenicity of hESCs with naturally low-expressed HLA-I, the HLA-I-deficient human immortalized erythroleukemia cells K562 were also injected into these mice strains for comparison. They survived in SCID-beige with defected NK function, but were quickly rejected in Balb/c and nude mice due to their high NK-susceptibility. In summary, the fact, that the T-cell competent recipients rejected hESCs while the NK function impaired recipients were not capable of rejecting hESCs, demonstrated a central role of T cell in mediating hESCs rejection in a xenogeneic setting, and the low expression level or knock down of HLA-I did not increase the NK susceptibility. It's in line with the finding in previous studies that human T cells are able to recognize the hESCs (123) and their derivatives (124), and the T cell- specific immunosuppression in immunocompetent mice recipients prolonged markedly the hESCs survival (109). And it's also in accordance with the phenomenon that human NK cells only were not capable to recognize hESCs *in vitro* (125).

To achieve the goal of hypoimmunogenicity in hESCs, siRNA technique and intrabody technique were used separately or together to silence the HLA-I at post-transcriptional level to generate HLA-I-knockdown hESCs. The differences with regard to the efficacy of generating these cells and the immunogenicity were characterized in the hESCs modified by siRNA technique (hESC^{siRNA}), intrabody (IB) technique (hESC^{IB}), and combined techniques (hESC^{siRNA+IB}). The transfection efficacy of siRNA and IB technique were 74±12% and 82±11%, respectively, while the transduction efficacy of siRNA+IB was 88±9%. The HLA expression in genetically modified hESCs was quantified by Fluorescence-activated Cell Sorting (FACS). The FACS analysis at different time points showed HLA-I expression was lowered to its trough level of 2.6±0.8 in hESC^{siRNA}, 2.1±0.7 in hESC^{IB}, and 1.1±0.1 in hESC^{siRNA+IB} (p=0.005, p=0.004, and p=0.002 compared to unmodified hESCs, respectively), in which hESC^{siRNA+IB} only had about 1% of the HLA-I surface expression in naïve hESCs. The lowered level of HLA-I expression in hESC^{siRNA+IB} was stably sustained through day 7 and day 42 (2.1±0.4).

Afterwards, both hESCs and hESC^{siRNA+IB} were characterized for immune marker surface expression and pluripotency. hESCs showed modest HLA-I and β 2-microglobulin expression, but those of hESC^{siRNA+IB} were remarkably reduced. Both hESCs and hESC^{siRNA+IB} were negative for HLA-II and the co-stimulatory molecules CD80, CD86 and CD40. hESCs showed positive for all the embryonic stem cell markers Oct-4, Sox-2, stage-specific embryonic antigen-3 (SSEA-3), and TRA-1-60. The same results for hESC^{siRNA+IB} showed that they maintain the pluripotency after HLA-I was knockdown, and both of them can still be differentiated into all three germ layers, proved by teratoma formation in SCID-beige mice, which is the gold standard to test pluripotency (126).

Since the hESC^{siRNA+IB} was established and proved to have very low HLA-I expression, they were transplanted into both Balb/c and SCID-beige recipients to test their immunogenicity. BLI was again used to trace the survival cells, and reflected an initial decrease in cell viability in the first few days in both two recipient strains, the same as the previous finding. Later on, hESCs injected into SCID-beige gradually regained the BLI signal up to the same level of beginning on day 21. By day 80 they formed teratomas containing tissues from all three germ layers, as proved by further histology staining. But all the hESCs were rejected by Balb/c recipients, and lost their BLI signal by day 5. However, the rejection triggered by hESC^{siRNA+IB} in Balb/c was significantly reduced and had remarkably improved survival. The BLI signals of six out of ten animals slowly dropped into background around day 28, but the other four animals remained their signals though the whole 42 days. Elispot of IFN- γ and IL-4, showing the Th1 and Th2 immune response, respectively, on day 5, indicated a significantly lowered spot frequency induced by hESC^{siRNA+IB} in immunocompetent Balb/c recipients compared with that induced by hESC ($p=0.002$ for IFN- γ , $p<0.001$ for IL-4). hESCs manipulated by either siRNA or intrabody were also transplanted i.m. into Balb/c mice. Compared to hESC^{siRNA+IB}, the immunogenicity of hESC^{siRNA} and hESC^{IB} was not as low as hESC^{siRNA+IB}. The Elispot on day 5 showed reduced IFN- γ spot frequencies in both hESC^{siRNA} and hESC^{IB} groups ($p=0.048$, $p=0.002$ vs. naïve hESCs respectively), but IL-4 production was brought down only in hESC^{IB} group ($p<0.001$ vs. naïve hESCs). Traced by BLI, all of the hESC^{siRNA} cells were rejected by day 10, and hESC^{IB} cells by d14.

Transduced with luciferase, the hESCs and hESC^{siRNA+IB} can be identified using anti-Luciferase antibody. The survival of hESCs and hESC^{siRNA+IB} and the infiltration of inflammatory cells can be revealed by immunohistochemistry. In the section of Balb/c gastrocnemius muscle injected with hESCs, massive infiltration of Mac-2+ macrophages and CD3+ lymphocytes, and only scarce killer cell lectin-like receptor sub-family A member 1 (KLRA1) positive NK cells were found. The densities of all the three kinds of inflammatory cells were reduced significantly in the hESC^{siRNA+IB} group ($p<0.001$). The IgM donor-specific

antibody was much higher in Balb/c mice injected with hESCs than those with hESC^{siRNA+IB} ($p < 0.001$). Luminex single-antigen assays found that the anti-HLA-I antibody was significantly induced only after hESCs transplantation ($p = 0.021$ vs. native animal), but not after hESC^{siRNA+IB} transplantation, since HLA-I had been knocked down. The induction of anti-HLA-II antibodies was not significantly higher in both groups compared to native animals. Negligible amount of naturally occurring anti-hESC xeno-antibodies was detected in Balb/c mice before cell transplantation. hESC re-injection into the Balb/c recipients one week after the first hESCs injection triggered a massive boost of anti-HLA-I antibody ($p = 0.007$), but not HLA-II. The same re-injection with hESC^{siRNA+IB} didn't induce hESC-specific HLA-I antibody significantly. The *in vitro* incubation with CD3⁺ CD56⁻ lymphocytes also showed significantly increased IFN- γ and IL-4 spot frequency in hESCs group but not in hESC^{siRNA+IB}.

Our study showed a pivot role of HLA-I expression in the recognition of hESCs by T cells in xenogeneic setting. Knock down of HLA-I by siRNA and intrabody technique could escape from the xenogeneic immune surveillance, resulting in diminished cellular and humoral immune responses, and prolonged stem cell survival.

6. Summary

In my doctoral study, a study on acute heart rejection was performed to evaluate the role JAK1/3 inhibitors in T cell immune response. Results showed both R507 and R545 were novel and potent immunosuppressants mainly acting on T cells, and the interruption of “Signal 3” transduction is promising way to diminish rejection. Studies on lung transplant involved establishing and comparing the mice models for OB. Both orthotopic and heterotopic tracheal transplant models are feasible and reliable. The choice of model depends on the question the study focuses on. Using the heterotopic model, we identified KCa3.1 as a crucial contributor in the development of OB and also as a potential new target to prevent the OB. Specific KCa3.1 blockade might be considered as an additional therapeutic strategy. Intimal hyperplasia, as a major manifestation of transplant vasculopathy, was also investigated. It showed the capacity of sustained inhibition on ϵ PKC to prevent the vascular smooth muscle cell activation and proliferation via inhibition of ERK and Ark pathways. A novel and reliable humanized model to study restenosis after stenting was invented and established, in which the disease pattern was very close to that in human. Besides solid organ transplantation, the studies also involved the immunobiology of stem cell transplantation for regenerative therapies. Islet-1, which was thought to be the marker for resident cardiac progenitors, was found to be expressed only in specific areas, all of which are well differentiated. The potential regenerative role of the Islet-1+ cells got questioned. Therefore, we strongly believe that allogeneic pluripotent stem cell sources are needed. The study on the immunogenicity of genetically modified hESC revealed a principal role of HLA-I expression in the hESC recognition in a xenotransplant setting, mainly mediated by T cells. And the HLA-I-knockdown using both the microRNA and intrabody technique could help the modified hESC escape immune attack from recipient and may lead to long-term graft survival. In the past century, with all the endeavors of clinicians and researchers, transplantation became clinical reality and has saved innumerable lives of patients with end-stage organ failure. To improve long-term outcomes and patients’ quality of life after transplantation, clinicians and researchers need to continue working together to reach the ultimate goal of transplantation: graft acceptance without affecting normal immune function. We believe that the achievement of this goal will eventually become reality.

7. Reference

1. Ullmann E. Experimental kidney-transplantation (reprinted from Wiener-klinische-wochenschrift, vol 15, p 281, 1902). Wiener Klinische Wochenschrift 1988; 100 (8): 258.
2. Matevossian E, Kern H, Huser N, et al. Surgeon Yuri Voronoy (1895-1961) - a pioneer in the history of clinical transplantation: in Memoriam at the 75th Anniversary of the First Human Kidney Transplantation. Transplant International 2009; 22 (12): 1132.
3. Stefoni S, Campieri C, Donati G, Orlandi V. The history of clinical renal transplant. Journal of Nephrology 2004; 17 (3): 475.
4. Simpson E. Reminiscences of Sir Peter Medawar: In hope of antigen-specific transplantation tolerance. American Journal of Transplantation 2004; 4 (12): 1937.
5. Murray JE, Hills W. The first successful organ transplants in man. Journal of the American College of Surgeons 2005; 200 (1): 5.
6. Richmond C. Jean Dausset. The Lancet; 374 (9698): 1324.
7. Germain RN, Paul WE. Baruj Benacerraf (1920-2011). Nature; 477 (7362): 34.
8. Murray JE, Dammin GJ, Dealy JB, Harrison JH, Alexandr.Gw, Merrill JP. Kidney transplantation in modified recipients. Annals of Surgery 1962; 156 (3): 337.
9. Murray JE, Harrison JH, Dammin GJ, Wilson RE, Merrill JP. Prolonged survival of human-kidney homografts by immunosuppressive drug therapy. New England Journal of Medicine 1963; 268 (24): 1315.
10. Hill RB, Dahrling BE, Starzl TE, Rifkind D. Death after transplantation - an analysis of sixty cases. American Journal of Medicine 1967; 42 (3): 327.
11. Calne RY, Pentlow BD, White DJG, et al. Cyclosporin-A in patients receiving renal-allografts from cadaver donors. Lancet 1978; 2 (8104): 1323.
12. Shiba N, Chan MCY, Kwok BWK, Valentine HA, Robbins RC, Hunt SA. Analysis of survivors more than 10 years after heart transplantation in the cyclosporine era: Stanford experience. Journal of Heart and Lung Transplantation 2004; 23 (2): 155.
13. Kino T, Hatanaka H, Miyata S, et al. FK-506, a novel immunosuppressant isolated from a streptomyces 2 immunosuppressive effect of FK-506 in vitro. Journal of Antibiotics 1987; 40 (9): 1256.
14. Starzl TE, Todo S, Fung J, Demetris AJ, Venkataramman R, Jain A. FK-506 for liver, kidney, and pancreas transplantation. Lancet 1989; 2 (8670): 1000.
15. Todo S, Fung JJ, Starzl TE, et al. Liver, kidney, and thoracic organ-transplantation under FK-506. Annals of Surgery 1990; 212 (3): 295.

16. Shapiro R, Jordan M, Fung J, et al. Kidney-transplantation under FK506 immunosuppression. *Transplantation Proceedings* 1991; 23 (1): 920.
17. Pirsch JD, Miller J, Deierhoi MH, Vincenti F, Filo RS. A comparison of tacrolimus (FK506) and cyclosporine for immunosuppression after cadaveric renal transplantation. *Transplantation* 1997; 63 (7): 977.
18. Busuttil RW, McDiarmid S, Klintmalm GB, et al. A comparison of tacrolimus (FK-506) and cyclosporine for immunosuppression in liver-transplantation. *New England Journal of Medicine* 1994; 331 (17): 1110.
19. Cho S, Danovitch G, Deierhoi M, et al. Mycophenolate mofetil in cadaveric renal transplantation. *American Journal of Kidney Diseases* 1999; 34 (2): 296.
20. Kahan BD, Rapamune USSG. Efficacy of sirolimus compared with azathioprine for reduction of acute renal allograft rejection: a randomised multicentre study. *Lancet* 2000; 356 (9225): 194.
21. Gaber AO, First MR, Tesi RJ, et al. Results of the double-blind, randomized, multicenter, phase III clinical trial of thymoglobulin versus Atgam in the treatment of acute graft rejection episodes after renal transplantation. *Transplantation* 1998; 66 (1): 29.
22. Kahan BD, Rajagopalan PR, Hall M, Grp USSRS. Reduction of the occurrence of acute cellular rejection among renal allograft recipients treated with basiliximab, a chimeric anti-interleukin-2-receptor monoclonal antibody. *Transplantation* 1999; 67 (2): 276.
23. Vincenti F, Kirkman R, Light S, et al. Interleukin-2-receptor blockade with daclizumab to prevent acute rejection in renal transplantation. *New England Journal of Medicine* 1998; 338 (3): 161.
24. Stehlik J, Edwards LB, Kucheryavaya AY, et al. The Registry of the International Society for Heart and Lung Transplantation: Twenty-eighth Adult Heart Transplant Report-2011. *Journal of Heart and Lung Transplantation*; 30 (10): 1078.
25. Christie JD, Edwards LB, Kucheryavaya AY, et al. The Registry of the International Society for Heart and Lung Transplantation: Twenty-eighth Adult Lung and Heart-Lung Transplant Report-2011. *Journal of Heart and Lung Transplantation*; 30 (10): 1104.
26. Nankivell BJ, Alexander SI. Rejection of the Kidney Allograft. *New England Journal of Medicine*; 363 (15): 1451.
27. Abt PL, Mange KC, Olthoff KM, Markmann JF, Reddy KR, Shaked A. Allograft survival following adult-to-adult living donor liver transplantation. *American Journal of Transplantation* 2004; 4 (8): 1302.

28. Alqahtani SA. Update in liver transplantation. *Current Opinion in Gastroenterology*; 28 (3): 230.
29. Dandel M, Lehmkuhl HB, Knosalla C, Hetzer R. Impact of different long-term maintenance immunosuppressive therapy strategies on patients' outcome after heart transplantation. *Transplant Immunology*; 23 (3): 93.
30. Olyaei AJ, de Mattos AM, Bennett WM. Nephrotoxicity of immunosuppressive drugs: new insight and preventive strategies. *Current opinion in critical care* 2001; 7 (6): 384.
31. Naesens M, Kuypers DRJ, Sarwal M. Calcineurin Inhibitor Nephrotoxicity. *Clinical Journal of the American Society of Nephrology* 2009; 4 (2): 481.
32. Dhar R, Human T. Central Nervous System Complications After Transplantation. *Neurologic Clinics*; 29 (4): 943.
33. Serkova N, Christians U, Benet AZ. Biochemical mechanisms of cyclosporine neurotoxicity. *Molecular Interventions* 2004; 4 (2): 97.
34. Boudreaux JP, McHugh L, Canafax DM, et al. The impact of cyclosporine and combination immunosuppression on the incidence of posttransplant diabetes in renal-allograft recipients. *Transplantation* 1987; 44 (3): 376.
35. van Hooff JP, Christiaans MHL, van Duijnhoven EM. Tacrolimus and posttransplant diabetes mellitus in renal transplantation. *Transplantation* 2005; 79 (11): 1465.
36. Prokai A, Fekete A, Pasti K, et al. The importance of different immunosuppressive regimens in the development of posttransplant diabetes mellitus. *Pediatric Diabetes*; 13 (1): 81.
37. Kasiske BL, Snyder JJ, Gilbertson D, Matas AJ. Diabetes mellitus after kidney transplantation in the United States. *American Journal of Transplantation* 2003; 3 (2): 178.
38. Barnard CN. Human cardiac transplantation - an evaluation of first 2 operations performed at Groote Schuur Hospital Cape Town. *American Journal of Cardiology* 1968; 22 (4): 584.
39. Shumay NE. Transplantation of an unpaired organ, heart. *Proceedings of the National Academy of Sciences of the United States of America* 1969; 63 (4): 1032.
40. Cooley DA, Bloodwell RD, Hallman GL, Nora JJ, Harrison GM, Leachman RD. Organ Transplantation for Advanced Cardiopulmonary Disease. *The Annals of Thoracic Surgery* 1969; 8 (1): 30.
41. Sivathanan C. Experience with cyclosporine in heart transplantation. *Transplantation Proceedings* 2004; 36 (2, Supplement): S346.

42. Caves PK, Stinson EB, Billingham ME, Shumway NE. Serial transvenous biopsy of the transplanted human heart - improved management of acute rejection episodes. *Lancet* 1974; 1 (7862): 821.
43. Reitz BA, Wallwork JL, Hunt SA, et al. Heart-Lung Transplantation. *New England Journal of Medicine* 1982; 306 (10): 557.
44. Cooper JD. Unilateral lung transplantation for pulmonary fibrosis. *New England Journal of Medicine* 1986; 314 (18): 1140.
45. Kaiser LR, Pasque MK, Trulock EP, Low DE, Dresler CM, Cooper JD. Bilateral sequential lung transplantation: The procedure of choice for double-lung replacement. *Ann Thorac Surg* 1991; 52 (3): 438.
46. DeMeo DL, Ginns LC. Lung transplantation at the turn of the century. *Annual Review of Medicine* 2001; 52: 185.
47. Todd JL, Palmer SM. Bronchiolitis Obliterans Syndrome. *Bronchiolitis Obliterans in Lung Transplantation: The Final Frontier for Lung Transplantation*. *CHEST Journal*; 140 (2): 502.
48. Hayes D. A review of bronchiolitis obliterans syndrome and therapeutic strategies. *Journal of Cardiothoracic Surgery*; 6: 9.
49. Taylor DO, Stehlik J, Edwards LB, et al. Registry of the International Society for Heart and Lung Transplantation: Twenty-sixth Official Adult Heart Transplant Report-2009. *Journal of Heart and Lung Transplantation* 2009; 28 (10): 1007.
50. Patel JK, Kobashigawa JA. Should we be doing routine biopsy after heart transplantation in a new era of anti-rejection? *Current Opinion in Cardiology* 2006; 21 (2): 127.
51. Costanzo MR, Dipchand A, Starling R, et al. The International Society of Heart and Lung Transplantation Guidelines for the care of heart transplant recipients. *Journal of Heart and Lung Transplantation*; 29 (8): 914.
52. Mills RM, Naftel DC, Kirklin JK, et al. Heart transplant rejection with hemodynamic compromise: A multiinstitutional study of the role of endomyocardial cellular infiltrate. *Journal of Heart and Lung Transplantation* 1997; 16 (8): 813.
53. Everitt MD, Pahl E, Schechtman KB, et al. Rejection with hemodynamic compromise in the current era of pediatric heart transplantation: A multi-institutional study. *Journal of Heart and Lung Transplantation*; 30 (3): 282.
54. Phelps CM, Tissot C, Buckvold S, et al. Outcome of Acute Graft Rejection Associated with Hemodynamic Compromise in Pediatric Heart Transplant Recipients. *Pediatric Cardiology*; 32 (1): 1.
55. Patel JK, Kittleson M, Kobashigawa JA. Cardiac allograft rejection. *The Surgeon*; 9 (3): 160.

56. Stewart S, Winters GL, Fishbein MC, et al. Revision of the 1990 Working Formulation for the Standardization of Nomenclature in the Diagnosis of Heart Rejection. *The Journal of Heart and Lung Transplantation* 2005; 24 (11): 1710.
57. Lindenfeld JA, Miller GG, Shakar SF, et al. Drug therapy in the heart transplant recipient - Part I: Cardiac rejection and immunosuppressive drugs. *Circulation* 2004; 110 (24): 3734.
58. Halloran PF. Immunosuppressive drugs for kidney transplantation. *New England Journal of Medicine* 2004; 351 (26): 2715.
59. Vincenti F. What's in the pipeline? New immunosuppressive drugs in transplantation. *American Journal of Transplantation* 2002; 2 (10): 898.
60. Changelian PS, Flanagan ME, Ball DJ, et al. Prevention of organ allograft rejection by a specific Janus kinase 3 inhibitor. *Science* 2003; 302 (5646): 875.
61. Behbod F, Erwin-Cohen RA, Wang ME, et al. Concomitant inhibition of janus kinase 3 and calcineurin-dependent signaling pathways synergistically prolongs the survival of rat heart allografts. *Journal of Immunology* 2001; 166 (6): 3724.
62. Ono K, Lindsey ES. Improved technique of heart transplantation in rats. *Journal of Thoracic and Cardiovascular Surgery* 1969; 57 (2): 225.
63. Li C, Kraemer FB, Ahlborn TE, Liu JW. Induction of low density lipoprotein receptor (LDLR) transcription by oncostatin M is mediated by the extracellular signal-regulated kinase signaling pathway and the repeat 3 element of the LDLR promoter. *Journal of Biological Chemistry* 1999; 274 (10): 6747.
64. Sundaresan S, Trulock EP, Mohanakumar T, Cooper JD, Patterson GA. Prevalence and outcome of bronchiolitis obliterans syndrome after lung transplantation. *The Annals of Thoracic Surgery* 1995; 60 (5): 1341.
65. Paradis I, Yousem S, Griffith B. Airway obstruction and bronchiolitis obliterans after lung transplantation. *Clin Chest Med* 1993; 14 (4): 751.
66. Burke C, Baldwin J, Morris A, et al. Twenty-right cases of human heart-lung transplantation. *The Lancet* 1986; 327 (8480): 517.
67. Griffith BP, Paradis IL, Zeevi A, et al. Immunologically mediated disease of the airways after pulmonary transplantation. *Ann Surg* 1988; 208 (3): 371.
68. Boehler A KS, Weder W, Speich R. Bronchiolitis obliterans after lung transplantation: a review. *Chest* 1998; 114 (5): 1411.
69. Adams BF, Brazelton T, Berry GJ, Morris RE. The role of respiratory epithelium in a rat model of obliterative airway disease. *Transplantation* 2000; 69 (4): 661.
70. Deuse T, Schrepfer S, Reichenspurner H, et al. Techniques for experimental heterotopic and orthotopic tracheal transplantations - When to use which model? *Transplant Immunology* 2007; 17 (4): 255.

71. Marck KW, Prop J, Wildevuur CR, Nieuwenhuis P. Lung transplantation in the rat: histopathology of left lung iso- and allografts. *The Journal of heart transplantation* 1985; 4 (2): 263.
72. Wiebe K, Fraund S, Steinmuller C, Steinhoff G. Rat cytomegalovirus and *Listeria monocytogenes* infection enhance chronic rejection after allogenic rat lung transplantation. *Transplant International* 2005; 18 (10): 1166.
73. Chung WS, Cho C, Kim S, et al. Review of significant microvascular surgical breakthroughs involving the heart and lungs in rats. *Microsurgery* 1999; 19 (2): 71.
74. Hertz MI, Jessurun J, King MB, Savik SK, Murray JJ. Reproduction of the obliterative bronchiolitis lesion after heterotopic transplantation of mouse airways. *American Journal of Pathology* 1993; 142 (6): 1945.
75. Hele DJ, Yacoub MH, Belvisi MG. The heterotopic tracheal allograft as an animal model of obliterative bronchiolitis. *Respiratory Research* 2001; 2 (3): 169.
76. McDyer JF. Human and murine obliterative bronchiolitis in transplant. *Proceedings of the American Thoracic Society* 2007; 4 (1): 37.
77. Schrepfer S, Deuse T, Hoyt G, et al. Experimental orthotopic tracheal transplantation: The Stanford technique. *Microsurgery* 2007; 27 (3): 187.
78. George Chandy K, Wulff H, Beeton C, Pennington M, Gutman GA, Cahalan MD. K⁺ channels as targets for specific immunomodulation. *Trends in Pharmacological Sciences* 2004; 25 (5): 280.
79. Gutman GA, Chandy KG, Adelman JP, et al. International Union of Pharmacology. XLI. Compendium of voltage-gated ion channels: potassium channels. *Pharmacol Rev* 2003; 55 (4): 583.
80. Cahalan MD, Chandy KG. The functional network of ion channels in T lymphocytes. *Immunol Rev* 2009; 231 (1): 59.
81. Rus H, Pardo CA, Hu L, et al. The voltage-gated potassium channel Kv1.3 is highly expressed on inflammatory infiltrates in multiple sclerosis brain. *Proc Natl Acad Sci U S A* 2005; 102 (31): 11094.
82. Fanger CM, Rauer H, Neben AL, et al. Calcium-activated potassium channels sustain calcium signaling in T lymphocytes. Selective blockers and manipulated channel expression levels. *J Biol Chem* 2001; 276 (15): 12249.
83. Ghanshani S, Wulff H, Miller MJ, et al. Up-regulation of the IKCa1 potassium channel during T-cell activation. Molecular mechanism and functional consequences. *J Biol Chem* 2000; 275 (47): 37137.
84. Khanna R, Chang MC, Joiner WJ, Kaczmarek LK, Schlichter LC. hSK4/hIK1, a Calmodulin-binding KCa Channel in Human T Lymphocytes. *Journal of Biological Chemistry* 1999; 274 (21): 14838.

85. Jensen BS, Hertz M, Christophersen P, Madsen LS. The Ca²⁺-activated K⁺ channel of intermediate conductance: a possible target for immune suppression. *Expert Opin Ther Targets* 2002; 6 (6): 623.
86. Chou CC, Lunn CA, Murgolo NJ. KCa_{3.1}: target and marker for cancer, autoimmune disorder and vascular inflammation? *Expert Rev Mol Diagn* 2008; 8 (2): 179.
87. Kohler R, Wulff H, Eichler I, et al. Blockade of the intermediate-conductance calcium-activated potassium channel as a new therapeutic strategy for restenosis. *Circulation* 2003; 108 (9): 1119.
88. Tharp DL, Wamhoff BR, Wulff H, Raman G, Cheong A, Bowles DK. Local delivery of the KCa_{3.1} blocker, TRAM-34, prevents acute angioplasty-induced coronary smooth muscle phenotypic modulation and limits stenosis. *Arterioscler Thromb Vasc Biol* 2008; 28 (6): 1084.
89. Toyama K, Wulff H, Chandy KG, et al. The intermediate-conductance calcium-activated potassium channel KCa_{3.1} contributes to atherogenesis in mice and humans. *J Clin Invest* 2008; 118 (9): 3025.
90. Grgic I, Kiss E, Kaistha BP, et al. Renal fibrosis is attenuated by targeted disruption of K(Ca)_{3.1} potassium channels. *Proceedings of the National Academy of Sciences of the United States of America* 2009; 106 (34): 14518.
91. Reznik SI, Jaramillo A, SivaSai KSR, et al. Indirect Allorecognition of Mismatched Donor HLA Class II Peptides in Lung Transplant Recipients with Bronchiolitis Obliterans Syndrome. *American Journal of Transplantation* 2001; 1 (3): 228.
92. Lu KC, Jaramillo As, Mendeloff EN, et al. Concomitant allorecognition of mismatched donor HLA class I, and class II, derived peptides in pediatric lung transplant recipients with bronchiolitis obliterans syndrome. *The Journal of Heart and Lung Transplantation* 2003; 22 (1): 35.
93. Sundaresan S, Mohanakumar T, Smith MA, et al. HLA-A locus mismatches and development of antibodies to HLA after lung transplantation correlate with the development of bronchiolitis obliterans syndrome. *Transplantation* 1998; 65 (5): 648.
94. Lau CL, Palmer SM, Posther KE, et al. Influence of panel-reactive antibodies on posttransplant outcomes in lung transplant recipients. *The Annals of Thoracic Surgery* 2000; 69 (5): 1520.
95. Schmauss D, Weis M. Cardiac allograft vasculopathy - Recent developments. *Circulation* 2008; 117 (16): 2131.
96. Mehra MR, Crespo-Leiro MG, Dipchand A, et al. International Society for Heart and Lung Transplantation working formulation of a standardized nomenclature for cardiac allograft vasculopathy 2010. *The Journal of Heart and Lung Transplantation*; 29 (7): 717.

97. Colvin-Adams M, Agnihotri A. Cardiac allograft vasculopathy: current knowledge and future direction. *Clinical Transplantation*; 25 (2): 175.
98. Lee MS, Finch W, Weisz G, Kirtane AJ. Cardiac Allograft Vasculopathy. *Reviews in Cardiovascular Medicine*; 12 (3): 143.
99. Koyanagi T, Noguchi K, Ootani A, Inagaki K, Robbins RC, Mochly-Rosen D. Pharmacological inhibition of epsilon PKC suppresses chronic inflammation in murine cardiac transplantation model. *Journal of Molecular and Cellular Cardiology* 2007; 43 (4): 517.
100. Deuse T, Erben RG, Ikeno F, et al. Introducing the first polymer-free leflunomide eluting stent. *Atherosclerosis* 2008; 200 (1): 126.
101. Dorn GW, Souroujon MC, Liron T, et al. Sustained in vivo cardiac protection by a rationally designed peptide that causes epsilon protein kinase C translocation. *Proceedings of the National Academy of Sciences of the United States of America* 1999; 96 (22): 12798.
102. Gray MO, Karliner JS, Mochly-Rosen D. A selective epsilon-protein kinase C antagonist inhibits protection of cardiac myocytes from hypoxia-induced cell death. *Journal of Biological Chemistry* 1997; 272 (49): 30945.
103. Li L, Blumenthal DK, Masaki T, Terry CM, Cheung AK. Differential effects of imatinib on PDGF-induced proliferation and PDGF receptor signaling in human arterial and venous smooth muscle cells. *Journal of Cellular Biochemistry* 2006; 99 (6): 1553.
104. Chamberlain J, Wheatcroft M, Arnold N, et al. A novel mouse model of in situ stenting. *Cardiovascular Research*; 85 (1): 38.
105. Finn AV, John M, Nakazawa G, et al. Differential Healing After Sirolimus, Paclitaxel, and Bare Metal Stent Placement in Combination With Peroxisome Proliferator-Activator Receptor gamma Agonists Requirement for mTOR/Akt2 in PPAR gamma Activation. *Circulation Research* 2009; 105 (10): 1003.
106. Tellez A, Krueger CG, Seifert P, et al. Coronary bare metal stent implantation in homozygous LDL receptor deficient swine induces a neointimal formation pattern similar to humans. *Atherosclerosis*; 213 (2): 518.
107. Suzuki Y, Yeung AC, Ikeno F. The Pre-Clinical Animal Model in the Translational Research of Interventional Cardiology. *Jacc-Cardiovascular Interventions* 2009; 2 (5): 373.
108. Velagaleti RS, Pencina MJ, Murabito JM, et al. Long-Term Trends in the Incidence of Heart Failure After Myocardial Infarction. *Circulation* 2008; 118 (20): 2057.
109. Swijnenburg RJ, Schrepfer S, Govaert JA, et al. Immunosuppressive therapy mitigates immunological rejection of human embryonic stem cell xenografts.

- Proceedings of the National Academy of Sciences of the United States of America 2008; 105 (35): 12991.
110. Cai CL, Liang XQ, Shi YQ, et al. Isl1 identifies a cardiac progenitor population that proliferates prior to differentiation and contributes a majority of cells to the heart. *Developmental Cell* 2003; 5 (6): 877.
 111. Sun YF, Liang XQ, Najafi N, et al. Islet 1 is expressed in distinct cardiovascular lineages, including pacemaker and coronary vascular cells. *Developmental Biology* 2007; 304 (1): 286.
 112. Moretti A, Caron L, Nakano A, et al. Multipotent embryonic Isl1(+) progenitor cells lead to cardiac, smooth muscle, and endothelial cell diversification. *Cell* 2006; 127 (6): 1151.
 113. Laugwitz KL, Moretti A, Lam J, et al. Postnatal isl1+cardioblasts enter fully differentiated cardiomyocyte lineages. *Nature* 2005; 433 (7026): 647.
 114. Khattar P, Friedrich FW, Bonne G, et al. Distinction Between Two Populations of Islet-1-Positive Cells in Hearts of Different Murine Strains. *Stem Cells and Development*; 20 (6): 1043.
 115. Genead R, Danielsson C, Andersson AB, et al. Islet-1 Cells Are Cardiac Progenitors Present During the Entire Lifespan: From the Embryonic Stage to Adulthood. *Stem Cells and Development*; 19 (10): 1601.
 116. Thor S, Andersson SGE, Tomlinson A, Thomas JB. A LIM-homeodomain combinatorial code for motor-neuron pathway selection. *Nature* 1999; 397 (6714): 76.
 117. Muller R, Lengerke C. Patient-specific pluripotent stem cells: promises and challenges. *Nat Rev Endocrinol* 2009; 5 (4): 195.
 118. Lui KO, Waldmann H, Fairchild PJ. Embryonic Stem Cells: Overcoming the Immunological Barriers to Cell Replacement Therapy. *Current Stem Cell Research & Therapy* 2009; 4 (1): 70.
 119. Chidgey AP, Layton D, Trounson A, Boyd RL. Tolerance strategies for stem-cell-based therapies. *Nature* 2008; 453 (7193): 330.
 120. Daley GQ, Scadden DT. Prospects for stem cell-based therapy. *Cell* 2008; 132 (4): 544.
 121. Lin G, Xie YB, OuYang Q, et al. HLA-Matching Potential of an Established Human Embryonic Stem Cell Bank in China. *Cell Stem Cell* 2009; 5 (5): 461.
 122. Tamaoki N, Takahashi K, Tanaka T, et al. Dental Pulp Cells for Induced Pluripotent Stem Cell Banking. *Journal of Dental Research*; 89 (8): 773.
 123. Drukker M, Katchman H, Katz G, et al. Human embryonic stem cells and their differentiated derivatives are less susceptible to immune rejection than adult cells. *Stem Cells* 2006; 24 (2): 221.

124. Preynat-Seauve O, de Rham C, Tirefort D, Ferrari-Lacraz S, Krause KH, Villard J. Neural progenitors derived from human embryonic stem cells are targeted by allogeneic T and natural killer cells. *Journal of Cellular and Molecular Medicine* 2009; 13 (9B): 3556.
125. Tseng HC, Arasteh A, Paranjpe A, et al. Increased Lysis of Stem Cells but Not Their Differentiated Cells by Natural Killer Cells; De-Differentiation or Reprogramming Activates NK Cells. *Plos One*; 5 (7): 16.
126. Brivanlou AH, Gage FH, Jaenisch R, Jessell T, Melton D, Rossant J. Setting standards for human embryonic stem cells. *Science* 2003; 300 (5621): 913.

8. Appendix

8.1 Abbreviations

| | |
|----------------|---|
| AChE | acetylcholinesterase |
| ACR | acute cardiac rejection |
| AVN | atrioventricular node |
| BLI | bioluminescence imaging |
| BOS | bronchiolitis obliterans syndrome |
| CAV | cardiac allograft vasculopathy |
| ChAT | choline acetyltransferase |
| CRAC | calcium-release activated calcium |
| Elispot | Enzyme-linked immunosorbent spot |
| ERK | extracellular signal-regulated kinase |
| ESCs | embryonic stem cells |
| FACS | Fluorescence-activated Cell Sorting |
| GFP | Green Fluorescent Protein |
| HCN4 | hyperpolarization-activated cyclic nucleotide-gated channel 4 |
| HDL | high-density lipoprotein |
| HLA | human leukocyte antigen |
| IB | intrabody |
| IMA | internal mammary artery |
| iPSCs | induced pluripotent stem cells |
| ISHLT | International Society for Heart and Lung Transplantation |
| JAK | Janus kinase |
| KCa3.1 | intermediate-conductance calcium-activated potassium channel |
| KLRA1 | killer cell lectin-like receptor sub-family A member 1 |
| LacZ | β -galactosidase gene |
| LAD | left anterior descending |
| LDL | low-density lipoprotein |
| MAPK | mitogen-activated protein kinase |
| MHC | major histocompatibility complex |
| mTOR | mammalian target of rapamycin |
| NF- κ B | nuclear factor kappa B |
| NK | natural killer |
| OB | Obliterative bronchiolitis |
| OCT | Optical Coherence Tomography |

| | |
|---------------------|--|
| PCWP | pulmonary capillary wedge pressure |
| PDGF | platelet-derived growth factor |
| POD | post-operation day |
| SAN | sinoatrial node |
| SCID | severe combined immunodeficiency |
| SCNT | somatic cell nuclear transfer |
| SMA | smooth muscle α -actin |
| SMCs | smooth muscle cells |
| SSEA-3 | stage-specific embryonic antigen-3 |
| β -gal | β -galactosidase |
| TCR | T cell receptor |
| Tyk | tyrosine kinase |
| VSMC | vascular smooth muscle cell |
| X-Gal | Bromo-Chloro-Indolyl-Galactopyranoside |
| ϵ PKC | epsilon protein kinase C |
| $\psi\epsilon$ RACK | $\psi\epsilon$ receptor for activated protein kinase C |

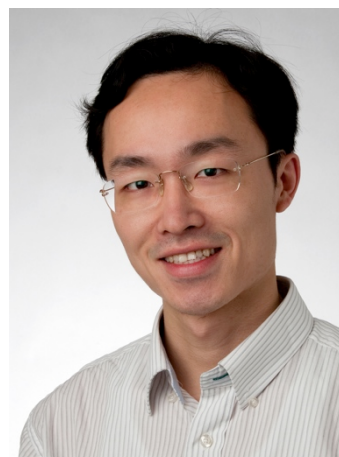
8.2 Peer-reviewed manuscripts listed in PubMed

1. Deuse T, **Hua X**, Taylor V, Stubbendorff M, Baluom M, Chen Y, Park G, Velden J, Streichert J, Reichenspurner H, Robbins RC, Schrepfer S. Significant reduction of acute cardiac allograft rejection by selective JAK1/3-inhibition using R507 and R545. *Transplantation* 2012 (in press).
2. **Hua X**, Deuse T, Tang-Quan KR, Robbins RC, Reichenspurner H, Schrepfer S. Heterotopic and orthotopic tracheal transplantation in mice used as models to study the development of obliterative airway disease. *J Vis Exp*. 2010 Jan 20; (35).
3. **Hua X**, Deuse T, Chen YJ, Wulff H, Köhler R, Stubbendorff M, Reichenspurner H, Robbins RC, Schrepfer S. The potassium channel KCa3.1 as new therapeutic target for preventing obliterative airway disease after lung transplant. *Transplantation* 2012 (in press).
4. Deuse T, Koyanagi T, Erben RG, **Hua X**, Velden J, Ikeno F, Reichenspurner H, Robbins RC, Mochly-Rosen D, Schrepfer S. Sustained inhibition of epsilon protein kinase C inhibits vascular restenosis after balloon injury and stenting. *Circulation*. 2010 Sep 14; 122(11 Suppl):S170-8.
5. **Hua X**, Deuse T, Michelakis ED, Tsao PS, Maegdefessel L, Erben R, Behnisch BB, Reichenspurner H, Robbins RC, Schrepfer S. Human IMA transplantation and stenting: A humanized model to study the development of intimal hyperplasia. *J. Vis. Exp.* (63), e3663, DOI: 10.3791/3663 (2012).
6. Weinberger F, Mehrkens D, Friedrich FW, Stubbendorff M, **Hua X**, Müller JC, Schrepfer S, Evans S, Carrier L, Eschenhagen T. Localization of Islet-1-Positive Cells in the Healthy and Infarcted Adult Murine Heart. *Circ Res*. 2012 May 11;110(10):1303-10. Epub 2012 Mar 15.
7. Deuse T, Seifert M, Phillips N, Fire A, Tyan D, Kay M, Tsao PS, **Hua X**, Velden J, Eiermann T, Volk HD, Reichenspurner H, Robbins RC, Schrepfer S. Human leukocyte antigen I knockdown human embryonic stem cells induce host ignorance and achieve prolonged xenogeneic survival. *Circulation*. 2011 Sep 13;124(11 Suppl):S3-9.
8. Deuse T, Seifert M, Tyan D, Tsao PS, **Hua X**, Velden J, Eiermann T, Volk HD, Reichenspurner H, Robbins RC, Schrepfer S. Immunobiology of naïve and genetically modified HLA-class-I-knockdown human embryonic stem cells. *J Cell Sci*. 2011 Sep 1;124(Pt 17):3029-37.

CURRICULUM VITAE

Xiaoqin Hua

Transplantation and Stem Cell Immunobiology (TSI) Lab
University Heart Center Hamburg-Eppendorf
Campus Research, N27, EG, R68
Martinistraße 52
20246 Hamburg
Germany
Phone: +49-40-741056568
Email: sphenoid_xq@hotmail.com



Personal Details

| | |
|----------------|-----------------------------------|
| Date of Birth | May 12 th , 1984 |
| Place of Birth | Wuxi, Jiangsu Province, P.R.China |
| Nationality | P.R.China |

Education

| | |
|-------------|--|
| 2009 - 2012 | Doctoral thesis, Transplantation and Stem Cell Immunobiology Lab, University Heart Center Hamburg, Germany |
| 2007 - 2009 | Master Degree of Clinical Medicine (All-in-English Teaching Program), Tongji Medical College, Huazhong University of Science and Technology, Wuhan, P.R.China. |
| 2002 - 2007 | Bachelor Degree of Clinical Medicine (All-in-English Teaching Program), Tongji Medical College, Huazhong University of Science and Technology, Wuhan, P.R.China. |
| 1999 - 2002 | No. 2 High School, Wuxi, Jiangsu, P.R.China. |

| | |
|-------------|---|
| 1996 - 1999 | Furen Middle School, Wuxi, Jiangsu, P.R.China. |
| 1990 - 1996 | Chongning Primary School, Wuxi, Jiangsu, P.R.China. |

Internships

| | |
|-----------|---|
| 2008-2009 | Internship (Senior, 9 months), specialized in hepatic surgery, Center of Hepatic Surgery, Tongji Hospital, Wuhan, P.R.China. |
| 2007-2008 | Internship Rotation (16 months), Tongji Hospital, Wuhan, P.R.China. |
| 2007 | Clerkship in General Surgery (1 month), Wuxi No.1 People's Hospital, Wuxi, Jiangsu, P.R.China. |
| 2006 | Clerkship in General Surgery (1 month), Wuxi No.1 People's Hospital, Wuxi, Jiangsu, P.R.China. |
| 2005-2006 | Clerkship Rotation (10 months), Tongji Hospital, Wuhan, P.R.China. |
| 2004 | Clerkship in Cardiology (1 month), Wuxi No.1 People's Hospital, Wuxi, Jiangsu, P.R.China |

Research Experience

| | |
|-----------|---|
| 2010 | Visiting research fellow at the University Alberta, Edmonton, Canada (Department of Cardiology and Pulmonary Hypertension) for 5 weeks |
| 2009-2012 | Doctoral research, Transplantation and Stem Cell Immunobiology Lab, University Heart Center, University Hospital Hamburg-Eppendorf, Germany |
| 2008-2009 | Master thesis, The significance of infrahepatic inferior vena cava clamping technique in hemorrhage reduction in hepatectomy: A Prospective Randomized Trial Center of Hepatic Surgery, Tongji Hospital, Wuhan, Hubei, China |
| 2005-2006 | Predoctoral fellow, Detecting Acetylcholine Level <i>in vivo</i> in AD-Like Animal Model Systems with Proton Magnetic Resonance Spectroscopy Department of Pathophysiology, School of Basic Medical Science, Tongji Medical College, Wuhan, P.R.China |

Honors and Awards

| | |
|-----------|--|
| 2012 | Basic Science Mentee-Mentor Award, The Transplant Society (TTS) |
| 2012 | Finalist in the Philip K. Caves Award Session of the International Society for Heart and Lung Transplant (ISHLT) |
| 2009-2012 | Scholarship under the State Scholarship Fund, Chinese Scholarship Council (CSC) |
| 2007 | Award and Scholarship for Outstanding Student, Tongji Medical College, HUST |
| 2006 | Rank 1 st in the presentation of thesis accomplished in the fundamental scientific research, Tongji Medical College |
| 2004 | Award and Scholarship for Outstanding Student, HUST |
| 2003 | Award and Scholarship for Outstanding Student, HUST |
| 2002 | Merit Student of Jiangsu Province |

Publications

1. **Hua X**, Deuse T, Chen YJ, Wulff H, Köhler R, Stubbendorff M, Reichenspurner H, Robbins RC, Schrepfer S. The potassium channel KCa3.1 as new therapeutic target for preventing obliterative airway disease after lung transplant. *Transplantation* 2012 (in press).
2. Deuse T, **Hua X**, Taylor V, Stubbendorff M, Baluom M, Chen Y, Park G, Velden J, Streichert J, Reichenspurner H, Robbins RC, Schrepfer S. Significant reduction of acute cardiac allograft rejection by selective JAK1/3-inhibition using R507 and R545. *Transplantation* 2012 (in press).
3. **Hua X**, Deuse T, Michelakis ED, Tsao PS, Maegdefessel L, Erben R, Behnisch BB, Reichenspurner H, Robbins RC, Schrepfer S. Human IMA transplantation and stenting: A humanized model to study the development of intimal hyperplasia. *J. Vis. Exp.* (63), e3663, DOI: 10.3791/3663 (2012).
4. Weinberger F, Mehrkens D, Friedrich FW, Stubbendorff M, **Hua X**, Müller JC, Schrepfer S, Evans S, Carrier L, Eschenhagen T. Localization of Islet-1-Positive Cells in the Healthy and Infarcted Adult Murine Heart. *Circ Res.* 2012 May 11;110(10):1303-10. Epub 2012 Mar 15.
5. Deuse T, Seifert M, Phillips N, Fire A, Tyan D, Kay M, Tsao PS, **Hua X**, Velden J, Eiermann T, Volk HD, Reichenspurner H, Robbins RC, Schrepfer S. Immunobiology of naïve and genetically modified HLA-class-I-knockdown human embryonic stem cells. *J Cell Sci.* 2011 Sep 1;124(Pt 17):3029-37.

6. Deuse T, Seifert M, Phillips N, Fire A, Tyan D, Kay M, Tsao PS, **Hua X**, Velden J, Eiermann T, Volk HD, Reichenspurner H, Robbins RC, Schrepfer S. Human leukocyte antigen I knockdown human embryonic stem cells induce host ignorance and achieve prolonged xenogeneic survival. *Circulation*. 2011 Sep 13;124(11 Suppl):S3-9.
7. Deuse T, Koyanagi T, Erben RG, **Hua X**, Velden J, Ikeno F, Reichenspurner H, Robbins RC, Mochly-Rosen D, Schrepfer S. Sustained inhibition of epsilon protein kinase C inhibits vascular restenosis after balloon injury and stenting. *Circulation*. 2010 Sep 14; 122(11 Suppl):S170-8.
8. **Hua X**, Deuse T, Tang-Quan KR, Robbins RC, Reichenspurner H, Schrepfer S. Heterotopic and orthotopic tracheal transplantation in mice used as models to study the development of obliterative airway disease. *J. Vis. Exp.* (35), e1437, DOI: 10.3791/1437 (2010).

Abstracts

-
1. Deuse T, Koyanagi T, Erben R, **Hua X**, Velden J, Reichenspurner H, Robbins R, Mochly-Rosen D, Schrepfer S. Sustained inhibition of epsilon protein kinase C inhibits vascular restenosis after balloon injury and stenting. *Transpl Int*. 2010 Oct 31:38.
 2. **Hua X**, Gossler T, Stubbendorff M, Deuse T, Taylor V, Chen Y, Reichenspurner H, Robbins R, Schrepfer S. Targeting the JAK1/3 pathway to suppress acute allograft rejection. *Transpl Int* 2011;24Suppl 3:276.
 3. **Hua X**, Deuse T, Wulff H, Köhler R, Chen Y, Reichenspurner H, Robbins R, Schrepfer S. Blockade of KCa3.1 as potential new therapeutic strategy for the prevention of chronic allograft rejection. *Transpl Int* 2011;24Suppl 3:P024.
 4. **Hua X**, Deuse T, Gossler T, Stubbendorff M, Haddad F, Reichenspurner H, Michelakis E, Schrepfer S. The mitochondria-K⁺channel axis is involved in the development of intimal hyperplasia. *Transpl Int* 2011;24Suppl 3:P026.
 5. Deuse T, Seifert M, Fire A, Volk HD, **Hua X**, Reichenspurner H, Robbins R, Schrepfer S. Genetically engineered human embryonic stem cells escape immune response. *Transpl Int* 2011;24Suppl 3:234.
 6. Deuse T, Gossler T, **Hua X**, Stubbendorff M, Haddad F, Velden J, Reichenspurner H, Robbins RC, Michelakis E, Schrepfer S. Metabolic Modulation – A feasible Concept to tackle intimal proliferation? *J Heart Lung Transpl* 2011;30 4S:400.
 7. Stubbendorff M, Deuse T, **Hua X**, Gossler T, Pahrman C, Tang-Quan KR, Reichenspurner H, Robbins RC, Schrepfer S. Immunogenicity and immunomodulatory properties of umbilical cord lining mesenchymal stem cells for regenerative therapies. *J Heart Lung Transpl* 2011;30 4S:545.

8. Deuse T, Seifert M, Fire A, Phillips N, **Hua X**, Velden J, Kay M, Volk H-D, Reichenspurner H, Robbins RC, Schrepfer S. Hypoimmunogenic HLA I knockdown human embryonic stem cells induce host ignorance and achieve prolonged xenogeneic survival. *J Heart Lung Transpl* 2011;30 4S:547.
9. Gossler T, Deuse T, **Hua X**, Stubbendorff M, Velden J, Robbins RC, Reichenspurner H, Michelakis E, Schrepfer S. Prevention, inhibition, and reversion of chronic allograft vasculopathy by mitochondrial modulation. *Thorac Cardiovasc Surg* 2012; 60: V133.
10. **Hua X**, Boeddinghaus J, Gossler T, Stubbendorff M, Deuse T, Michelakis E, Tsao PS, Maegdefessel L, Erben R, Reichenspurner H, Robbins RC, Schrepfer S. Translational models: A humanized model to study the development of intimal hyperplasia after stenting. *Thorac Cardiovasc Surg* 2012; 60: V134.
11. **Hua X**, Deuse T, Velden J, Kirak O, Jaenisch R, Weissman I, Ricklefs F, Reichenspurner H, Robbins R.C, Schrepfer S. Regenerative therapy after myocardial infarction: role of mtDNA in SCNT derived embryonic stem cells. *J Heart Lung Transpl* 2012;31 4S:S117. **[Philip K. Caves Award Session for the best scientific abstract.]**
12. Deuse T, **Hua X**, Stubbendorff M, Gossler T, Velden J, Taylor, V, Park G, Chen Y, Reichenspurner H, Robbins R.C, Schrepfer S. The JAK1/3-inhibitor R507 diminishes acute and chronic rejection while demonstrating immune cell specificity. *J Heart Lung Transpl* 2012;31 4S:S125.
13. **Hua X**, Deuse T, Stubbendorff M, Gossler T, Velden J, Reichenspurner H, Robbins R.C, E Michelakis, Schrepfer S. Role of mitochondrial activity in the development of chronic allograft vasculopathy. *J Heart Lung Transpl* 2012;31 4S:S125.
14. Deuse T, **Hua X**, Länger F, Gossler T, Stubbendorff M, Rakovic A, Klein C, Sutendra G, Dromparis P, Maegdefessel L, Tsao P.S, Velden J, Reichenspurner H, Robbins R.C, Haddad F, E Michelakis, Schrepfer S. Pyruvate dehydrogenase kinase 2 controls vascular remodeling. *J Heart Lung Transpl* 2012;31 4S:S126.

Posters

-
1. **Hua X**, Deuse T, Chen YJ, Wulff H, Köhler R, Reichenspurner H, Robbins RC, Schrepfer S. Identifying the potassium channel KCa3.1 as new therapeutic target to prevent airway allograft rejection. *J Heart Lung Transpl* 2011;30 4S:563.
 2. **Hua X**, Deuse T, Robbins R, Reichenspurner H, Schrepfer S. Immunosuppressive agents differently suppress T cell subpopulations. *Transpl Int.* 2010 Oct 31:34-35.
 3. Arunagirinathan U, Stubbendorff M, Deuse T, **Hua X**, Velden J, Haddad F, Robbins RC, Reichenspurner H, Schrepfer S. Using skin transplants as early *in vivo* indicators for graft rejection in heart transplantation. *Thorac Cardiovasc Surg* 2012; 60: PP141.

4. **Hua X**, Deuse T, Stubbendorff M, Velden J, Reichenspurner H, Robbins R.C, Schrepfer S. Translational models: a humanized model to study the development of obliterative airway disease. *J Heart Lung Transpl* 2012;31 4S:S144.
5. **Hua X**, Deuse T, Stubbendorff M, Haddad F, Reichenspurner H, Robbins R.C, Schrepfer S. Vascular biology: dichloroacetate inhibits the development of intimal hyperplasia, but not atherosclerotic lesions. *J Heart Lung Transpl* 2012;31 4S:S144.
6. Schmidt S, Conradi L, **Hua X**, Peters L, Deuse T, Hansen A, Eder A, Reichenspurner H, Robbins R.C, Eschenhagen T, Schrepfer S. Clinical aspects in regenerative medicine: Immunobiology of engineered heart tissue. *J Heart Lung Transpl* 2012;31 4S:S218.

Research Techniques

Animal Micro-operation Technique: Heterotopic and orthotopic tracheal transplantation in mice and rats, Heterotopic heart Transplantation in rats.

Histology: Tissue processing, Paraffin and cryo sectioning, Routine biological staining (H&E, Masson-Goldner Trichrome, PAS, etc.), Immunofluorescence, Immunohistochemistry

Microscopic Imaging Techniques: Light Microscope and conventional fluorescent microscope imaging, Confocal imaging (by PerkinElmer UltraVIEWVoX system, basic technique on spinning disc system), Image process by Volocity (3D Opacity Reconstruction and 3D movie making)

Cell and Molecular Biochemistry: Donor specific antibody essay, ELISPOTs, Cell culture, Western blot/Immunoblot

Language

| | |
|-----------|--|
| 2010-2011 | German as foreign language, (400 study hours, equivalent to level B1) |
| 2008 | TOEFL iBT: 94/120 |
| 2007 | GRE: Verbal part: 550, Quantitative part: 800, Analytical Writing: 3.5 |
| 2005 | Advanced Interpreter Training (2 months) |
| 2004 | Basis of German (120 study hours) |
| 2004 | Chinese College English Test (Level 6): 86/100 |
| 2003 | Chinese College English Test (Level 4): 94.5/100 |

Hamburg, den 06.09.2012

Xiaoqin Hua

9. Acknowledgement

My doctoral thesis could not have been done without my supervisor Prof. Dr. Sonja Schrepfer, who trained and encouraged me throughout my doctoral study. I am extremely grateful to her for her expert and valuable guidance on the diverse exciting projects, and for all the opportunities she generously provided. I believe that her critical thinking, hardworking and meticulousness, will enlighten me on the way of my future academic career. I'm very grateful to PD Dr. Tobias Deuse. Every time it's such a pleasure to discuss projects with him, and I'm deeply impressed by his transplant operations. I also wish to express my sincere thanks to Prof. Dr. Dr. Hermann Reichenspurner for all the supports he offered.

I would like to appreciate the support from my motherland, China, especially from the Chinese Scholarship Council. Life abroad would have never been easy without the scholarship. Thanks to my Alma mater, Tongji Medical College, Huazhong University of Science and Technology, for all the medical knowledge and skills I learnt. I really appreciated the English program I attended, which not only helped me improve my language, but also build a bridge with respect to the different cultures, ideas, and ways of thinking.

I take this opportunity to acknowledge and extend my heartfelt gratitude to all my colleagues and friends I met here in Germany, especially Ms. Christiane Pahrman and Dr. Mandy Stubbendorff. Thanks for every help and happiness they brought to me in these three years.

I'm particularly indebted to my parents. You raise me up, to more than I can be.

Last but not least, lots of thanks from my bottom of heart to Roumu. Es ist schön dass es dich gibt.

10. Eidesstattliche Versicherung

Ich versichere ausdrücklich, dass ich die Arbeit selbständig und ohne fremde Hilfe verfasst, andere als die von mir angegebenen Quellen und Hilfsmittel nicht benutzt und die aus den benutzten Werken wörtlich oder inhaltlich entnommenen Stellen einzeln nach Ausgabe (Auflage und Jahr des Erscheinens), Band und Seite des benutzten Werkes kenntlich gemacht habe.

Ferner versichere ich, dass ich die Dissertation bisher nicht einem Fachvertreter an einer anderen Hochschule zur Überprüfung vorgelegt oder mich anderweitig um Zulassung zur Promotion beworben habe.

Ich erkläre mich einverstanden, dass meine Dissertation vom Dekanat der Medizinischen Fakultät mit einer gängigen Software zur Erkennung von Plagiaten überprüft werden kann.

Hamburg, den 06.09.2012

Xiaoqin Hua

Significant Reduction of Acute Cardiac Allograft Rejection by Selective Janus Kinase-1/3 Inhibition Using R507 and R545

AQ1

Tobias Deuse,^{1,2} Xiaoqin Hua,^{1,2} Vanessa Taylor,³ Mandy Stubbendorff,^{1,2} Muhammad Baluom,³ Yan Chen,³ Gary Park,³ Joachim Velden,⁴ Thomas Streichert,⁵ Hermann Reichenspurner,^{1,2} Robert C. Robbins,⁶ and Sonja Schrepfer^{1,2,6,7}

Background. Selective inhibition of lymphocyte activation through abrogation of signal 3-cytokine transduction emerges as a new strategy for immunosuppression. This is the first report on the novel Janus kinase (JAK)1/3 inhibitors R507 and R545 for prevention of acute allograft rejection.

Methods. Pharmacokinetic and in vitro enzyme inhibition assays were performed to characterize the drugs. Heterotopic Brown Norway–Lewis heart transplantations were performed to study acute cardiac allograft rejection, graft survival, suppression of cellular host responsiveness, and antibody production. Therapeutic and subtherapeutic doses of R507 (60 and 15 mg/kg 2 times per day) and R545 (20 and 5 mg/kg 2 times per day) were compared with those of tacrolimus (Tac; 4 and 1 mg/kg once per day).

Results. Plasma levels of R507 and R545 were sustained high for several hours. Cell-based enzyme assays showed selective inhibition of JAK1/3-dependent pathways with 20-fold or greater selectivity over JAK2 and Tyk2 kinases. After heart transplantation, both JAK1/3 inhibitors reduced early mononuclear graft infiltration, even significantly more potent than Tac. Intra-graft interferon- γ release was significantly reduced by R507 and R545, and for interleukin-10 suppression, they were even significantly more potent than Tac. Both JAK1/3 inhibitors and Tac were similarly effective in reducing the host Th1 and Th2, but not Th17, responsiveness and similarly prevented donor-specific immunoglobulin M antibody production. Subtherapeutic and therapeutic R507 and R545 doses prolonged the mean graft survival and were similarly effective as 1 and 4 mg/kg Tac, respectively. In combination regimens, however, only R507 showed highly beneficial synergistic drug interactions with Tac.

Conclusions. Both R507 and R545 are potent novel immunosuppressants with favorable pharmacokinetics and high JAK1/3 selectivity, but only R507 synergistically interacts with Tac.

Keywords: JAK1/3 inhibitor, Acute cardiac allograft rejection, Novel immunosuppression.

(*Transplantation* 2012;94: 00–00)

AQ2

AQ3

Immunosuppressive drug therapy after heart transplantation significantly contributes to the overall morbidity and mortality of recipients by inducing pleiotropic side effects (1). Novel immunosuppressive agents target a variety of molecules at different levels of the antigen presenting cell (APC)–T-cell

interaction (2). Targets for small-molecule drugs at various stages of the preclinical development include tyrosine kinases, mitogen-activated protein kinases (3), phosphoinositide-3-kinase (4), and chemokine receptors (5). In the future, we hope to have tailored patient-individualized drug regimens, combined from an arsenal of available substances, taking into account the patient's immune responsiveness

AQ5

S.S. received funding from the Deutsche Forschungsgemeinschaft (SCHR992/3-1; SCHR992/4-1) and the International Society for Heart and Lung Transplantation.

V.T., M.B., Y.C., and G.P. are affiliated with Rigel Pharmaceuticals.

¹ Transplant and Stem Cell Immunobiology Laboratory, University Heart Center Hamburg, Hamburg, Germany.

² Cardiovascular Research Center and Deutsches Zentrum für Herz-Kreislaufforschung University Hamburg, Hamburg, Germany.

³ Rigel Pharmaceuticals, South San Francisco, CA.

⁴ Institute of Pathology, University Hospital Hamburg, Hamburg, Germany.

⁵ Institute of Clinical Chemistry, University Hospital Hamburg, Hamburg, Germany.

⁶ Department of Cardiothoracic Surgery, Stanford University School of Medicine, Stanford, CA.

⁷ Address correspondence to: Sonja Schrepfer, M.D., Ph.D., Department of Cardiothoracic Surgery, Stanford University School of Medicine, 300 Pasteur Dr, CVRB MC 5407, Stanford, CA 94305.

E-mail: schrepfer@stanford.edu

T.D., V.T., Y.C., G.P., and S.S. participated in research design. T.D., X.H., V.T., H.R., R.C.R., and S.S. participated in the writing of the paper. T.D., X.H., M.S., J.V., V.T., M.B., Y.C., G.P., T.S., and S.S. participated in the performance of the research. T.D., X.H., V.T., and S.S. participated in data analysis. Supplemental digital content (SDC) is available for this article. Direct URL citations appear in the printed text, and links to the digital files are provided in the HTML text of this article on the journal's Web site (www.transplantjournal.com).

Received 11 December 2011. Revision requested 23 May 2012.

Accepted 21 June 2012.

Copyright © 2012 by Lippincott Williams & Wilkins

ISSN: 0041-1337/12/9407-00

DOI: 10.1097/TP.0b013e3182660496

AQ4

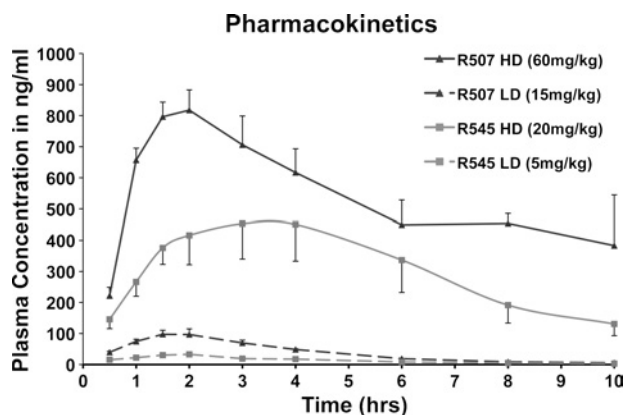


FIGURE 1. Pharmacokinetics of R507 and R545. Male Lew rats were orally dosed with R507 or R545 at therapeutic or subtherapeutic doses, and plasma concentrations were quantified at serial time points.

and comorbidities. However, the last decade has been disappointing for transplant therapeutics, because no new immunosuppression agents have been approved (6). Instead, highly anticipated drugs failed to sustain clinical trials (FTY720 (7), FK778 (8)) after showing promising effects in preclinical models (9, 10). Basic researchers and industry partners are therefore prompted to team up and advance the development of new, much-needed immunosuppressants.

The cytoplasmic Janus kinases (JAKs) participate in the signaling of a broad range of cell surface receptors, particularly cytokine receptors, and are among the most promising and most intensely studied immune targets (11). Although immunosuppressive efficacy could be demonstrated for different molecules (12–18), increased selectivity for JAK1/3 inhibition and improved JAK2 avoidance is the an ongoing challenge (6). We present the first data on the 2 JAK1/3 inhibitors R507 and R545 in experimental cardiac allograft survival, quantifying cellular immune inhibition and assessing interaction with tacrolimus (Tac).

RESULTS

Pharmacokinetics

R507 and R545 plasma levels peaked between 2 and 3 hours after administration (Fig. 1). The area under the concentration-time curve in the R507 high-dose (HD) group was approximately 13.8-fold higher than that for R507 low-dose (LD) group. Plasma levels in the R545 HD group resulted even in a 22.6-fold higher area under the concentration-time curve compared with R545 LD.

Pharmacodynamics

R507 and R545 inhibited JAK1/3-dependent signal transducer and activator of transcription (STAT)-5 phosphorylation in response to interleukin (IL)-2 and blocked the resulting T-cell proliferation (Table 1; see Figure 1, SDC 1, <http://links.lww.com/TP/A696>). Consistent with this, R507 and R545 potently inhibited the proliferative response of T cells to dendritic cell (DC) costimulation in mixed lymphocyte reactions (MLRs). In human primary T cells, R507 and R545 also inhibited JAK1/Tyk2-dependent phosphorylation of STAT-1 in response to interferon (IFN)- α but only weakly inhibited JAK2/Tyk2-dependent phosphorylation of STAT-4 in response to IL-12. Furthermore, R507 and R545 showed limited inhibition of JAK2-dependent cultured human erythroid progenitor cell (CHEP) survival in response to erythropoietin (EPO), and JAK1/2-dependent intercellular adhesion molecule (ICAM)-1 expression in U937 cells in response to IFN- γ . Taken together, these data show that R507 and R545 are potent inhibitors of JAK1 and JAK3 kinases with 20-fold or greater selectivity over JAK2 and Tyk2 kinases in cells. In contrast, CP-690,550 potently inhibited IFN- γ - and EPO-dependent signaling and IL-2- and IFN- α -dependent signaling but was only weakly active against IL-12. This suggests that CP-690,550 is a potent inhibitor of JAK1, JAK2, and JAK3 but not Tyk2. The pan-JAK inhibitor R369 broadly inhibited all of the JAK-dependent cell-based assays. The JAK selectivity of the inhibitors was also assessed in whole blood assays using intracellular flow

TABLE 1. Activity of CP-609,550, R545, R507, and the pan-JAK inhibitor R369 in a cell-based assay panel assessing JAK selectivity and a panel of cytokine-induced STAT phosphorylation assays in blood lymphocytes and granulocytes

| Assay | Upstream kinases | EC ₅₀ , μ M | | | |
|--|------------------|----------------------------|-------------------|-------------------|--------------------|
| | | CP-690,550 | R545 | R507 | R369 |
| MLR | | 0.148 \pm 0.085 | 0.022 \pm 0.006 | 0.016 \pm 0.007 | 0.005 (n=1) |
| JAK-dependent cell-based activity | | | | | |
| IL-2 T-cell proliferation | JAK1/3 | 0.046 \pm 0.021 | 0.030 \pm 0.013 | 0.021 \pm 0.007 | 0.022 \pm 0.009 |
| IL-2 T-cell phospho-STAT-5 | JAK1/3 | 0.038 \pm 0.019 | 0.035 \pm 0.015 | 0.021 \pm 0.009 | 0.026 \pm 0.016 |
| IFN- α T-cell phospho-STAT-1 | JAK1/Tyk2 | 0.035 \pm 0.010 | 0.007 \pm 0.001 | 0.009 \pm 0.007 | 0.002 \pm 0.0005 |
| IL-12 T-cell phospho-STAT-4 | JAK2/ Tyk2 | 4.717 \pm 2.571 | 1.564 \pm 0.971 | 0.463 (n=1) | 0.094 \pm 0.067 |
| IFN- γ U937 ICAM-1 | JAK1/2 | 0.072 \pm 0.047 | 0.791 \pm 0.352 | 0.417 \pm 0.211 | 0.041 \pm 0.028 |
| EPO CHEP survival | JAK2 | 0.239 \pm 0.121 | 1.111 \pm 0.339 | 0.490 \pm 0.246 | 0.099 \pm 0.055 |
| Whole blood activity | | | | | |
| IL-2 whole blood lymphocytes phospho-STAT-5 | JAK1/3 | 0.058 \pm 0.026 | 0.887 \pm 0.295 | 0.416 \pm 0.152 | 0.260 \pm 0.135 |
| IFN- α whole blood lymphocytes phospho-STAT-1 | JAK1/ Tyk2 | 0.116 \pm 0.048 | 0.511 \pm 0.279 | 0.153 \pm 0.033 | 0.086 \pm 0.055 |
| IL-6 whole blood lymphocytes phospho-STAT-3 | JAK1/2 /Tyk2 | 0.557 \pm 0.226 | 6.690 \pm 1.61 | 3.838 \pm 1.522 | 1.287 \pm 0.936 |
| GM-CSF whole blood granulocytes phospho-STAT-5 | JAK2 | 0.871 \pm 0.353 | >50 | 32.7 \pm 9.51 | 0.801 \pm 0.608 |

cytometry. R545 and R507 were potent inhibitors of JAK1/3-dependent lymphocyte STAT-5 phosphorylation (see **Figure 2**, **SDC 1**, <http://links.lww.com/TP/A696>) but not JAK2-dependent granulocyte STAT-5 phosphorylation (see **Figure 3**, **SDC 1**, <http://links.lww.com/TP/A696>). Whereas the potency of R545 and R507 was significantly reduced in blood, likely owing to serum protein binding or red blood cell partitioning, the selective inhibition of IL-2 and IFN- α signaling was retained. In contrast, CP-690,550, which has very low protein binding, retains similar potency in whole blood assays as in purified T cells, consistent with previous reports (19). R507 and R545 were further profiled in a panel of cell-based assays to assess their activity against a range of kinase targets, including cytoplasmic tyrosine kinases such as Syk, Lck, and ZAP70; the receptor tyrosine kinases vascular endothelial growth factor receptor (VEGFR), INSR, and EGFR; a multitude of serine threonine kinases involved in signaling downstream of these receptors; and receptor-proximal kinases (eg, phosphatidylinositol 3-kinase pathway, mitogen-activated protein kinase pathways, protein kinase C, and nuclear factor- κ B pathways; not shown). R507 and R545 show very limited inhibition of all of these other kinase targets in cells (see **Table 1**, **SDC 1**, <http://links.lww.com/TP/A696>). In vivo inhibition of JAK1/3-dependent lymphocyte STAT-5 phosphorylation by R545 and R507 was dose and time dependent (see **Figure 4**, **SDC 1**, <http://links.lww.com/TP/A696>). R545 and R507, however, did not inhibit JAK2-dependent granulocyte STAT-5 phosphorylation. Splenocyte cell proliferation from animals treated with R545 or R507 was significantly inhibited (see **Figure 5**, **SDC 1**, <http://links.lww.com/TP/A696>).

Histology and Immunohistochemistry

In 5-day grafts of untreated recipients, lymphocyte p-JAK1 and p-JAK3 expressions were high, serving as abundant

targets for pharmacotherapy, whereas p-JAK2 was scarce (Fig. 2; see **SDC**, **Videos 1-4**, <http://links.lww.com/TP/A697>, <http://links.lww.com/TP/A698>, <http://links.lww.com/TP/A699>, <http://links.lww.com/TP/A700>). The high levels of intragraft p-JAK1 and p-JAK3 correlate with the observed massive CD3+ cell infiltration, suggesting infiltration of activated lymphocytes. Syngeneic 5-day grafts showed no pathologic signs of cellular rejection, whereas the allogeneic no-medication group showed destroyed myocardial tissue, massive mononuclear cell infiltration, hemorrhages, edema, and vasculitis (Fig. 3A), resulting in moderate-to-severe rejection ratings (Fig. 3B). Grafts in the 3 LD groups ranged from 1R to 3R rejection. Among the HD groups, R545 achieved the most 0R and the least ≥ 2 R category ratings. A dose-dependent effect was observed for all medication groups. Massive CD3+ and even more CD68+ cells were observed in the no-medication group (Fig. 3C,D). The heart tissue of the syngeneic group showed some cell accumulation, which was attributed mainly to the surgical trauma and showed a subendocardial pattern. The 3 LD groups were ineffective to relevantly reduce cell infiltration. Although all 3 HD groups showed a significant decrease of CD3+ cell infiltration compared with the no-medication group ($P < 0.001$), both JAK1/3 inhibitors proved to be especially strong inhibitors of graft infiltration ($P < 0.001$ vs. Tac HD).

Enzyme-Linked Immunospot Assays, Donor-Specific Antibodies, and T-Cell Subsets

The no-medication group showed a strong cellular IFN- γ , IL-4, and IL-17-release in response to donor antigens ($P < 0.001$ for each cytokine vs. the syngeneic group; Fig. 4A-C). Tac and both HD JAK1/3 inhibitors were very effective and similarly potent in reducing IFN- γ and IL-4 spot frequencies ($P < 0.001$ each vs. no medication), but had only marginal

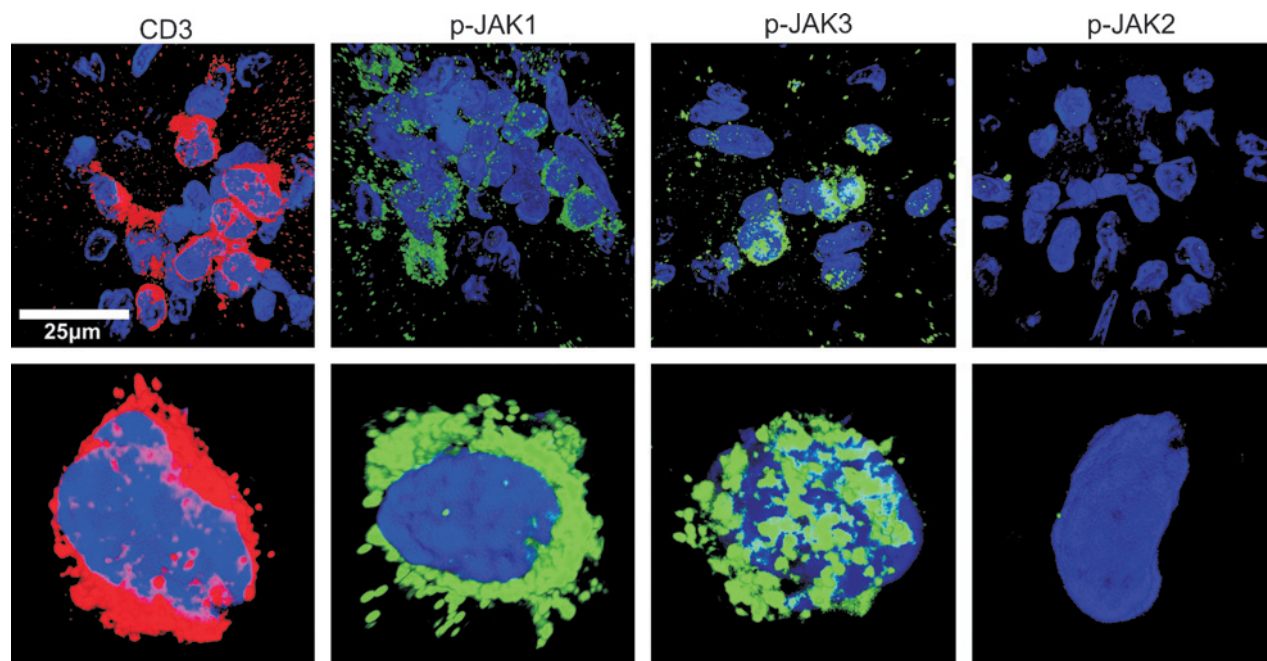


FIGURE 2. Intragraft lymphocyte p-JAK expression. Untreated 5-day grafts were stained for CD3, p-JAK1, p-JAK2, and p-JAK3 expression. Graft-infiltrating lymphocytes showed strong p-JAK1 and p-JAK3 but only weak p-JAK2 expression.

Fig 3 4/C

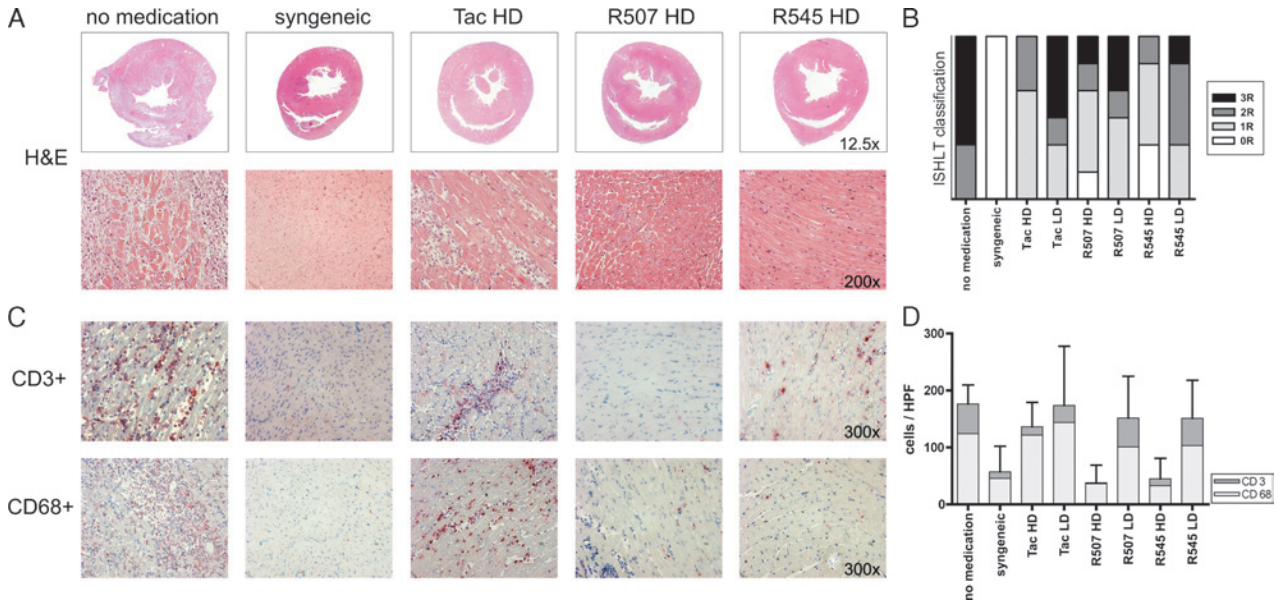


FIGURE 3. Graft histology. A, Overview and detail of representative mid-graft cross sections for the control and HD-medication groups. Rejection was scored according to the revised ISHLT classification. B, Distribution of rejection classes within the groups. Graft-infiltrating cell types were identified by immunohistochemical stainings for CD3 and CD68 (C) and quantified (D).

impact on IL-17. R507 LD and especially R545 LD showed surprisingly reduced IFN- γ spots in this test. However, the JAK1/3 inhibitor LD treatments also significantly decreased IL-4 spot frequencies compared with Tac LD ($P < 0.001$).

We observed a significant decrease of immunoglobulin M antibodies in all LD- and HD-medication groups ($P < 0.001$ vs. no medication; Fig. 4D). This assay showed no dose dependency on the effects of donor-specific antibody suppression.

Intragraft Cytokine Release

Figure 4E demonstrates the intragraft cytokine levels of IFN- γ , which is mostly released by T cells and natural killer cells. IFN- γ release was significantly less in the R507 HD- and R545 HD-medication groups ($P < 0.05$). IL-10 release (Fig. 4F) was again significantly reduced in the 2 JAK1/3-inhibitor HD groups when compared with the no-medication group (both $P < 0.05$) and also with the Tac HD group (both $P < 0.05$).

Fig 4 4/C

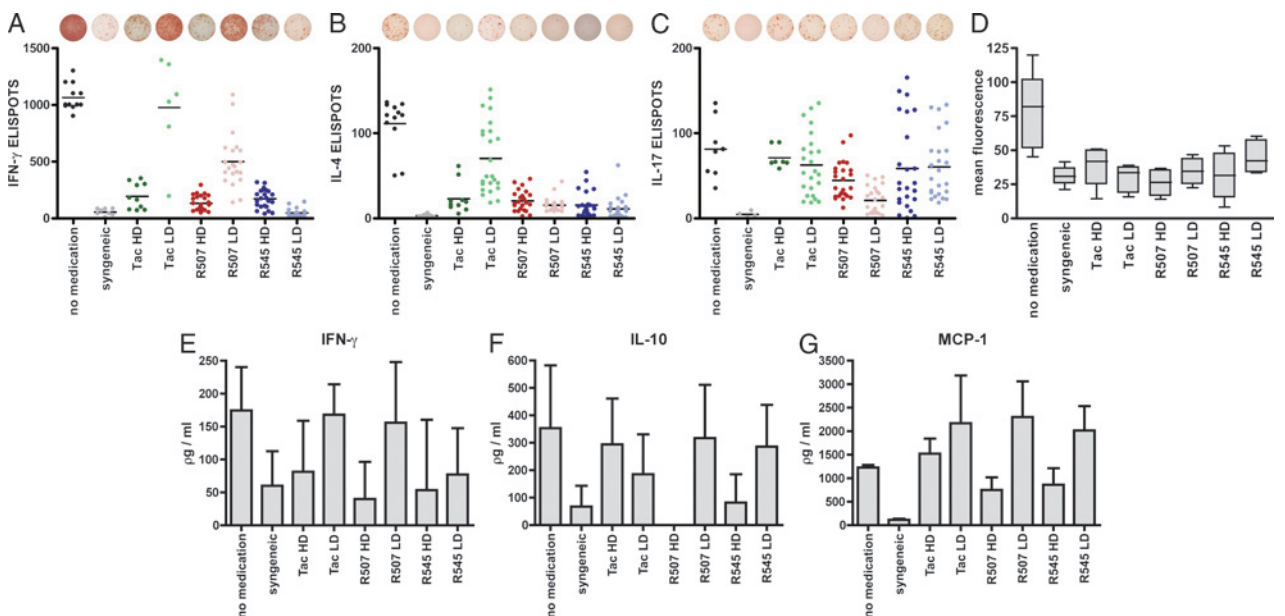


FIGURE 4. Immune response after 5 days. Elispot assays were performed to assess the cellular host responses. Spot frequencies for IFN- γ (A), IL-4 (B), and IL-17 (C). Five days after transplantation, all treatment groups showed significant suppression of alloreactive antibody production (D). Intragraft IFN- γ (E), IL-10 (F), and MCP-1 (G) were quantified.

AQ13 Monocyte chemoattractant protein (MCP)-1 levels (Fig. 4G) showed no significant differences in the treatment groups compared with the no-medication group.

Side Effects

No obvious signs of discomfort, gastrointestinal symptoms such as diarrhea, or neurological dysfunctions were observed in any animals during the treatment period. No anemia was observed. Tac HD, R507 HD, and R545 HD showed increased high-density lipoprotein values and decreased low-density lipoprotein (LDL) values compared with the no-medication group. All 3 drugs HD showed elevated serum alanine aminotransferase levels but not aspartate aminotransferase levels. In complete blood counts, R507 HD and R545 HD did not alter erythrocyte or hemoglobin levels. However, total leukocyte numbers were reduced, and whereas lymphocyte counts decreased, basophil counts were increased (for details see **Table 2**, **SDC 1**, <http://links.lww.com/TP/A696>).

Graft Survival Study

Syngeneic grafts did not undergo rejection. Mean allograft survival was significantly prolonged in all LD and HD groups ($P < 0.05$ each vs. no medication; Fig. 5). Dose-dependent effects were observed for all drugs, and all HD-medication groups extended graft survival significantly further than their respective LD groups ($P < 0.002$ each). No significant differences in graft survival were found among the 3 HD groups. The interaction of the JAK1/3 inhibitors with Tac, however, revealed great disparity. The combination of R507 LD with Tac LD was similarly effective as R507 HD, significantly better than either drug alone, and the combination index (CI) of 0.584 showed synergism. The interaction of R545 LD with Tac LD was rather antagonistic (CI, 3.0), and drug combination did not increase survival.

DISCUSSION

T-cell activation by APC requires cellular interactions through direct and indirect signaling. Signal 1 is delivered by major histocompatibility complex-bound antigen peptides to specific T-cell receptors and is amplified by costimulatory signals by multiple contacts between APCs and T cells, encompassed as signal 2 (20). The third signal is mediated by cytokines and growth factors in an autocrine or paracrine fashion and drives T-cell proliferation and clonal expansion. JAK3 is a lymphoid-specific tyrosine kinase involved in

signaling cascades of many signal 3-cytokines utilizing γ c receptors. JAK1 is also associated with intracellular domains of signal 3-cytokines, but it is more widely expressed and binds to the α - and β -receptor chains, whereas JAK3 binds to γ c-chain (21–23). The γ c-chain is paired with either the α - or β -chain, and cytokine signaling requires both JAK1 and JAK3. Cells lacking JAK1 or JAK3 are thus unable to respond to γ c cytokines (24, 25). Defects of the JAK3 gene have been identified in patients with severe combined immunodeficiency (26), indicating its importance for the maintenance of a functionally competent immune system (27). However, JAK1 has recently been identified to play a dominant role over JAK3 in signal transduction through γ c-containing cytokine receptors, and that JAK3 kinase activity merely enhances the effect of JAK1 (28). Because JAK3 is always paired with JAK1, and inhibition of both kinases is more effective in blocking γ c-cytokine effects than inhibition of either kinase alone, dual inhibitory function may be desirable for an immunosuppressive agent. Nevertheless, strong selectivity against JAK1/3 versus JAK2 is highly warranted. JAK2 mediates signaling through EPO receptor, thrombopoietin receptor, and cytokine receptors that harbor the common β -chain, like the IFN- γ receptors (29, 30). JAK2 is essential for pathways that control erythroid, myeloid, and megakaryocytic development, and JAK2 inhibitors are currently evaluated for treatment of myeloproliferative neoplasms. In clinical trials with the JAK2 inhibitor CEP701, toxicity included myelosuppression (anemia, thrombocytopenia) and gastrointestinal toxicity (diarrhea, nausea, vomiting) (31, 32), both of which are believed to be avoided by JAK1/3 selectivity. Also, JAK2 phosphorylation has been shown to be essential for opioid-induced (33), thrombopoietin-induced (34), and leptin-induced (35) cardioprotection, and JAK2 inhibition was associated with an increase in infarct size after ischemia-reperfusion injury. Avoidance of JAK2 inhibition may thus be beneficial in the setting of heart transplantation where ischemia is a major risk factor for early graft failure. Using confocal immunofluorescence, we could demonstrate that activated, graft-infiltrating lymphocytes showed high levels of p-JAK1 and p-JAK3 expression and thus provide abundant targets for JAK1/3 inhibitors. JAK2 has also been described to mediate lymphocyte cell signaling like DC-T-cell interaction (36) or the response to IFN- γ receptor activation (37). However, the latter study demonstrated that only in the presence of functional JAK1 are JAK2 and Tyk2 activated by IFNs. The functionality of JAK2 in lymphocytes exposed to JAK1/3 inhibitors remains to be elucidated.

One JAK inhibitor (CP-690,550), used with IL-2R antagonist induction and mycophenolate mofetil-steroid maintenance, has already been evaluated in clinical trials with kidney transplant patients. In a phase 2A pilot study, the efficacy at 15 mg 2 times per day was comparable with that of Tac, but higher doses of CP-690,550 led to over-immunosuppression with an increased incidence of polyoma virus nephropathy and cytomegalovirus infections (38). In a subsequent phase 2B trial using reduced drug doses, CP-690,550-treated patients had statistically noninferior acute rejection rates and improved renal functions as compared with cyclosporine A but, unfortunately, excessive rates of infection and myelosuppression (39). Whereas the authors

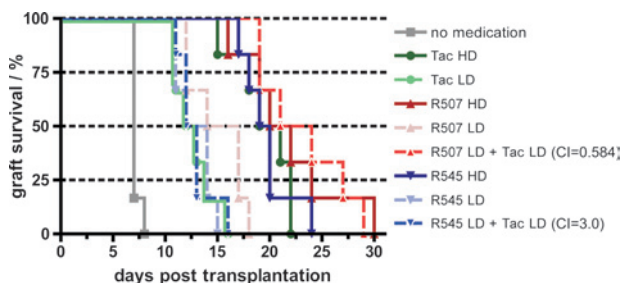


FIGURE 5. Graft survival. Allograft survival was evaluated after a 10-day treatment period. Single-drug and combination regimens are shown. There were no differences in graft survival among the 3 HD groups. Of the JAK1/3 inhibitors, only R507 showed synergistic interaction with Tac.

claim that further analyses on the optimal dosing of CP-690,550 were warranted, others question its JAK3 selectivity (20). The binding preference of CP-690,550 for JAK3 over JAK2 was recently observed to be only about 2-fold (40). Our own results are in line with the latter report and show that both R545 and R507 are more specific inhibitors of JAK1 and JAK3 with 20-fold or greater selectivity over JAK2 and Tyk2 kinases in cells. We did not observe the development of anemia with R507 or R545, but our study period was rather short and may not reflect long-term trends.

Favorable effects on cholesterol levels, with an increase of high-density lipoprotein and a decrease of LDL, have been observed with the 2 JAK1/3 inhibitors in our study. The current state of knowledge let us suspect that inhibition of JAK1 in the oncostatin M pathway prevents suppression of the LDR receptor, increases LDL uptake, and decreases LDL blood level in the R507- and R545-medication groups (41). That, however, contradicts observations in CP-690,550-treated patients, who frequently developed hyperlipidemia (38, 42).

Intra-graft inflammatory cytokine expression depends on the amount of infiltration cells and their release of factors. IFN- γ production by lymphocytes has been shown to be inhibited by CP-690,550 in a dose-dependent fashion (43), and we found significantly reduced IFN- γ levels in the grafts of R507 and R545 HD-treated animals. Recent data suggest that monocyte MCP-1 expression is regulated by the JAK2-STAT-5 pathway (44), and the intra-graft MCP-1 expression in our study failed to demonstrate significant differences.

Recently, STAT-5 and STAT-3 have been considered as opposing regulators of Treg versus Th17 generation and function. Whereas STAT-5 promoted Treg and inhibited Th17 function, STAT-3 had the opposite effect (45). On the other hand, STAT-3 phosphorylation was shown to be mandatory for Foxp3 expression, and STAT-3 ablation inhibited Foxp3 expression and the suppressive functions of CD4+CD25+ T lymphocytes (46). In a separate rat collagen-induced arthritis study, we observed that JAK1/3 inhibition with R545 treatment reduced the numbers of effector and regulatory T cells without altering the Tc-to-Treg ratio (unpublished data). To date, however, we have limited data to speculate on tolerance induction and long-term graft acceptance during JAK1/3 inhibitor therapy.

In this head-to-head comparison of 2 novel JAK1/3 inhibitors, R507 and R545 demonstrated comparable overall immunosuppressive potency. They achieved a comparable dose-dependent reduction of cardiac allograft infiltration and intra-graft cytokine release, similar alleviation of cellular graft rejection (mildly favoring R545), and similar prolongation of allograft survival (mildly favoring R507). R507 most potently decreased IL-17 spot frequencies. Although the Th17 population remains incompletely understood, recent studies suggest a harmful role of Th17 graft infiltration, promoting cellular rejection (47–49). The biggest difference between R507 and R545 was revealed when combined with Tac, inasmuch as only R507 interacted synergistically. Calcineurin inhibitor-free immunosuppression is already being used in selected patients early after heart transplantation (50); however, safety remains to be proven. For the time being, calcineurin inhibitors are indispensable, and favorable

interactions by novel immunosuppressive drugs are required. R507 will therefore be the focus of further drug development.

In conclusion, highly selective JAK1/3 inhibition provides powerful immunosuppression by interrupting signal transduction of signal 3-cytokines. Although CP-690,550 has made its way into clinical trials, some side effects may arise from its lack of selectivity. More selective compounds could present an improved effect-to-side effect ratio, and R507 is a very promising candidate.

MATERIALS AND METHODS

Pharmacokinetics

Male Lewis (Lew) rats received either R507 at 60 mg/kg (HD) or 15 mg/kg (LD) 2 times per day or R545 at 20 mg/kg (HD) or 5 mg/kg (LD) 2 times per day by oral gavage. The plasma levels of R507 and R545 were quantified using LC/MS/MS. In the graft survival study, 2 combination regimens (R507 LD+ Tac LD and R545 LD+ Tac LD) were tested to evaluate drug interactions.

Pharmacodynamics

The activity and selectivity of R507 and R545 were assessed in a panel of cell-based assays and compared with those of CP-690,550 (51). Data for a nonselective JAK inhibitor from the same chemical series, R369, are shown for reference.

Mixed Lymphocyte Reactions

MLRs were performed by incubating freshly prepared naive human peripheral blood lymphocytes with CD80+/CD86+ mature DCs, derived from a different donor for 5 days. The percentage of CD3+/CD71+ (anti-CD3-APC, anti-CD71-FITC; BD Biosciences, San Jose, CA) proliferating cells was assessed by a fluorescence-activated cell sorter (FACS; BD Biosciences). AQ16

Cell Viability Assay

IL-2-dependent human primary T-cell proliferation was assessed using Promega's CellTiter-Glo Luminescent Cell Viability Assay (Promega, Madison, WI). The EPO-dependent survival of CHEPs was again determined using Promega's assay.

Fluorescence-Activated Cell Sorter Analyses

STAT phosphorylation induced by different cytokines in human primary T cells was measured by intracellular FACS analysis (anti-pY694-STAT-5 AlexaFluor488, anti-pY701-STAT-1 AlexaFluor488, and anti-pY693-STAT-4 AlexaFluor488; BD Biosciences). STAT phosphorylation induced by different cytokines in whole blood was measured after red blood cell lysis (Lyse/Fix buffer; BD Biosciences) and methanol permeabilization. IFN- γ signaling was assessed in the U937 monocytic cell line by measuring ICAM-1 surface expression by FACS (ICAM-1-APC; BD Biosciences). B-cell receptor-dependent Erk phosphorylation was measured in Ramos cells by intracellular FACS (anti-pT202/pY204-ERK1/2-AlexaFluor488; BD Biosciences).

Enzyme-Linked Immunosorbent Assays

Human primary T-cell activation was assessed by measuring IL-2 production by enzyme-linked immunosorbent assay (R&D Systems, Minneapolis, MI) after plate-bound anti-CD3 and anti-CD28 stimulation (anti-CD3; BD Biosciences; anti-CD28; Immunotech, Prague, Czech Republic). Human umbilical vein endothelial cells were stimulated with VEGF, and VEGFR2 phosphorylation was assessed by enzyme-linked immunosorbent assay (100 ng/mL VEGF165; R&D Systems; rabbit anti-phospho-VEGFR2 mAb; Cell Signaling, Danvers, MA).

Tryptase Activity

The enzymatic activity of tryptase released by human cultured mast cells on stimulation with immunoglobulin E was quantified by fluorescence (MP Biomedicals, Solon, OH) in tryptase buffer.

Cell Proliferation Assay

Cell proliferation assays were performed with A549 epithelial cells and H1299 lung carcinoma cells using nuclear staining to measure cell numbers (DAPI; Invitrogen, Darmstadt, Germany).

Chemiluminescence

Growth factor-dependent protein phosphorylation was detected in HeLa cells by staining permeabilized cells with phospho-specific antibodies and quantified by chemiluminescence (Luminator, Wallac Multilabel Counter; Perkin Elmer). Akt phosphorylation was measured after insulin (1 μ M) stimulation, and EGFR phosphorylation was measured after EGF (200 ng/mL) stimulation (phospho-Akt; Cell Signaling; phospho-EGFR; Cell Signaling).

Animals and Heterotopic Heart Transplantations

Male Brown Norway (BN) and Lew rats weighing 350 g were purchased from Charles River (Sulzfeld, Germany) and were housed under conventional conditions at the animal care facilities of the University Hospital Hamburg, Germany. All animals were fed standard rat chow and water ad libitum and received humane care in compliance with the Principles of Laboratory Animal Care. Allogeneic (BN-to-Lew) and syngeneic (Lew-to-Lew) heterotopic heart transplantations were performed as previously described (52).

Immunosuppression and Study Groups

R507 and R545 were provided by Rigel (San Francisco, CA), and Tac by Astellas (Munich, Germany). All drugs were administered orally either in HD suggesting maximal efficacy or LD, which was 25% of the HD. The doses of R507 and R545 were defined by previous studies in the rat collagen-induced arthritis model, where R507 HD and R545 HD achieved 100% suppression of disease (unpublished data). Lew recipients of BN hearts were randomly assigned to their groups; Lew recipients of Lew hearts remained untreated and served as syngeneic controls ($n=6$ in each group). In the 5-day study, animals received their group-specific treatment. Hearts and spleens were recovered after 5 days, and EDTA and serum were analyzed for differential blood count and clinical chemistry. Animals in the graft survival study were treated for a total of 10 days and were followed up by daily abdominal graft palpation. A heart beating score from 4 (strong and regular contraction) to 0 (no palpable contraction) was defined every day, and the time of rejection was defined as the last day of palpable cardiac contractions. In the LD drug combination groups, the quality of drug interaction was described using the CI introduced by Chou (53). A computer software (Calculus; Biosoft, Cambridge, United Kingdom) was used to determine the CI values, which indicate synergism for CI less than 1 and additive or antagonistic interaction for CI equal to 1 and CI greater than 1, respectively.

Histology and Immunohistochemistry

Grafts were embedded in paraffin, sliced, and stained with hematoxylin-eosin (Waldeck, Carl Roth GmbH, Münster, Germany). Slides were examined by an experienced pathologist (J.V.), and cellular rejection was classified according to the revised ISHLT working formulation (54). Specific antibodies against rat CD3 and CD68 (Serotec, Raleigh, NC) were applied to identify macrophages and lymphocytes, respectively. Inflammatory cell densities are expressed as cells per high power field. Intra-graft lymphocyte p-JAK1, p-JAK2, and p-JAK3 expression in untreated grafts was stained using primary antibodies against CD3 (Abcam, Cambridge, United Kingdom) and JAK1, JAK2, and JAK3 (Santa Cruz Biotechnology, Santa Cruz, CA) with appropriate AlexaFluor488 secondary antibodies (Invitrogen) and evaluated by confocal laser scanning microscopy.

Enzyme-Linked Immunospot Assays and Donor-Specific Antibodies

Lymphocytes were isolated from spleens. Enzyme-linked immunospot (Elispot) assays with 1×10^7 /mL mitomycin-inhibited BN splenocytes and 1×10^6 /mL Lew splenocytes were performed according to the manufacturer's protocol (BD Biosciences). Spots were automatically enumerated using an Elispot plate reader (CTL, Cincinnati, Ohio) for scanning and analyzing. Donor-specific antibodies were quantified as previously described

(55). Fluorescence data were expressed as mean fluorescence intensity using Flowjo (Tree Star, Inc, Ashland, OR).

Quantibody Arrays

Cytokine antibody arrays (Raybiotech, Norcross, GA) were performed according to the manufacturer's protocol. All values were normalized to the standard curve.

Statistical Analyses

Data are presented as mean \pm SD. Comparisons between groups were done by analysis of variance between groups with least significant difference post hoc tests (SPSS 17.0; SPSS, Chicago, IL). $P < 0.05$ was considered significant.

ACKNOWLEDGMENTS

The authors thank Christiane Pahrman for her technical assistance and Ethicon (Norderstedt, Germany) for providing the sutures. The confocal images were taken at the UMIF, University Hospital Hamburg-Eppendorf (Bernd Zobiak).

REFERENCES

1. Stehlik J, Edwards LB, Kucheryavaya AY, et al. The Registry of the International Society for Heart and Lung Transplantation: twenty-seventh official adult heart transplant report—2010. *J Heart Lung Transplant* 2010; 29: 1089.
2. Halloran PF. Immunosuppressive drugs for kidney transplantation. *N Engl J Med* 2004; 351: 2715.
3. Wang S, Guan Q, Diao H, et al. Prolongation of cardiac allograft survival by inhibition of ERK1/2 signaling in a mouse model. *Transplantation* 2007; 83: 323.
4. Haidinger M, Werzowa J, Weichhart T, et al. Targeting the dysregulated mammalian target of rapamycin pathway in organ transplantation: killing 2 birds with 1 stone. *Transplant Rev (Orlando)* 2011; 25: 145.
5. Li J, Chen G, Ye P, et al. CCR5 blockade in combination with cyclosporine increased cardiac graft survival and generated alternatively activated macrophages in primates. *J Immunol* 2011; 186: 3753.
6. Vincenti F, Kirk AD. What's next in the pipeline. *Am J Transplant* 2008; 8: 1972.
7. Hoitsma AJ, Woodle ES, Abramowicz D, et al. FTY720 Phase II Transplant Study Group. FTY720 combined with tacrolimus in de novo renal transplantation: 1-year, multicenter, open-label randomized study. *Nephrol Dial Transplant* 2011; 26: 3802.
8. Guasch A, Roy-Chaudhury P, Woodle ES, et al. Assessment of efficacy and safety of FK778 in comparison with standard care in renal transplant recipients with untreated BK nephropathy. *Transplantation* 2010; 90: 891.
9. Zeng H, Waldman WJ, Yin DP, et al. Mechanistic study of mal-ononitrileamide FK778 in cardiac transplantation and CMV infection in rats. *Transplantation* 2005; 79: 17.
10. Pan S, Mi Y, Pally C, et al. A monoselective sphingosine-1-phosphate receptor-1 agonist prevents allograft rejection in a stringent rat heart transplantation model. *Chem Biol* 2006; 13: 1227.
11. O'Shea JJ, Pesu M, Borie DC, et al. A new modality for immunosuppression: targeting the JAK/STAT pathway. *Nat Rev Drug Discov* 2004; 3: 555.
12. Higuchi T, Shiraishi T, Shirakusa T, et al. Prevention of acute lung allograft rejection in rat by the janus kinase 3 inhibitor, tyrphostin AG490. *J Heart Lung Transplant* 2005; 24: 1557.
13. Borie DC, Changelian PS, Larson MJ, et al. Immunosuppression by the JAK3 inhibitor CP-690,550 delays rejection and significantly prolongs kidney allograft survival in nonhuman primates. *Transplantation* 2005; 79: 791.
14. Wang LH, Kirken RA, Erwin RA, et al. JAK3, STAT, and MAPK signaling pathways as novel molecular targets for the tyrphostin AG-490 regulation of IL-2-mediated T cell response. *J Immunol* 1999; 162: 3897.
15. Behbod F, Erwin-Cohen RA, Wang ME, et al. Concomitant inhibition of Janus kinase 3 and calcineurin-dependent signaling pathways synergistically prolongs the survival of rat heart allografts. *J Immunol* 2001; 166: 3724.
16. Stepkowski SM, Nagy ZS, Wang ME, et al. PNU156804 inhibits Jak3 tyrosine kinase and rat heart allograft rejection. *Transplant Proc* 2001; 33: 3272.

17. Velotta JB, Deuse T, Haddad M, et al. A novel JAK3 inhibitor, R348, attenuates chronic airway allograft rejection. *Transplantation* 2009; 87: 653.
18. Deuse T, Velotta JB, Hoyt G, et al. Novel immunosuppression: R348, a JAK3- and Syk-inhibitor attenuates acute cardiac allograft rejection. *Transplantation* 2008; 85: 885.
19. Meyer DM, Jesson MI, Li X, et al. Anti-inflammatory activity and neutrophil reductions mediated by the JAK1/JAK3 inhibitor, CP-690,550, in rat adjuvant-induced arthritis. *J Inflamm (Lond)* 2010; 7: 41.
20. Kahan BD. Frontiers in immunosuppression. *Transplant Proc* 2011; 43: 822.
21. Gaffen SL. Signaling domains of the interleukin 2 receptor. *Cytokine* 2001; 14: 63.
22. Johnston JA, Kawamura M, Kirken RA, et al. Phosphorylation and activation of the Jak-3 Janus kinase in response to interleukin-2. *Nature* 1994; 370: 151.
23. Johnston JA, Bacon CM, Riedy MC, et al. Signaling by IL-2 and related cytokines: JAKs, STATs, and relationship to immunodeficiency. *J Leukoc Biol* 1996; 60: 441.
24. Rodig SJ, Meraz MA, White JM, et al. Disruption of the Jak1 gene demonstrates obligatory and nonredundant roles of the Jaks in cytokine-induced biologic responses. *Cell* 1998; 93: 373.
25. Thomis DC, Gurniak CB, Tivol E, et al. Defects in B lymphocyte maturation and T lymphocyte activation in mice lacking Jak3. *Science* 1995; 270: 794.
26. Notarangelo LD, Giliani S, Mella P, et al. Combined immunodeficiencies due to defects in signal transduction: defects of the gammac-JAK3 signaling pathway as a model. *Immunobiology* 2000; 202: 106.
27. O'Shea JJ, Husa M, Li D, et al. Jak3 and the pathogenesis of severe combined immunodeficiency. *Mol Immunol* 2004; 41: 727.
28. Haan C, Rolvering C, Raulf F, et al. Jak1 has a dominant role over Jak3 in signal transduction through gammac-containing cytokine receptors. *Chem Biol* 2011; 18: 314.
29. Parganas E, Wang D, Stravopodis D, et al. Jak2 is essential for signaling through a variety of cytokine receptors. *Cell* 1998; 93: 385.
30. Neubauer H, Cumano A, Muller M, et al. Jak2 deficiency defines an essential developmental checkpoint in definitive hematopoiesis. *Cell* 1998; 93: 397.
31. Smith BD, Levis M, Beran M, et al. Single-agent CEP-701, a novel FLT3 inhibitor, shows biologic and clinical activity in patients with relapsed or refractory acute myeloid leukemia. *Blood* 2004; 103: 3669.
32. Hexner EO, Serdikoff C, Jan M, et al. Lestaurtinib (CEP701) is a JAK2 inhibitor that suppresses JAK2/STAT5 signaling and the proliferation of primary erythroid cells from patients with myeloproliferative disorders. *Blood* 2008; 111: 5663.
33. Gross ER, Hsu AK, Gross GJ. The JAK/STAT pathway is essential for opioid-induced cardioprotection: JAK2 as a mediator of STAT3, Akt, and GSK-3 beta. *Am J Physiol Heart Circ Physiol* 2006; 291: H827.
34. Baker JE, Su J, Hsu A, et al. Human thrombopoietin reduces myocardial infarct size, apoptosis, and stunning following ischemia/reperfusion in rats. *Cardiovasc Res* 2008; 77: 44.
35. Smith CC, Dixon RA, Wynne AM, et al. Leptin-induced cardioprotection involves JAK/STAT signaling that may be linked to the mitochondrial permeability transition pore. *Am J Physiol Heart Circ Physiol* 2010; 299: H1265.
36. Betts BC, Abdel-Wahab O, Curran SA, et al. Janus kinase-2 inhibition induces durable tolerance to alloantigen by human dendritic cell-stimulated T cells yet preserves immunity to recall antigen. *Blood* 2011; 118: 5330.
37. Muller M, Briscoe J, Laxton C, et al. The protein tyrosine kinase JAK1 complements defects in interferon-alpha/beta and -gamma signal transduction. *Nature* 1993; 366: 129.
38. Busque S, Leventhal J, Brennan DC, et al. Calcineurin-inhibitor-free immunosuppression based on the JAK inhibitor CP-690,550: a pilot study in de novo kidney allograft recipients. *Am J Transplant* 2009; 9: 1936.
39. Vincenti F, Tedesco Silva H, Busque S, et al. A phase 2B study of CNIfree immunosuppression with the JAK inhibitor CP-690,550 in de novo kidney transplant patients: 6-month interim analysis. *Am J Transplant* 2010; 10: 211.
40. Karaman MW, Herrgard S, Treiber DK, et al. A quantitative analysis of kinase inhibitor selectivity. *Nat Biotechnol* 2008; 26: 127.
41. Li C, Kraemer FB, Ahlborn TE, et al. Induction of low density lipoprotein receptor (LDLR) transcription by oncostatin M is mediated by the extracellular signal-regulated kinase signaling pathway and the repeat 3 element of the LDLR promoter. *J Biol Chem* 1999; 274: 6747.
42. Riese RJ, Krishnaswami S, Kremer J. Inhibition of JAK kinases in patients with rheumatoid arthritis: scientific rationale and clinical outcomes. *Best Pract Res Clin Rheumatol* 2010; 24: 513.
43. Paniagua R, Si MS, Flores MG, et al. Effects of JAK3 inhibition with CP-690,550 on immune cell populations and their functions in non-human primate recipients of kidney allografts. *Transplantation* 2005; 80: 1283.
44. Tanimoto A, Murata Y, Wang KY, et al. Monocyte chemoattractant protein-1 expression is enhanced by granulocyte-macrophage colony-stimulating factor via Jak2-Stat5 signaling and inhibited by atorvastatin in human monocytic U937 cells. *J Biol Chem* 2008; 283: 4643.
45. Wei L, Laurence A, O'Shea JJ. New insights into the roles of Stat5a/b and Stat3 in T cell development and differentiation. *Semin Cell Dev Biol* 2008; 19: 394.
46. Pallandre JR, Brillard E, Crehange G, et al. Role of STAT3 in CD4+CD25+FOXP3+ regulatory lymphocyte generation: implications in graft-versus-host disease and antitumor immunity. *J Immunol* 2007; 179: 7593.
47. Heidt S, Segundo DS, Chadha R, et al. The impact of Th17 cells on transplant rejection and the induction of tolerance. *Curr Opin Organ Transplant* 2010; 15: 456.
48. Booth AJ, Bishop DK. TGF-beta, IL-6, IL-17 and CTGF direct multiple pathologies of chronic cardiac allograft rejection. *Immunotherapy* 2010; 2: 511.
49. Wang S, Li J, Xie A, et al. Dynamic changes in Th1, Th17, and FoxP3+ T cells in patients with acute cellular rejection after cardiac transplantation. *Clin Transplant* 2011; 25: E177.
50. Celik S, Doesch AO, Konstantin MH, et al. Increased incidence of acute graft rejection on calcineurin inhibitor-free immunosuppression after heart transplantation. *Transplant Proc* 2011; 43: 1862.
51. Changelian PS, Flanagan ME, Ball DJ, et al. Prevention of organ allograft rejection by a specific Janus kinase 3 inhibitor. *Science* 2003; 302: 875.
52. Ono K, Lindsey ES. Improved technique of heart transplantation in rats. *J Thorac Cardiovasc Surg* 1969; 57: 225.
53. Chou T. The median-effect principle and combination index for quantitation of synergism. In: Chou TC RD, ed. *Synergism and Antagonism in Chemotherapy*. San Diego, CA: Academic Press; 1991: 61.
54. Stewart S, Winters GL, Fishbein MC, et al. Revision of the 1990 working formulation for the standardization of nomenclature in the diagnosis of heart rejection. *J Heart Lung Transplant* 2005; 24: 1710.
55. Schrepfer S, Deuse T, Koch-Nolte F, et al. FK778 in experimental xenotransplantation: a detailed analysis of drug efficacy. *J Heart Lung Transplant* 2007; 26: 70.

Video Article

Heterotopic and Orthotopic Tracheal Transplantation in Mice used as Models to Study the Development of Obliterative Airway Disease

Xiaoqin Hua¹, Tobias Deuse^{1,2}, Karis R. Tang-Quan^{1,2,3}, Robert C. Robbins³, Hermann Reichenspurner^{1,2}, Sonja Schrepfer^{1,2,3}¹Transplant and Stem Cell Immunobiology Lab (TSI), University Heart Center Hamburg²CVRC, University Hospital Hamburg³Department of CT Surgery, Stanford University School of MedicineCorrespondence to: Sonja Schrepfer at schrepfer@stanford.eduURL: <http://www.jove.com/index/Details.stp?ID=1437>

DOI: 10.3791/1437

Citation: Hua X., Deuse T., Tang-Quan K.R., Robbins R.C., Reichenspurner H., Schrepfer S. (2010). Heterotopic and Orthotopic Tracheal Transplantation in Mice used as Models to Study the Development of Obliterative Airway Disease. JoVE. 35. <http://www.jove.com/index/Details.stp?ID=1437>, doi: 10.3791/1437

Abstract

Obliterative airway disease (OAD) is the major complication after lung transplantations that limits long term survival (1-7).

To study the pathophysiology, treatment and prevention of OAD, different animal models of tracheal transplantation in rodents have been developed (1-7). Here, we use two established models of trachea transplantation, the heterotopic and orthotopic model and demonstrate their advantages and limitations.

For the heterotopic model, the donor trachea is wrapped into the greater omentum of the recipient, whereas the donor trachea is anastomosed by end-to-end anastomosis in the orthotopic model.

In both models, the development of obliterative lesions histological similar to clinical OAD has been demonstrated (1-7).

This video shows how to perform both, the heterotopic as well as the orthotopic tracheal transplantation technique in mice, and compares the time course of OAD development in both models using histology.

Protocol

1. Male Balb/C mice (8-12 weeks) are purchased from Charles River Laboratories (Sulzfeld, Germany). The mice are housed under conventional conditions, fed standard mice food and water ad libitum.
2. 2% Isoflurane is used for anesthesia.

DONOR PREPARATION

1. Shave the abdominal hair and disinfect the area using betaisodona.
2. Under microscopic view, perform a midline cervical incision from the level of the larynx to the sternum.
3. Remove the subcutaneous fat and the strap muscles to get a clear view of the trachea.
4. Dissect the trachea from any surrounding tissues, like the esophagus, nerves, arteries, and connective tissue.
5. Remove the whole trachea (from the larynx to the bifurcation).
6. Flush the transplant with cold saline and store the graft at 4°C.
7. The donor is euthanized by cervical dislocation following the harvest of the trachea.

RECIPIENT: HETEROTOPIC TRANSPLANTATION

1. Shave the abdominal hair in a wide margin around the incision site and disinfect the area three times using betaisodona (betadine) followed by alcohol. Eyes should be lubricated with an ophthalmic ointment product to prevent the corneas from drying out.
2. Perform a median laparotomy and place the intestine into a sterile, moistened glove.
3. Spread the greater omentum carefully. Place the graft into the center and fixate it with a single suture using 8-0 (Prolene, Ethicon, Germany).
4. Fully cover the transplant with the greater omentum and fix the graft with one single suture 8-0 (Prolene, Ethicon, Germany).
5. Relocate the intestines back into the abdomen and flush with warm, sterile saline prior to closure.
6. Close up in 2 layers - abdominal wall and skin layer with continuous pattern using 7-0 Prolene for the muscle and 7-0 Vicryl for the skin.

RECIPIENT: ORTHOTOPIC TRANSPLANTATION

1. Shave the abdominal hair in a wide margin around the incision site and disinfect the area three times using betaisodona (betadine) followed by alcohol. Eyes should be lubricated with an ophthalmic ointment product to prevent the corneas from drying out.
2. Divide the strap muscles to visualize the entire laryngotracheal complex.
3. Carefully dissect the trachea from the surrounding tissues, take care to preserve the recurrent laryngeal nerves.
4. Divide the trachea three rings caudal from the cricoid. The animal maintains physiologic respiration via the tracheostomy.
5. Ensure clean tracheal edges in the recipient as well as in the graft.
6. The graft is interposed between the recipient tracheal defects and orientated to maintain anatomic polarity.
7. Using 8-0 (Prolene, Ethicon, Germany) anastomose the donor graft with the distal (mediastinal) trachea. The posterior aspect of the anastomosis is performed in continuous running fashion. The anterior aspect is then completed using interrupted stitches.
8. Remove any secretions from the airway.

9. The proximal anastomosis is then completed in the same way as the distal one.
10. Ensure integrity of the airway and adequate, spontaneous breathing.
11. Relocate the strap muscles and close the subcutaneous tissue and skin layer using 6-0 sutures (Vicryl, Ethicon, Germany) with continuous pattern.
12. Use injection anesthesia for the recipient, therefore the animal will retain physiological respiration through the trachea. A combination of 75/1/0.2 mg/kg of propofol, medetomidine and fentanyl, respectively, is used for i.p. anaesthesia in mice.

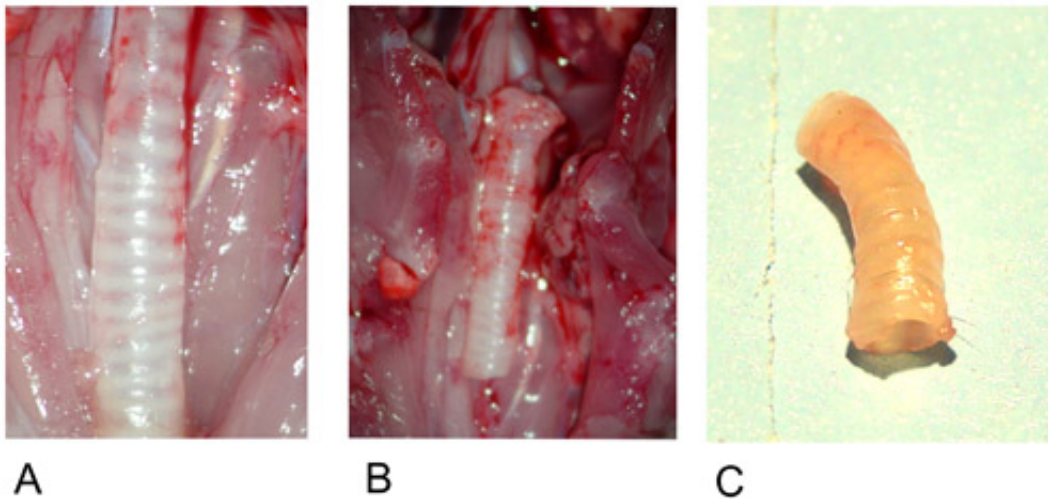


Figure 1: Donor trachea.

- 1A: Donor trachea in situ after preparation.
 1B: Excised donor trachea.
 1C: Donor trachea after explantation.

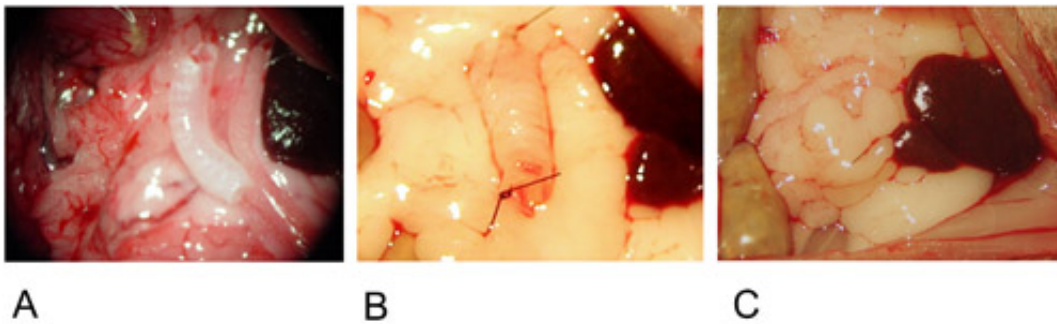


Figure 2: Heterotopic Model.

- 2A: The graft is positioned in the center of the greater omentum.
 2B: The graft is fixed on both ends with a single suture.
 2C: The graft is wrapped into the greater omentum and fixed with a single suture.

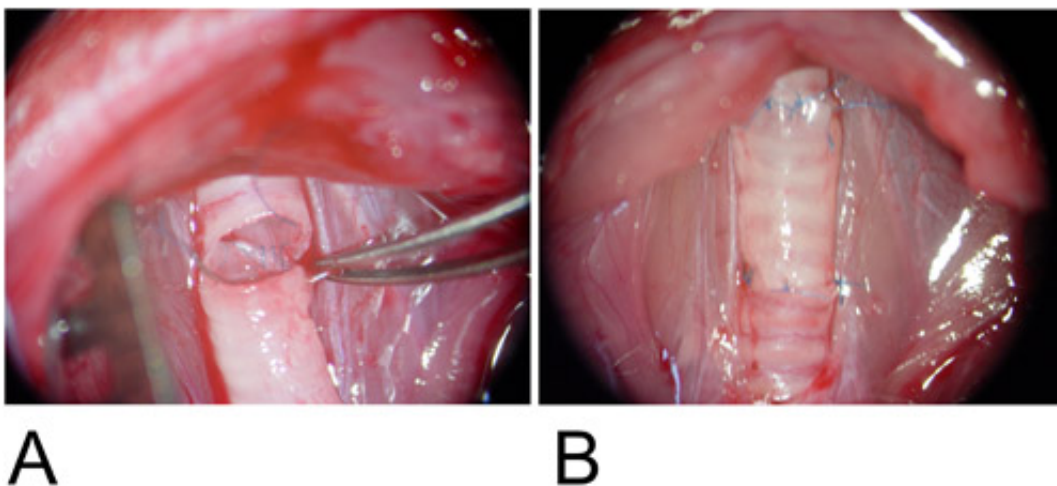


Figure 3: Orthotopic Model.

- 3A: The graft is interposed between the recipient tracheal defects and the posterior wall is anastomosed in continuous running fashion.
 3B: The anterior wall is completed using a single suture.

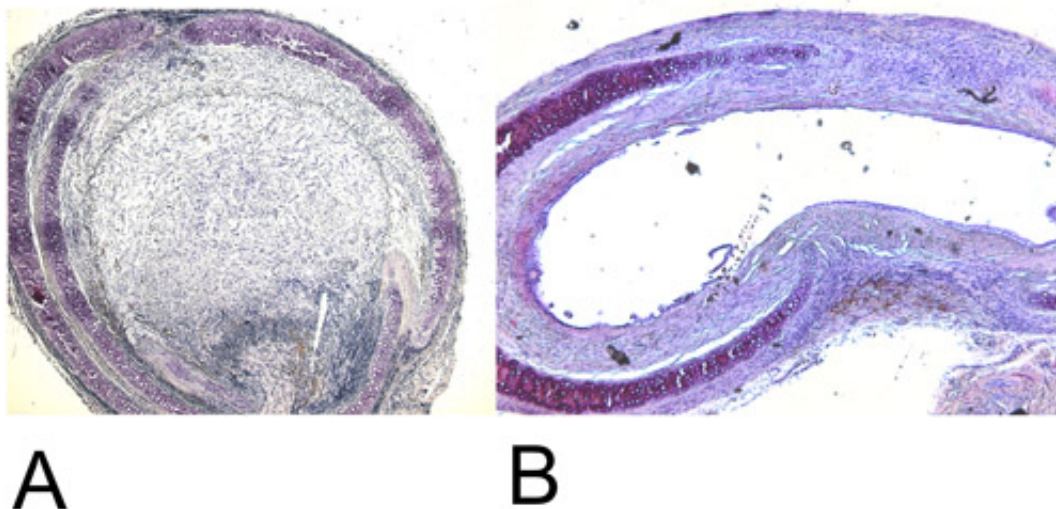


Figure 4: Histology.
 4A: Recovered heterotopic transplanted trachea after 28 days in the H+E staining (15x). Note the 100% luminal obliteration.
 4B: Recovered orthotopic transplanted trachea after 60 days in the H+E staining (15x). Maximal achieved luminal obliteration is approximately 45%.

| | Heterotopic Tracheal Transplantation Model | Orthotopic Tracheal Transplantation Model |
|----------------------|--|--|
| Advantages | <ul style="list-style-type: none"> + Easy to perform + Luminal obliteration with complete airway occlusion after 28 days + No physical affection of animals by OAD | <ul style="list-style-type: none"> + Physical ventilation of the graft + Inhaled drug administration possible + Strong immunological reactions such as alloreactive IgM antibody production + Physiological thoracic milieu + Tracheal-tracheal anastomosis imitates the clinical setting |
| Disadvantages | <ul style="list-style-type: none"> - No ventilation of transplanted trachea - No evaluation of inhaled pathogens possible - Inhibition of mucociliary clearance and retained secretions - Peritoneal microenvironment instead of thoracic milieu | <ul style="list-style-type: none"> - Surgical training necessary - Luminal obliteration with luminal occlusion app. 45% after 60 days - Animals may develop symptoms of OAD |

Table 1: Advantages and Disadvantages of Heterotopic and Orthotopic Tracheal Transplantation.

Discussion

Mice are available in different transgenic and knockout model, and therefore suitable to study mechanistic questions related to OAD (4). Both models of tracheal transplantation shown in this video can be used as reliable models for studying OAD development. However, each model demonstrates advantages and limitations.

The **heterotopic tracheal transplantation** is easy to perform and does not require special surgical training (3, 5). After heterotopic transplantation, luminal obliteration will occur fast and complete airway occlusion appears after 28 days (3, 4, 6). Animals are not physically affected by the OAD development, since their organism does not depend on the heterotopic transplanted trachea.

A disadvantage is the lack of ventilation of the transplanted trachea (7, 6), therefore it is not possible to evaluate the influence of inhaled pathogens (3, 7). Due to the inhibition of mucociliary clearance and retained secretions the results may differ from physiologic reactions seen in clinical OAD (7). The peritoneal microenvironment differs from the thoracic milieu which may also lead to altered results (3).

To perform the **orthotopic tracheal transplantation** surgical training is necessary and luminal obliteration of the transplanted trachea appears after 60 days instead of 28 days in the heterotopic model (3, 7). Also, maximal luminal obliteration achieved is app. 45% instead of 100% in the heterotopic model (3, 7). However, in the orthotopic model, physiologic ventilation is obtained and inhaled drug administration is possible (3). Immunological response, such as alloreactive IgM antibody production has been shown to be much stronger in this model than the heterotopic model (3). The tracheal-tracheal anastomosis and the reactions in this site are more comparable with the anastomosis performed in the clinic (7).

Advantages and limitations of each model are shown in detail in Table 1.

In summary, this video shows that both, the heterotopic as well as the orthotopic tracheal transplantation technique in mice can be used as reproducible and reliable models to study OAD.

However, the model should be chosen carefully depending on the basic question of the study.

Acknowledgements

The authors thank Christiane Pahrman (Lab Manager).

References

1. Adams B., Berry G., Huang X., Shorthouse R., Brazelton T., Morris R.; Immunosuppressive therapies for the prevention and treatment of obliterative airway disease in heterotopic rat trachea allografts; *Transplantation* Vol. 69 (11), (2000), 2260-2266.
2. Adams B., Brazelton T., Berry G., Morris R.; The role of respiratory epithelium in a rat model of obliterative airway disease; *Transplantation* Vol. 69 (4), (2000), 661-665.
3. Deuse T., Schrepfer S., Reichenspurner H., Hoyt G., Fischbein M., Robbins R., Pelletier M.; Techniques for experimental heterotopic and orthotopic tracheal transplantations – when to use which model; *Transplant Immunology* 17 (2007), 255-261.
4. Hele D., Yacoub M., Belvisi M.; The heterotopic tracheal allograft as an animal model of obliterative bronchiolitis; *Respiratory Research* 2 (2001), 169-183.
5. Hertz M., Jessurun J., King M., Savic S., Murray J.; Reproduction of the obliterative bronchiolitis lesion after heterotopic transplantation of mouse airways; *American Journal of Pathology* Vol. 142, No 6 (1993), 1945-191.
6. McDyer J., Human and murine obliterative bronchiolitis in transplant; *Proceedings of the American Thoracic Society* Vol. 4 (2007), 37-43.
7. Schrepfer S., Deuse T., Hoyt G., Sheikh A., Hoffmann J., Reichenspurner H., Robbins R., Pelletier M.; Experimental orthotopic tracheal transplantation: the stanford technique; *Microsurgery* 27 (2007), 187-9.

The potassium channel KCa3.1 as new therapeutic target for the prevention of obliterative airway disease

Xiaoqin Hua¹, Tobias Deuse¹, Yi-Je Chen², Heike Wulff², Mandy Stubbendorff¹, Ralf Köhler³, Hiroto Miura⁴, Florian Länger⁵, Hermann Reichenspurner¹, Robert C. Robbins⁶, Sonja Schrepfer^{1,6}

¹University of Hamburg, University Heart Center Hamburg, Transplant and Stem Cell Immunobiology (TSI) Lab, CVRC (Cardiovascular Research Center Hamburg) and DZHK (Deutsches Zentrum für Herz- und Kreislau fforschung, E.V., University Hamburg).

²University of California, Davis, Department of Pharmacology, California, USA.

³University of Southern Denmark, Cardiovascular and Renal Research, Institute of Molecular Medicine, Odense, DK; Aragon Institute of Health Sciences I+CS, Zaragoza, Spain.

⁴University of Nevada, Department of Physiology and Cell Biology, Reno, Nevada, USA.

⁵Institute of Pathology, Hannover Medical School, Hannover, Germany.

⁶Stanford University, School of Medicine, CT Surgery, Stanford, USA.

Key words: KCa3.1, Obliterative airway disease, TRAM-34, Chronic rejection, Heterotopic tracheal transplantation.

Word count for text: 3099

Word count for abstract: 249

Figure count: 4; table count: 1

Reference count: 58

Address for Correspondence:

Sonja Schrepfer, M.D., Ph.D.

Department of Cardiothoracic Surgery

Stanford University School of Medicine

300 Pasteur Dr., CVRB MC 5407

Stanford, CA 94305, USA

Tel: (650) 736-8592; Fax: (650) 725-3846

E-mail: schrepfer@stanford.edu

Authorship

T.D., H.W., R.C.R. and S.S. participated in research design

X.H., T.D., H.W., R.K., H.R., R.C.R., and S.S. wrote the paper

X.H., Y.C., M.S., F.L., H.M. and S.S. performed the research

X.H., T.D., Y.C., H.W., R.K. and S.S. participated in data analysis

H.W. and R.K. contributed the new reagent (TRAM-34) and the KCa3.1^{-/-} mouse strain

Funding

S.S. received funding from the Deutsche Forschungsgemeinschaft (DFG) (SCHR992/3-1; SCHR992/4-1) and the International Society for Heart and Lung Transplantation (ISHLT).

H.W. was funded by the National Institute of Health (RO1 GM076063).

Conflict of interests

none

Abstract

Background

The calcium-activated potassium channel KCa3.1 is critically involved in T cell activation, as well as in the proliferation of smooth muscle cells and fibroblasts. We sought to investigate whether KCa3.1 contributes to the pathogenesis of obliterative airway disease (OAD) and whether knockout or pharmacological blockade would prevent the development of OAD.

Methods

Tracheas from CBA donors were heterotopically transplanted into the omentum of C57Bl/6J wild-type or KCa3.1^{-/-} mice. C57Bl/6J recipients were either left untreated or received the KCa3.1 blocker TRAM-34 (120mg/kg/d). Histopathology and immunological assays were performed on postoperative days (POD) 5 or 28.

Results

Subepithelial T cell and macrophage infiltration on POD 5, as seen in untreated allografts, was significantly reduced in the KCa3.1^{-/-} and TRAM-34 groups. Also, systemic Th1 activation was significantly, and Th2 mildly reduced by KCa3.1 knockout or blockade. After 28 days, luminal obliteration of tracheal allografts was reduced from 89±21% in untreated recipients to 53±26% (p=0.010) and 59±33% (p=0.032) in KCa3.1^{-/-} and TRAM-34-treated animals, respectively. The airway epithelium was mostly preserved in syngeneic grafts, mostly destroyed in the KCa3.1^{-/-} and TRAM-34 groups, and absent in untreated allografts. Allografts triggered an antibody response in untreated recipients, which was significantly reduced in KCa3.1^{-/-} animals. KCa3.1 was detected in T cells, airway epithelial cells and myofibroblasts. TRAM-34 dose-dependently suppressed proliferation of wild-type C57B/6J splenocytes, but did not show any effect on KCa3.1^{-/-} splenocytes.

Conclusions

Our findings suggest that KCa3.1 channels are involved in the pathogenesis of OAD and that KCa3.1 blockade holds promise to reduce OAD development.

Introduction

Obliterative airway disease (OAD) remains the most common chronic complication and major obstacle to the long-term graft survival in lung transplant recipients (1, 2). Alloimmunogenic T cell activation drives the development of fibroproliferative lesions, but the detailed pathogenesis of OAD remains incompletely understood (3-7). No specific or effective treatments have been developed yet.

Recent studies have shown that the intermediate-conductance Ca^{2+} -activated potassium channel KCa3.1 plays an important role in Ca^{2+} -signaling and T cell activation (8, 9). The KCa3.1 channel is composed of four α -subunits each containing 6 trans-membrane segments with calmodulin complexed to its C-terminus as calcium sensor (10). Opening of this channel due to elevated intracellular Ca^{2+} leads to K^{+} efflux, membrane hyperpolarization, and increases the driving force for store-operated Ca^{2+} -entry through calcium-release activated calcium (CRAC) channels (11). The resulting increase in cytosolic Ca^{2+} turns on the calcineurin pathway and induces T cell activation.. Interestingly, the expression of KCa3.1 increases from 5-35 channels per cell in resting T cells to 500 channels per cell in activated naïve and memory T cells (12), suggesting that activated T cells might be more sensitive to selective KCa3.1 blockade.

Pharmacological KCa3.1 blockade depolarizes T cells, reduces Ca^{2+} -influx, and inhibits T cell proliferation and cytokine production *in vitro* (13-15), while *in vivo* studies have demonstrated that KCa3.1 blockers can prevent experimental autoimmune encephalomyelitis and anti-collagen antibody-induced arthritis in mice and contribute to the prevention of kidney graft rejection in rats (16, 17). Based on the additional involvement of KCa3.1 in smooth muscle cell and fibroblast proliferation and the efficacy of the KCa3.1 blocker TRAM-34 in models of restenosis (18, 19), atherosclerosis (20), and kidney fibrosis (21), KCa3.1 has also been proposed as a possible therapeutic target for cardiovascular diseases. However, whether the KCa3.1 channel could be considered as a novel therapeutic target for the prevention of OAD has not been investigated before.

Results

Tracheas from CBA donors were heterotopically transplanted into the greater omentum of C57Bl/6J mice. Recipients in the treatment group received TRAM-34 (120mg/kg/d, i.p.) for 5 days or 28 days. KCa3.1^{-/-} mice receiving grafts from CBA donors and C57Bl/6J receiving syngeneic grafts were used as control (see table 1).

5-day study

Inflammatory Cell Infiltration

In untreated heterotopic tracheal allografts harvested on POD5, massive F4/80⁺ macrophage and CD3⁺ T lymphocyte infiltration occurred in the subepithelial area (Fig. 1A). The degree of infiltration was two- to three-fold higher than in the KCa3.1^{-/-} and TRAM-34 groups ($p < 0.001$ for both CD3⁺ and F4/80⁺ cells, Fig. 1B). Only a few infiltrating cells were found in syngeneic grafts and the differences to the KCa3.1^{-/-} and TRAM-34 groups did not reach statistical significance.

Elispot

Elispot assays on POD 5 revealed that knockout (KCa3.1^{-/-}) or pharmacological blockade (TRAM-34) of the KCa3.1 channel resulted in decreased cellular immune activation. Spot frequencies for IFN- γ in the no medication group were significantly higher than those in the KCa3.1^{-/-} ($p = 0.007$) and TRAM-34 groups ($p = 0.015$; Fig. 1C). Spots were lowest in the syngeneic group ($p = 0.004$ vs. KCa3.1^{-/-}, $p = 0.002$ vs. TRAM-34, $p < 0.001$ vs. no medication). The IL-4 spot frequencies, representing the Th2 response, were significantly lower in the TRAM-34 than the no medication group ($p = 0.005$; Fig. 1D).

28-day study

Luminal obliteration

In the 28-day study, we observed myoproliferative tissue of high cellularity in the allogeneic no medication group causing luminal obliteration of $88.7 \pm 20.9\%$ (Fig. 2A). Tracheal grafts in the TRAM-34 and KCa3.1^{-/-} groups showed significantly reduced luminal obliteration ($p = 0.032$, $p = 0.010$; Fig. 2B). However, KCa3.1 blockade or knockout did not completely

prevent obliteration ($p=0.014$ and $p=0.007$, respectively vs. the syngeneic group). Only syngeneic grafts presented without fibrotic tissue growth in the epithelial or subepithelial areas.

Donor-Specific Antibody (DSA) Assay

DSAs were evaluated on POD 28. The mean value of donor-reactive IgG in the no medication group was significantly higher than that of the syngeneic group ($p=0.001$). DSAs of the KCa3.1^{-/-} group ($p=0.018$) and the TRAM-34 group ($p=ns$) were lower than those of the no medication group (Fig. 2C).

Epithelial coverage

Tracheal allografts of the no medication group showed a complete loss of epithelial coverage. In contrast, the epithelium in the syngeneic group was well preserved for most of the luminal circumference, with 91.8% respiratory morphology ($p<0.001$ vs. no medication). Syngeneic transplants using transgenic donors expressing firefly luciferase showed that the epithelium was donor-derived and not recipient-type 'neo-epithelium' (SDC, Fig. 1). In the KCa3.1^{-/-} and TRAM-34 groups, scattered areas of flattened cuboidal epithelia (7.8% and 10.1%, respectively) remained ($p=0.453$ and $p=0.356$, vs. no medication, respectively), but we did not observe any epithelium of respiratory type ($p<0.001$ for both vs. no medication; Fig. 3).

mRNA-Expression of KCa3.1 in Tracheal Grafts

Semi-quantitative RT-PCR on POD 28 revealed similar amounts of KCa3.1 mRNA in whole grafts from the allogeneic no medication group and the syngeneic group (Fig. 4A), while KCa3.1 mRNA was hardly detectable in allografts of KCa3.1^{-/-} recipients ($p<0.001$ vs. no medication; $p=0.005$ vs. syngeneic). KCa3.1 mRNA amounts were significantly lower in the TRAM-34 group than in the no medication group ($p=0.008$), which most likely reflected lower numbers of infiltrating KCa3.1-expressing mononuclear cells, as well as reduced luminal obliteration by KCa3.1-expressing fibroblasts.

KCa3.1 Protein Expression in Tracheal Grafts

In the no medication group, intense KCa3.1 staining was found in the subepithelial area, which was confined mostly to immune cell infiltrates. Within the luminal granulation tissue, we observed very intense staining of fibroblast-like cells as well as T lymphocytes and macrophages. In the syngeneic group, KCa3.1-staining was most intense within the intact respiratory epithelium, which is in line with the reported physiological expression of the channel in this tissue (Fig. 4B). Significantly less KCa3.1 staining was observed in the KCa3.1^{-/-} and TRAM-34 groups, which showed mostly destroyed epithelium, little myoproliferation, and only a few infiltrating cells.

Side Effects

Mice of all groups recovered well from surgery and there were no significant differences in body weight over the study period (data not shown). The mice did not show any obvious signs of discomfort, or side effects arising from TRAM-34 treatment or KCa3.1 knockout. Complete blood counts and blood biochemistry (AST, ALT, creatinine, and BUN) were in the normal range in all groups (data not shown). To screen for epithelial toxicity of TRAM-34, native C57B/6J mice and C57B/6J recipients of syngeneic tracheal grafts were treated for 28 days with TRAM-34 (SDC, Fig. 2). We did not observe any epithelial damage in the native lung or GI tract, nor in syngeneic tracheal grafts demonstrating that TRAM-34 does not exhibit any epithelial toxicity despite KCa3.1 being expressed in epithelia

Proliferation Assay *in vitro*

In vitro proliferation of ConA-stimulated splenocytes from C57B/6J wild-type (WT) or KCa3.1^{-/-} mice under increasing concentrations of TRAM-34 is shown in Fig. 4C. In WT splenocytes, TRAM-34 dose-dependently suppressed proliferation (p=0.007 for 100nM, p=0.006 for 250nM, p=0.0007 for 1µM, and p=0.0006 for 5µM). However, the same TRAM-34 concentrations did not affect the proliferation of ConA-stimulated KCa3.1^{-/-} splenocytes, confirming that the TRAM-34 effect was mediated through inhibition of KCa3.1 and not through an unspecific off-target effect.

KCa3.1 in human OAD

To assess the relevance of the KCa3.1 channel in human disease, tissue specimens retrieved

from lung transplant patients with OAD were studied (SDC, Fig. 3). KCa3.1 staining was abundant in human lung tissue, most prominent in the epithelium and myoproliferative areas.

Discussion

Based on previous studies showing that KCa3.1 is involved in the activation and proliferation of inflammatory cells (14, 22) the channel has been proposed as a novel target for immunomodulation (8). In this study, we demonstrate that KCa3.1 is also involved in the pathogenesis of OAD, and that KCa3.1 blockade or knockout slows disease progression.

KCa3.1 protein expression was observed in different cell populations of tracheal grafts, mainly infiltrating mononuclear cells, proliferating myofibroblasts, and respiratory epithelium. Semi-quantitative RT-PCR showed only negligible amounts of KCa3.1-mRNA in the KCa3.1^{-/-} recipients. In keeping with the previously reported increased expression of KCa3.1 in activated T cells (23), we observed high amounts of KCa3.1-mRNA and intensive KCa3.1 protein staining on inflammatory cells in the no medication group demonstrating marked KCa3.1 channel up-regulation in this allogeneic transplant setting. Compared to the no medication group, KCa3.1-mRNA expression was significantly lower in the TRAM-34 group, most likely due to lower numbers of KCa3.1-expressing inflammatory cells (14), destruction of the epithelium, and reduced myoproliferation.

OAD development has been shown to be mediated by alloimmune-activated T cells (24-26). Macrophages play a role in further recruiting inflammatory cells (27, 28) and producing pro-proliferative cytokines and growth factors (29, 30). We observed dense CD3⁺ T cell and F4/80⁺ macrophage infiltration in the subepithelial areas of untreated allografts, which were significantly reduced in both the KCa3.1^{-/-} and TRAM-34 groups. Also, IFN- γ Elispot frequencies, reflecting the degree of cellular immune activation, were significantly reduced in both groups. IFN- γ increases the expressions of MHC-I and -II, adhesion molecules, and co-stimulatory ligands on APCs after lung transplantation (31, 32), and is considered a central cytokine in cellular rejection. Pharmacologic blockade or knockout of KCa3.1 alone was sufficient to mitigate allo-immune Th1 activation. However, it was reported that the functions of Th17 and regulatory T cells in KCa3.1^{-/-} mice seemed unchanged (33). Furthermore, while Ca²⁺ influx and IL-2 production following TCR ligation was reduced in KCa3.1^{-/-} T cells, the absolute numbers of peripheral T cells and the CD4/CD8 ratio, as well as the macroscopic appearance of all lymphoid organs was normal. KCa3.1-deficiency may either be compensated for by the up-regulation of other channels or KCa3.1 may not be crucial for

maintaining T cell numbers. The specificity of TRAM-34 for KCa3.1 was confirmed *in vitro*. Proliferation assays showed that TRAM-34 dose-dependently reduced cell proliferation in WT, but not KCa3.1^{-/-} splenocytes.

The DSA assays revealed reduced donor-specific IgG production in the KCa3.1^{-/-} group compared to untreated animals. Cumulating evidence suggests that allogeneic antibody responses play an important role in acute lung graft rejection as well as in the development of OAD. Lung transplant recipients with pre-existing anti-HLA antibodies show a significantly higher risk for early graft dysfunction and have a poor prognosis (26, 34). The reduced antibody response of the KCa3.1^{-/-} group may result from impaired T cell-mediated B cell activation.

The donor airway epithelium is considered to be the primary target for the allogeneic immune response (35), and epithelial injury plays a pivotal role in triggering rejection and OAD formation (36, 37). Preserved epithelial coverage of the airway lumen was found to slow the progression of OAD (7, 38). In our study, no airway epithelium was found in untreated animals after 28 days. In KCa3.1^{-/-} and TRAM-34-treated animals, there were some scattered, flattened cuboidal epithelial cells visible, which occupied less than 10% of the whole circumference, while the syngeneic group exhibited well preserved ciliated epithelium. It therefore seems that neither KCa3.1 channel knockout nor blockade protect the epithelium from being destroyed or facilitate epithelial recovery. Because this is a non-ventilated model, the airway epithelium is more prone to injury and destruction and our results may exaggerate the epithelial damage with KCa3.1 blockade. In the clinical setting and ventilated trachea transplant models, the airway epithelium is preserved despite OAD development (39).

TRAM-34 treatment induced no significant side-effects in keeping with previous studies (18-20, 40). We also did not observe any differences between the KCa3.1^{-/-} mice and the WT animals before or after transplantation and the KCa3.1^{-/-} mouse strain is viable and fertile (41). Senicapoc, another potent and selective KCa3.1 blocker, already passed through clinical phase I to III trials for sickle cell disease and proved efficacy in its biological endpoint of reducing hemolysis (42, 43). Although, senicapoc did not prevent clinically-relevant vaso-occlusive pain crises, these studies showed that KCa3.1 blockade was safe and well-tolerated in humans (44).

Human OAD is a form of chronic lung allograft dysfunction from allo- and innate immune injury, autoimmunity, environmental pathogens, and contributing conditions like acid reflux disease. Its aggressiveness and clinical course are likely related to the extent of immunologic and non-immunologic insults (45). It is pathohistologically characterized by collagen-rich myoproliferative tissue that progressively obliterates the small airway lumen in the terminal and respiratory bronchioles (46, 47). Current treatment strategies involve switching to other calcineurin (48) or mTOR inhibitors (49), the addition of azithromycin (50) or statins (51), and extracorporeal photopheresis (52). Some patients with more active immune responses seem to be better amenable to the treatment of OAD, while the disease progresses steadily despite aggressive therapy in others. Although the heterotopic murine tracheal transplant model may not well represent human OAD in its whole complexity, it nicely mimics immune activation, graft infiltration, epithelial damage, and mice also mount a DSA response. The lack of environmental and viral challenges as well as the lack of airway clearance from secretions, however, somewhat restrict the transferability of results to the lung transplant setting.

To link our results to the human disease, we demonstrated similar KCa3.1 channel expression in mouse and human lung tissue. In accordance with the murine distribution, human KCa3.1 expression was most prominent in epithelial and myofibrotic cells. KCa3.1 blockade might therefore also benefit patients with OAD in the clinic. Because KCa3.1 channel blockers are mild immunosuppressants that double up as anti-proliferative agents, they are unlikely to replace current immunosuppressive agents, but may be useful additions for long-term maintenance therapy.

In conclusion, the present study demonstrates that KCa3.1 blockade or knockout significantly decreases T cell activation and reduces the development of OAD suggesting KCa3.1 blockade as an additional maintenance strategy for patients after lung transplantation.

Materials and Methods

Animals

Male CBA mice were used as allogeneic and C57Bl/6J mice as syngeneic trachea donors, and male C57Bl/6J mice, or KCa3.1^{-/-} mice on C57Bl/6J background, were used as recipients. Mice weighing 25 to 35 g were purchased from Charles River Laboratories (Sulzfeld, Germany) and KCa3.1^{-/-} mice derived from our own breeding colonies were genotyped as described previously (53). All animals received humane care in compliance with the guide for the principles of laboratory animals, prepared by the Institute of Laboratory Animal Resources, and published by the National Institutes of Health. The animals were maintained in the animal care facilities of the University Hospital Hamburg-Eppendorf.

Heterotopic Tracheal Transplantations, Graft Recovery, and Tissue Processing

The heterotopic tracheal transplant model in mice was chosen because of its reliability in presenting the characteristics of OAD pathogenesis and its high reproducibility (54, 55). Transplantations were performed as previously described (55). For analysis, tracheal grafts were recovered from the greater omentum and cut into two segments. One segment was fixed in 4% paraformaldehyde solution, dehydrated, and embedded in paraffin. The second segment was snap-frozen in liquid nitrogen and stored at -80°C.

Experimental Groups

Eight groups were involved in this study (see table 1). All animals were randomly assigned to one of the groups prior to tracheal transplantation and there were no animal deaths due to technical failures. Mice in groups 4 and 8 were treated with 120mg/kg TRAM-34 intra peritoneally (18, 56) once daily. TRAM-34 was freshly dissolved in Miglyol 812 (Pharmacy of University Hospital Hamburg-Eppendorf) prior to use. Grafts were recovered 5 days after transplantation to investigate cellular rejection and immune activation (groups 1-4) or 28 days after transplantation for the study of OAD (groups 5-8).

Side Effect Screening

Blood was drawn during graft recovery for complete blood count, liver, and kidney toxicity. All recipients were examined daily for signs of discomfort or diarrhea.

Histology

General Histology

Sections of 5µm were cut and stained with hematoxylin and eosin (H&E) or Masson-Goldner trichrome. Histologic analyses were done using image-processing software (Leica, Bensheim, Germany). Luminal obliteration was quantified as previously described (57). Since the tissue inside the tracheal cartilage contains submucosal and epithelial tissue, the value for luminal obliteration in native tracheas is approximately 10% (58). The airway epithelium was classified as intact respiratory epithelium or flattened cuboidal epithelium. By computerized morphometry, the length of the respective epithelium along the whole luminal circumference was measured and calculated in percent. Mononuclear infiltrating cells were identified using monoclonal antibodies against CD3 (DakoCytomation, Glostrup, Denmark) and the macrophage marker F4/80 (Clone BM8, BMA Biomedicals, Augst, Switzerland). Antigens were retrieved in epitope-retrieval solution (Dako, pH 9) by the heating method in a steamer, or by trypsin digestion (Dako), respectively. After overnight incubation with the primary antibody at 4°C, the biotinylated rabbit-anti-rat secondary antibody (Dako) was used if necessary. These antibodies were further bound with alkaline phosphatase conjugated enzyme polymer (AP Polymer Kit, Zytomed Systems, Berlin, Germany) and finally visualized by New Fuchsin Substrate System (Dako). Sections were counterstained with hematoxylin. Three high power fields were analyzed per animal to quantify cell infiltration (expressed as cells/mm²).

KCa3.1 channel expression

After antigen retrieval in sodium citrate (10mM, pH 6), KCa3.1 channel proteins were identified by an anti-KCNN4 antibody (Sigma-Aldrich, St. Louis, MO). A biotinylated secondary antibody was further labeled by horseradish peroxidase-conjugated avidin complex (Vector Laboratories, CA) and finally visualized by DAB (Vector Laboratories) as previously

described (40).

Elispot Assays

The cellular immune response was investigated on POD5. Recipient spleens were harvested and splenocytes were isolated and freshly used. Elispot assays using 1×10^5 mitomycin-inhibited donor splenocytes as stimulator cells and 1×10^6 recipient splenocytes as responder cells were performed according to the manufacturer's protocol (BD Biosciences, CA) using IFN- γ and IL-4-coated plates. Duplicates or quadruplicates were done for each animal. Spots were counted automatically by an ELISPOT plate reader (CTL, St. Louis, OH) for scanning and analyzing.

DSA Assay

On POD28, sera from recipient mice were decomplexed by heating to 56°C for 30 min. Equal amounts of sera and donor splenocyte suspensions (5×10^6 /ml) were incubated for 30 min at 37°C. Bound allogeneic IgG antibodies were labelled with the FITC-conjugated goat anti-mouse IgG F(ab')₂ fragment (Sigma-Aldrich) and analyzed by flow cytometry (BD Bioscience).

KCa3.1 mRNA-Expression

mRNA was extracted and purified from tracheal transplants using the RNeasy Mini Kit (Qiagen). Semi-quantitative RT-PCR was conducted using iQ™ CYBR® Green Supermix (Bio-Rad) and a Stratagene MX3000p cycler. Primer sequences were as follows: mKCa3.1: F, GTGGCCAAGCTGTACATGA; R, GCCACAGTGTGTCTGTGAGG; mGAPDH: F, CAATGAATACGGCTACAGCAAC; R, AGGGAGATGCTCAGTGTTGG. Expression levels were normalized to the house keeping gene, glyceraldehyde-3-phosphate dehydrogenase (GAPDH) as reference gene by calculating the ΔC_t values ($\Delta C_t = C_t(\text{target}) - C_t(\text{GAPDH})$) and the ratios to GAPDH (ratio = $2^{-\Delta C_t}$). Results were expressed as percentage of GAPDH (% GAPDH).

Proliferation Assay *in vitro*

Proliferation assays were performed by stimulating 1×10^5 splenocytes from either C57Bl/6J WT or KCa3.1^{-/-} mice with 5 μ g/ml ConA (Sigma-Aldrich). Cells were incubated with different concentrations of TRAM-34 in flat-bottom 96 well plates for 48 hours. [³H]-TdR incorporation was measured, normalized to ConA-activated controls, and the background was subtracted.

Statistical analysis

Data are presented as mean \pm standard deviation. Comparisons between groups were performed by analysis of variance (ANOVA) between groups with Fisher's Least Significant Difference (LSD) post hoc tests. Probability values (p) smaller than 0.05 were considered significant. Statistical analysis was performed using the SPSS statistical software package 17.0 for Windows (SPSS Inc., Chicago, IL).

Acknowledgements

The authors thank Christiane Pahrman for her technical support and Ethicon (Norderstedt, Germany) for providing the sutures. Special thanks to the UKE Microscopy Imaging Facility (umif) at the University Hospital Hamburg-Eppendorf (Bernd Zobiak) for their help and equipment support.

References

1. Christie JD, Edwards LB, Kucheryavaya AY, et al. The Registry of the International Society for Heart and Lung Transplantation: Twenty-seventh official adult lung and heart-lung transplant report--2010. *The Journal of Heart and Lung Transplantation*; 29 (10): 1104.
2. Sundaresan S, Trulock EP, Mohanakumar T, Cooper JD, Patterson GA. Prevalence and outcome of bronchiolitis obliterans syndrome after lung transplantation. *The Annals of Thoracic Surgery* 1995; 60 (5): 1341.
3. Paradis I, Yousem S, Griffith B. Airway obstruction and bronchiolitis obliterans after lung transplantation. *Clin Chest Med* 1993; 14 (4): 751.
4. Burke C, Baldwin J, Morris A, et al. Twenty-eight cases of human heart-lung transplantation. *The Lancet* 1986; 327 (8480): 517.
5. Griffith BP, Paradis IL, Zeevi A, et al. Immunologically mediated disease of the airways after pulmonary transplantation. *Ann Surg* 1988; 208 (3): 371.
6. Boehler A KS, Weder W, Speich R. Bronchiolitis obliterans after lung transplantation: a review. *Chest* 1998; 114 (5): 1411.
7. Adams BF, Brazelton T, Berry GJ, Morris RE. The role of respiratory epithelium in a rat model of obliterative airway disease. *Transplantation* 2000; 69 (4): 661.
8. George Chandy K, Wulff H, Beeton C, Pennington M, Gutman GA, Cahalan MD. K⁺ channels as targets for specific immunomodulation. *Trends in Pharmacological Sciences* 2004; 25 (5): 280.
9. Gutman GA, Chandy KG, Adelman JP, et al. International Union of Pharmacology. XLI. Compendium of voltage-gated ion channels: potassium channels. *Pharmacol Rev* 2003; 55 (4): 583.
10. Wulff H, Gutman GA, Cahalan MD, Chandy KG. Delineation of the clotrimazole/TRAM-34 binding site on the intermediate conductance calcium-activated potassium channel, IKCa1. *J Biol Chem* 2001; 276 (34): 32040.
11. Cahalan MD, Chandy KG. The functional network of ion channels in T lymphocytes. *Immunol Rev* 2009; 231 (1): 59.
12. Rus H, Pardo CA, Hu L, et al. The voltage-gated potassium channel Kv1.3 is highly expressed on inflammatory infiltrates in multiple sclerosis brain. *Proc Natl Acad Sci U S A* 2005; 102 (31): 11094.
13. Fanger CM, Rauer H, Neben AL, et al. Calcium-activated potassium channels sustain calcium signaling in T lymphocytes. Selective blockers and manipulated channel expression levels. *J Biol Chem* 2001; 276 (15): 12249.
14. Ghanshani S, Wulff H, Miller MJ, et al. Up-regulation of the IKCa1 potassium channel during T-cell activation. Molecular mechanism and functional consequences. *J Biol Chem* 2000; 275 (47): 37137.
15. Khanna R, Chang MC, Joiner WJ, Kaczmarek LK, Schlichter LC. hSK4/hIK1, a Calmodulin-binding K⁺ Channel in Human T Lymphocytes. *Journal of Biological Chemistry* 1999; 274 (21): 14838.
16. Jensen BS, Hertz M, Christophersen P, Madsen LS. The Ca²⁺-activated K⁺ channel

- of intermediate conductance: a possible target for immune suppression. *Expert Opin Ther Targets* 2002; 6 (6): 623.
17. Chou CC, Lunn CA, Murgolo NJ. KCa3.1: target and marker for cancer, autoimmune disorder and vascular inflammation? *Expert Rev Mol Diagn* 2008; 8 (2): 179.
 18. Kohler R, Wulff H, Eichler I, et al. Blockade of the intermediate-conductance calcium-activated potassium channel as a new therapeutic strategy for restenosis. *Circulation* 2003; 108 (9): 1119.
 19. Tharp DL, Wamhoff BR, Wulff H, Raman G, Cheong A, Bowles DK. Local delivery of the KCa3.1 blocker, TRAM-34, prevents acute angioplasty-induced coronary smooth muscle phenotypic modulation and limits stenosis. *Arterioscler Thromb Vasc Biol* 2008; 28 (6): 1084.
 20. Toyama K, Wulff H, Chandy KG, et al. The intermediate-conductance calcium-activated potassium channel KCa3.1 contributes to atherogenesis in mice and humans. *J Clin Invest* 2008; 118 (9): 3025.
 21. Grgic I, Kiss E, Kaistha BP, et al. Renal fibrosis is attenuated by targeted disruption of K(Ca)3.1 potassium channels. *Proceedings of the National Academy of Sciences of the United States of America* 2009; 106 (34): 14518.
 22. Wulff H, Knaus HG, Pennington M, Chandy KG. K⁺ channel expression during B cell differentiation: implications for immunomodulation and autoimmunity. *J Immunol* 2004; 173 (2): 776.
 23. Wulff H, Calabresi PA, Allie R, et al. The voltage-gated Kv1.3 K⁺ channel in effector memory T cells as new target for MS. *The Journal of Clinical Investigation* 2003; 111 (11): 1703.
 24. Reznik SI, Jaramillo A, SivaSai KSR, et al. Indirect Allorecognition of Mismatched Donor HLA Class II Peptides in Lung Transplant Recipients with Bronchiolitis Obliterans Syndrome. *American Journal of Transplantation* 2001; 1 (3): 228.
 25. Lu KC, Jaramillo As, Mendeloff EN, et al. Concomitant allorecognition of mismatched donor HLA class I, Ì and class II, Ì derived peptides in pediatric lung transplant recipients with bronchiolitis obliterans syndrome. *The Journal of Heart and Lung Transplantation* 2003; 22 (1): 35.
 26. Sundaresan S, Mohanakumar T, Smith MA, et al. HLA-A locus mismatches and development of antibodies to HLA after lung transplantation correlate with the development of bronchiolitis obliterans syndrome. *Transplantation* 1998; 65 (5): 648.
 27. Sekine Y, Yasufuku K, Heidler KM, et al. Monocyte chemoattractant protein-1 and RANTES are chemotactic for graft infiltrating lymphocytes during acute lung allograft rejection. *American Journal of Respiratory Cell and Molecular Biology* 2000; 23 (6): 719.
 28. Schmid-Antomarchi H, Schmid-Alliana A, Romey G, et al. Extracellular ATP and UTP control the generation of reactive oxygen intermediates in human macrophages through the opening of a charybdotoxin-sensitive Ca²⁺-dependent K⁺ channel. *Journal of Immunology* 1997; 159 (12): 6209.
 29. Hertz MI, Henke CA, Nakhleh RE, et al. Obliterative bronchiolitis after lung transplantation - A fibroproliferative disorder associated with platelet-derived growth factor. *Proceedings of the National Academy of Sciences of the United States of*

- America* 1992; 89 (21): 10385.
30. Oyaizu T, Okada Y, Shoji W, et al. Reduction of recipient macrophages by gadolinium chloride prevents development of obliterative airway disease in a rat model of heterotopic tracheal transplantation. *Transplantation* 2003; 76 (8): 1214.
 31. Smith CR, Jaramillo As, Duffy BF, Mohanakumar T. Airway epithelial cell damage mediated by antigen-specific T cells: implications in lung allograft rejection. *Human Immunology* 2000; 61 (10): 985.
 32. Nakajima J, Ono M, Takeda M, Kawauchi M, Furuse A, Takizawa H. Role of costimulatory molecules on airway epithelial cells acting as alloantigen-presenting cells. *Transplantation Proceedings* 1997; 29 (4): 2297.
 33. Di L, Srivastava S, Zhdanova O, et al. Inhibition of the K(+) channel KCa3.1 ameliorates T cell-mediated colitis. *Proceedings of the National Academy of Sciences of the United States of America* 2010; 107 (4): 1541.
 34. Lau CL, Palmer SM, Posther KE, et al. Influence of panel-reactive antibodies on posttransplant outcomes in lung transplant recipients. *The Annals of Thoracic Surgery* 2000; 69 (5): 1520.
 35. Mauck KA, Hosenpud JD. The bronchial epithelium: A potential allogeneic target for chronic rejection after lung transplantation. *Journal of Heart and Lung Transplantation* 1996; 15 (7): 709.
 36. Kuo E, Bharat A, Shih J, et al. Role of Airway Epithelial Injury in Murine Orthotopic Tracheal Allograft Rejection. *The Annals of Thoracic Surgery* 2006; 82 (4): 1226.
 37. Qu N, de Vos P, Schelfhorst M, de Haan A, Timens W, Prop J. Integrity of Airway Epithelium Is Essential Against Obliterative Airway Disease in Transplanted Rat Tracheas. *The Journal of Heart and Lung Transplantation* 2005; 24 (7): 882.
 38. Ikonen TS, Brazelton TR, Berry GJ, Shorthouse RS, Morris RE. Epithelial re-growth is associated with inhibition of obliterative airway disease in orthotopic tracheal allografts in non-immunosuppressed rats. *Transplantation* 2000; 70 (6): 857.
 39. Deuse T, Schrepfer S, Reichenspurner H, et al. Techniques for experimental heterotopic and orthotopic tracheal transplantations - When to use which model? *Transpl Immunol* 2007; 17 (4): 255.
 40. Chen YJ, Raman G, Bodendiek S, O'Donnell ME, Wulff H. The KCa3.1 blocker TRAM-34 reduces infarction and neurological deficit in a rat model of ischemia/reperfusion stroke. *Journal of Cerebral Blood Flow and Metabolism* 2011; 31 (12): 2363.
 41. Hu L, Mullen K, Allie R, Calabresi P. Blockade of Kv1.3 potassium channels inhibits granzyme B production in human CD8+T lymphocytes. *Clinical Immunology* 2006; 119: S45.
 42. Ataga KI, Orringer EP, Styles L, et al. Dose-escalation study of ICA-17043 in patients with sickle cell disease. *Pharmacotherapy* 2006; 26 (11): 1557.
 43. Ataga KI, Smith WR, De Castro LM, et al. Efficacy and safety of the Gardos channel blocker, senicapoc (ICA-17043), in patients with sickle cell anemia. *Blood* 2008; 111 (8): 3991.
 44. Wulff H, Castle NA. Therapeutic potential of KCa3.1 blockers: recent advances and promising trends. *Expert Rev Clin Pharmacol* 2010; 3 (3): 385.

45. Todd JL, Palmer SM. Bronchiolitis obliterans syndrome: the final frontier for lung transplantation. *Chest* 2011; 140 (2): 502.
46. Jaramillo A, Fernández FG, Kuo EY, Trulock EP, Patterson GA, Mohanakumar T. Immune mechanisms in the pathogenesis of bronchiolitis obliterans syndrome after lung transplantation. *Pediatric Transplantation* 2005; 9 (1): 84.
47. Burke CM, Theodore J, Dawkins KD, et al. Post-transplant obliterative bronchiolitis and other late sequelae in human heart-lung transplantation. *Chest* 1984; 86 (6): 824.
48. Cairn J, Yek T, Banner NR, Khaghani A, Hodson ME, Yacoub M. Time-related changes in pulmonary function after conversion to tacrolimus in bronchiolitis obliterans syndrome. *J Heart Lung Transplant* 2003; 22 (1): 50.
49. Groetzner J, Wittwer T, Kaczmarek I, et al. Conversion to sirolimus and mycophenolate can attenuate the progression of bronchiolitis obliterans syndrome and improves renal function after lung transplantation. *Transplantation* 2006; 81 (3): 355.
50. Gottlieb J, Szangolies J, Koehnlein T, Golpon H, Simon A, Welte T. Long-term azithromycin for bronchiolitis obliterans syndrome after lung transplantation. *Transplantation* 2008; 85 (1): 36.
51. Johnson BA, Iacono AT, Zeevi A, McCurry KR, Duncan SR. Statin use is associated with improved function and survival of lung allografts. *Am J Respir Crit Care Med* 2003; 167 (9): 1271.
52. Morrell MR, Despotis GJ, Lublin DM, Patterson GA, Trulock EP, Hachem RR. The efficacy of photopheresis for bronchiolitis obliterans syndrome after lung transplantation. *J Heart Lung Transplant* 2010; 29 (4): 424.
53. Si H, Heyken W-T, Wölfle SE, et al. Impaired Endothelium-Derived Hyperpolarizing Factor-Mediated Dilations and Increased Blood Pressure in Mice Deficient of the Intermediate-Conductance Ca²⁺-Activated K⁺ Channel. *Circulation Research* 2006; 99 (5): 537.
54. Hele DJ YM, Belvisi MG. The heterotopic tracheal allograft as an animal model of obliterative bronchiolitis. *Respir Res* 2001; 2 (3): 169.
55. Hua X, Deuse T, Tang-Quan KR, Robbins RC, Reichenspurner H, Schrepfer S. Heterotopic and orthotopic tracheal transplantation in mice used as models to study the development of obliterative airway disease. *J Vis Exp* 2010 (35).
56. Wulff H, Miller MJ, Hansel W, Grissmer S, Cahalan MD, Chandy KG. Design of a potent and selective inhibitor of the intermediate-conductance Ca²⁺-activated K⁺ channel, IKCa1: a potential immunosuppressant. *Proc Natl Acad Sci U S A* 2000; 97 (14): 8151.
57. Reichenspurner H, Soni V, Nitschke M, et al. Obliterative airway disease after heterotopic tracheal xenotransplantation: pathogenesis and prevention using new immunosuppressive agents. *Transplantation* 1997; 64 (3): 373.
58. Velotta JB, Deuse T, Peter C, et al. 330: Effects of the JAK3-Inhibitor R348 on Different Cell Types Involved in Obliterative Airway Disease. *The Journal of Heart and Lung Transplantation* 2009; 28 (2, Supplement 1): S180.

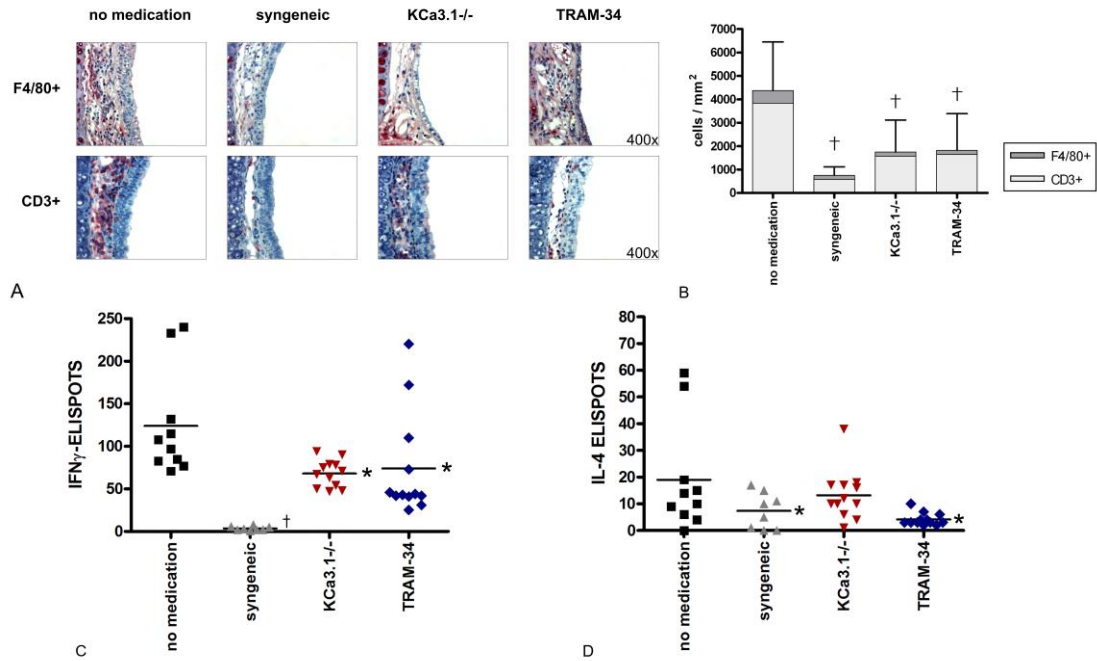
Tables

| Study | No. | Group | Donor | Recipients | Treatment |
|----------------------------------|-----|---------------|--------|------------|-----------|
| <i>Grafts recovered on POD5</i> | | | | | |
| | 1 | no medication | CBA | C57B16 | - |
| | 2 | syngeneic | C57B16 | C57B16 | - |
| | 3 | knockout | CBA | KCa3.1 -/- | - |
| | 4 | TRAM-34 | CBA | C57B16 | TRAM-34 |
| <i>Grafts recovered on POD28</i> | | | | | |
| | 5 | no medication | CBA | C57B16 | - |
| | 6 | syngeneic | C57B16 | C57B16 | - |
| | 7 | knockout | CBA | KCa3.1 -/- | - |
| | 8 | TRAM-34 | CBA | C57B16 | TRAM-34 |

Table 1. *Study groups.* Grafts were recovered on POD5 in groups 1-4 to investigate acute rejection and immune activation, or after 28 days in groups 5-8 to assess OAD development

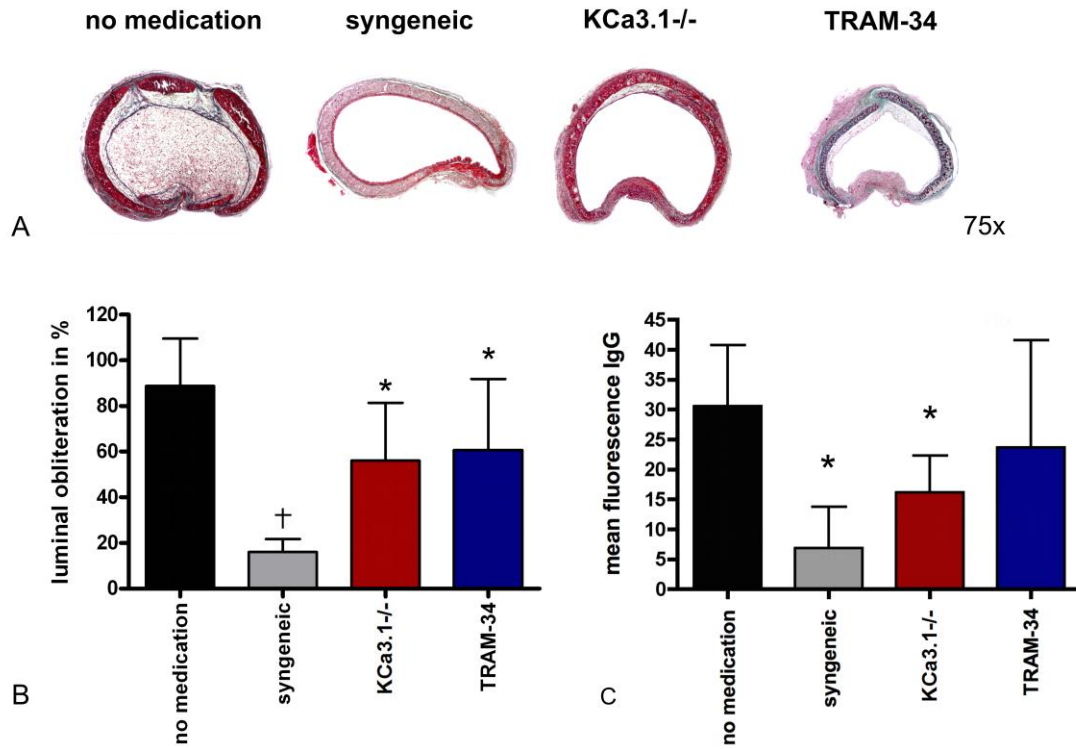
Figure Legends

Figure 1: Graft infiltrating cells and systemic cellular immune response.



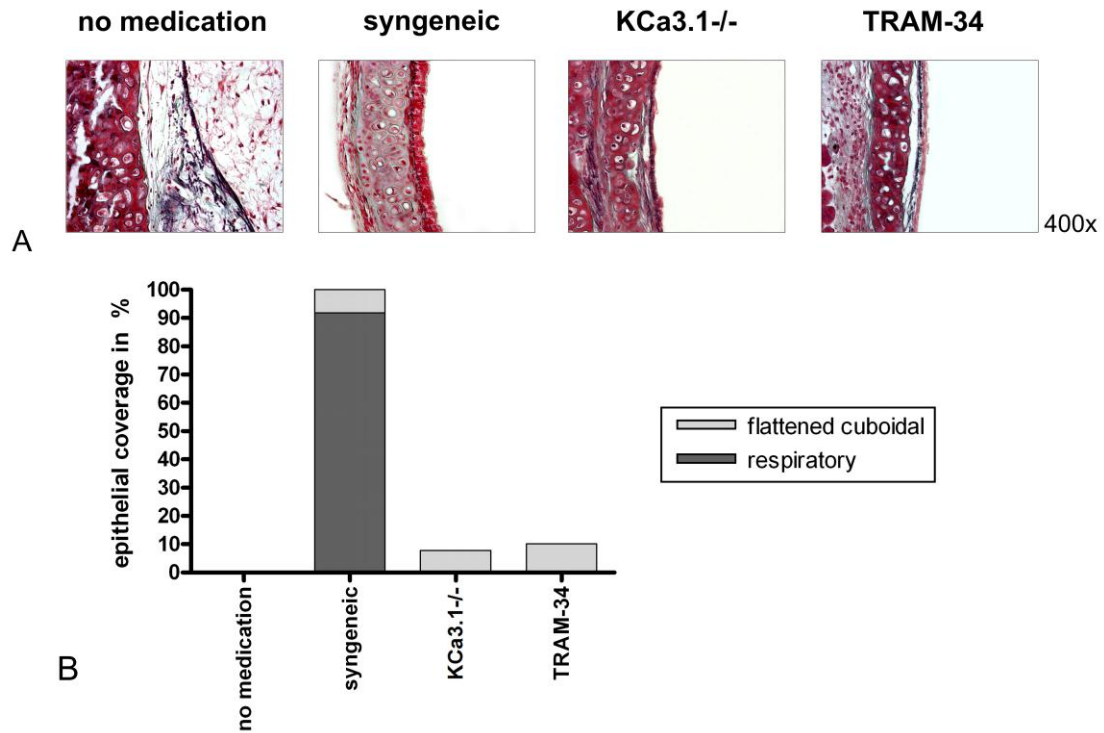
Graft infiltration of F4/80+ macrophages and CD3+ lymphocytes within the subepithelial area on POD5 is shown by immunohistochemistry (A; magnification 400 \times). Mean numbers of F4/80+ macrophages (N=5 for no medication, N=6 for syngeneic, N=6 for KCa3.1-/-, N=5 for TRAM-34) and CD3+ T cells (N=4 for all groups) are expressed as cells/mm² (B; †p<0.001 vs. no medication). On POD5, Elispot assays revealed attenuated systemic responses of IFN- γ producing Th1 cells (C) and IL-4 producing Th2 cells (D) in the KCa3.1-/- (N=4) and TRAM-34 (N=5) groups (*p<0.05 vs. no medication; †p<0.001 vs. no medication (N=3), N=3 for syngeneic).

Figure 2: Histopathology, luminal obliteration, and donor-reactive antibodies.



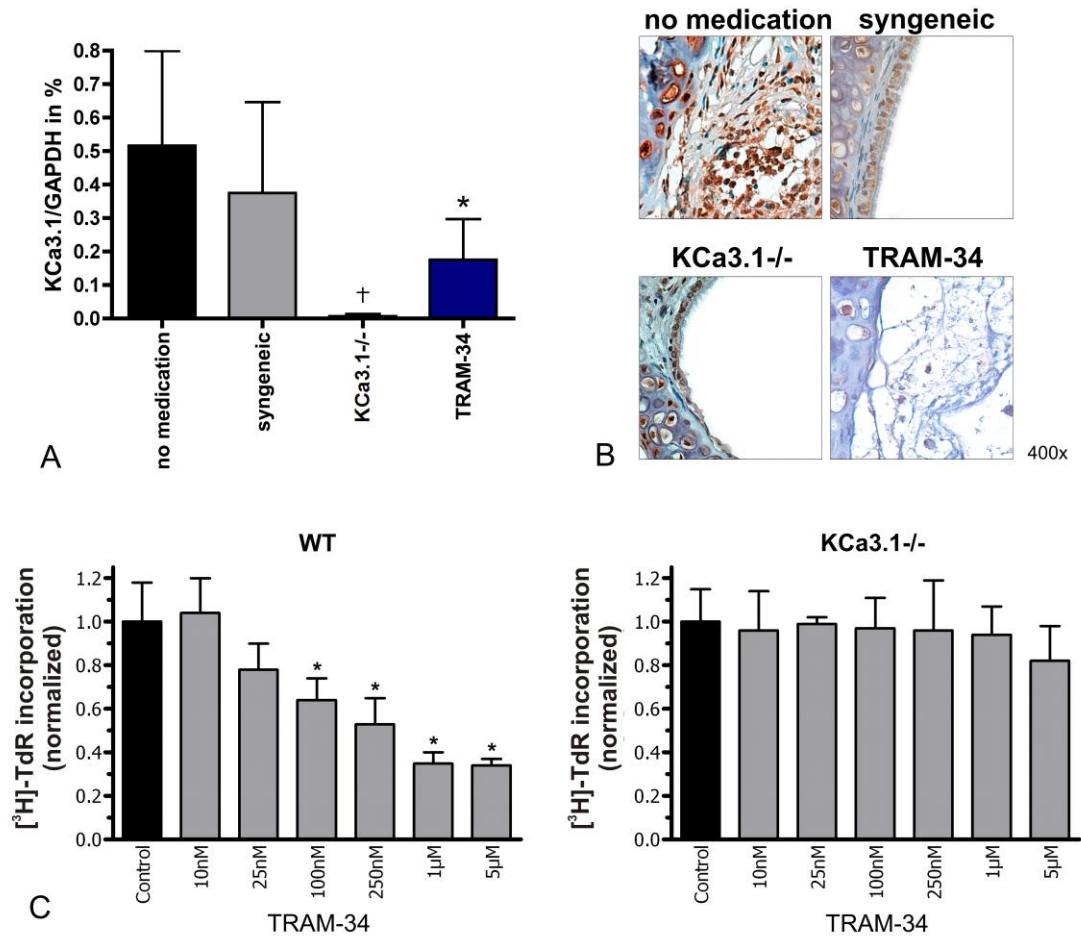
Representative cross sections of tracheal grafts on POD 28 stained with Masson-Goldner Trichrome at a magnification 75x are depicted (A). The average percent luminal obliteration is shown (B; *p<0.05 vs. no medication; †p<0.001 vs. no medication; N=7 for no medication and TRAM-34, N=5 for syngeneic, N=8 for KCa3.1 -/-). Mean fluorescence of IgG demonstrates a significant reduction in DSAs in the syngeneic (N=5) and KCa3.1 -/- (N=9) groups (C; p=0.001 and p=0.018, respectively, vs. no medication (n=7); N=7 for TRAM-34).

Figure 3: Airway epithelium.



Representative sections of the tracheal epithelia on POD 28, stained with Masson-Goldner trichrome, are shown at a magnification of 400 \times (A). The respiratory epithelium of the syngeneic group (N=5) is widely preserved (B). The KCa3.1-/- (N=10) and TRAM-34 (N=8) groups show cuboidal or flattened epithelia, whereas the epithelium in the no medication group (N=8) is totally destroyed.

Figure 4: *KCa3.1* expression and *in vitro* proliferation assay.



KCa3.1 mRNA-expression in tracheal grafts was analyzed by semi-quantitative RT-PCR (A; * $p < 0.008$; † $p < 0.001$ vs. no medication (N=6), N=4 for syngeneic, N=8 for KCa3.1^{-/-}, N=5 for TRAM-34). Representative stainings for the KCa3.1 channel in tracheal graft are shown at a magnification of 400× (B). The results of the *in vitro* proliferation assay for WT or KCa3.1^{-/-} splenocytes are shown as [³H]-TdR incorporation normalized to the ConA-stimulated controls (C; * $p < 0.05$ vs. controls).

Sustained Inhibition of ϵ Protein Kinase C Inhibits Vascular Restenosis After Balloon Injury and Stenting

Tobias Deuse, MD; Tomoyoshi Koyanagi, MD; Reinhold G. Erben, MD; Xiaoqin Hua, MD; Joachim Velden, MD; Fumiaki Ikeno, MD; Hermann Reichenspurner, MD; Robert C. Robbins, MD; Daria Mochly-Rosen, MD; Sonja Schrepfer, MD, PhD

Background— ϵ Protein kinase C (ϵ PKC) is involved in vascular smooth muscle cell (VSMC) activation, but little is known about its function in vascular pathology. We aimed at assessing the role of ϵ PKC in the development of restenosis.

Methods and Results—Rat models of aortic balloon injury with or without subsequent stenting were used. Rats were treated with the selective ϵ PKC activator $\psi\epsilon$ receptor for activated protein kinase C ($\psi\epsilon$ RACK), the selective ϵ PKC inhibitor ϵ V1–2, or saline. Both down-stream cascades of the platelet-derived growth factor receptor via extracellular signal-regulated kinase and Akt, respectively, were evaluated in vivo and in VSMC cultures. Intimal hyperplasia with luminal obliteration developed in saline-treated balloon-injured rat aortas ($20.3\pm 8.0\%$), and $\psi\epsilon$ RACK significantly promoted neointima development ($32.4\pm 4.9\%$, $P=0.033$), whereas ϵ V1–2 significantly inhibited luminal narrowing ($9.2\pm 4.3\%$, $P=0.039$). ϵ PKC inhibition led to significantly reduced VSMC extracellular signal-regulated kinase phosphorylation in vivo, whereas Akt phosphorylation was not markedly affected. Neointimal proliferation in vivo and platelet-derived growth factor-induced VSMC proliferation/migration in vitro were significantly inhibited by ϵ V1–2. The inhibition of the platelet-derived growth factor pathway was mediated by inhibiting down-stream extracellular signal-regulated kinase and Akt phosphorylation. In vitro, ϵ V1–2 showed inhibitory properties on endothelial cell proliferation, but that did not prevent reendothelialization in vivo. ϵ V1–2 showed proapoptotic effects on VSMC in vitro. After stent implantation, luminal restenosis (quantified by optical coherence tomography imaging) was significantly reduced with ϵ V1–2 ($8.0\pm 2.0\%$) compared with saline ($20.2\pm 9.8\%$, $P=0.028$).

Conclusions— ϵ PKC seems to be centrally involved in the development of neointimal hyperplasia. We suggest that ϵ PKC inhibition may be mediated via inhibition of extracellular signal-regulated kinase and Akt activation. ϵ PKC modulation may become a new therapeutic target against vascular restenosis. (*Circulation*. 2010;122[suppl 1]:S170–S178.)

Key Words: ϵ protein kinase C ■ vascular restenosis ■ platelet-derived growth factor pathway

Eleven related serine/threonine protein kinases form the protein kinase C (PKC) family.¹ Recent developments of isozyme-specific activators and inhibitors provided us with tools to differentially study isozyme-specific functions. It appears that α PKC and ϵ PKC, together with the atypical PKCs, mediate cell proliferation and survival, whereas δ PKC and ϵ PKC are important regulator of apoptosis.² ζ PKC has been shown to play a role in promoting early medial infiltration in a carotid artery balloon injury model, thus aiding in controlling neointimal inflammation and growth.³ The δ PKC and ϵ PKC isozymes have been shown to play opposing roles in cardiac ischemia and reperfusion, with ϵ PKC mediating cardioprotection against ischemic injury and δ PKC mediating

reperfusion-induced cell damage.^{2,4} Selective sustained ϵ PKC inhibition has been shown to suppress chronic inflammation and the development of perivascular fibrosis in a murine cardiac transplantation model.⁵ In hypertensive rats, ϵ PKC inhibition prolonged survival, reduced cardiac hypertrophy, excessive fibrosis, vascular remodeling, inflammation, and corrected cardiac dysfunction.⁶ However, the selective ϵ PKC activator $\psi\epsilon$ receptor for activated protein kinase C ($\psi\epsilon$ RACK) conferred cardioprotection from ischemia-reperfusion injury under cell culture conditions and in animal models of acute myocardial infarction, when delivered acutely before the ischemic event.^{4,7,8} ϵ PKC activation may appear as a “double-edged sword”, acutely increasing mito-

From the Departments of Cardiothoracic Surgery (T.D., R.C.B., S.S.); Cardiovascular Medicine (F.I.), Stanford University School of Medicine, Stanford, CA; Department of Cardiovascular Surgery, Transplant and Stem Cell Immunobiology Lab (T.D., X.H., H.R., S.S.); Cardiovascular Research Center (T.D., X.H., H.R., S.S.); Department of Pathology (J.V.), University Hospital Hamburg, Hamburg, Germany; Department of Chemical and Systems Biology, Stanford University, Stanford, CA (T.K., D.M.-R.); University of Veterinary Medicine Vienna, Vienna, Austria (R.G.E.).

Presented at the 2010 American Heart Association meeting in Orlando, Fla, November 14–18, 2009.

The online Data Supplement can be found with this article at <http://circ.ahajournals.org/cgi/content/full/CIRCULATIONAHA.109.927640/DCI>.

Correspondence to Sonja Schrepfer, MD, PhD, Department of Cardiothoracic Surgery, Stanford University School of Medicine, 300 Pasteur Dr, Cardiovascular Research Building 5407, Stanford, CA 94305. E-mail schrepfer@stanford.edu

© 2010 American Heart Association, Inc.

Circulation is available at <http://circ.ahajournals.org>

DOI: 10.1161/CIRCULATIONAHA.109.927640

chondrial function and preventing cell death, but chronically increasing inflammatory responses. The complex involvement of PKC isozymes in cardiovascular physiology needs further research before targets for therapeutic interventions can be identified. Especially the role of ϵ PKC on vascular remodeling is not known. In this study, we sought to investigate the role of ϵ PKC on the development of intimal hyperplasia after mechanical injury.

Methods

Rat Restenosis Models

Male Sprague–Dawley rats weighing 550 to 600 g were purchased from Harlan. All rats were housed under conventional conditions in the animal care facilities. All animals received humane care in compliance with the Principles of Laboratory Animal Care formulated by the National Society for Medical Research and the Guide for the Care and Use of Laboratory Animals. Aortic endothelial denudation and stent placement (Yukon Plus, 2.5×12 mm; Translumina) was performed as previously reported⁹ and described in the supplemental data, available online at <http://circ.ahajournals.org>.

Animals were treated with the selective ϵ PKC activator, $\psi\epsilon$ RACK,⁷ the selective ϵ PKC inhibitor, ϵ V1–2,¹⁰ the cell-penetrating TAT carrier peptide (TAT_{47–57}), or saline. Both PKC modifying peptides were conjugated to TAT_{47–57}, which greatly enhances cell permeation of these intracellularly acting peptides in vivo and in vitro. The selectivity of the peptides to ϵ PKC was previously reported in many independent studies in vitro^{7,10} and in vivo.¹¹ All drugs were administered in a sustained fashion via implanted osmotic pumps (Alzet), which were replaced every second week. Peptides were each delivered at 3 mg/kg per day. Denuded aortas were harvested after 4 weeks and stented aortas after 6 weeks.

Histology

Cross-sections of denuded aortas were stained with Elastica van Giesson and Masson–Goldner trichrome (Merck). Cell proliferation was detected by PCNA staining (Dako) after antigen retrieval (Dako) using the AP development system (Zytomed). Paraffin sections were stained for α -actin (red; Sigma), 4',6-diamidino-2-phenylindole (DAPI) (blue; Invitrogen), and elastin (green; Abcam). Quantification of neointimal fibrosis and cell density was performed as outlined in supplemental data. Reendothelialization was determined by RECA-1 immunofluorescence stainings (Serotec). Aortas housing stents were processed as previously reported,⁹ sectioned at 5- μ m thickness, and stained with hematoxylin and eosin. For details, please see supplemental data.

Optical Coherence Tomography (OCT) Imaging

OCT images were obtained with the M2 OCT imaging system (LightLab Imaging). Motorized pullback was performed at a rate of 1.0 mm per second as described in the supplemental data. Neointimal cross-sectional areas were measured, and luminal obliteration was calculated.

Western Blot Analysis

Rat aortic tissue was homogenized in homogenization buffer (50 mmol/L Tris-HCl, pH 7.5/150 mmol/L NaCl/1% SDS/protease inhibitor cocktail [Sigma-Aldrich]). After removal of tissue debris by centrifugation, 20 or 50 μ g of proteins were separated on an 8 or 10% SDS-PAGE and were transferred to immobilon-P transfer membrane (Millipore). Antibodies against platelet-derived growth factor (PDGF) receptor- β , phosphorylated Akt (S453) and extracellular signal-regulated kinase (ERK), and β -actin (Santa Cruz Biotechnology, Inc; Cell Signaling Technology) were used for immunoblotting followed by HRP-conjugated antimouse, rabbit or goat IgG antibodies (GE Healthcare; Santa Cruz Biotechnology, Inc). All samples were loaded equally for each gel based on protein concentration.

In Vitro VSMC and Endothelial Cell (EC) Culture Assays

Proliferation assays with mitogen-stimulated rat aortic VSMC (PDGF 25 ng/mL) and EC (VEGF 10 ng/mL) were performed in the presence of TAT_{47–57} only (control), $\psi\epsilon$ RACK, or ϵ V1–2 (1 μ mol/L each). To assess VSMC migration, a standard scratch was made across a VSMC culture slide, and the number of cells that migrated into this “wound” within 4 days was counted. The TUNEL assay (Invitrogen) was used to detect apoptotic cells. For details, please see supplemental data.

In Vitro PKC Translocation Assay and Western Blot Analysis

Levels of active ϵ PKC in VSMC were determined by cell fractionation and Western blot analysis. Cells were pretreated with ϵ V1–2 or TAT_{47–57} and stimulated with 25 ng/mL PDGF as outlined in supplemental data. Cells were homogenized, spun, and supernatants were collected. All samples were separated by 10% SDS-PAGE, and the proteins were transferred to immobilon-P transfer membranes for immunoblotting. Akt, ERK, phosphorylated Akt, and ERK levels were measured as described above.

Statistical Analysis

Data are presented as mean \pm SD. Comparisons were done by ANOVA between groups with Bonferroni post hoc tests (SPSS). $P<0.05$ was considered significant.

Results

Rat Restenosis Models

All denudation and stenting procedures were tolerated well by the animals and no stent-related complications occurred. All animals survived the study period, and all stents were suitable for OCT imaging and histological evaluation.

Intimal Hyperplasia in Balloon-Injured Aortas

Intimal hyperplasia developed in denuded rat aortas as determined 4 weeks after aortic balloon injury (Figure 1A). Histology revealed a high density of spindle-shaped cells and only very few mononuclear inflammation cells. Trichrome staining showed a cell-rich neointima containing fibrotic connective tissue (Figure 1B). Cell proliferation, detected by PCNA staining, was observed in 19 \pm 6, 25 \pm 4, and 20 \pm 4% of neointimal cells in the saline, $\psi\epsilon$ RACK, and TAT_{47–57} groups, respectively, and was significantly reduced by ϵ V1–2 (9 \pm 3%, $P=0.003$ versus saline) (Figure 1C). Planimetric measurements showed that luminal obliteration in saline-treated animals was approximately 20% and was not affected by the carrier peptide TAT_{47–57}. Interestingly, sustained treatment with the ϵ PKC activator, $\psi\epsilon$ RACK, significantly promoted neointima development, whereas sustained ϵ PKC inhibition with ϵ V1–2 significantly inhibited luminal narrowing (Figure 1D). Accordingly, the maximal plaque thickness in the $\psi\epsilon$ RACK group was significantly greater than with ϵ V1–2 (Figure 1E). Although the total neointimal areas differed among groups, the fractional areas of neointimal fibrosis (35 \pm 5, 36 \pm 5, 36 \pm 6, and 33 \pm 5%; $P=0.704$) and the VSMC densities (24 \pm 5, 28 \pm 10, 23 \pm 5, and 22 \pm 5 VSMCs per 100 μ m² of neointimal cross-sectional area; $P=0.643$) (Figure 1F) were similar for saline, $\psi\epsilon$ RACK, TAT_{47 to 57}, and ϵ V1–2, respectively. We found virtually complete reendothelialization 4 weeks after denuda-

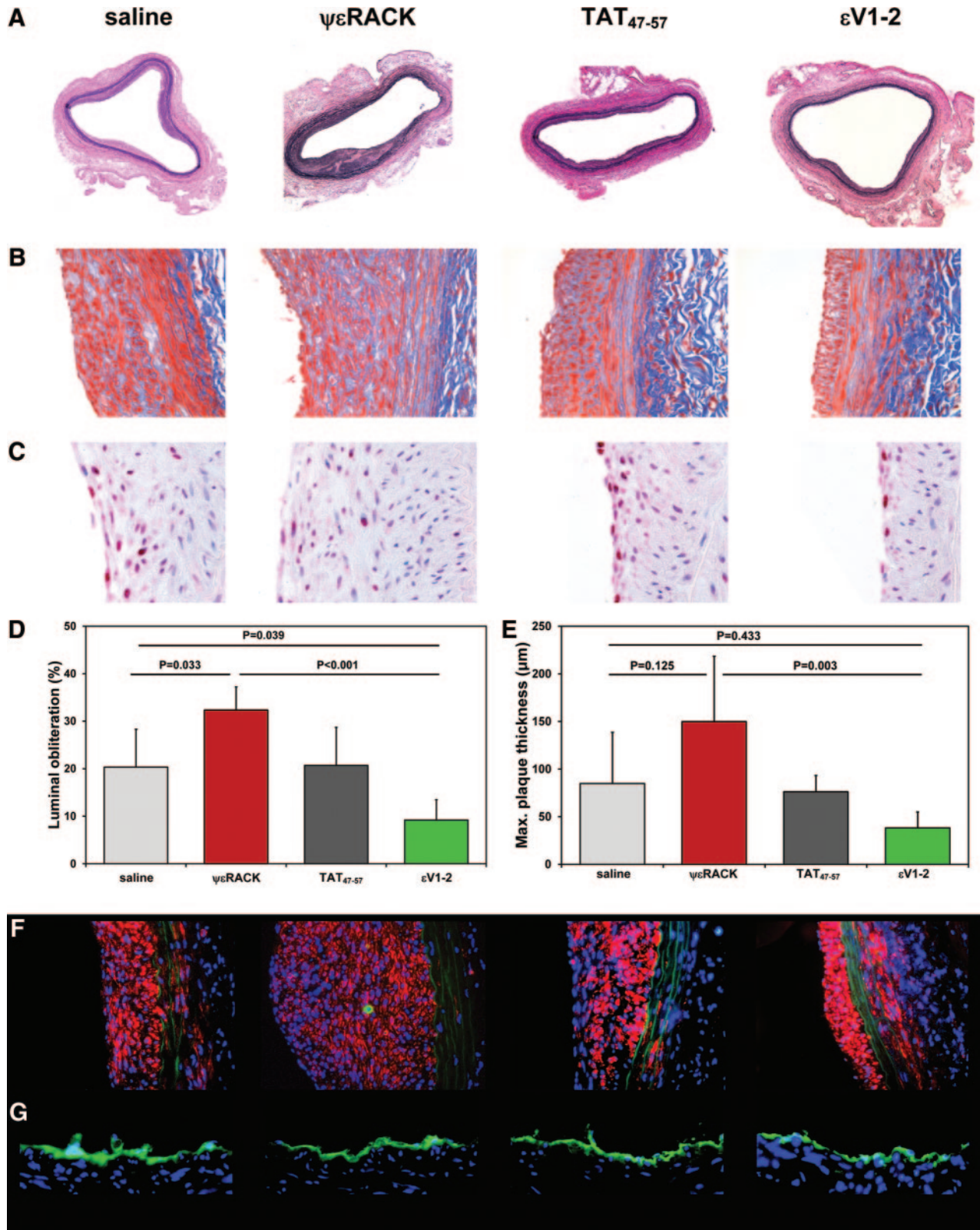


Figure 1. Intimal hyperplasia in balloon-injured aortas. Aortic cross-sections in hematoxylin and eosin staining are shown depicting the degree of intimal hyperplasia 4 weeks after balloon injury (magnification, $\times 15$; $n=6$ animals per group) (A). Neointimal fibrosis was visualized by trichrome staining (magnification, $\times 400$) (B), and cell proliferation was detected by PCNA staining (magnification, $\times 600$) (C). Mean percentage luminal obliteration (D) and maximal plaque thickness (E) of the aortas are presented. Treatment with the ϵ PKC activator $\psi\epsilon$ RACK significantly promoted neointima development, whereas ϵ PKC inhibition with ϵ V1-2 significantly inhibited luminal narrowing. Sections were stained for α -actin (red), DAPI (blue), and elastin (green) (F). Reendothelialization (RECA-1, green; DAPI, blue) was complete in all groups (G).

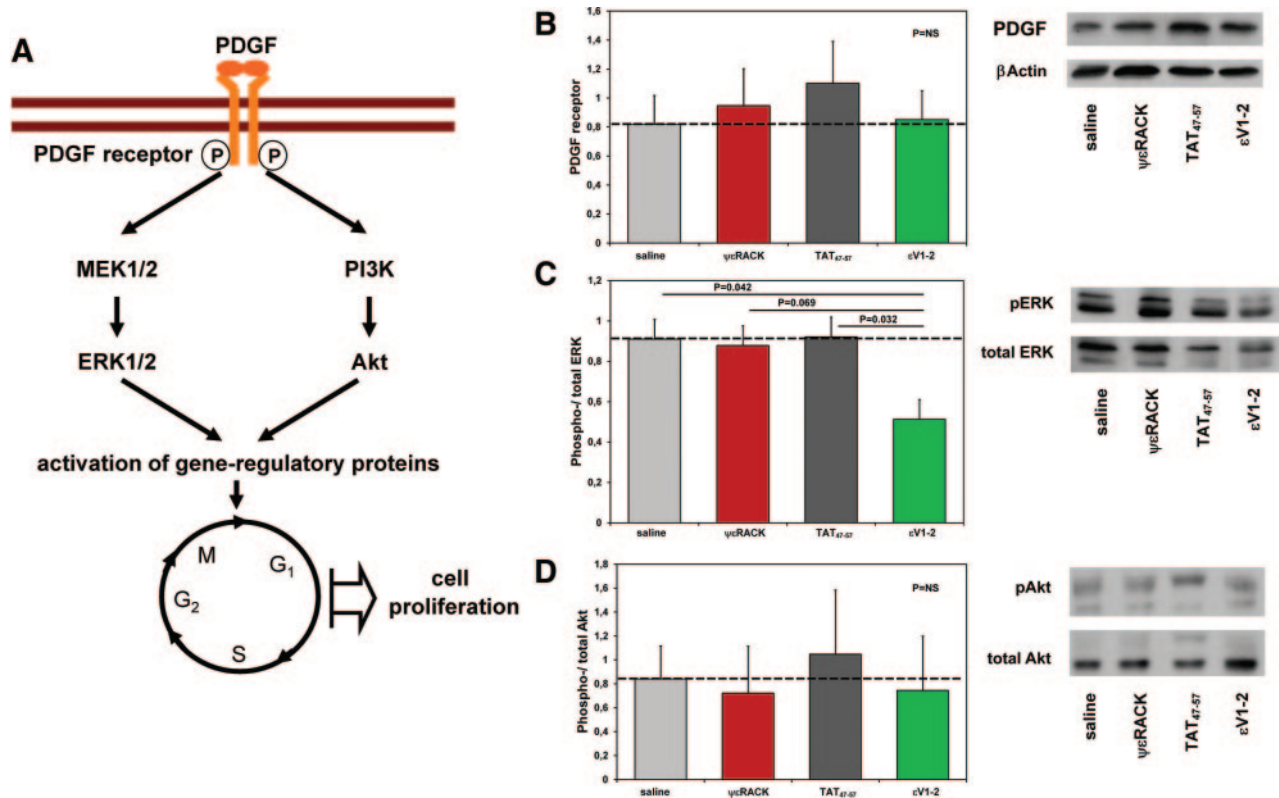


Figure 2. In vivo VSMC PDGF pathway activation. PDGF pathway-mediated VSMC cell cycle control involves the ERK/MEK and phosphatidylinositol 3-kinase/Akt down-stream cascades (A). PDGF receptor expression was not affected by ϵ PKC modulation (B). A significant reduction of ERK phosphorylation (C), but not for Akt phosphorylation (D), could be shown after the administration of ϵ V1-2. Western blot analysis images from the same gel are rearranged in the presented order ($n=6$ samples per group).

tion in all slides without differences related to the treatment with ϵ PKC modulators (Figure 1G).

In Vivo VSMC PDGF Pathway Activation

Both down-stream cascades of the PDGF pathway controlling VSMC cell cycle (Figure 2A) were explored. The levels of PDGF receptor expression were not affected by ϵ PKC modulation (Figure 2B). ϵ V1-2 administration led to a significantly reduced ERK phosphorylation, suggesting an involvement of ϵ PKC in ERK activation (Figure 2C). Neither $\psi\epsilon$ RACK nor ϵ V1-2 markedly affected Akt phosphorylation (Figure 2D).

In Vitro VSMC and EC Culture Assays

We set out to determine whether ϵ PKC plays a direct role in VSMC and EC proliferation and VSMC migration. First, PDGF-induced ϵ PKC activation was determined. PKC translocation (or movement from the cell soluble to the cell particulate fraction) is an established method to assess PKC activation.¹² We found that PDGF stimulation significantly activated ϵ PKC (Figure 3A) and that this activation was blocked by pretreatment of the cells with ϵ V1-2. We further show that VSMC proliferation induced by PDGF treatment was moderately stimulated by $\psi\epsilon$ RACK and significantly inhibited by ϵ V1-2 treatment (Figure 3B). We also performed the assay with 100 ng/mL of PDGF stimulation and observed similar magnitudes of growth enhancement and significant inhibition by treatment with ϵ V1-2 (data not

shown). VSMC migration was assessed in culture slide scratch assays (Figure 3C) and revealed that VSMC migration was similarly influenced by ϵ PKC modulation. We found significant stimulation of VSMC migration by $\psi\epsilon$ RACK in vitro and significant inhibition by ϵ V1-2 (Figure 3D). Cell proliferation of VEGF-stimulated EC in vitro is quantified in Figure 3E and depicted in Figure 3F. EC proliferation was significantly stimulated by $\psi\epsilon$ RACK and significantly inhibited with ϵ V1-2. A possible implication of ϵ PKC modulators on VSMC apoptosis was further investigated using the TUNEL assay (Figure 3G). There was mild reduction of apoptosis by $\psi\epsilon$ RACK, but we found significantly increased numbers of apoptotic VSMCs with ϵ V1-2 treatment (Figure 3H).

Effect of ϵ V1-2 Treatment on Down-Stream Signaling of PDGF

To investigate the molecular mechanism of VSMC growth inhibition by ϵ V1-2 treatment, we next determined ERK and Akt activation, which are postulated to play a role in VSMC proliferation.¹³ As demonstrated by Western blot analysis, 5 minutes of PDGF stimulation significantly increased the levels of phosphorylated ERK and Akt, but ϵ V1-2 treatment did not have a significant effect at this time point (Figure 4A). However, after 6 hours of ϵ V1-2 treatment, there was a significant decrease in phosphorylated ERK levels in cells treated with or without PDGF as compared with cells treated with control peptide (Figure 4B). Similar effects of ϵ V1-2 on

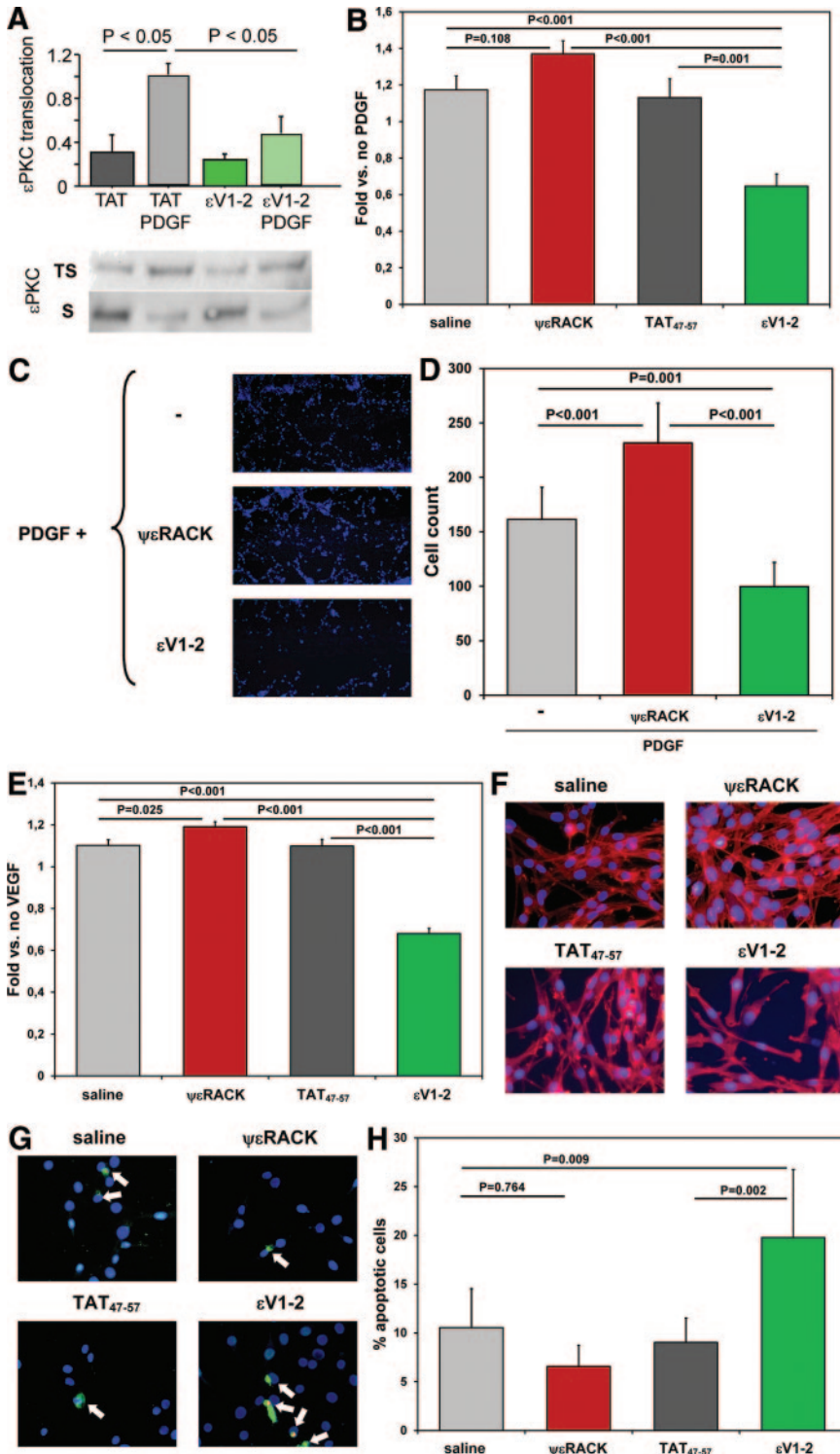


Figure 3. In vitro VSMC and EC culture assays. ϵ PKC translocation from the cell soluble (S) to the cell particulate fraction (TS) was observed after PDGF stimulation, and this activation was blocked by ϵ V1-2 (n=3 per group) (A). PDGF-induced VSMC proliferation was significantly inhibited by ϵ V1-2 treatment (B). A standard scratch (600 μ m wide) was made into VSMC monolayers and, 4 days later, 1080- μ m-long segments of the scratch were photographed (DAPI staining; original magnification, $\times 100$) (C), and the amount of PDGF-stimulated VSMCs that had migrated into the scratch was counted (n=8 per group) (D). $\psi\epsilon$ RACK significantly promoted VSMC migration, whereas it was significantly inhibited by ϵ V1-2. In vitro EC proliferation was quantified (n=3 per group) (E) in EC cultures (phalloidin [red], DAPI [blue]; original magnification, $\times 600$) (F). EC proliferation was significantly stimulated by $\psi\epsilon$ RACK and inhibited by ϵ V1-2. In vitro VSMC apoptosis was determined using the TUNEL test (n=6 per group; original magnification, $\times 600$) (G). Cell nuclei were stained with Hoechst 33342 (blue), and fragmented DNA is labeled with Alexa Fluor 488 (green). The percentage of apoptotic cells was determined (H). Apoptosis was only very mildly reduced with $\psi\epsilon$ RACK but significantly increased with ϵ V1-2.

Akt and phosphorylated Akt were also found. Although there was no effect of ϵ V1-2 treatment after 5 minutes with PDGF, there was a significant decrease in the levels of phosphorylation ratio of Akt after 6 hours. Because PDGF signaling is long lasting in injured vessels, such changes may be physiologically relevant. Together, our data suggest that ϵ PKC inhibition of PDGF-induced VSMC proliferation is likely mediated, at least in part, through inhibition of ERK and Akt activation.

Intimal Hyperplasia in Stented Aortas

Figure 5A shows histological cross-sections of the stented aortas. The stent struts were eliminated during the processing, leaving behind open spaces at their former locations. The systemic release of ϵ V1-2 significantly reduced the development of the neointimal plaque area from 1.0 ± 0.4 to 0.5 ± 0.8 mm² ($P = 0.047$) (Figure 5B). Representative OCT frames are shown in Figure 5C. OCT-derived luminal obliteration (Figure 5D) was $12.2 \pm 9.8\%$ in saline-treated rats and

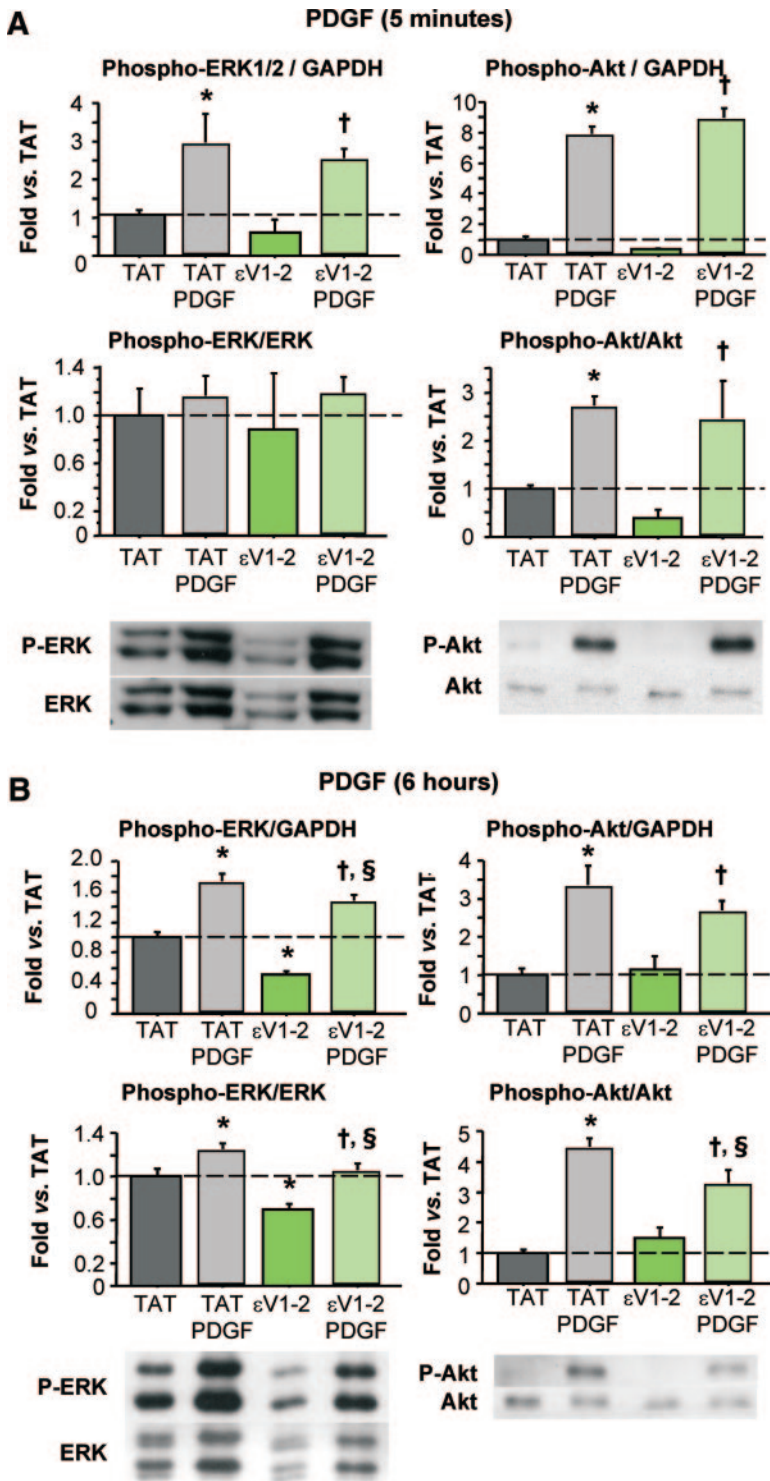


Figure 4. Effect of ϵ V1-2 treatment on downstream signaling of PDGF. Five minutes of PDGF stimulation (25 ng/mL) significantly increased ERK and Akt phosphorylation ($n=3$ per group). ϵ V1-2 treatment did not show a significant early effect on these cascades ($*P<0.05$ vs TAT; $\dagger P<0.05$ vs ϵ V1-2) (A). However, after 6 hours, there was a significant decrease in phosphorylated ERK and Akt levels ($*P<0.05$ vs TAT; $\dagger P<0.05$ vs ϵ V1-2; $\S P<0.05$ vs TAT+PDGF) (B), suggesting that ϵ PKC inhibition of PDGF-induced VSMC proliferation may be mediated via inhibition of ERK and Akt activation.

was significantly reduced by a 6-week treatment with ϵ V1-2 to $8.0 \pm 2.0\%$ ($P=0.028$).

Discussion

Clinical results of percutaneous coronary interventions with or without stenting have been limited by restenosis and patients frequently require repeat revascularization procedures. VSMC proliferation and migration with subsequent synthesis of extracellular matrix are central cellular events

resulting in neointimal formation. Rat models of aortic balloon injury with¹⁴ and without¹⁵ subsequent stent placement are established models for the development of arterial restenosis and have been used in this study.

Role of ϵ PKC in the Development of Intimal Hyperplasia

Although the importance of PKC signaling for VSMC growth and restenosis has been shown previously,¹⁶ the specific roles

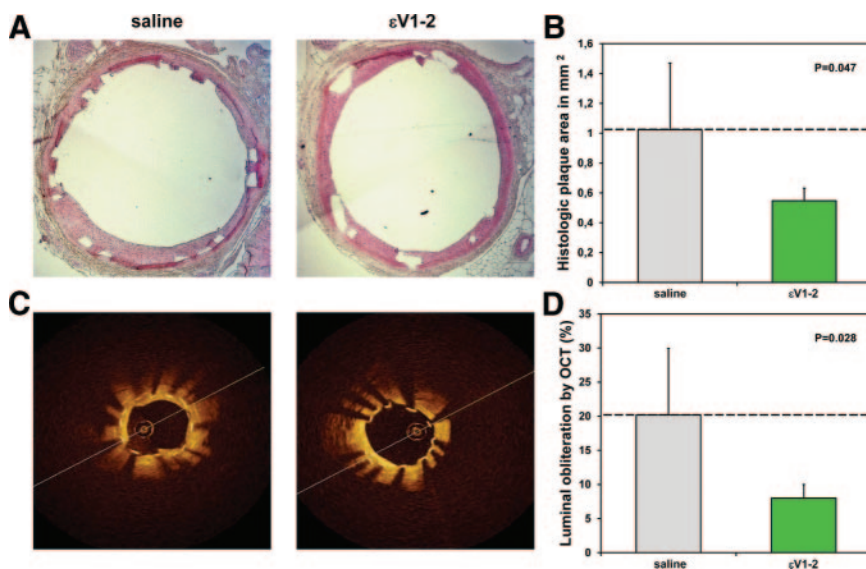


Figure 5. Intimal hyperplasia in stented aortas. Histological cross-sections of stented aortas are shown 6 weeks after implantation subsequent to mechanical injury (n=6 animals per group) (A). ϵ V1-2 treatment significantly reduced neointimal plaque development (B). Luminal obliteration, quantified by OCT (C), was also significantly reduced in ϵ V1-2-treated animals (D).

of its isoforms remained unknown. We used a selective ϵ PKC activator and inhibitor, respectively, to elucidate the role of ϵ PKC in vascular restenosis. In a rat model of balloon injury, we here show that sustained ϵ PKC activation significantly increases neointimal hyperplasia, whereas it is reduced with sustained ϵ PKC inhibition. The suppression of neointimal development by ϵ PKC inhibition could be shown to result from an antiproliferative capacity of ϵ V1-2 in vivo. The cellularity of the neointima and the neointimal fractional area of fibrosis were found to be similar among groups. Therefore, both cellular proliferation and the increase of extracellular fibrosis seem to be affected to similar extents by ϵ PKC modulation. Reendothelialization is crucial for physiological healing of mechanically injured arteries. ϵ V1-2 treatment, although shown to inhibit in vitro EC proliferation, did not prevent reendothelialization until 4 weeks after injury. Our data, however, cannot determine whether endothelial healing was slowed down by ϵ PKC inhibition, because only 1 time point was assessed.

Molecular Basis of ϵ PKC Inhibition on PDGF-Stimulated VSMC Proliferation

PDGF induces VSMC proliferation by triggering the activation of both the ERK/mitogen-activated protein kinase and phosphatidylinositol 3-kinase-Akt pathways.¹⁷ To further examine the molecular basis for the inhibition of VSMC proliferation in rat aortas treated with ϵ V1-2, we used VSMC in primary cultures. ϵ V1-2 treatment decreased PDGF-induced ϵ PKC activation and cell proliferation in VSMC cultures in vitro. ERK is a key transducer of extracellular signals and promotes cell growth and migration. ERK1 and ERK2 play pivotal roles in proliferation of VSMC in vitro and in vivo. PDGF-induced proliferation is inhibited by dominant negative mutants¹⁸ or antisense oligonucleotides¹⁹ of ERKs. In addition, dominant negative mutation of Akt causes delays in G_{1/2} exit in the cell cycle and controls proliferation of primary rat aortic VSMC.²⁰ Independent but synergistic effects of the phosphatidylinositol 3-kinase-Akt pathway and the MEK1/2-ERK pathway in PDGF-induced responses were observed using inhibitors of these kinases,

LY294002 and PD98059, respectively.¹³ In addition to the relationship between ERK activity and VSMC proliferation, a correlation between ERK and neointimal hyperplasia in rat aorta has been previously observed following balloon angioplasty-induced injury.^{18,21} Mechanical injury-induced VSMC proliferation involves ERK phosphorylation,²² and ERK activation is among the earliest of biochemical changes detected after arterial injury.²³ ERK transmits mitogenic signals by translocation to the nucleus where multiple genes implicated in the pathogenesis of atherosclerosis and restenosis are induced.²⁴

Here, we showed that the ϵ PKC inhibitor ϵ V1-2 did not affect early PDGF-induced ERK and Akt activation, suggesting that ϵ PKC is probably not an immediate upstream regulator of these enzymes. However, after 6 hours of PDGF stimulation, ERK levels were significantly decreased following ϵ V1-2 treatment, which resulted in decreased amounts of active ERKs in PDGF-stimulated VSMC. ϵ PKC activation may also control ERK activity by reducing protein stability and/or decreasing its expression in VSMC. Saito et al²⁵ reported involvement of ϵ PKC in the activation of Grb2-associated binder-1, an adapter protein related to the insulin receptor substrate family. Because ERK2 is downstream of Grb2-associated binder-1, the ϵ PKC-mediated PDGF effect that we observed may be due to inhibition of the ϵ PKC-mediated PDGF-Grb2-associated binder-1 pathway activation. Although we only found mild decreases of Akt levels by ϵ PKC inhibition in vivo, Akt phosphorylation levels were significantly decreased in vitro by ϵ V1-2 treatment when determined 6 hours after PDGF treatment. These data suggest that ϵ PKC also controls Akt activity by direct or indirect phosphorylation in VSMC. However, the moderate $\approx 12\%$ (versus saline) to 29% (versus TAT₄₇₋₅₇) reduction of Akt activity observed in our ϵ V1-2-treated balloon-denuded aortas failed to reach significance.

ϵ PKC inhibition may also attenuate VSMC chemotaxis following stimulation with PDGF. ERK activation is required for PDGF-induced VSMC chemotaxis²⁶ as well as for hyperglycemia-induced chemotaxis of VSMC and cross-talk between ERK and Akt signals.²⁷ Therefore, although not

assessed directly in this study, inhibition of chemotaxis of VSMC may also contribute to the benefit of ϵ V1–2 treatment on neointimal hyperplasia.

ϵ PKC is the only PKC isozyme that has been considered an oncogene, because it collaborates with Ras/Raf/ERK and Akt pathways to regulate cell survival and death.²⁸ Reverse, cytosolic translocation of ϵ PKC was shown to correlate with ceramide-induced apoptosis in leukemic cells.²⁹ ϵ PKC knockout mice exhibited significantly decreased survival,³⁰ whereas overexpression of ϵ PKC in rat embryo fibroblasts inhibited apoptosis induced by cisplatin.³¹ Antiapoptotic ϵ PKC further enhances antiapoptotic Bcl-2 members while inhibiting the proapoptotic members of the family.³² Our results reveal mild antiapoptotic effects of ϵ PKC activation in VSMC and demonstrate that ϵ PKC inhibition by ϵ V1–2 significantly increases apoptosis. In the context of postangioplasty restenosis, the inhibition of VSMC proliferation and the induction of VSMC apoptosis is appealing and has led to regression of experimental vascular lesions.³³ However, VSMC apoptosis in advanced plaques may also contribute to fibrous cap weakening and thereby promote plaque rupture and vessel thrombosis.

ϵ PKC Inhibition for the Prevention of Restenosis After Stent Placement

Driven by the success of reducing arterial restenosis with ϵ PKC inhibition, we next determined whether the effect would reproduce in a model of restenosis following stent placement. Because the ϵ PKC inhibitor ϵ V1–2 is a peptide, we could not use it for stent coating, and the drug delivery again was performed systemically via SC pumps. ϵ V1–2 significantly reduced both neointimal plaque area as determined by histology and luminal obliteration quantified by OCT. Similarly, the first studies demonstrating inhibition of restenosis by sirolimus were done using systemic drug administration.³⁴

In conclusion, ϵ PKC seems to be centrally involved in the development of neointimal hyperplasia, because contrarious modulations of ϵ PKC activation result in opposing effects. Interference with ϵ PKC-mediated activation of downstream PDGF pathway enzymes by ϵ V1–2 may be the mechanism of action. Targeting ϵ PKC may be a novel approach to control arterial restenosis.

Sources of Funding

This work was supported by the Falk Research Fund for the Department of Cardiothoracic Surgery at Stanford University School of Medicine, Stanford, CA; and by the Deutsche Forschungsgemeinschaft Research Grant SCHR992/3–1 (to S.S.).

Disclosures

D.M.-R. is the founder of KAI Pharmaceuticals. However, none of the research in her laboratory is supported by the company. The other authors have no disclosures to make.

References

- Roffey J, Rosse C, Linch M, Hibbert A, McDonald NQ, Parker PJ. Protein kinase C intervention: the state of play. *Curr Opin Cell Biol*. 2009;21:268–279.
- Murriel CL, Mochly-Rosen D. Opposing roles of δ and ϵ PKC in cardiac ischemia and reperfusion: targeting the apoptotic machinery. *Arch Biochem Biophys*. 2003;420:246–254.
- Parmentier JH, Zhang C, Estes A, Schaefer S, Malik KU. Essential role of PKC- ζ in normal and angiotensin II-accelerated neointimal growth

- after vascular injury. *Am J Physiol Heart Circ Physiol*. 2006;291:H1602–H1613.
- Chen L, Hahn H, Wu G, Chen CH, Liron T, Schechtman D, Cavallaro G, Banci L, Guo Y, Bolli R, Dorn GW II, Mochly-Rosen D. Opposing cardioprotective actions and parallel hypertrophic effects of δ PKC and ϵ PKC. *Proc Natl Acad Sci U S A*. 2001;98:11114–11119.
- Koyanagi T, Noguchi K, Ootani A, Inagaki K, Robbins RC, Mochly-Rosen D. Pharmacological inhibition of ϵ PKC suppresses chronic inflammation in murine cardiac transplantation model. *J Mol Cell Cardiol*. 2007;43:517–522.
- Inagaki K, Koyanagi T, Berry NC, Sun L, Mochly-Rosen D. Pharmacological inhibition of ϵ -protein kinase C attenuates cardiac fibrosis and dysfunction in hypertension-induced heart failure. *Hypertension*. 2008;51:1565–1569.
- Dorn GW II, Souroujon MC, Liron T, Chen CH, Gray MO, Zhou HZ, Csukai M, Wu G, Lorenz JN, Mochly-Rosen D. Sustained in vivo cardiac protection by a rationally designed peptide that causes ϵ protein kinase C translocation. *Proc Natl Acad Sci U S A*. 1999;96:12798–12803.
- Inagaki K, Begley R, Ikeno F, Mochly-Rosen D. Cardioprotection by ϵ -protein kinase C activation from ischemia: continuous delivery and antiarrhythmic effect of an ϵ -protein kinase C-activating peptide. *Circulation*. 2005;111:44–50.
- Deuse T, Erben RG, Ikeno F, Behnisch B, Boeger R, Connolly AJ, Reichen-spurner H, Bergow C, Pelletier MP, Robbins RC, Schrepfer S. Introducing the first polymer-free leflunomide eluting stent. *Atherosclerosis*. 2008;200:126–134.
- Gray MO, Karliner JS, Mochly-Rosen D. A selective ϵ -protein kinase C antagonist inhibits protection of cardiac myocytes from hypoxia-induced cell death. *J Biol Chem*. 1997;272:30945–30951.
- Begley R, Liron T, Barya J, Mochly-Rosen D. Biodistribution of intracellularly acting peptides conjugated reversibly to Tat. *Biochem Biophys Res Commun*. 2004;318:949–954.
- Kraft AS, Anderson WB. Phorbol esters increase the amount of Ca²⁺, phospholipid-dependent protein kinase associated with plasma membrane. *Nature*. 1983;301:621–623.
- Li L, Blumenthal DK, Masaki T, Terry CM, Cheung AK. Differential effects of imatinib on PDGF-induced proliferation and PDGF receptor signaling in human arterial and venous smooth muscle cells. *J Cell Biochem*. 2006;99:1553–1563.
- Langeveld B, Roks AJ, Tio RA, van Boven AJ, van der Want JJ, Henning RH, van Beusekom HM, van der Giessen WJ, Zijlstra F, van Gilst WH. Rat abdominal aorta stenting: a new and reliable small animal model for in-stent restenosis. *J Vasc Res*. 2004;41:377–386.
- Hamdan AD, Quist WC, Gagne JB, Feener EP. Angiotensin-converting enzyme inhibition suppresses plasminogen activator inhibitor-1 expression in the neointima of balloon-injured rat aorta. *Circulation*. 1996;93:1073–1078.
- Han O, Takei T, Basson M, Sumpio BE. Translocation of PKC isoforms in bovine aortic smooth muscle cells exposed to strain. *J Cell Biochem*. 2001;80:367–372.
- Choudhury GG, Mahimainathan L, Das F, Venkatesan B, Ghosh-Choudhury N. c-Src couples PI 3 kinase/Akt and MAPK signaling to PDGF-induced DNA synthesis in mesangial cells. *Cell Signal*. 2006;18:1854–1864.
- Izumi Y, Kim S, Namba M, Yasumoto H, Miyazaki H, Hoshiga M, Kaneda Y, Morishita R, Zhan Y, Iwao H. Gene transfer of dominant-negative mutants of extracellular signal-regulated kinase and c-Jun NH2-terminal kinase prevents neointimal formation in balloon-injured rat artery. *Circ Res*. 2001;88:1120–1126.
- Liu B, Fisher M, Groves P. Down-regulation of the ERK1 and ERK2 mitogen-activated protein kinases using antisense oligonucleotides inhibits intimal hyperplasia in a porcine model of coronary balloon angioplasty. *Cardiovasc Res*. 2002;54:640–648.
- Stabile E, Zhou YF, Saji M, Castagna M, Shou M, Kinnaird TD, Baffour R, Ringel MD, Epstein SE, Fuchs S. Akt controls vascular smooth muscle cell proliferation in vitro and in vivo by delaying G1/S exit. *Circ Res*. 2003;93:1059–1065.
- Zhan Y, Kim S, Izumi Y, Izumiya Y, Nakao T, Miyazaki H, Iwao H. Role of JNK, p38, and ERK in platelet-derived growth factor-induced vascular proliferation, migration, and gene expression. *Arterioscler Thromb Vasc Biol*. 2003;23:795–801.
- Hu Y, Cheng L, Hochleitner BW, Xu Q. Activation of mitogen-activated protein kinases (ERK/JNK) and AP-1 transcription factor in rat carotid arteries after balloon injury. *Arterioscler Thromb Vasc Biol*. 1997;17:2808–2816.

23. Poppel K, Zhang L, Orman ES, Hagen PO, Amalfitano A, Brian L, Freedman NJ. Activation of vascular smooth muscle cells by TNF and PDGF: overlapping and complementary signal transduction mechanisms. *Cardiovasc Res*. 2005;65:674–682.
24. Kawai-Kowase K, Owens GK. Multiple repressor pathways contribute to phenotypic switching of vascular smooth muscle cells. *Am J Physiol Cell Physiol*. 2007;292:C59–C69.
25. Saito Y, Hojo Y, Tanimoto T, Abe J, Berk BC. Protein kinase C- α and protein kinase C- ϵ are required for Grb2-associated binder-1 tyrosine phosphorylation in response to platelet-derived growth factor. *J Biol Chem*. 2002;277:23216–23222.
26. Graf K, Xi XP, Yang D, Fleck E, Hsueh WA, Law RE. Mitogen-activated protein kinase activation is involved in platelet-derived growth factor-directed migration by vascular smooth muscle cells. *Hypertension*. 1997;29:334–339.
27. Campbell M, Allen WE, Sawyer C, Vanhaesebroeck B, Trimble ER. Glucose-potentiated chemotaxis in human vascular smooth muscle is dependent on cross-talk between the PI3K and MAPK signaling pathways. *Circ Res*. 2004;95:380–388.
28. Basu A, Sivaprasad U. Protein kinase C ϵ makes the life and death decision. *Cell Signal*. 2007;19:1633–1642.
29. Sawai H, Okazaki T, Takeda Y, Tashima M, Sawada H, Okuma M, Kishi S, Umehara H, Domae N. Ceramide-induced translocation of protein kinase C- δ and - ϵ to the cytosol. Implications in apoptosis. *J Biol Chem*. 1997;272:2452–2458.
30. Castrillo A, Pennington DJ, Otto F, Parker PJ, Owen MJ, Bosca L. Protein kinase C ϵ is required for macrophage activation and defense against bacterial infection. *J Exp Med*. 2001;194:1231–1242.
31. Basu A, Cline JS. Oncogenic transformation alters cisplatin-induced apoptosis in rat embryo fibroblasts. *Int J Cancer*. 1995;63:597–603.
32. Gubina E, Rinaudo MS, Szallasi Z, Blumberg PM, Mufson RA. Overexpression of protein kinase C isoform ϵ but not δ in human interleukin-3-dependent cells suppresses apoptosis and induces bcl-2 expression. *Blood*. 1998;91:823–829.
33. Lemay J, Hale TM, deBlois D. Neointimal-specific induction of apoptosis by losartan results in regression of vascular lesion in rat aorta. *Eur J Pharmacol*. 2009;618:45–51.
34. Gallo R, Padurean A, Jayaraman T, Marx S, Roque M, Adelman S, Chesebro J, Fallon J, Fuster V, Marks A, Badimon JJ. Inhibition of intimal thickening after balloon angioplasty in porcine coronary arteries by targeting regulators of the cell cycle. *Circulation*. 1999;99:2164–2170.

Video Article

Human Internal Mammary Artery (IMA) Transplantation and Stenting: A Human Model to Study the Development of In-Stent Restenosis

Xiaoqin Hua^{1,2}, Tobias Deuse^{1,2}, Evangelos D. Michelakis³, Alois Haromy³, Phil S. Tsao⁴, Lars Maegdefessel⁴, Reinhold G. Erben⁵, Claudia Bergow⁵, Boris B. Behnisch⁶, Hermann Reichenspurner^{1,2}, Robert C. Robbins⁷, Sonja Schrepfer^{1,2,7}

¹University Heart Center Hamburg, TSI-Lab, Germany

²Cardiovascular Research Center, University of Hamburg

³Department of Medicine, Cardiology Division, Pulmonary Hypertension Program, University of Alberta

⁴Department of Medicine, Stanford University School of Medicine

⁵Department of Biomedical Sciences, Institute of Physiology, Pathophysiology, and Biophysics, University of Veterinary Medicine, Vienna

⁶Translumina GmbH, Hechingen

⁷Department of Cardiothoracic Surgery, Stanford University School of Medicine

Correspondence to: Sonja Schrepfer at schrepfer@stanford.edu

URL: <http://www.jove.com/video/3663/>

DOI: 10.3791/3663

Keywords: ,

Date Published: //

Citation: Hua, X., Deuse, T., Michelakis, E.D., Haromy, A., Tsao, P.S., Maegdefessel, L., Erben, R.G., Bergow, C., Behnisch, B.B., Reichenspurner, H., Robbins, R.C., Schrepfer, S. Human Internal Mammary Artery (IMA) Transplantation and Stenting: A Human Model to Study the Development of In-Stent Restenosis. *J. Vis. Exp.* (), e3663, DOI : 10.3791/3663 ().

Abstract

Preclinical *in vivo* research models to investigate pathobiological and pathophysiological processes in the development of intimal hyperplasia after vessel stenting are crucial for translational approaches^{1,2}.

The commonly used animal models include mice, rats, rabbits, and pigs³⁻⁵. However, the translation of these models into clinical settings remains difficult, since those biological processes are already studied in animal vessels but never performed before in human research models^{6,7}. In this video we demonstrate a new humanized model to overcome this translational gap. The shown procedure is reproducible, easy, and fast to perform and is suitable to study the development of intimal hyperplasia and the applicability of diverse stents.

This video shows how to perform the stent technique in human vessels followed by transplantation into immunodeficient rats, and identifies the origin of proliferating cells as human.

Video Link

The video component of this article can be found at <http://www.jove.com/video/3663/>

Protocol

1. IMA preparation

1. The arterial endothelium is denuded by the passage of a 2-french Fogarty arterial embolectomy catheter (Baxter Healthcare, Deerfield, IL, USA). The catheter is pulled through the whole vessel length twice to ensure endothelial damage.
2. Use any human stent of 8mm length and 2.5 mm-3 mm in diameter (e.g. Translumina, Yukon stent). CAUTION: The diameter of the stent should not exceed the vessel diameter by more than 10% to avoid pre- and post-stent stenosis. CAUTION: Don't switch the length of the stent within the same study.
3. Deploy the stent using the appropriate balloon pressure (which is noted on the stent package) to achieve the desired diameter.
4. Store stented IMA in 4 °C RPMI + heparin (500 IE/10 ml) on ice until transplantation.

2. Animal preparation

RNU Nude (Cri:NIH-*Foxn1^{tmu}*) rats (300-350 g) are housed under conventional conditions in scantainer ventilated cabinets, fed standard rat chow and autoclaved water ad libidum.

1. Anesthetize rat with isoflurane (2.5-3%) using an induction chamber.
2. Shave the abdominal hair and place the rat on its back and place a facemask over its nose and mouth to keep up the anesthesia.
3. Disinfect the abdominal area widely using Provo-Iodine, next use 80% ethanol - repeat this step twice. Check reflexes pinching the hind feet to be sure that the rat is sufficient anesthetized.
4. Under microscopic view, perform an upper median laparotomy to expose the infrarenal abdominal aorta.
5. Place the intestines in a saline moisturized glove. Fold the glove around the intestines to prevent loss of moisture.
6. Dissect the aorta from the infrarenal region to the bifurcation, carefully not to cause damage on the branches of the vessels.
7. Use micro clamps to stop the aortic blood flow. Place the proximal clamp first, followed by the distal clamp.

8. Remove an app. 0.5-0.7 mm aortic segment and flush the remaining aorta with heparin (200 units).
9. Take the stented IMA and shorten it to the adequate length and position it into the gap.10. Connect the IMA to the recipient aorta, by running sutures using 8-0 prolene suture (Ethicon, Norderstedt, Germany).
10. Connect the IMA to the recipient aorta, by running sutures using 8-0 prolene suture (Ethicon, Norderstedt, Germany).
11. Carefully open the cranial clamp.
12. There should be a visible pulse in the transplanted IMA and at the distal end of the aorta.
13. Place the intestines back into the abdomen.
14. Flush the abdomen with prewarmed sterile saline.
15. Close the muscle layer of the abdominal wall using 6-0 prolene running sutures (Ethicon, Norderstedt, Germany).
16. While the rat is still in anesthesia, inject 4-5 mg/kg Carprofen subcutaneously.
17. Metamizol is added to the drinking water (50mg Metamizol per 100 mL) for pain medication for 3 days post surgery.

3. Representative Results

For histology, the specimens were fixed in 4% formalin, dehydrated in a graded series of alcohol, and infiltrated in a mixture (MMA I) of 80% methylmethacrylate and 20% dibutylphthalate for 1 day, MMA I with 1% dry benzoyl peroxide for 1 day, and MMA I with 3% dry benzoyl peroxide (MMA III) for 1-2 days at 4 °C. Thereafter, the specimens were polymerized in fresh MMA III in glass vials in a water bath on a pre-polymerized base. Slow polymerization was achieved by keeping the vials at 26 °C overnight, increasing the temperature to 28 °C the next morning, and then increasing the temperature gradually by 0.5 °C over 12 h until polymerization occurred. The polymerized blocks were sectioned at 5 µm thickness using a MICROM HM 360 microtome equipped with a tungsten carbide knife.

To identify the origin of proliferating cells (figure 1), slides were stained with antibodies identifying either the green fluorescent protein (GFP) or rat MHC-I and human smooth muscle cells. For these studies, human IMA was incubated with the reporter gene GFP overnight using lentiviral particles for stable transduction of IMA cells. Dividing daughter cells from human origin could be identified by expressing GFP. After deparaffinization, heat-induced epitope retrieval is performed by heating the slides in antigen retrieval solution using a steamer. The Image-iT FX signal enhancer can be used for the blocking step. Cells of human origin are identified using the mouse monoclonal antibodies against GFP (1:100 diluted in primary antibody diluent (Dako)), and further labeled with goat-anti-mouse IgG, Alexa Fluor 488 (1:1000 diluted in secondary antibody diluent). The smooth muscle cells were marked with the rabbit polyclonal anti-smooth muscle α-actin (1:100 diluted in primary antibody diluent), followed by goat-anti-rabbit IgG, Alexa Fluor 555 (1:1000 diluted in secondary antibody diluents). Each antibody incubation step is performed at 37 °C for 1 hour with three times PBS washing in between. Nuclei are stained with DAPI for 10 minutes. After mounting of the slides using Prolong Gold antifade reagent, samples were analyzed using confocal microscopy.

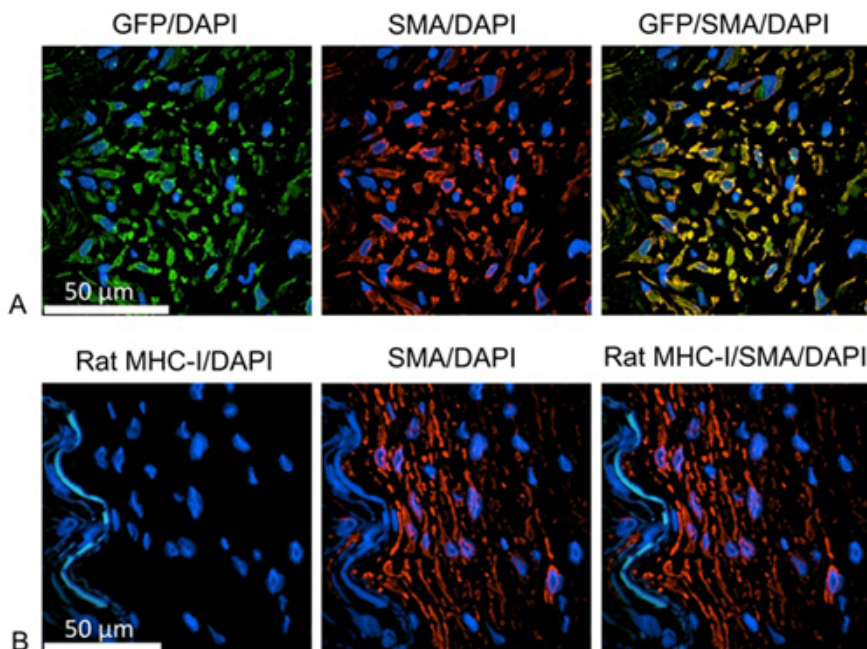


Figure 1. the neointimal cells as human smooth muscle cells.

A: Green= anti GFP, labeling cells of human origin; red=anti human smooth muscle cell actin; blue=DAPI, identifying cell nuclei.

B: Green= anti rat MHC-I, labeling cells of rat origin; red=anti human smooth muscle cell actin; blue=DAPI, identifying cell nuclei.

Proliferating cells are identified as smooth muscle cells and positive for GFP, but negative for the rat MHC-I molecule. Therefore, proliferating cells are human origin.

Discussion

Although different *in vivo* research models are existing to investigate the development of intimal hyperplasia after stent placement, these models still facing translational hurdles to overcome. Furthermore, large animal models are expensive and special housing conditions as well as surgical equipment is not available for all laboratories.

Using a human IMA to study the development of human intimal proliferation and in-stent restenosis was studied before *ex situ* in organ cultures^{8,9}. The new humanized IMA model constitutes a translational approach to address the issue of in stent re-stenosis *in vivo*, by implanting the

human IMA into the abdominal aortic position of immunodeficient rats. Human IMA's are a perfect match to the size of the abdominal aorta of rats. Therefore, our presented model is reproducible, easy and fast to perform, does not require special surgical training, and is inexpensive.

The identification of the neointimal cells as human smooth muscle cells closes the translational gap to clinical settings and shows the opportunity to investigate human pathophysiological processes *in vivo*.

Disclosures

No conflicts of interest declared.

Acknowledgements

The authors thank Christiane Pahrman for her contribution. Special thanks to Ethicon, Norderstedt, Hamburg (Germany) for providing the suture material.

Funding

Sonja Schrepfer has received a research grant from the Deutsche Forschungsgemeinschaft (DFG) (SCHR992/3 1 and SCHR992/4-1).] The work was supported by the ISHLT Shumway Career Development Grant 2010 and the Falk Research Funding (Stanford University).

References

1. Deuse, T., Ikeno, F., Robbins, R.C., & Schrepfer, S. Imaging in-stent restenosis: an inexpensive, reliable, and rapid preclinical model. *Journal of visualized experiments : JoVE*. doi:10.3791/1346 (2009).
2. Oyamada, S., *et al.* Trans-iliac rat aorta stenting: a novel high throughput preclinical stent model for restenosis and thrombosis. *J. Surg. Res.* **166**, e91-95, doi:10.1016/j.jss.2010.11.882 (2011).
3. Chamberlain, J., *et al.* A novel mouse model of in situ stenting. *Cardiovascular research.* **85**, 38-44, doi:10.1093/cvr/cvp262 (2010).
4. Deuse, T., *et al.* Introducing the first polymer-free leflunomide eluting stent. *Atherosclerosis.* **200**, 126-134, doi:10.1016/j.atherosclerosis.2007.12.055 (2008).
5. Finn, A.V., *et al.* Differential healing after sirolimus, paclitaxel, and bare metal stent placement in combination with peroxisome proliferator-activator receptor gamma agonists: requirement for mTOR/Akt2 in PPARgamma activation. *Circulation research.* **105**, 1003-1012, doi:10.1161/CIRCRESAHA.109.200519 (2009).
6. Tellez, A., *et al.* Coronary bare metal stent implantation in homozygous LDL receptor deficient swine induces a neointimal formation pattern similar to humans. *Atherosclerosis.* **213**, 518-524, doi:10.1016/j.atherosclerosis.2010.09.021 (2010).
7. Suzuki, Y., Yeung, A.C., & Ikeno, F. The pre-clinical animal model in the translational research of interventional cardiology. *JACC Cardiovasc. Interv.* **2**, 373-383, doi:10.1016/j.jcin.2009.03.004 (2009).
8. Holt, C.M., *et al.* Intimal proliferation in an organ culture of human internal mammary artery. *Cardiovascular research.* **26**, 1189-1194 (1992).
9. Swanson, N., Javed, Q., Hogrefe, K., & Gershlick, A. Human internal mammary artery organ culture model of coronary stenting: a novel investigation of smooth muscle cell response to drug-eluting stents. *Clin Sci (Lond).* **103**, 347-353, doi:10.1042/ (2002).

Localization of Islet-1–Positive Cells in the Healthy and Infarcted Adult Murine Heart

Florian Weinberger,* Dennis Mehrkens,* Felix W. Friedrich, Mandy Stubbendorff, Xiaoqin Hua, Jana Christina Müller, Sonja Schrepfer, Sylvia M. Evans, Lucie Carrier, Thomas Eschenhagen

Rationale: The transcription factor Islet-1 is a marker of cardiovascular progenitors during embryogenesis. The isolation of Islet-1–positive (Islet-1⁺) cells from early postnatal hearts suggested that Islet-1 also marks cardiac progenitors in adult life.

Objective: We investigated the distribution and identity of Islet-1⁺ cells in adult murine heart and evaluated whether their number or distribution change with age or after myocardial infarction.

Methods and Results: Distribution of Islet-1⁺ cells in adult heart was investigated using gene targeted mice with nuclear β -galactosidase inserted into the Islet-1 locus. nLacZ-positive cells were only present in 3 regions of the adult heart: clusters in the interatrial septum and around the pulmonary veins, scattered within the wall of the great vessels, and a strictly delimited cluster between the right atrium and superior vena cava. Islet-1⁺ cells in the first type of clusters coexpressed markers for parasympathetic neurons. Positive cells in the great arteries coexpressed smooth muscle actin and myosin heavy chain, indicating a smooth muscle cell identity. Very few Islet-1⁺ cells within the outflow tract expressed the cardiomyocyte marker α -actinin. Islet-1⁺ cells in the right atrium coexpressed the sinoatrial node pacemaker cell marker HCN4. Cell number and localization remained unchanged between 1 to 18 months of age. Consistently Islet-1 mRNA was detected in human sinoatrial node. Islet-1⁺ cells could not be detected in the infarct zone 2 to 28 days after myocardial infarction, aside from 10 questionable cells in 1/13 hearts.

Conclusions: Our results identify Islet-1 as a novel marker of the adult sinoatrial node and do not provide evidence for Islet-1⁺ cells to serve as cardiac progenitors. (*Circ Res.* 2012;110:1303-1310.)

Key Words: cardiac transcription factors ■ cardiac progenitor cells ■ sinoatrial node

Myocardial damage after myocardial infarction or other cardiac diseases results in loss of working myocardium and subsequent heart failure. Within the past years, improved revascularization strategies have enabled more patients to survive myocardial infarction, thereby increasing the incidence of heart failure.¹ Despite new pharmacological and device-based therapies prognosis for heart failure remains poor, and new therapeutic options are urgently needed. In this context, regenerative approaches have gained increasing attention. Adult cardiac myocytes were classically regarded as withdrawn from the cell cycle. This dogma has been challenged by recent findings suggesting that a very small fraction of adult cardiomyocytes in human heart is regenerated.² Fate-mapping experiments in mice provided

evidence that cells from an unknown source differentiate into cardiomyocytes after myocardial injury, but not in healthy hearts.³ A subsequent study showed that this effect can be stimulated by bone marrow cell therapy, probably due to stimulation of endogenous cardiac progenitors.⁴ A study using a feline model also suggested cardiac regeneration by endogenous progenitor cells.⁵ These data lend support to the concept of resident cardiac stem or progenitor cells as proposed earlier.⁶ These cell types have been characterized by the expression of general (c-kit,⁷ and sca-1⁸) or more restricted (Islet-1⁹) stem or progenitor cell marker proteins. Their stimulation might be a particularly attractive therapeutic strategy as it avoids immunologic problems and could be achieved pharmacologically. Yet,

Original received October 25, 2011; revision received March 7, 2012; accepted March 8, 2012. In February 2012, the average time from submission to first decision for all original research papers submitted to *Circulation Research* was 13.77 days.

From the Department of Experimental Pharmacology and Toxicology, Cardiovascular Research Center, University Medical Center Hamburg-Eppendorf, Hamburg, Germany (F.W., D.M., F.W.F., L.C., T.E.); the Department of Cardiovascular Surgery, TSI-Lab, Cardiovascular Research Center, University Medical Center Hamburg-Eppendorf, Hamburg, Germany (M.S., X.H., S.S.); the Institute of Cellular and Integrative Physiology, Cardiovascular Research Center, University Medical Center Hamburg-Eppendorf, Hamburg, Germany (J.C.M.); the Skaggs School of Pharmacy and Pharmaceutical Science, University of California San Diego, San Diego, CA (S.M.E.); and Inserm UMR-S974, CNRS UMR7215, Institut de Myologie, IFR14, Paris6 University, Paris, France (L.C.).

*F.W. and D.M. contributed equally to this work.

The online-only Data Supplement is available with this article at <http://circres.ahajournals.org/lookup/suppl/doi:10.1161/CIRCRESAHA.111.259630/-DC1>.

Correspondence to Thomas Eschenhagen, MD, Department of Experimental Pharmacology and Toxicology, University Medical Center Hamburg-Eppendorf, Martinistraße 52, 20246 Hamburg, Germany. E-mail t.eschenhagen@uke.de

© 2012 American Heart Association, Inc.

Circulation Research is available at <http://circres.ahajournals.org>

DOI: 10.1161/CIRCRESAHA.111.259630

Non-standard Abbreviations and Acronyms

| | |
|--------------|--|
| AChE | acetylcholinesterase |
| AVN | atrioventricular node |
| ChAT | choline acetyltransferase |
| HGN4 | potassium/sodium hyperpolarization-activated cyclic nucleotide-gated channel 4 |
| SAN | sinoatrial node |
| X-gal | bromo-chloro-indolyl-galactopyranoside |

the existence, relevance and character of resident cardiac progenitors remain ambiguous.¹⁰

Editorial, see p 1267
In This Issue, see p 1265

Cells that express the transcription factor Islet-1 are attractive candidates as resident cardiac progenitors because the role of Islet-1 in early cardiac development has been unambiguously demonstrated. Islet-1 is a transcription factor of the LIM-homeodomain family, which was first identified in the β -cells of the pancreas as an enhancer of the insulin gene.¹¹ It has been extensively studied in the nervous system, where it is essential for the differentiation of motor neurons.^{12,13} Islet-1 became popular in the field of cardiovascular research after the discovery of severe cardiac malformation in Islet-1-deficient mice. These animals lack the outflow tract, the right ventricle, and most of the atria. Lineage tracing studies revealed that these structures originate from Islet-1 positive (Islet-1⁺) precursors.¹⁴ Islet-1⁺ cells do not only differentiate into cardiac myocytes but also contribute to the formation of the sinoatrial node (SAN), the atrioventricular node (AVN), and smooth muscle cells of the coronary arteries.¹⁵ Importantly, murine Islet-1⁺ cells retain this wide cardiovascular differential potential *in vitro* when isolated

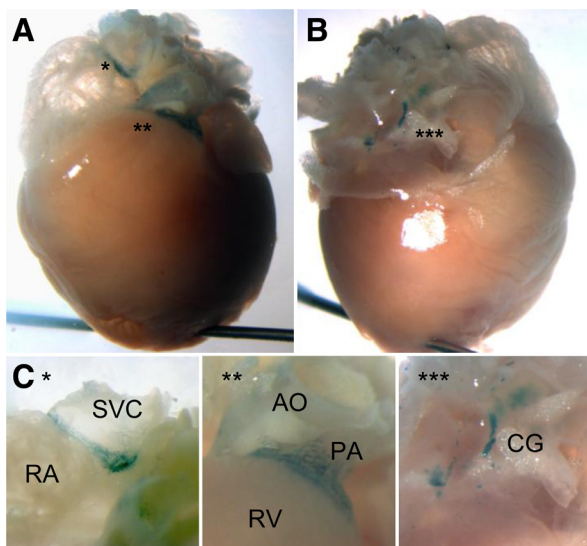


Figure 1. nLacZ⁺ cells in an Isl-1-nLacZ adult mouse heart. **A**, Anterior view, and **B**, posterior view of a 20-week-old Isl-1-nLacZ-mouse heart after X-gal staining. **C**, Magnification of the nLacZ⁺ structures marked with asterisks in **A** and **B**. AO indicates aorta; CG, cardiac ganglion; PA, pulmonary artery; RA, right atrium; RV, right ventricle; and SVC, superior vena cava.

from embryonic and neonatal hearts^{16,17} or from murine or human embryonic stem cells.^{9,16} Islet-1⁺ cells from embryonic and neonatal hearts can therefore be regarded as real cardiac progenitors. Recently, small numbers of Islet-1⁺ cells were identified in adult heart.^{18,19} Khattar et al differentiated 2 clusters of Islet-1⁺ cells in adult murine hearts,¹⁸ and Genead et al detected Islet-1⁺ cells in hearts of young adult rats.¹⁹ Both studies relied on immunofluorescent methods, which are subject to ambiguity because of the extremely low expression level of Islet-1. Furthermore, they are not well suited to analyze the exact anatomic localization of scattered cells in 3D. The present study used a genetic approach to improve the sensitivity and specificity of detection of Islet-1⁺ cells and evaluated their localization and number throughout adult life and after myocardial infarction.

Methods

An expanded Methods section is available in the Online Data Supplement.

Animals

The investigation conforms to the *Guide for the Care and Use of Laboratory Animals* published by the NIH (Publication No. 85-23, revised 1985). Isl-1-nLacZ-mice were created by targeted insertion of a DNA cassette containing nLacZ in exon 1 of the Islet-1 gene.¹³ Final investigations were done in heterozygous Isl-1-nLacZ-mice on a mixed Blackswiss and C57BL/6J background, and wild-type littermates were used as controls.

Bromo-Chloro-Indolyl-Galactopyranoside Staining

Hearts were perfusion-fixed with 4% paraformaldehyde, washed in 0.9% NaCl, and afterward incubated in a staining solution containing

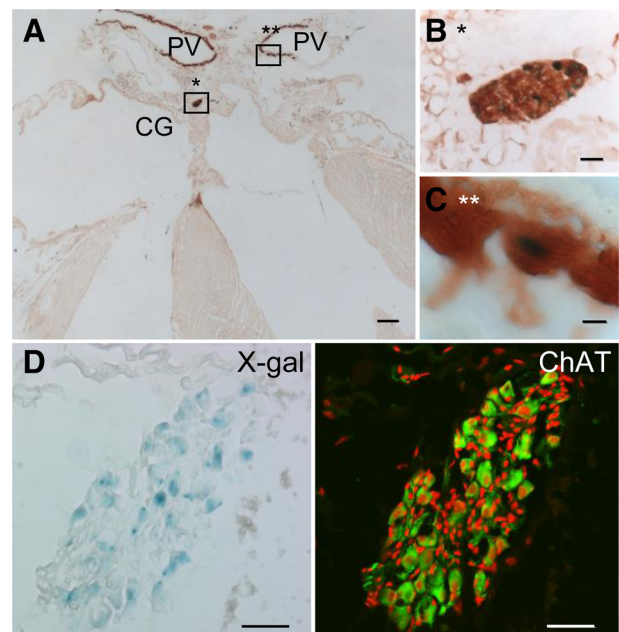


Figure 2. Characterization of nLacZ⁺ cells in the interatrial septum and around the pulmonary veins. AChE⁺ (brown) and nLacZ⁺ cells (blue nucleus) in a cardiac parasympathetic ganglion in **A**, low magnification, and **B**, high magnification. **C**, Single nLacZ⁺ cell around a pulmonary vein. Asterisks in **A** mark structures showed in higher magnification in **B** and **C**. **D**, Brightfield and confocal microscopy showing coexpression of ChAT (green) and β -gal in a parasympathetic ganglion. Nuclei are stained red (DRAQ5). CG indicates cardiac ganglion; PV, pulmonary vein. Scale bars: 500 μ m (**A**), 20 μ m (**B**), and 10 μ m (**C** and **D**).

potassium ferrocyanide (5 mmol/L), potassium ferricyanide (5 mmol/L), MgCl₂ (2 mmol/L), 0.02% NP-40, 0.01% sodium deoxycholate, Tris pH 7.4 (20 mmol/L), and 1 mg/mL bromo-chloro-indolyl-galactopyranoside (X-Gal) in phosphate-buffered saline for 2 hours at 37°C. Cells were fixed in 0.05% glutaraldehyde for 10 minutes at 4°C and afterward incubated in the staining solution overnight. Islet-1⁺ cells could be visualized by a blue nuclear signal.

Histology

Serial cryosections (10 μm) were either performed in a 4-chamber view or a transversal short-axis view. All sections were collected. Sections were postfixed in 4% paraformaldehyde for 10 minutes at room temperature and eosin-counterstained to allow for an overview. Consecutive sections were used for immunofluorescence, immunohistochemistry, and staining for cholinesterase activity.

Isolation of Smooth Muscle Cells

The ascending aorta and the pulmonary artery were excised, cleared of connective tissue, and longitudinally opened. Aorta and pulmonary artery were cut into 5 to 10 pieces, which were transferred onto 35-mm cell culture plates. These pieces were cultured in DMEM containing 10% FCS, and 1% penicillin/streptomycin and immunofluorescence was performed before the cells formed a confluent monolayer.

Preparation of mRNA From Murine and Human SAN Tissue

Mice were euthanized by cervical dislocation. Hearts were quickly removed and placed in modified Tyrode solution (NaCl 119.8 mmol/L, KCl 5.4 mmol/L, CaCl₂ 0.2 mmol/L, MgCl₂ 1.05 mmol/L, NaHCO₃ 22.6 mmol/L, NaH₂PO₄ 0.42 mmol/L, glucose 5.05 mmol/L, Na₂EDTA 0.05 mmol/L, ascorbic acid 0.56 mmol/L). The SAN region (approximately 1 × 1 mm) was carefully dissected using a Stemi SV6 stereo microscope (Zeiss). We obtained human SAN tissue, which was routinely prepared from postmortem human hearts, as described by Hudson,²⁰ during scientific autopsy (between 1–3 days postmortem). RNA was isolated using the High-Capacity cDNA RT-Kit (Applied Biosystem).

Isolation of Mouse SAN Cells

Isolation of SAN cells was performed according to Mangoni et al.²¹ The SAN region was dissected as described above and isolation of

SAN cells was achieved by digestion using Liberase TH (Roche Applied Science) and manual agitation.

Results

The distribution of Islet-1⁺ cells was investigated in 30 heterozygous Islet-1–LacZ mice at different time points after birth (10 weeks to 18 months). After light perfusion-fixation and X-gal staining, nLacZ⁺ cells were easily recognizable by eye or stereo microscopy when present in clusters. Microscopic identification of even single isolated nLacZ⁺ cells was unambiguous due to the nuclear restriction of the blue signal and immunohistochemistry showed that nLacZ⁺ cells expressed Islet-1 (Online Figure I and Sun et al¹⁵). Hearts from 6 nontransgenic littermates that were subjected to identical fixation and staining procedures did not show any comparable signal (Online Figure II).

nLacZ⁺ cells were not randomly distributed within the heart but were strictly confined to certain anatomic structures. There was no macroscopic or microscopic evidence for nLacZ⁺ cells in the muscular layer of the left or right ventricular walls (Online Figure III; n=20, ≈500–600 slices per heart). In contrast, we consistently identified three different regions of nLacZ⁺ cells in adult heart (Figure 1A through 1C). Two regions were visible in an anterior view of the heart (Figure 1A) and a third region was located at the back of the heart (Figure 1B). A cluster of nLacZ⁺ cells was located in the border zone between right atrium and the superior vena cava. nLacZ⁺ cells were also scattered around the proximal part of the great vessels (aorta and pulmonary artery). The additional clusters on the back of the heart contained only few nLacZ⁺ cells (2–50 cells). These small clusters were located around the pulmonary veins and inside the interatrial septum. Very few single nLacZ⁺ cells were localized along the wall of the pulmonary veins. We identified positive cells in these 3 anatomic regions in all transgenic animals that were analyzed and did not observe alterations of localization or cell number with age.

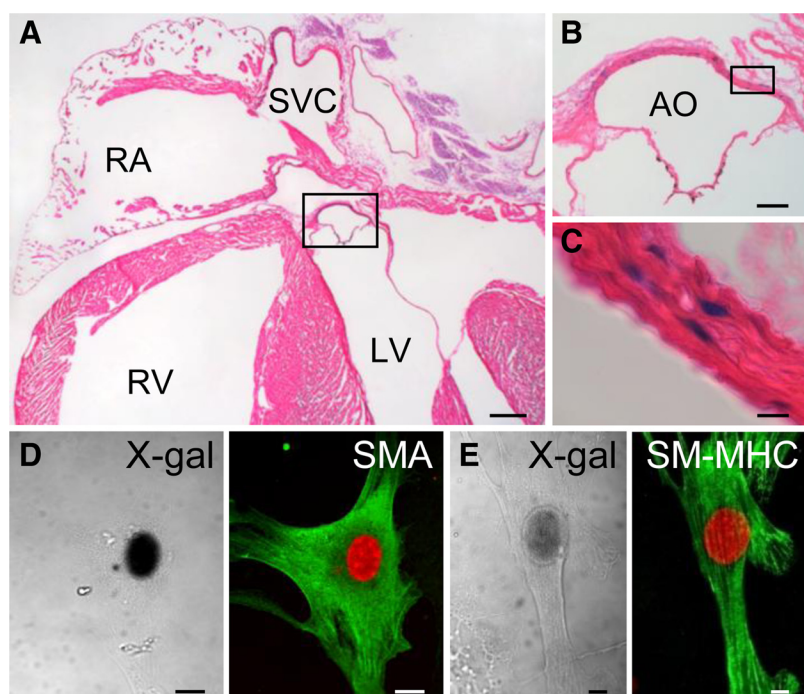


Figure 3. Characterization of nLacZ⁺ cells in the proximal aorta and pulmonary artery. A through C, nLacZ⁺ cells in the muscular layer of the proximal aorta after X-gal staining and eosin counterstaining. D and E, nLacZ⁺ cells cultured after isolation from the proximal pulmonary artery, stained with X-gal and antibodies against smooth muscle α -actin (D, green) and smooth muscle myosin heavy chain (E, green). Nuclei are stained red (DRAQ5). Visualization by differential interference contrast confocal microscopy (DIC) and confocal fluorescent microscopy. Note the black nucleus in DIC as sign of nLacZ⁺ positivity. AO indicates aorta; LV, left ventricle; RA, right atrium; RV, right ventricle; and SVC, superior vena cava. Scale bars: 500 μm (A), 100 μm (B), and 10 μm (C through E).

The clusters of nLacZ⁺ cells on the posterior side of the heart consisted of round, large cells. Further characterization revealed that these were cardiac ganglia, as shown by the coexpression of acetylcholinesterase (AChE; Figure 2A through 2C). Coexpression of β -galactosidase (β -gal) and the parasympathetic marker choline acetyltransferase (ChAT) characterized them as parasympathetic ganglia (Figure 2D). Very few single nLacZ⁺ neurons were located in the nervous plexus surrounding the pulmonary veins (Figure 2C).

nLacZ⁺ cells were also detected in the proximal part of the aorta and the trunk of the pulmonary artery (Figure 1 and Figure 3A through 3C). The absolute majority of these cells were located in the muscular layer above the aortic and pulmonary valve. We isolated these cells for further characterization. They coexpressed β -gal and the smooth muscle markers smooth muscle actin and smooth muscle myosin heavy chain (Figure 3D and 3E). Very few single nLacZ⁺ cells were present in the aortic valve leaflets (Figure 4A and 4C). A third type of nLacZ⁺ cells existed in the left ventricular outflow tract region (Figure 4A through 4E), where a small number of nLacZ⁺ cells coexpressed β -gal and the cardiomyocyte marker α -actinin, indicating that these were cardiomyocytes.

A fourth type of nLacZ⁺ cells was located in the muscular wall of the right atrium. These cells were aligned along the border zone between the right atrium and the vena cava superior (Figure 1 and Online Figure IV) and expressed the cardiomyocyte marker α -actinin (Figure 5A and 5D). Because of the peculiar localization between right atrium and vena cava superior and the typical “comma-shaped” form, we performed staining for the SAN marker hyperpolarization-activated cyclic nucleotide-gated channel 4 (HCN4). Costaining for HCN4 and X-gal indicated that these cells were SAN cells (Figure 5B, 5C, 5E, and 5F). Interestingly, only a subpopulation (approximately 50%) of HCN4-positive cells stained positive for nLacZ. The AChE-positive and HCN4-positive AVN was consistently negative for nLacZ⁺ cells (Online Figure V). Isolation of cells from the SAN region resulted in single cells showing typical heterogeneous morphology (spindle-shaped, elongated spindle-shaped, atrial-like). Compared with whole-mount histologies, a much smaller subpopulation (0.1% to 5%) of the isolated cells stained positive for β -gal (Figure 6).

To investigate whether Islet-1 is also expressed in murine wild-type and human SAN, we isolated RNA from murine and postmortem human SAN tissue. Islet-1 mRNA was detectable in all tissue samples containing the SAN in C57BL/6J from 12 to 44 weeks of age (n=31), but not from the corresponding atrial or ventricular myocardium (Figure 7A). Islet-1 mRNA was also detectable in human postmortem samples containing the SAN, but not from the corresponding ventricular myocardium (n=4; Figure 7B).

To investigate the role of Islet-1⁺ cells after myocardial injury, we subjected a group of Isl-1-LacZ mice to myocardial infarction and examined the hearts at different time points after ischemic injury (2, 7, 14, and 28 days after left anterior descending artery ligation, n=3–4; Figure 8A through 8D). nLacZ⁺ cells could still be detected in the SAN, the trunk of the great vessels, and cardiac ganglia (Online VI, A through C) but were not present in the infarct region in 12 of 13 examined hearts

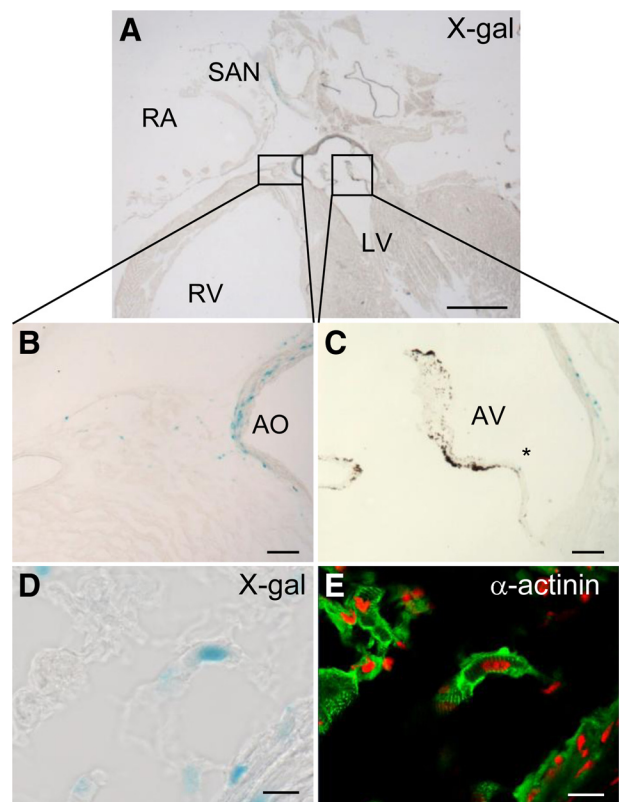


Figure 4. nLacZ⁺ cells in the outflow tract and the aortic valve. **A**, Histological overview, showing the localization of nLacZ⁺ cells in the muscular layer of the outflow tract, and **B**, high magnification after X-gal staining. **C**, Asterisk marks a single nLacZ⁺ cell in the aortic valve in high magnification. **D**, Brightfield visualization of nLacZ⁺ cells scattered in the myocardium of the outflow tract and the muscular layer of the proximal aorta. **E**, Corresponding staining for α -actinin (**E**, green), showing the typical cross-striation in a nLacZ⁺ cell in the myocardium of the outflow tract. AO indicates aorta; AV, aortic valve; LV, left ventricle; RA, right atrium; RV, right ventricle; and SAN, sinoatrial node. Scale bars: 500 μ m (**A**), 100 μ m (**B**), and 10 μ m (**C**).

2, 14, and 28 days after myocardial infarction (in >4000 analyzed sections). However, in 1 heart examined 7 days after myocardial infarction, we observed 10 questionable cells in the infarct area showing atypical but clearly nuclear LacZ staining (Online Figure VII, A).

Discussion

The transcription factor Islet-1 marks a population of cardiovascular progenitors of the second heart field in early murine development.¹⁴ The observation that few Islet-1⁺ cells are also present in the early postnatal heart and can differentiate into cells of all 3 cardiovascular cell types *in vitro*^{16,17} led to the idea that Islet-1⁺ cells represent a resident cardiac progenitor cell population with therapeutic potential.²² By using gene targeted Islet-1 nLacZ knock-in mice we provide evidence that the postnatal (1–18 months) murine heart is essentially devoid of Islet-1⁺ cells except well defined and consistent populations in the SAN, a fraction of cardiac ganglia, the media of the proximal aspects of the aorta, and pulmonary artery and very few single cells in the outflow tract area. Given the high sensitivity and specificity of nLacZ staining and the consistency of the staining pattern we believe that the findings are unambiguous.

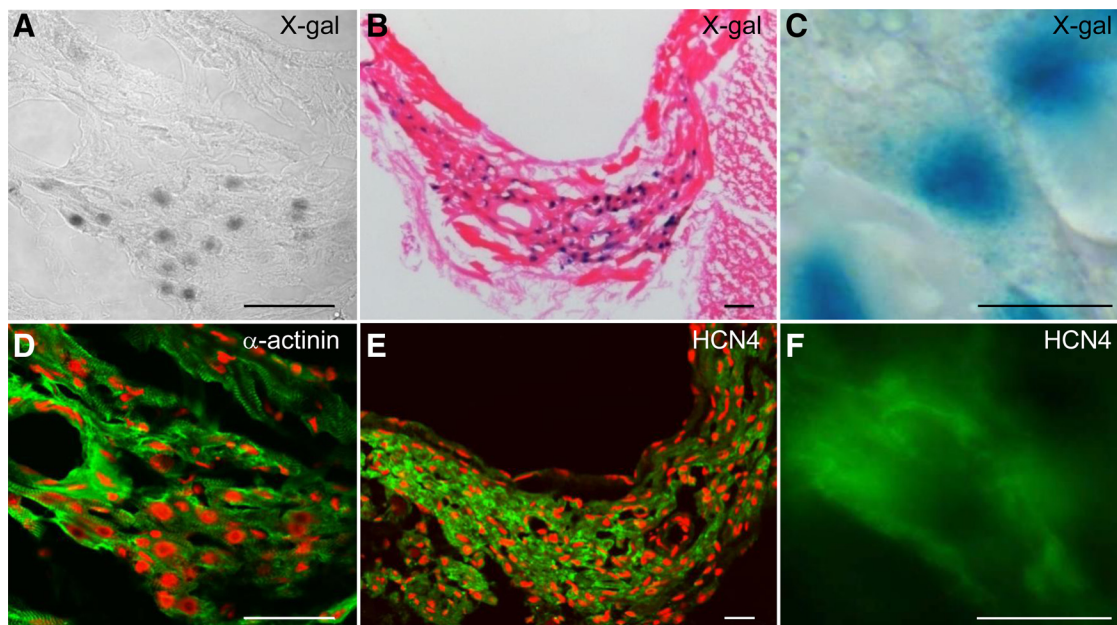


Figure 5. nLacZ⁺ cells in the sinoatrial node. **A**, Differential interference contrast confocal microscopy, and **B** and **C**, brightfield microscopy. **D** through **F**, Corresponding immunofluorescence staining for α -actinin (**D**, green) and HCN4 (**E** and **F**, green). Nuclei are stained red (DRAQ5). Scale bars: 20 μ m (**A** and **B**) and 10 μ m (**C**).

Our results are mainly consistent with 2 recent findings and significantly expand them.^{18,19} Khattar et al described Islet-1-expressing cells in 2 types of clusters in close proximity to the heart basis. One consisted of neuronal cells and a second one was formed by cardiomyocytes. In a longitudinal study, Genead et al identified single Islet-1⁺ cells in the outflow tract of young adult rats that expressed the cardiomyocyte marker troponin T. Both studies mainly relied on classic immunohistological techniques. The difference between these findings may indicate species differences. On the other hand they might also be due to technical limitations. In the light of the present findings, the first cluster most likely represented parasympathetic ganglia, the second one the SAN and the troponin T⁺/Islet-1⁺ cells in the outflow tract of rats correspond to the few nLacZ⁺ cardiomyocytes in our model.

The first, also macroscopically visible clusters of nLacZ⁺ cells, were located in the posterior aspects of the atria and around the pulmonary veins. These cells were marked as parasympathetic neurons by their coexpression of AChE and ChAT. AChE marks neuronal structures in general, whereas ChAT almost exclusively marks parasympathetic neurons.^{23,24} The finding of Islet-1 expression in differentiated neurons was not surprising since it was known from chicken embryos that Islet-1 expression persists in neurons after leaving the cell cycle.²⁵ Additionally, recent studies by Sun et al have demonstrated a key role for Islet-1 in sensory neuron development.²⁶ Interestingly, not all cardiac ganglia contained nLacZ⁺ cells. Rysevaite et al described about twenty AChE-positive cardiac ganglia in the adult murine heart.²⁷ Similar to their results, we observed cardiac ganglia of different size and cell

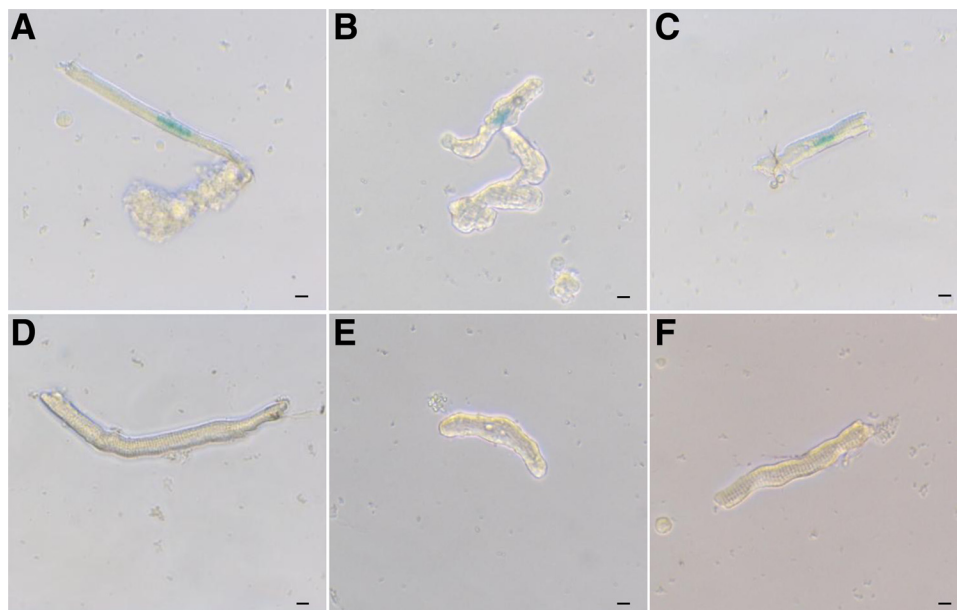


Figure 6. Isolated sinoatrial node cells after X-gal staining. **A** through **E**, Isolated cells from murine SAN with heterogeneous cellular morphology. Brightfield microscopy of elongated spindle-shaped cells (**A** and **D**), spindle-shaped cells (**B** and **E**), and atrial-like-shaped cells (**C** and **F**) showing nLacZ⁺ (**A** through **C**) and nLacZ⁻ cells (**D** through **F**), respectively. Scale bars: 5 μ m.

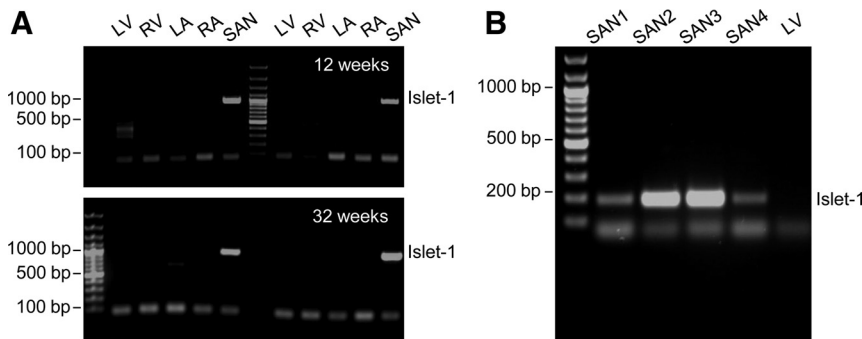


Figure 7. Islet-1 mRNA in murine and human sinoatrial node tissue. **A**, Qualitative detection of Islet-1 mRNA by RT-PCR in murine SAN tissue from four C57/BL6J wild-type animals (12 and 32 weeks), and **B**, human SAN tissue samples from 4 different patients. LV indicates left ventricular tissue; RV, right ventricular tissue; LA, left atrial tissue; RA, right atrial tissue; and SAN, sinoatrial node tissue.

number (2–50 cells), most of them being localized around the pulmonary veins. These nLacZ⁺ ganglia were detectable in up to 1.5-year-old mice, which had a mixed genetic background of Blackswiss and C57BL/6J. In this respect, our findings are identical to the clusters of Islet-1⁺ cells observed in 129SvJ×C57BL/6J and in 129SvJ mice by Khattar et al.¹⁸

The second cluster of Islet-1⁺ cells clearly marks the SAN. Approximately 50% of the HCN4 and α-actinin–positive cells of the SAN were also nLacZ⁺, suggesting the existence of at least 2 populations of pacemaker cells in the adult murine SAN, an Islet-1⁺ and an Islet-1[−] subpopulation. In all likelihood, the Islet-1⁺ subpopulation of the SAN is identical to the second cluster of cells described by Khattar et al.¹⁸ The authors described this cluster to be located in the right atrium and the interatrial septum. We were not able to detect any nLacZ⁺ cardiomyocytes in the interatrial septum. The difference might be species- or even strain-dependent, as Khattar et al showed differences between mouse strains. Alternatively, it may be a question of labeling techniques. In any case, the existence of a robust Islet-1⁺ SAN subpopulation is in agreement with recent data from Mommersteg et al²⁸ showing that the SAN develops partly from cells that coexpress Islet-1 and Tbx18. This is a very small population, resulting from an overlap of Islet-1⁺ progenitors from the second heart field and Tbx18⁺ sinus venosus progenitors. These cells maintain Islet-1 positivity after myocardial differentiation during embryonic development. Further-

more, it fits to the data by Sun et al,¹⁵ who showed that even though the Islet-1 expression in the right atria becomes more and more locally confined during embryonic development, it persists in the SAN up to 3 days postnatally (the latest time point evaluated in their study). Sun et al¹⁵ described attenuation of Islet-1 expression during this process, suggesting that Islet-1 expression would diminish within weeks. Our data now show that Islet-1 positivity of the SAN remains unaltered for at least 18 months, indicating that it serves a continuous, as yet unidentified, function in pacemaker cells. After isolation of SAN cells we observed that only a small subpopulation of sinoatrial node cells stained positive for β-gal. nLacZ⁺ cells were not restricted to one of the previously described SAN cell types.²¹ The proportion of nLacZ⁺ cells varied markedly between the different preparations (0.1% to 5%) but was always much lower than that observed in histology. The low proportion of nLacZ⁺ cells probably is due to the technical difficulties in obtaining isolated single SAN cells and suggests that nLacZ⁺ SAN cells were more susceptible to the digestion process. In any case, it confirms the existence of a subset of Islet-1⁺ SAN pacemaker cells. These results are in accordance with previous findings of Sun et al,¹⁵ who observed colocalization of Islet-1 and GFP in a HCN4-H2B-GFP knock-in mouse model during cardiac development. Of note, Islet-1 was also expressed in AVN during cardiac development, whereas we could not detect nLacZ⁺ cells within the AVN of adult animals. The mRNA data

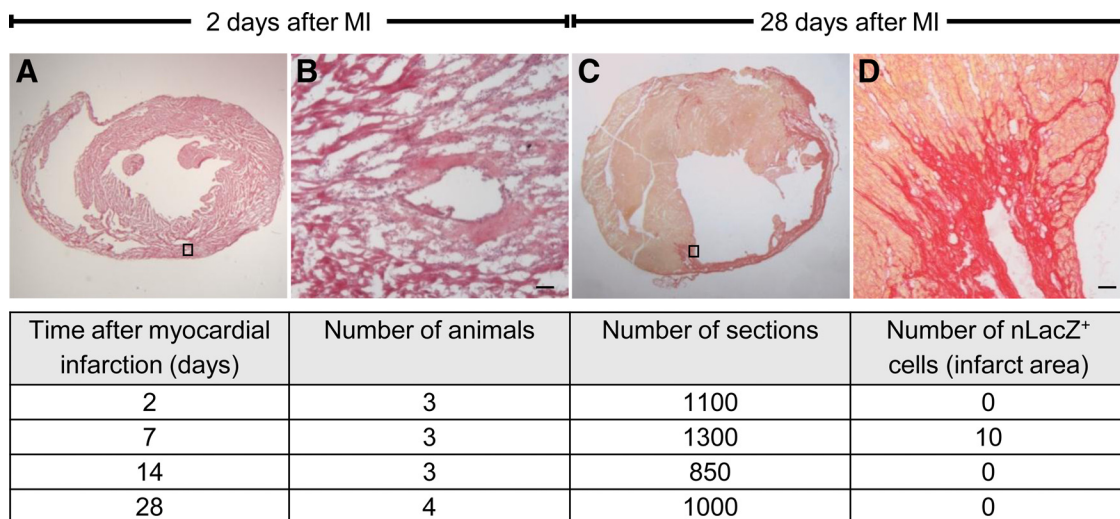


Figure 8. Islet-1-nLacZ-hearts after myocardial infarction. Histological overview, showing nLacZ-hearts 2 days (**A**) and 28 days (**C**) after left anterior descending artery ligation. Insets mark the regions shown in higher magnification (**B** and **D**). Examples of the infarct border zone 2 days (**B**) (hematoxylin and eosin staining) and 28 days (**D**) after myocardial infarction (sirius red staining). Scale bars: 50 μm.

from human heart samples suggest that the murine findings extend to the human SAN as well.

Besides the 2 compact clusters of Islet-1⁺ cells, we identified significant numbers of more disseminated nLacZ⁺ smooth muscle cells in the proximal aorta and the trunk of the pulmonary artery. Since Islet-1 progenitors can give rise to smooth muscle cells^{14–15} and Sun et al showed persistent Islet-1 expression in this particular region of the heart on the third postnatal day,¹⁵ we were not surprised by this finding. Again, the specific function of Islet-1⁺ compared with the majority of Islet-1⁻ smooth muscle cells in the media of the great vessels remains unknown at present.

In contrast to adult newt hearts, which contain Islet-1–expressing cardiomyocytes,²⁹ Islet-1 expression was considered to be down-regulated during murine cardiac differentiation.^{12,13,16,21} Therefore, we were surprised by the finding that a small number of ventricular cardiomyocytes exhibit Islet-1 positivity, all of them located in the outflow tract area. This could suggest that these cells are cardiomyogenic progenitors. Indeed, Smart et al showed that by priming mice with thymosin β 4, cardiac progenitors marked by the expression of Wilms tumor 1 gain Islet-1 expression during cardiac differentiation³⁰ after myocardial injury. However, although our study cannot exclude the possibility that Islet-1 plays a role during cardiac regeneration, several findings argue against the proposed role of Islet-1⁺ cardiovascular progenitors remaining in the adult heart. Recent data in mice, in contrast to zebrafish,³¹ support the hypothesis that cardiac regeneration occurs from an undifferentiated precursor rather than from cardiac myocytes.³ We found different cell types that expressed Islet-1, all of them highly differentiated. Furthermore, the localization of these cells and especially the absence of Islet-1⁺ cells from the working myocardium of the left and right ventricle (except for the very few cells in the outflow tract) make it unlikely that these cells play a significant role for myocardial regeneration. When analyzing >4000 sections (and thereby more than 100 Mio cells) we found that 12 of 13 hearts did not contain any nLacZ⁺ cells after myocardial infarction. In 1 heart with a very large myocardial infarction, we detected 10 cells that showed an atypical but nuclear LacZ staining in the subendocardial infarct region 7 days after myocardial infarction. Whether the staining in these cells really reflects Islet-1 is unknown at present, but the frequency would then account for 10 of >25 Mio analyzed cells at this time point and therefore is unlikely to be of biological relevance.

Limitations

Genetic models such as the one used in our study have the inherent limitation that the expression of the marker is never present in 100% of the cells intended for transgene expression and that the expression pattern may vary between different lines of mice. Moreover, we had to use heterozygous Isl-1–LacZ-mice because insertion of nLacZ into the Islet-1 gene locus caused disruption of the endogenous Islet-1 gene and homozygous knockout of Islet-1 is lethal. Therefore, the mice were functionally heterozygous Islet-1 knockout mice. This was not associated with apparent abnormalities, but unrecognized pathologies cannot be excluded completely. On the other hand, partial allele usage may have caused underestimation of the number of Islet-1⁺ cells. The fact that we found very consistent distribution of nLacZ⁺ cells in 25 animals of different ages suggests that such error, if existing, was minor. In addition, costaining with an Islet-1 antibody confirmed that nLacZ⁺ cells were indeed Islet-1

positive (Online Figure D). Staining for β -gal can also give rise to nonspecific positivity, but nontransgenic littermate controls were consistently negative and the strict nuclear localization of the signal facilitated discrimination between a true signal and noise in almost all cases. Nevertheless, we observed 10 cells in the subendocardial infarct region of 1 heart 7 days after myocardial infarction that showed an atypical but nuclear LacZ staining (Online Figure VII, A). We could not definitely discriminate between a true positive signal and false positivity (eg, caused by macrophages that are able to catalyze X-gal³²). Although it might be possible that Islet-1 was expressed between the analyzed time points, the long half-life of β -gal protein of \approx 30 hours³³ render it unlikely that such transient expression would go unnoticed.

In conclusion, our results identify Islet-1 as a novel marker of a subpopulation of SAN cells, parasympathetic neurons, a subpopulation of smooth muscle cells in the proximal aspects of the great arteries and few cardiac myocytes in the outflow tract of the adult heart. The role of Islet-1 in these distinct heart regions deserves further studies.

Acknowledgments

We thank the Mouse Pathology Core Facility (University Medical Center of Hamburg-Eppendorf) for immunohistochemical staining for Islet-1, K. Püschel (University Medical Center of Hamburg-Eppendorf) for providing the human SAN samples, and J. Starbatty for excellent technical assistance.

Sources of Funding

This study was supported by the LeDucq Foundation. D.M. was supported by the Werner Otto Stiftung.

Disclosures

None.

References

1. Velagaleti RS, Pencina MJ, Murabito JM, Wang TJ, Parikh NI, D'Agostino RB, Levy D, Kannel WB, Vasan RS. Long-term trends in the incidence of heart failure after myocardial infarction. *Circulation*. 2008; 118:2057–2062.
2. Bergmann O, Bhardwaj RD, Bernard S, Zdunek S, Barnabé-Heider F, Walsh S, Zupicich J, Alkass K, Buchholz BA, Druid H, Jovinge S, Frisén J. Evidence for cardiomyocyte renewal in humans. *Science*. 2009;324:98–102.
3. Hsieh PCH, Segers VFM, Davis ME, MacGillivray C, Gannon J, Molkentin JD, Robbins J, Lee RT. Evidence from a genetic fate-mapping study that stem cells refresh adult mammalian cardiomyocytes after injury. *Nature Med*. 2007;13:970–974.
4. Loffredo FS, Steinhauser ML, Gannon J, Lee RT. Bone marrow-derived cell therapy stimulates endogenous cardiomyocyte progenitors and promotes cardiac repair. *Cell Stem Cell*. 2011;8:389–398.
5. Angert D, Berretta RM, Kubo H, Zhang H, Chen X, Wang W, Ogorek B, Barbe M, Houser SR. Repair of the injured adult heart involves new myocytes potentially derived from resident cardiac stem cells. *Circ Res*. 2011.
6. Beltrami AP, Barlucchi L, Torella D, Baker M, Limana F, Chimenti S, Kasahara H, Rota M, Musso E, Urbanek K, Leri A, Kajstura J, Nadal-Ginard B, Anversa P. Adult cardiac stem cells are multipotent and support myocardial regeneration. *Cell*. 2003;114:763–776.
7. Orlic D, Kajstura J, Chimenti S, Bodine DM, Leri A, Anversa P. Bone marrow stem cells regenerate infarcted myocardium. *Pediatr Transplant*. 2003;7(Suppl 3):86–88.
8. Matsuura K, Nagai T, Nishigaki N, Oyama T, Nishi J, Wada H, Sano M, Toko H, Akazawa H, Sato T, Nakaya H, Kasanuki H, Komuro I. Adult cardiac Sca-1-positive cells differentiate into beating cardiomyocytes. *J Biol Chem*. 2004;279:11384–11391.
9. Bu L, Jiang X, Martin-Puig S, Caron L, Zhu S, Shao Y, Roberts DJ, Huang PL, Domian IJ, Chien KR. Human ISL1 heart progenitors generate diverse multipotent cardiovascular cell lineages. *Nature*. 2009;460:113–117.

10. Mignone JL, Murry CE. A repair “kit” for the infarcted heart. *Cell Stem Cell*. 2011;8:350–352.
11. Karlsson O, Thor S, Norberg T, Ohlsson H, Edlund T. Insulin gene enhancer binding protein Isl-1 is a member of a novel class of proteins containing both a homeo- and a Cys-His domain. *Nature*. 1990;344:879–882.
12. Ericson J, Thor S, Edlund T, Jessell TM, Yamada T. Early stages of motor neuron differentiation revealed by expression of homeobox gene *Islet-1*. *Science*. 1992;256:1555–1560.
13. Thor S, Andersson SGE, Tomlinson A, Thomas JB. A LIM-homeodomain combinatorial code for motor- neuron pathway selection system, although expression was also observed in precursors of the. *Nature*. 1999;397:76–80.
14. Cai C-L, Liang X, Shi Y, Chu P-H, Pfaff SL, Chen J, Evans S. Isl1 identifies a cardiac progenitor population that proliferates prior to differentiation and contributes a majority of cells to the heart. *Dev Cell*. 2003;5:877–889.
15. Sun Y, Liang X, Najafi N, Cass M, Lin L, Cai C-L, Chen J, Evans SM. *Islet 1* is expressed in distinct cardiovascular lineages, including pacemaker and coronary vascular cells. *Dev Biol*. 2007;304:286–296.
16. Moretti A, Caron L, Nakano A, Lam JT, Bernshausen A, Chen Y, Qyang Y, Bu L, Sasaki M, Martin-Puig S, Sun Y, Evans SM, Laugwitz K-L, Chien KR. Multipotent embryonic *isl1+* progenitor cells lead to cardiac, smooth muscle, and endothelial cell diversification. *Cell*. 2006;127:1151–1165.
17. Laugwitz K-L, Moretti A, Lam J, Gruber P, Chen Y, Woodard S, Lin L-Z, Cai C-L, Lu MM, Reth M, Platoshyn O, Yuan JX-J, Evans S, Chien KR. Postnatal *isl1+* cardioblasts enter fully differentiated cardiomyocyte lineages. *Nature*. 2005;433:647–653.
18. Khattar P, Friedrich FW, Bonne G, Carrier L, Eschenhagen T, Evans SM, Schwartz K, Fiszman MY, Vilquin J-T. Distinction between two populations of *islet-1*-positive cells in hearts of different murine strains. *Stem Cell Dev*. 2011;20:1043–1052.
19. Genead R, Danielsson C, Andersson AB, Corbascio M, Franco-Cereceda A, Sylvén C, Grinnemo K-H. *Islet-1* cells are cardiac progenitors present during the entire lifespan: from the embryonic stage to adulthood. *Stem Cell Dev*. 2010;19:1601–1615.
20. Hudson REB. The human conducting-system and its examination. *J Clin Pathol*. 1963;16:492–498.
21. Mangoni ME, Nargeot J. Properties of the hyperpolarization-activated current (*I*(f)) in isolated mouse sino-atrial cells. *Cardiovasc Res*. 2001;52: 51–64.
22. Bollini S, Smart N, Riley PR. Resident cardiac progenitor cells: at the heart of regeneration. *J Mol Cell Cardiol*. 2010;50:296–303.
23. Koelle GB. The histochemical identification of acetylcholinesterase in cholinergic, adrenergic and sensory neurons. *J Pharmacol Exp Ther*. 1955;114:167–184.
24. Hoover DB, Ganote CE, Ferguson SM, Blakely RD, Parsons RL. Localization of cholinergic innervation in guinea pig heart by immunohistochemistry for high-affinity choline transporters. *Cardiovasc Res*. 2004;62:112–121.
25. Avivi C, Goldstein RS. Differential expression of *Islet-1* in neural crest-derived ganglia: *Islet-1* + dorsal root ganglion cells are post-mitotic and *Islet-1* + sympathetic ganglion cells are still cycling. *Brain Res Dev Brain Res*. 1999;115:89–92.
26. Sun Y, Dykes IM, Liang X, Eng SR, Evans SM, Turner EE. A central role for *Islet1* in sensory neuron development linking sensory and spinal gene regulatory programs. *Nat Neurosci*. 2008;11:1283–1293.
27. Rysevaite K, Saburkina I, Pauziene N, Vaitkevicius R, Noujaim SF, Jalife J, Pauza DH. Immunohistochemical characterization of the intrinsic cardiac neural plexus in whole-mount mouse heart preparations. *Heart Rhythm*. 2011;8:731–738.
28. Mommersteeg MT, Dominguez JN, Wiese C, Norden J, de Gier-de Vries C, Burch JB, Kispert A, Brown NA, Moorman AF, Christoffels VM. The sinus venosus progenitors separate and diversify from the first and second heart fields early in development. *Cardiovasc Res*. 2010;87:92–101.
29. Witman N, Murtuza B, Davis B, Amer A, Morrison JI. Recapitulation of developmental cardiogenesis governs the morphological and functional regeneration of adult newt hearts following injury. *Dev Biol*. 2011;354:67–76.
30. Smart N, Bollini S, Dubé KN, Vieira JM, Zhou B, Davidson S, Yellon D, Riegler J, Price AN, Lythgoe MF, Pu WT, Riley PR. De novo cardiomyocytes from within the activated adult heart after injury. *Nature*. 2011;474:640–644.
31. Kikuchi K, Holdway JE, Werdich AA, Anderson RM, Fang Y, Egnaczyk GF, Evans T, Macrae CA, Stainier DYS, Poss KD. Primary contribution to zebrafish heart regeneration by *gata4(+)* cardiomyocytes. *Nature*. 2010;464:601–605.
32. Kiernan JA. Indigogenic substrates for detection and localization of enzymes. *Biotech Histochem*. 2007;82:73–103.
33. Gonda DK, Bachmair A, Wünnig I, Tobias JW, Lane WS, Varshavsky A. Universality and structure of the N-end rule. *J Biol Chem*. 1989;264:16700–16712.

Novelty and Significance

What Is Known?

- In early cardiac development, cells expressing the transcription factor *Islet-1* form the right ventricle, the outflow tract, parts of the atria (the “second heart field”) and the sinoatrial node (SAN) and atrioventricular node (AVN).
- *Islet-1*⁺ cells from fetal hearts or embryonic stem cells form cardiac myocytes, smooth muscle and endothelial cells when placed in cell culture, suggesting that *Islet-1*⁺ cells may also serve a cardiovascular progenitor role in the adult heart.
- In the adult mouse heart, *Islet-1* positivity was detected by antibody staining in distinct clusters in the heart basis whose identity remained unclear.

What New Information Does This Article Contribute?

- Genetic labeling experiments showed that *Islet-1* in the adult mouse heart is expressed in HCN4⁺ pacemaker cells of the SAN, but not the AVN, parasympathetic nervous ganglia, smooth muscle cells of the proximal part of the great arteries, and few cardiac myocytes of the outflow tract area.
- The expression pattern was highly reproducible and stable for up to 18 months.

- No *Islet-1*⁺ cells were found in healthy ventricular myocardium. These cells were found only in an atypical form in 10/ ≈100 000 000 cells in >4000 sections of hearts 2 to 28 days after myocardial infarction.

Islet-1 is an established marker of early cardiovascular development; however, its role in the adult heart, specifically its progenitor role, remains obscure. Given the technical difficulties in studying *Islet-1* distribution in the heart by immunologic means, we used a genetic approach, that is, a mouse in which *Islet-1* expression drives a nuclear localized β -galactosidase. This technique allows not only histological identification of *Islet-1*⁺ cells with high sensitivity and specificity but even the macroscopic identification in the whole heart, facilitating the analysis of regional distribution. *Islet-1*⁺ cells were undetectable in >5000 sections from normal or injured myocardium. This is important because it provides strong evidence against the idea that *Islet-1*⁺ cells could serve a progenitor role in the normal or injured postnatal heart. Stable *Islet-1*⁺ expression in very distinct and functionally specialized cells suggest that *Islet-1*⁺ expression in the postnatal heart is not a spurious “left-over” from development but serves an important role that warrants further studies. The findings of this study also establish *Islet-1* as a new and, compared with HCN4, a specific marker of a subpopulation of SAN pacemaker cells.

Human Leukocyte Antigen I Knockdown Human Embryonic Stem Cells Induce Host Ignorance and Achieve Prolonged Xenogeneic Survival

Tobias Deuse, MD; Martina Seifert, PhD; Neil Phillips, PhD; Andrew Fire, PhD; Dolly Tyan, PhD; Mark Kay, PhD; Philip S. Tsao, PhD; Xiaoqin Hua, MD; Joachim Velden, MD; Thomas Eiermann, MD; Hans-Dieter Volk, MD; Hermann Reichenspurner, MD, PhD; Robert C. Robbins, MD; Sonja Schrepfer, MD, PhD

Background—Although human embryonic stem cells (hESC) have enormous potential for cell replacement therapy of heart failure, immune rejection of hESC derivatives inevitably would occur after transplantation. We therefore aimed to generate a hypoantigenic hESC line with improved survival characteristics.

Methods and Results—Using various in vivo, nonischemic, hindlimb xenotransplant models (immunocompetent and defined immunodeficient mouse strains) as well as human in vitro T-cell and natural killer (NK)-cell assays, we revealed a central role for T cells in mediating hESC rejection. The NK-cell susceptibility of hESC in vivo was found to be low, and the NK response to hESC challenge in vitro was negligible. To reduce the antigenicity of hESC, we successfully generated human leukocyte antigen (HLA) I knockdown cells (hESC^{siRNA+IB}) using both HLA I RNA interference (siRNA) and intrabody (IB) technology. HLA I expression was $\approx 99\%$ reduced after 7 days and remained low for weeks. Cellular immune recognition of these hESC^{siRNA+IB} was strongly reduced in both xenogeneic and allogeneic settings. Immune rejection was profoundly mitigated after hESC^{siRNA+IB} transplantation into immunocompetent mice, and even long-term graft survival was achieved in one third of the animals without any immunosuppression. The survival benefit of hESC^{siRNA+IB} was further confirmed under ischemic conditions in a left anterior descending coronary artery ligation model.

Conclusions—HLA I knockdown hESC^{siRNA+IB} provoke T-cell ignorance and experience largely mitigated xenogeneic rejection. By generating hypoantigenic hESC lines, the generation of acceptable hESC derivatives may become a practical concept and push cell replacement strategies forward. (*Circulation*. 2011;124[suppl 1]:S3–S9.)

Key Words: cells ■ gene therapy ■ immunology

Human embryonic stem cells (hESC) display true pluripotency and have the capacity to propagate indefinitely without senescence. These characteristics make them valuable candidates for cell replacement therapy in the treatment of degenerative diseases, especially heart failure. With transplantation of hESC-derived cardiac progenitor cells that form contractile intracardiac grafts¹ or functional, in vitro-generated engineered heart tissue from hESC,² substantial improvements in cardiac function have been reported. However, because of the human leukocyte antigen (HLA) disparity between hESC-derived donor cells and recipients, immune rejection inevitably occurs. Therefore, improvement of rodent cardiac function after acute myocardial infarction so far has only been achieved by transplanting hESC-derived cardio-

myocytes into either immunodeficient³ or heavily immunosuppressed⁴ recipients. Immunosuppressive drugs, however, are associated with severe morbidity and may hamper cell engraftment and cell survival.⁵

We and others⁶ believe that the best way to overcome immune rejection is to generate hypoimmunogenic pluripotent cell lines that are barely visible to the immune system and, thereby, can serve as universal cell sources for generating off-the-shelf cellular grafts or tissues. Herein, we present a strategy to generate hypoimmunogenic hESC by HLA I knockdown. The results demonstrate that HLA I knockdown is both necessary and sufficient to diminish graft rejection and to achieve long-term survival, even in a stringent xenogeneic model.

From the Departments of Cardiothoracic Surgery (T.D., R.C.R., S.S.), Pediatrics, Human Gene Therapy (N.P., M.K.), Pathology (A.F., D.T.), and Cardiovascular Medicine (P.T.), Stanford University, Stanford, CA; Institute of Medical Immunology and Berlin-Brandenburg Center for Regenerative Therapies (M.S., H.-D.V.), Berlin, Germany; and Cardiovascular Surgery (T.D., H.R., S.S.), TSI-Laboratory, Cardiovascular Research Center (T.D., H.R., X.H., S.S.), Pathology (J.V.), and Transfusion Medicine (T.E.), University Hospital Hamburg, Hamburg, Germany.

Presented at the 2010 American Heart Association meeting in Chicago, IL, November 12–16, 2010.

The online-only Data Supplement is available at <http://circ.ahajournals.org/lookup/suppl/doi:10.1161/CIRCULATIONAHA.111.020727/-/DC1>.

Correspondence to Tobias Deuse, MD, Department of Cardiovascular Surgery, University Heart Center Hamburg, Martinistr 52, 20246 Hamburg, Germany. E-mail t.deuse@uke.de

© 2011 American Heart Association, Inc.

Circulation is available at <http://circ.ahajournals.org>

DOI: 10.1161/CIRCULATIONAHA.111.020727

Methods

Animals

Male BALB/c, SCID Beige (CB17.Cg-Prkdc^{scid}Lyst^{bg}/CrI), nude (Cby.Cg-Foxn1^{nu}/J), beige (C57BL/6J-Lyst^{bg-J}/J), and perforin^{-/-} mice (C57BL/6-Prp^{tm1.5dz}) were purchased from Charles River Laboratories (Sulzfeld, Germany) and received humane care in compliance with the *Guide for the Principles of Laboratory Animals*. Myocardial infarctions were induced by ligation of the left anterior descending coronary artery (LAD) through an anterolateral thoracotomy.

ESC Culture and Cell Transplantation

H9 hESC (Wicell; Madison, WI) were maintained on inactivated murine embryonic fibroblast feeder layers (Millipore; Billerica, MA) in hESC medium. The hESC colonies were separated from the murine embryonic fibroblasts by incubation with dispase (Invitrogen; Frederick, MD) and subcultured on feeder-free matrigel-coated (BD Biosciences; San Jose, CA) plates before their use. HLA I surface expression was assessed on a FACSCalibur system (Becton Dickinson; Heidelberg, Germany) [HLA A/B/C (clone DX17) from BD Biosciences]. Mean fluorescence intensity of HLA I was compared to that of the associated negative isotype control. Normalized expression was calculated as the mean fluorescence intensity of the molecule divided by the mean fluorescence intensity of the isotype control. Therefore, a normalized expression of 1 corresponds to no (0%) molecule expression. Before transplantation, hESC were trypsinated and resuspended in sterile PBS at 1×10^6 cells per 50 μ L. The hESC viability was $\approx 95\%$ as determined by trypan blue staining. The hESC were transplanted either into the right-side gastrocnemius muscle (nonischemic hindlimb model) or into the border zone of an acute myocardial infarction (LAD ligation model, divided into 4 injections) using a 27-gauge syringe.

Bioluminescence Imaging

Bioluminescence imaging (BLI) was performed using the Xenogen in vivo imaging system (Caliper Life Sciences; Hopkinton, MA) as reported earlier⁷ (online-only Data Supplement). The recipient mice were scanned repetitively on days 0, 1, 3, 5, 7, 14, 21, 28, 35, and 42 or until the signal dropped into the background. BLI signals were quantified in units of photons per second (total flux) and are presented on a logarithmic scale.

Immune Response Assays

Elispot Assays

Allogeneic Elispot assays were done with 5×10^5 hESC and 5×10^5 human peripheral blood mononuclear cells (PBMC) or natural killer (NK) cells (Lonza; Cologne, Germany) according to the manufacturer's (BD Biosciences) protocol using interferon- γ (IFN- γ) and interleukin-4 (IL-4)-coated plates. Spots were automatically enumerated using an Elispot plate reader (CTL; Shaker Heights, OH) for scanning and analyzing.

Degranulation Assay With NK Cells

Cell-mediated cytotoxicity of human NK cells was evaluated in a CD107a degranulation assay. This assay sensitively detects the surface expression of CD107a as a result of activation-induced degranulation and secretion of the lytic granule contents. NK cells were incubated for 6 hours with FITC-labeled anti-CD107a monoclonal antibody (BD Biosciences). K562, hESC, or hESC^{siRNA+IB} were added at ratios of 1:10, and surface expression of CD107a was determined by FACS (BD Biosciences).

HLA I Knockdown Technologies

Both technologies of gene silencing using small interfering RNA (siRNA) at the posttranscriptional level⁸ and intrabody (IB) protein knockout at the posttranslational level⁹ were used separately (hESC^{siRNA} and hESC^{IB}) or in combination (hESC^{siRNA+IB}). For details, see the online-only Data Supplement.

Statistical Analysis

Data are presented as mean \pm SD, unless otherwise indicated. Comparisons between groups were done by independent sample *t* tests or ANOVA with Bonferroni post hoc tests where appropriate. Differences were considered significant for $P < 0.05$. Statistical analysis was performed using SPSS for Windows (SPSS Inc; Chicago, IL) software.

Results

hESC Survival After Xenogeneic Transplantation

A total of 1×10^6 hESC were injected into the gastrocnemius muscles of immunocompetent BALB/c or various immunocompromised mouse strains and were followed by BLI (Figure 1A). There was an early decline in cell numbers over the first few days, which occurred in all strains and, therefore, seemed not to be immune mediated. At later time points, the survival curves rapidly diverged (Figure 1B through 1E). The BLI signals dropped into the background in BALB/c mice by day 5, and all cell transplants were rejected. In immunodeficient SCID Beige mice, which lack lymphocytes and NK function, BLI signals steadily increased to regain their initial value by day 21 (Figure 1B). Up to day 80, total BLI flux increased ≈ 50 times, and macroscopic tumor growth was observed at the site of injection. In nude mice lacking only T cells, 7 of 9 cell transplants survived (Figure 1C), and after 80 days, tumor growth also was observed. Mice with the beige mutation (Figure 1D) and perforin^{-/-} mice (Figure 1E) both had defective cytotoxic NK activity but still rejected all cellular hESC transplants at a similar pace compared with immunocompetent BALB/c mice. Adoptive transfer of beige splenocytes into SCID Beige recipients on days -2, 0, 5, and 14 was sufficient to cause hESC rejection in otherwise accepting mice (Figure 1F). When the HLA I-deficient human erythroleukemia cell line K562 was transplanted, all cells were quickly rejected in immunocompetent BALB/c mice but formed tumors in SCID Beige recipients (Figure 1G). The highly NK-susceptible K562 cells were rapidly killed in athymic nude mice devoid of T cells but harboring functional NK cells (Figure 1H). The susceptibility of hESC to Fas-induced cytotoxicity was evaluated. Fas expression was negligible on hESC (1.3 ± 0.1) but could be significantly upregulated by in vitro IFN- γ stimulation (3.9 ± 0.4 , $P < 0.001$). Blocking of both NK killing (in beige mice [Figure 1I] or perforin^{-/-} mice [Figure 1J]) and Fas-dependent cytotoxicity (using the Fas-blocking antibody ANT-205) did not markedly improve hESC survival.

Allogeneic Cytotoxic Killing of hESC

Human PBMC were incubated with hESC or hESC^{siRNA+IB} in vitro (Figure 2A and 2B). Only hESC ($P = 0.001$ and

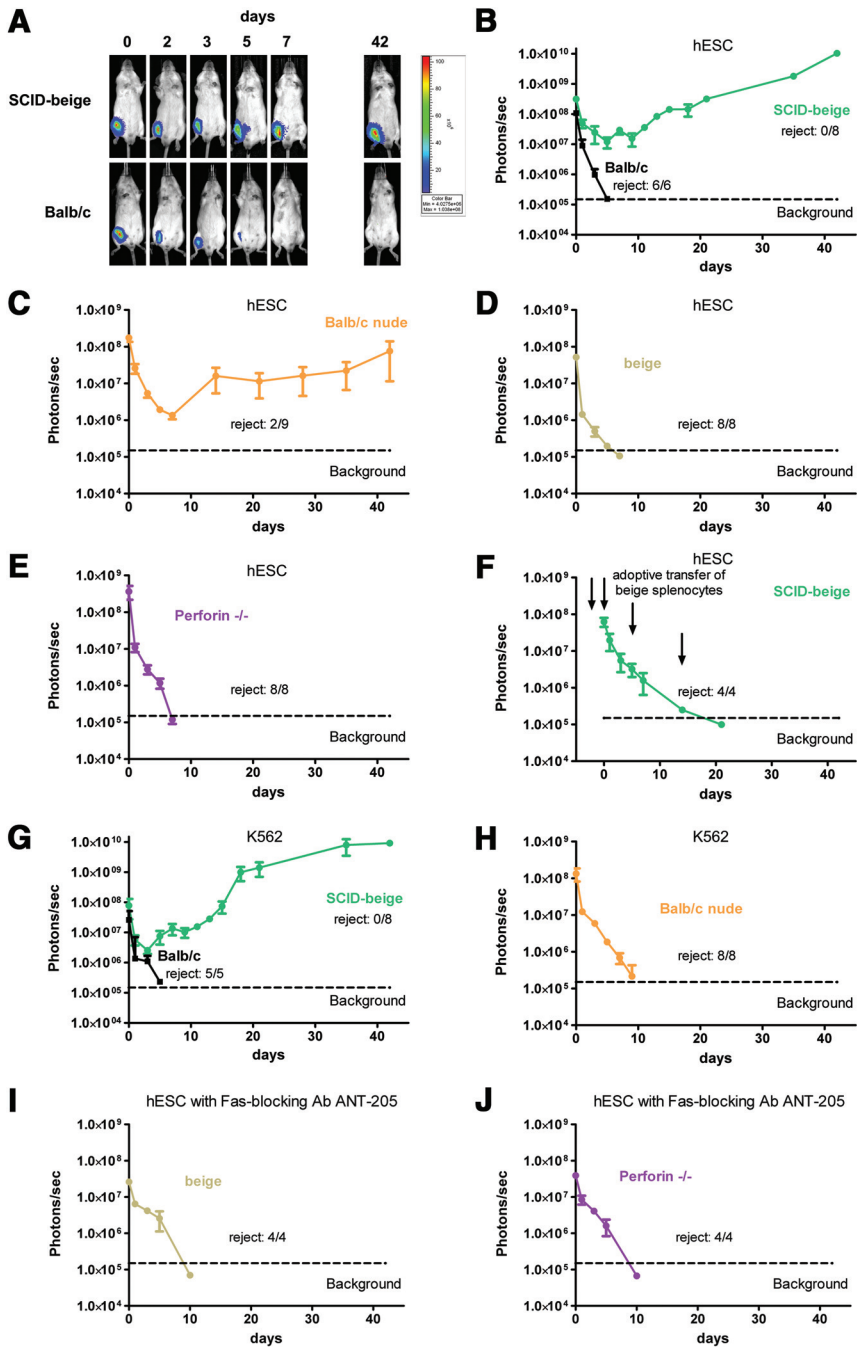


Figure 1. Survival of hESC after xenogeneic transplantation. A total of 106 hESC or K562 cells were transplanted into the gastrocnemius muscles of either immunocompetent BALB/c mice or mouse strains carrying different immune defects. Cell survival was longitudinally followed by bioluminescence imaging. All BALB/c mice rapidly rejected the hESC transplants, whereas the cells survived in severely immunodeficient SCID Beige mice (A and B). Whereas in athymic BALB/c nude mice only 2 of 9 hESC transplants were rejected (C), all hESC grafts were rejected in natural killer-cell-defective beige mice (D) and perforin^{-/-} mice (E). Repetitive adoptive transfers of beige splenocytes (arrows) were sufficient to cause hESC rejection in SCID Beige mice (F). K562 formed tumors in SCID Beige recipients but were rejected in BALB/c (G) and nude mice (H). The survival of hESC was not markedly improved by Fas blockade with ANT-205 in beige (I) or perforin^{-/-} mice (J). Data are presented as mean ± SEM. Ab indicates antibody; hESC, human embryonic stem cells.

$P=0.002$) but not hESC^{siRNA+IB} ($P=1.0$ and $P=0.428$) significantly increased the spot frequencies for IFN- γ and IL-4, respectively, compared to resting responder PBMC. Elispots also were then done with NK cells instead of PBMC (Figure 2C). NK-susceptible K562-induced substantial NK-cell activation that was similar to the effect of PMA/ionomycin incubation. Neither hESC ($P<0.001$ versus K562) nor hESC^{siRNA+IB} ($P<0.001$ versus K562) induced relevant IFN- γ release. Additionally, only NK cells incubated with K562 but not hESC ($P<0.001$ versus K562) or hESC^{siRNA+IB} ($P<0.001$ versus K562) showed increased CD107a surface expression (Figure 2D).

Generation and Transplantation of Hypoantigenic hESC

The siRNA and IB transfection was achieved with an efficacy of $\approx 74 \pm 12\%$ and $82 \pm 11\%$, respectively, and the transduction efficacy of siRNA+IB was $88 \pm 9\%$. After 7 days, siRNA and IB significantly lowered HLA I surface expression from 11.1 ± 3.1 on hESC to 2.6 ± 0.8 ($P=0.005$) and 2.1 ± 0.7 ($P=0.004$), respectively. Combined use of siRNA and IB even reduced HLA I down to 1.1 ± 0.1 ($P=0.002$) (Figure 3A), which corresponds to $\approx 99\%$ HLA I reduction. Between days 7 and 42, the lowered HLA I expression remained stable in all 3 groups. After 42 days, HLA I expression in the hESC^{siRNA+IB} group was still significantly

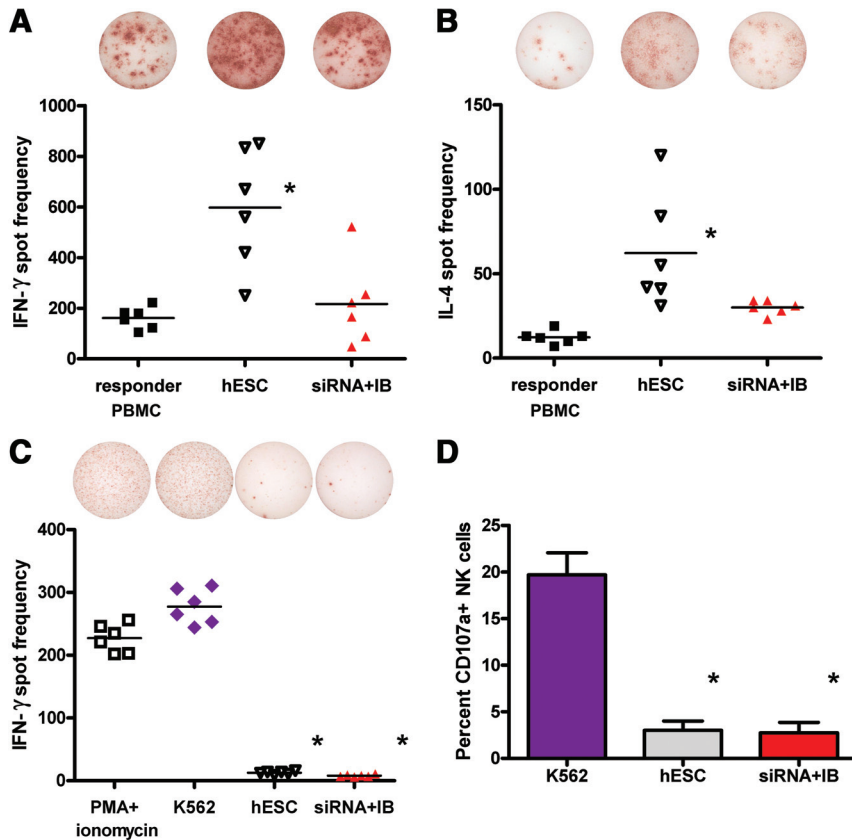


Figure 2. Cytotoxic killing of hESC. Allogeneic in vitro IFN- γ (A) and IL-4 (B) Elispot assays with human PBMC and hESC or hESC^{siRNA+IB} revealed elevated spot frequencies for hESC only (* $P < 0.05$ versus responder PBMC). K562 but not hESC or hESC^{siRNA+IB} induced significant natural killer (NK)-cell activation (C) (* $P < 0.05$ versus PMA/ionomycin) in allogeneic in vitro NK Elispot assays, and only K562 induced significant NK-cell CD107a expression (D) (* $P < 0.05$ versus K562). IB indicates intrabody; IFN- γ , interferon- γ ; IL-4, interleukin-4; siRNA, small interfering RNA. Other abbreviation as in Figure 1.

lower than in either the hESC^{siRNA} or the hESC^{IB} group ($P = 0.003$).

The survival of the 3 generated hESC groups in an immunocompetent host was assessed next. Five days after transplantation into the hindlimb of BALB/c mice, the Elispot assays (Figure 3B) showed that IFN- γ spot frequencies were highest for hESC and were significantly reduced with hESC^{siRNA} ($P = 0.048$), hESC^{IB} ($P = 0.002$), and hESC^{siRNA+IB} ($P = 0.002$). Similarly, IL-4 spot frequencies were significantly reduced for hESC^{IB} and hESC^{siRNA+IB} ($P < 0.001$ each). Longitudinal follow-up on cell survival showed that the last detectable BLI signals for hESC^{siRNA} and hESC^{IB} were found after 10 and 14 days, respectively, and all grafts were rejected (Figure 3C). The rejection of hESC^{siRNA+IB}, however, was profoundly mitigated, and the survival was markedly prolonged. In two thirds of the animals, the BLI signals slowly dropped into the background after 28 days, but in one third of the animals, the signals remained stable and showed a slight upward slope after 4 weeks. In these animals carrying long-term surviving grafts, BLI signals were still detectable after 2 months. Thus, with hESC^{siRNA+IB}, we were able to achieve long-term cell survival in a stringent xenogeneic setting.

Survival of hESC was further evaluated in a more clinically relevant model of acute myocardial infarction (Figure 4A through 4C). Similar to the results of the hindlimb model, hESC were rapidly rejected within 5 days in BALB/c mice but achieved long-term survival with the development of local teratomas in immunodeficient SCID Beige recipients (Figure 4D). The survival of hESC^{siRNA+IB} in immunocompetent BALB/c mice was greatly prolonged compared to

hESC, with 2 of 7 animals presenting steady BLI signals beyond 42 days.

Discussion

In the present study, we have described the fate of hESC after transplantation into several immunologically well-established mouse models. The survival of hESC in severely immunodeficient SCID Beige recipients exhibiting defective T-cell, B-cell, and NK-cell responses contrasted the rapid cell death in immunocompetent BALB/c mice and underlines the immunologic nature of cell death. Cell stress and injury from needle injection were universally seen in all recipient strains and may be accountable for nonimmunologic early cell losses over the first 5 days. Nude mice lacking T cells but possessing regular NK-cell, B-cell, and antigen-presenting cell activity were unable to reject the majority of hESC transplants. In contrast, in mice with NK-cell impairment because of either the beige mutation or lack of the perforin gene, T-cell-mediated hESC rejection reliably occurred. Additionally, adoptive transfer of beige splenocytes into SCID Beige recipients was sufficient to induce rapid hESC rejection. As previously reported by our group,¹⁰ T-cell-specific immunosuppression significantly prolongs xenogeneic hESC survival in immunocompetent mice. It has been demonstrated earlier that hESC¹¹ or their derivatives¹² can be recognized by human T cells and that T-cell recognition is strongly facilitated by inflammatory cytokines. The absence of HLA II and costimulatory molecules on hESC excludes direct antigen presentation,¹³ and hESC uniformly escaped rejection in a

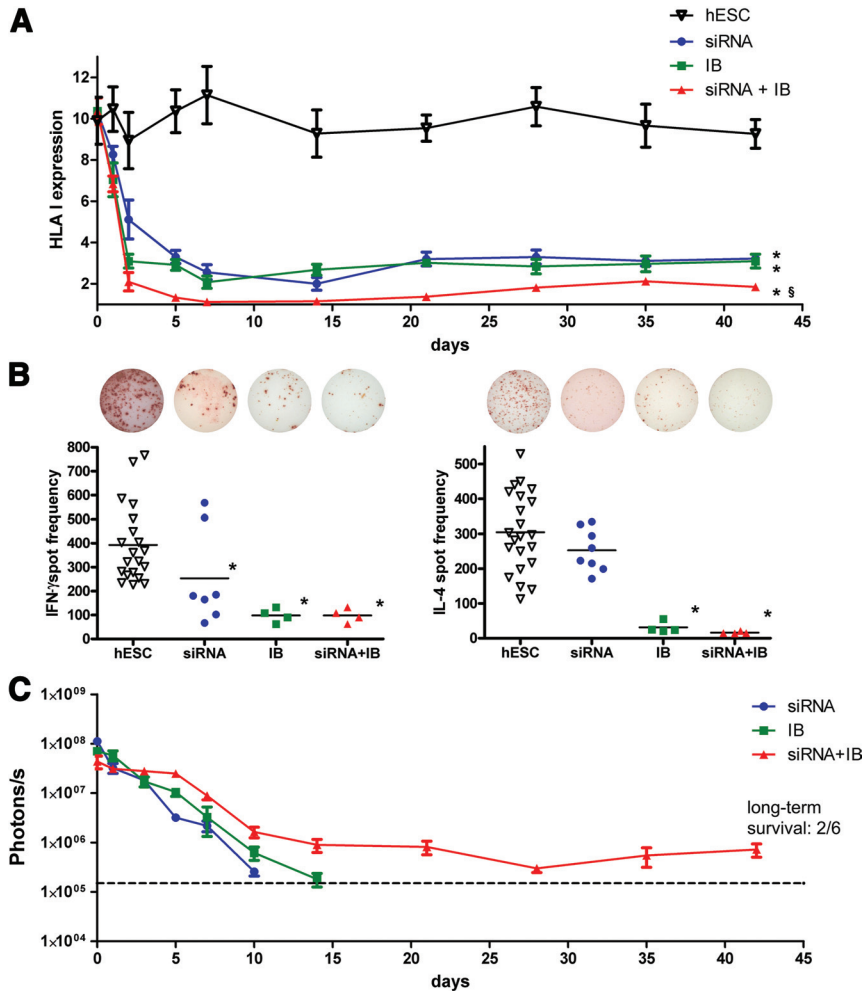


Figure 3. Generation and transplantation of hypoantigenic hESC. Flow cytometry was used to assess hESC HLA I surface expression before and after HLA I knockdown using siRNA, IB, or both. **A**, Longitudinal analyses demonstrated that once maximal knockdown was achieved after ≈ 7 days, the lowered HLA I expression remained stable for 42 days in all 3 knockdown groups. Data are presented as mean \pm SEM. * $P < 0.05$ versus hESC. $\$P < 0.05$ versus hESC^{IB} and hESC^{siRNA}. **B**, Cell transplants of hESC hESCsiRNA, hESCIB, or hESCsiRNA+IB were transplanted into immunocompetent BALB/c mice. After 5 days, IFN- γ and IL-4 spot frequencies were reduced in the knockdown groups. The last time points of above-background bioluminescence imaging signals were days 10 and 14 for hESC^{siRNA} and hESC^{IB}, respectively. * $P < 0.05$ versus hESC. **C**, Two of 6 hESC^{siRNA+IB} injections became long-term surviving cellular grafts. Data are presented as mean \pm SEM. HLA, indicates human leukocyte antigen. Other abbreviations as in Figures 1 and 2.

humanized mouse model with defective indirect immune recognition pathway.¹¹

Although T cells clearly seem to be required for hESC recognition, other effector cells may participate in the killing. Blocking both perforin- and FasL-dependent killing, 2 major cytotoxic effector mechanisms of T cells, did not prevent hESC rejection. Similarly, allogeneic leukemia cells were shown previously to be rejected in perforin/FasL double-deficient mice with macrophages identified as the effector cell population.¹⁴ Komatsu et al¹⁵ further demonstrated that T cells can mediate rejection of allogeneic marrow progenitor cells through alternative effector pathways independent of perforin-, FasL-, TWEAK (tumor necrosis factor-like weak inducer of apoptosis)-, and TRAIL (tumor necrosis factor-related apoptosis-inducing ligand)-dependent cytotoxicity.¹⁵ Effector mechanisms involving antibodies¹⁶ and complement¹⁷ have been suggested to contribute to hESC killing in vivo.

The naturally low HLA I expression of hESC could make them susceptible to NK killing, but in our experiments, only T-cell-deficient animals failed to reject hESC, whereas the lack of NK cells did not prevent vigorous hESC rejection. Other groups using murine ESCs reported substantial¹⁸ or negligible¹⁹ in vitro NK responses, presumably depending on the experimental conditions. Murine ESCs uniformly have

been reported to form teratomas in syngeneic^{17,20} but not allogeneic^{17,20} or xenogeneic hosts,²⁰ throwing into question the relevance of NK rejection in immunocompetent hosts. The hESC were shown not to be effectively recognized by human NK cells in vitro, only after additional in vitro NK stimulation.²¹ The present allogeneic in vitro results confirmed that human NK cells barely responded to hESC challenge and that NK susceptibility did not increase with HLA I knockdown.

Strategies involving the gene transfer of an anti-HLA I single-chain IB⁹ or plasmids containing siRNA²² recently were introduced to downregulate surface HLA I. Although we could demonstrate in the present study that either technique worked with hESC, only their combination provided the needed level of HLA I knockdown to generate hypoantigenic hESC^{siRNA+IB}. To our knowledge, our hESC^{siRNA+IB} is the first human cell line to achieve long-term survival in a stringent xenogeneic model without any immunosuppression. The results further demonstrate that the kinetics of immune rejection are similar in the nonischemic hindlimb and ischemic LAD ligation models. The ischemic conditions also may hamper cell engraftment but do not narrow the survival benefit of HLA I knockdown hESC^{siRNA+IB}. Differences in the level and endurance of HLA I knockdown still may determine which graft undergoes slow rejection or proceeds

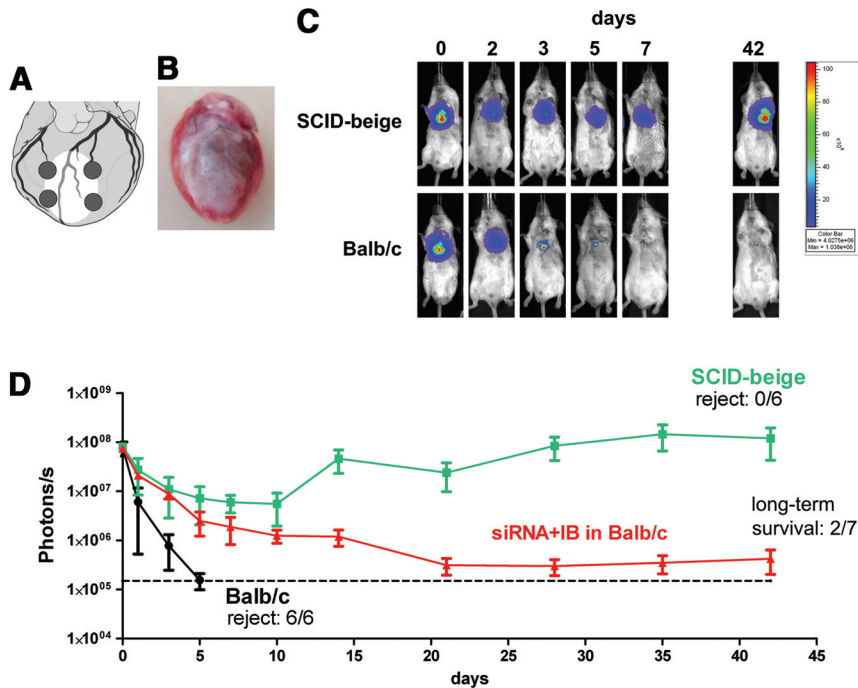


Figure 4. Survival of hESC under ischemic conditions. **A**, After creating an acute myocardial infarction by left anterior descending coronary artery ligation, 10^6 hESC, divided into 4 injections, were transplanted into the infarction border zone. **B**, Left anterior descending coronary artery ligation after the proximal third created large anteriolateral infarcts (heart explanted after 4 weeks). Longitudinal bioluminescence imaging analyses (**C**) showed rapid hESC rejection within 5 days in BALB/c mice but long-term survival in SCID Beige recipients (**D**). Data are presented as mean \pm SEM. Cell survival of hESC^{siRNA+IB} in BALB/c mice was greatly prolonged, and 2 of 7 cellular grafts survived beyond the study period. Abbreviations as in Figures 1 and 2.

to long-term survival. Future efforts will focus on engineering a reliable level of HLA I knockdown to facilitate routine long-term survival.

In summary, we herein highlight a central role for T cells in the rejection of hESC and demonstrate that hypoantigenic HLA I knockdown hESC^{siRNA+IB} experience strongly diminished T-cell responses without triggering substantial NK activity. We provide proof of concept that HLA I knockdown on hESC is both necessary and sufficient to achieve long-term graft survival. As progress is made toward the use of hESC therapeutics in human systems, it will be of great interest to determine the effect of HLA I knockdown in an allogeneic human setting.

Sources of Funding

Dr Schrepfer received funding from the Deutsche Forschungsgemeinschaft (SCHR 992/3-1, SCHR 992/4-1) and the International Society for Heart and Lung Transplantation (Norman Shumway Career Development Award 2010). The present study was supported by the Falk Research Fund for the Department of Cardiothoracic Surgery at Stanford University.

Disclosures

None.

References

- Laflamme MA, Chen KY, Naumova AV, Muskheli V, Fugate JA, Dupras SK, Reinecke H, Xu C, Hassanipour M, Police S, O'Sullivan C, Collins L, Chen Y, Minami E, Gill EA, Ueno S, Yuan C, Gold J, Murry CE. Cardiomyocytes derived from human embryonic stem cells in pro-survival factors enhance function of infarcted rat hearts. *Nat Biotechnol.* 2007;25:1015–1024.
- Domian IJ, Chiravuri M, van der Meer P, Feinberg AW, Shi X, Shao Y, Wu SM, Parker KK, Chien KR. Generation of functional ventricular heart muscle from mouse ventricular progenitor cells. *Science.* 2009;326:426–429.
- van Laake L, Passier R, Monshouwer-Kloots J, Verkleij A, Lips D, Freund C, den Ouden K, Oostwaard D, Korving J, Tertoolen L, van Echteld C, Doevendans P, Mummery C. Human embryonic stem cell-derived cardiomyocytes survive and mature in the mouse heart and transiently improve function after myocardial infarction. *Stem Cell Res.* 2007;1:9–24.
- Caspi O, Huber I, Kehat I, Habib M, Arbel G, Gepstein A, Yankelson L, Aronson D, Beyar R, Gepstein L. Transplantation of human embryonic stem cell-derived cardiomyocytes improves myocardial performance in infarcted rat hearts. *J Am Coll Cardiol.* 2007;50:1884–1893.
- Puymirat E, Geha R, Tomescot A, Bellamy V, Larghero J, Trinquart L, Bruneval P, Desnos M, Hagege A, Puceat M, Menasche P. Can mesenchymal stem cells induce tolerance to cotransplanted human embryonic stem cells? *Mol Ther.* 2009;17:176–182.
- Daley GQ, Scadden DT. Prospects for stem cell-based therapy. *Cell.* 2008;132:544–548.
- Cao F, Lin S, Xie X, Ray P, Patel M, Zhang X, Drukker M, Dylla SJ, Connolly AJ, Chen X, Weissman IL, Gambhir SS, Wu JC. In vivo visualization of embryonic stem cell survival, proliferation, and migration after cardiac delivery. *Circulation.* 2006;113:1005–1014.
- Caplen NJ, Parrish S, Imani F, Fire A, Morgan RA. Specific inhibition of gene expression by small double-stranded RNAs in invertebrate and vertebrate systems. *Proc Natl Acad Sci U S A.* 2001;98:9742–9747.
- Beyer F, Doebeis C, Busch A, Ritter T, Mhashilkar A, Marasco WM, Laube H, Volk HD, Seifert M. Decline of surface MHC I by adenoviral gene transfer of anti-MHC I intrabodies in human endothelial cells—new perspectives for the generation of universal donor cells for tissue transplantation. *J Gene Med.* 2004;6:616–623.
- Swijnenburg R-J, Schrepfer S, Govaert J, Cao F, Ransohoff K, Sheikh A, Haddad M, Connolly A, Davis M, Robbins R, Wu J. Immunosuppressive therapy mitigates immunological rejection of human embryonic stem cell xenografts. *Proc Natl Acad Sci U S A.* 2008;105:12991–12996.
- Drukker M, Katchman H, Katz G, Friedman S, Shezen E, Hornstein E, Mandelboim O, Reisner Y, Benvenisty N. Human embryonic stem cells and their differentiated derivatives are less susceptible to immune rejection than adult cells. *Stem Cells.* 2006;24:221–229.
- Preynat-Seauve O, de Rham C, Tirefort D, Ferrari-Lacraz S, Krause KH, Villard J. Neural progenitors derived from human embryonic stem cells are targeted by allogeneic T and natural killer cells. *J Cell Mol Med.* 2009;13:3556–3569.
- Grinnemo KH, Kumagai-Braesch M, Mansson-Broberg A, Skottman H, Hao X, Siddiqui A, Andersson A, Stromberg AM, Lahesmaa R, Hovatta O, Sylven C, Corbascio M, Dellgren G. Human embryonic stem cells are

- immunogenic in allogeneic and xenogeneic settings. *Reprod Biomed Online*. 2006;13:712–724.
14. Nomi H, Tashiro-Yamaji J, Yamamoto Y, Miura-Takeda S, Miyoshi-Higashino M, Takahashi T, Azuma H, Ueda H, Katsuoka Y, Kubota T, Yoshida R. Acute rejection of allografted CTL-susceptible leukemia cells from perforin/Fas ligand double-deficient mice. *J Immunol*. 2007;179: 2180–2186.
 15. Komatsu M, Mammolenti M, Jones M, Jurecic R, Sayers TJ, Levy RB. Antigen-primed CD8+ T cells can mediate resistance, preventing allogeneic marrow engraftment in the simultaneous absence of perforin-, CD95L-, TNFR1-, and TRAIL-dependent killing. *Blood*. 2003;101: 3991–3999.
 16. Drukker M, Benvenisty N. The immunogenicity of human embryonic stem-derived cells. *Trends Biotechnol*. 2004;22:136–141.
 17. Koch CA, Jordan CE, Platt JL. Complement-dependent control of teratoma formation by embryonic stem cells. *J Immunol*. 2006;177: 4803–4809.
 18. Dressel R, Nolte J, Elsner L, Novota P, Guan K, Streckfuss-Bomeke K, Hasenfuss G, Jaenisch R, Engel W. Pluripotent stem cells are highly susceptible targets for syngeneic, allogeneic, and xenogeneic natural killer cells. *FASEB J*. 2010;24:2164–2177.
 19. Mammolenti M, Gajavelli S, Tsoulfas P, Levy R. Absence of major histocompatibility complex class I on neural stem cells does not permit natural killer cell killing and prevents recognition by alloreactive cytotoxic T lymphocytes in vitro. *Stem Cells*. 2004;22:1101–1110.
 20. Dressel R, Schindehutte J, Kuhlmann T, Elsner L, Novota P, Baier PC, Schillert A, Bickeboller H, Herrmann T, Trenkwalder C, Paulus W, Mansouri A. The tumorigenicity of mouse embryonic stem cells and in vitro differentiated neuronal cells is controlled by the recipients' immune response. *PLoS One*. 2008;3:e2622.
 21. Tseng HC, Arasteh A, Paranjpe A, Teruel A, Yang W, Behel A, Alva JA, Walter G, Head C, Ishikawa TO, Herschman HR, Cacalano N, Pyle AD, Park NH, Jewett A. Increased lysis of stem cells but not their differentiated cells by natural killer cells; de-differentiation or reprogramming activates NK cells. *PLoS One*. 5:e11590.
 22. Gonzalez S, Castanotto D, Li H, Olivares S, Jensen MC, Forman SJ, Rossi JJ, Cooper LJ. Amplification of RNAi—targeting HLA mRNAs. *Mol Ther*. 2005;11:811–818.

Immunobiology of naïve and genetically modified HLA-class-I-knockdown human embryonic stem cells

Tobias Deuse^{1,2,3}, Martina Seifert⁴, Neil Phillips⁵, Andrew Fire⁶, Dolly Tyan⁶, Mark Kay⁵, Philip S. Tsao⁷, Xiaoqin Hua^{2,3}, Joachim Velden⁸, Thomas Eiermann⁹, Hans-Dieter Volk⁴, Hermann Reichenspurner^{2,3}, Robert C. Robbins¹ and Sonja Schrepfer^{1,2,3,*}

¹Cardiothoracic Surgery, Stanford University, Stanford, CA 94305, USA

²Cardiovascular Surgery, TSI-laboratory, University Hospital Hamburg, Hamburg 20246, Germany

³Cardiovascular Research Center, University Hospital Hamburg, Hamburg 20246, Germany

⁴Institute of Medical Immunology and Berlin-Brandenburg Center for Regenerative Therapies (BCRT) Charité Campus Virchow-Klinikum, Berlin 13353, Germany

⁵Pediatrics, Human Gene Therapy, Stanford University, Stanford, CA 94305, USA

⁶Pathology, Stanford University, Stanford, CA 94305, USA

⁷Cardiovascular Medicine, Stanford University, Stanford, CA 94305, USA

⁸Pathology, University Hospital Hamburg, Hamburg 20246, Germany

⁹Transfusion Medicine, University Hospital Hamburg, Hamburg 20246, Germany

*Author for correspondence (schrepfer@stanford.edu)

Accepted 10 May 2011

Journal of Cell Science 124, 3029–3037

© 2011. Published by The Company of Biologists Ltd

doi: 10.1242/jcs.087718

Summary

Human embryonic stem cells (hESCs) can serve as a universal cell source for emerging cell or tissue replacement strategies, but immune rejection of hESC derivatives remains an unsolved problem. Here, we sought to describe the mechanisms of rejection for naïve hESCs and upon HLA class I (HLA I) knockdown (hESC^{KD}). hESCs were HLA I-positive but negative for HLA II and co-stimulatory molecules. Transplantation of naïve hESC into immunocompetent Balb/c mice induced substantial T helper cell 1 and 2 (Th1 and Th2) responses with rapid cell death, but hESCs survived in immunodeficient SCID-beige recipients. Histology revealed mainly macrophages and T cells, but only scattered natural killer (NK) cells. A surge of hESC-specific antibodies against hESC class I, but not class II antigens, was observed. Using HLA I RNA interference and intrabody technology, HLA I surface expression of hESC^{KD} was 88%–99% reduced. T cell activation after hESC^{KD} transplantation into Balb/c was significantly diminished, antibody production was substantially alleviated, the levels of graft-infiltrating immune cells were reduced and the survival of hESC^{KD} was prolonged. Because of their very low expression of stimulatory NK ligands, NK-susceptibility of naïve hESCs and hESC^{KD} was negligible. Thus, HLA I recognition by T cells seems to be the primary mechanism of hESC recognition, and T cells, macrophages and hESC-specific antibodies participate in hESC killing.

Key words: Human embryonic stem cells, Immunology, Rejection, HLA class I knockdown

Introduction

Human embryonic stem cells (hESCs) are pluripotent with the capacity to differentiate into any cell line. It is therefore conceivable that complex tissues can be rebuilt by hESC-based therapy after tissue injury. In the case of myocardial damage, therapeutic strategies currently pursued include the transplantation of hESC-derived cardiac progenitor cells to form contractile intracardiac grafts (Laflamme et al., 2007; Xue et al., 2005) and the transplantation of functional in-vitro-generated engineered heart tissue from hESCs (Domian et al., 2009). Both approaches have already shown substantial improvements in cardiac function. The reestablishment of contractile cells contributing to the cardiac mechanics is aspired, and great progress has recently been achieved in differentiating hESCs into cardiomyocytes (Burrige et al., 2007; Passier et al., 2005) and in sorting highly purified hESC-derived cardiomyocyte populations (Anderson et al., 2007; Hattori et al., 2010; Mummery, 2010). However, it has to be emphasized that improvements of cardiac function in experimental settings have so far only been achieved by transplanting hESC-

derived cardiomyocytes into either immunodeficient (van Laake et al., 2007) or heavily immunosuppressed recipients (Caspi et al., 2007). Former beliefs of an immune privilege of hESCs or hESC-derived tissues have been thoroughly disproven (Drukker et al., 2006; Swijnenburg et al., 2008a) and human leukocyte antigen [HLA; the major histocompatibility complex (MHC) in humans] disparity between the hESC-derived donor cells and the recipient's immune cells during transplantation inevitably provokes immune rejection (Chidgey et al., 2008; Lui et al., 2009).

Although autologous induced pluripotent stem (iPS) cells can be generated from adult somatic cells as a potential pluripotent cell source for patients, thereby avoiding immune barriers, the generation of individualized cellular grafts for every patient might be impractical. This is because of the complexity of stem cell generation, requirements for quality assurance, timely and costly manufacturing process, the possibility of genetic abnormalities in donor cells and the uncertain availability at the time of need (Daley and Scadden, 2008). iPS-derived cells or tissues will more probably, at least in part, be transplanted in an

allogeneic setting. Therefore, efforts are currently being undertaken to establish both hESC (Lin et al., 2009) and iPSC cell banks (Tamaoki et al., 2010) in order to achieve at least partial HLA matching and reduce the risk for rejection. However, immunosuppressive protocols might still be needed at various levels.

Our group aims at generating hypoimmunogenic hESC lines that would conserve immune non-responsiveness and might therefore serve as cell sources for generating universally compatible 'off-the-shelf' cell grafts or tissues. We herein present our studies evaluating the contributions of cellular and humoral immune components to the killing of hESCs and demonstrate that HLA class I (HLA I)-knockdown hESCs (hESC^{KD}) induce a substantially reduced immune activation and show extended survival.

Results

Characterization of hESCs and hESC^{KD}

hESCs showed modest HLA I and β_2 -microglobulin surface expression, whereas these antigens were dramatically reduced in 7-day hESC^{KD} (Fig. 1). Both hESCs and hESC^{KD} were negative for HLA II and the co-stimulatory molecules CD80, CD86 and CD40. They were also negative for SSEA-1, a marker for maturity, but positive for SSEA-4 and the embryonic stem cell markers Oct-4, Sox-2, SSEA-3 and TRA-1-60. HLA phenotyping revealed the presence of A2, A3, B35, B44, Cw4, Cw7, DR15, DR16, DQ5 and DQ6.

Transplantation of hypoantigenic hESC^{KD}

The mean HLA I expression on hESC^{KD} over time was followed by fluorescence-activated cell sorting (FACS) (Fig. 2a). After around 7 days, HLA I expression reached its trough at 1.1 ± 0.1 ($P < 0.001$ compared with hESCs), which corresponds to $\sim 1\%$ of

the surface expression of naïve hESCs. Between days 7 and 42, the lowered HLA I expression remained stable, at between 1.1 ± 0.1 and 2.1 ± 0.4 .

To reveal whether the lowered HLA I surface expression was due to retainment of intracellular HLA I, the intracellular HLA I accumulation was quantified (supplementary material Fig. S1). Intracellular HLA I was hardly detectable in naïve hESCs and was not increased in hESCs after small interfering RNA (siRNA) application. In hESCs treated with intrabody (IB), however, accumulated intracellular HLA I was found. When IB was used as an adjunct to siRNA in hESC^{KD}, retainment of HLA I was not observed.

An early decline in BLI signals over the first few days was observed in Balb/c and SCID-beige recipients of hESCs (Fig. 2b). This initial decrease in cell viability was attributed to the transplant procedure itself, whereas the subsequent course of the bioluminescence imaging (BLI) signal reflected the impact of immune rejection on the proliferating viable hESC fraction. All hESCs were rapidly rejected in Balb/c mice and BLI signals were lost beyond the fifth day. In immunodeficient SCID-beige mice, which lack both lymphocytic and natural killer (NK) cell killing, BLI signals steadily increased to regain their initial values by around day 21. On day 80, macroscopic tumor growth was observed at the site of injection (supplementary material Fig. S2a) with ~ 50 times increased BLI signals (supplementary material Fig. S2b). Upon histological evaluation, the local tumors that had formed were clearly identified as teratomas, containing tissues from all three germ layers (supplementary material Fig. S2c). The rejection of hESC^{KD} in Balb/c recipients was profoundly mitigated compared with that of naïve hESC and their survival was markedly prolonged (Fig. 2b). In six of the ten animals, the BLI signals slowly dropped into the background at around day 28, but in four animals the signals remained stable

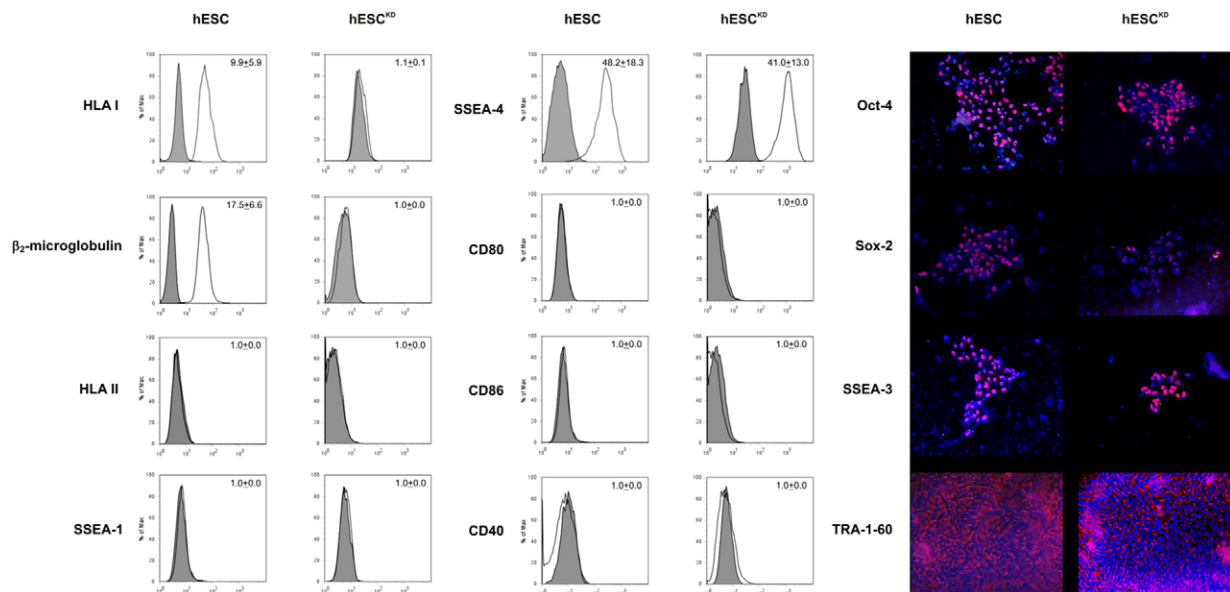


Fig. 1. Characterization of hESC and hESC^{KD}. Normalized surface molecule expression was assessed by flow cytometry. HLA I and β_2 -microglobulin were modestly expressed on hESCs and were successfully knocked down after 7 days in hESC^{KD}. Both hESC and hESC^{KD} were negative for HLA II and co-stimulatory molecules. They were also negative for SSEA-1 but positive for SSEA-4. Prominent expression of Oct-4, Sox-2, SSEA-3 and Tra-1-60 was confirmed by immunofluorescence (right-hand panel).

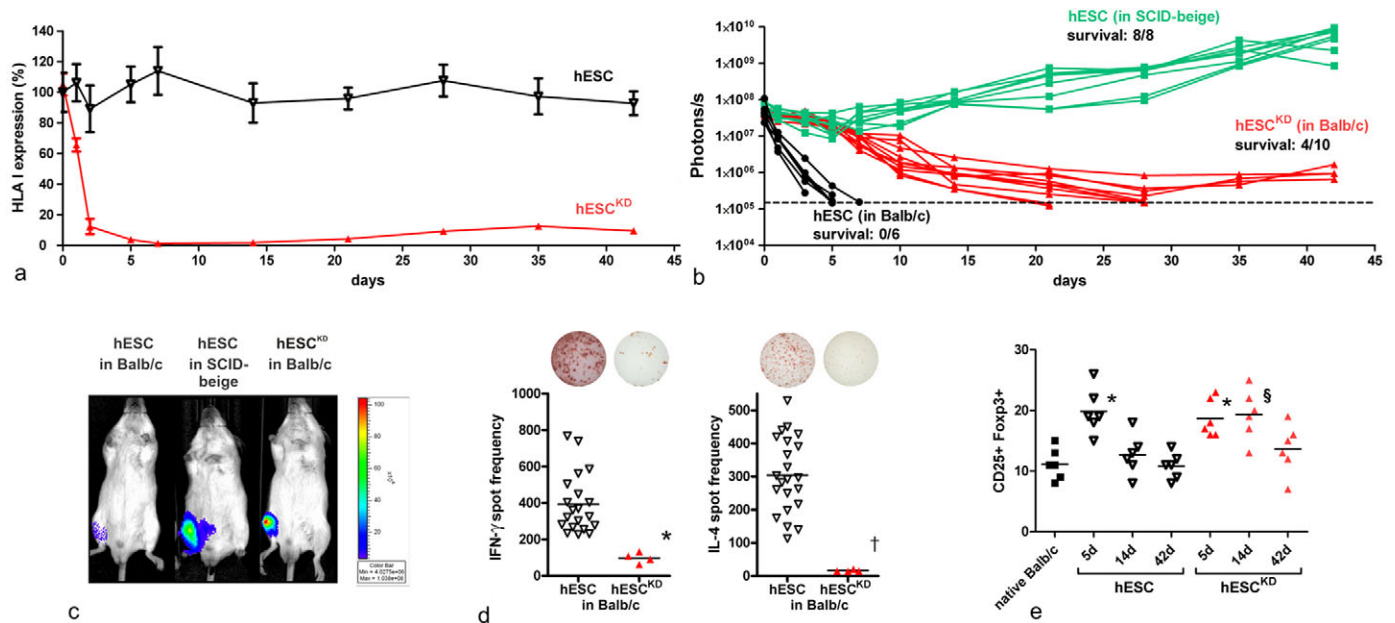


Fig. 2. Transplantation of hypoantigenic hESC. (a) HLA I knockdown in hESC^{KD} was followed by flow cytometry and showed levels between 1% and 12% of those of naïve hESC between days 7 and 42 (means \pm s.e.m.). (b) A total of 10^6 hESC or hESC^{KD} were transplanted into the gastrocnemius muscle of either immunocompetent Balb/c or severely immunocompromised SCID-beige mice. All Balb/c mice rapidly rejected the hESC transplants, whereas the cells survived in SCID-beige recipients. Rejection of hESC^{KD} was markedly attenuated and four out of ten hESC^{KD} grafts achieved long-term survival. (c) On day 5, BLI signals from hESCs in SCID-beige and hESC^{KD} in Balb/c were similarly strong, whereas signals from hESCs in Balb/c were negligible. (d) Balb/c cellular immune activation on the same day was significantly stronger after hESC rather than hESC^{KD} transplantation. * $P < 0.05$ compared with hESCs; † $P < 0.001$ compared with hESCs. (e) The percentage of Treg cells (CD25+ Foxp3+ cells) among the CD4+ population in inguinal lymph nodes was monitored over time. The Treg fraction increased after both hESC and hESC^{KD} transplantation (* $P < 0.05$ compared with native Balb/c) but remained elevated only in the hESC^{KD} group (§ $P < 0.01$ compared with hESC after 14 days).

and lasted for more than 42 days. Therefore, long-term cell survival in a stringent xenogeneic setting was achieved with hESC^{KD} in 40% of the animals.

At 5 days after the transplantation, the BLI signals from hESCs in SCID-beige mice and hESC^{KD} in Balb/c mice were similar, whereas signals from hESCs in Balb/c mice were hardly detectable (Fig. 2c). Because SCID-beige mice lack lymphocytes and NK cells, Elispot assays cannot be performed. Balb/c Elispot assays performed on day 5 were strikingly different between the naïve hESC and hESC^{KD} groups (Fig. 2d). Interferon (IFN)- γ ($P = 0.002$) and interleukin (IL)-4 spot frequencies ($P < 0.001$) were significantly lower after hESC^{KD} transplantation. Within the regional lymph nodes, the regulatory T cell (Treg) fraction (CD25+ Foxp3+) of CD4+ cells significantly increased 5 days after transplantation of hESCs ($P = 0.002$) or hESC^{KD} ($P = 0.010$) compared with control mice. After 14 days, a substantial time after all hESC grafts had been rejected, the Treg population had decreased to basal values. However, all hESC^{KD} grafts still showed viable BLI signals and the Treg fraction remained elevated ($P = 0.033$ among the 14-day groups). No differences were observed after 42 days (Fig. 2e).

Histology of hESC rejection

Gastrocnemius muscles of Balb/c mice were harvested on day 5 after hESC or hESC^{KD} transplantation and the composition of the cellular infiltrates was analyzed by immunohistochemistry. hESC grafts had a mainly round cell morphology and were identified by their firefly luciferase (Fluc) positivity (Fig. 3a–c). The main cell populations were macrophages and CD3+ lymphocytes, and only

scarce KLRA1+ NK cells were found (Fig. 3d). All inflammatory cell populations were significantly lower within hESC^{KD} grafts (Fig. 3e; $P < 0.001$ each compared with hESC).

Antibody response after hESC transplantation

Untreated Balb/c mice (before transplantation) showed negligible amounts of naturally occurring anti-hESC xenoantibodies, but cell transplantation rapidly induced IgM donor-specific antibody (DSA) production (Fig. 4a). However, the percentage of IgM-antibody-loaded cells was found to be significantly higher after hESC transplantation compared with hESC^{KD} transplantation ($P < 0.001$). Next, the specificity of these antibodies was determined in Luminex single-antigen assays for HLA I and II. Class I antibody production was only induced after hESC transplantation ($P = 0.021$ compared with native animals), but not after transplantation of hypoantigenic hESC^{KD} (Fig. 4b). There was no significant induction of class II antibodies in both transplant groups. hESC re-injection 1 week after the first hESC transplantation resulted in a massive boost of class I ($P = 0.007$ compared with hESCs), but not class II, antibodies, verifying the specificity of the antibody response. In recipients of hESC, the mean Z-score of hESC-specific class I antibodies was significantly higher than that of non-hESC-specific antibodies (Fig. 4c; $P = 0.049$) and all of the six hESC-specific HLA-A, -B and -C antibody Z-scores were above a threshold of three (Fig. 4d). In recipients of hESC^{KD}, no hESC-specific class I antibodies were significantly induced. All HLA-DR and -DQ antibody Z-scores remained far below the threshold after both hESC and hESC^{KD} transplantation.

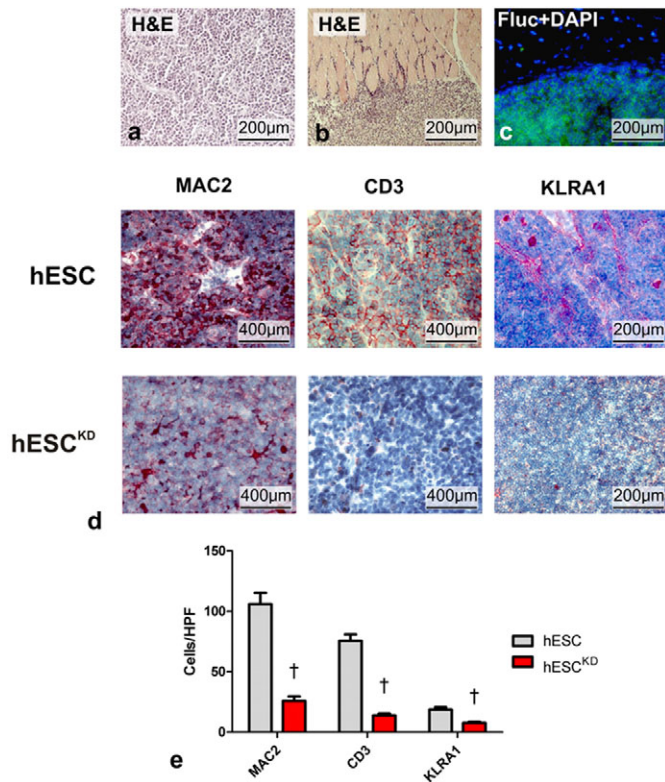


Fig. 3. Histology of hESC transplants. Intramuscularly-injected hESCs were identified according to their morphology in hematoxylin and eosin (a,b) and their Fluc-positivity (c). At 5 days after transplantation, hESC grafts showed markedly more dense infiltrates of MAC2⁺ macrophages and CD3⁺ lymphocytes than hESC^{KD} grafts (d). Only a few KLRA1⁺ NK cells were found after hESC or hESC^{KD} transplantation. (e) Cell numbers of all three cell populations were significantly lower within hESC^{KD} rather than hESC grafts. † $P < 0.001$ compared with hESCs.

Allogeneic cytotoxic killing of hESC

After incubation with CD3⁺ CD56⁻ lymphocytes, hESCs ($P = 0.001$ and $P = 0.002$), but not hESC^{KD} ($P = 1.0$ and $P = 0.428$), significantly increased the spot frequencies for IFN- γ (Fig. 5a) and IL-4 (Fig. 5b), respectively, compared with resting responder lymphocytes. hESC^{KD} were therefore incapable of inducing relevant in vitro lymphocyte activation. Elispots were then performed with CD3⁻ CD56⁺ NK cells. NK-susceptible K562 cells ($P < 0.001$ compared with responder NK cells) induced substantial NK cell activation that was similar to the effect of incubation with PMA plus ionomycin ($P < 0.001$ compared with responder NK). Neither hESCs nor hESC^{KD} induced relevant IFN- γ release (Fig. 5c). Similarly, CD107a surface expression on NK cells was only significantly increased upon either incubation with PMA plus ionomycin ($P < 0.001$) or K562 challenge ($P = 0.001$). hESC and hESC^{KD} incubation ($P = 1.0$ compared with responder NK cells) did not alter CD107a expression (Fig. 5d).

Differences in expression patterns of stimulatory and inhibitory NK ligands, more than differences in HLA I expression, might account for the differences in NK cytotoxicity between K562 cells and hESC^{KD} (Table 1). The stimulatory danger signals MHC class I polypeptide-related

sequence A (MICA) ($P = 0.012$), MICB ($P < 0.001$) and, most obviously, Hsp70 ($P < 0.001$) were expressed at significantly higher levels on K562 cells. The stimulatory NK ligands ULBP1, 2 and 3 and the NK inhibitory ligands HLA-E and HLA-G were similarly low on hESC, hESC^{KD} and K562 cells and might therefore not account for the different NK susceptibilities of these cells.

Discussion

The present study aimed at revealing the mechanisms of hESC rejection and describing the survival benefits of HLA I knockdown (hESC^{KD}). The immunological nature of cell fate after xenogeneic transplantation could be demonstrated by the rapid hESC death in immunocompetent Balb/c mice and the survival in severely immunodeficient SCID-beige recipients, exhibiting defective T cell, B cell and NK cell responses. We could clearly demonstrate strong Th1 (IFN γ release) and Th2 (IL-4 release) responses in Balb/c recipients of hESC transplants. In addition, we showed that those T cell activations were mainly triggered by hESC HLA I expression because hESC^{KD} largely failed to induce T cell responses. Differences in the completeness and durability of HLA I knockdown might therefore determine which graft undergoes slowed rejection or proceeds to long-term survival. We could further show that stem cell transplantation increased the fraction of CD4⁺ CD25⁺ Foxp3⁺ Tregs in regional lymph nodes and that only recipients of hESC^{KD} showed a prolonged polarization of T cells toward a regulatory phenotype. The induction of transplantation tolerance for ESCs by host conditioning with antibodies specific for the CD4 and CD8 receptors (Robertson et al., 2007) or by costimulatory blockade (Grinnemo et al., 2008; Pearl et al., 2011) has been successful in prolonging cell survival. Tregs have been identified as central regulators for this state of acquired immune privilege. Interestingly, hESC^{KD} seem to induce similar tolerogenic responses in non-conditioned immunocompetent hosts. The regulatory properties of Tregs might be most crucial in the induction phase of tolerance early after cell transplantation (Muller et al., 2010).

Strategies involving the gene transfer of an anti-HLA I single chain IB (Beyer et al., 2004) or plasmids containing siRNA (Gonzalez et al., 2005) were recently developed to downregulate surface HLA I. Using the IB technology as a second line of capture mechanism for the very few HLA I molecules that still were synthesized despite the use of siRNA caused no retainment of intracellular HLA I molecules. Such retainment has been reported with IB alone (Busch et al., 2004) and might paradoxically increase the antigenicity of cell transplants.

Table 1. Stimulatory and inhibitory ligands for NK activation

| Ligand | hESCs | hESC ^{KD} | K562 | P-value (ANOVA) |
|-------------|-----------|--------------------|------------|-----------------|
| MICA | 1.1 ± 0.1 | 1.2 ± 0.1 | 4.9 ± 2.1 | 0.012 |
| MICB | 1.2 ± 0.2 | 1.1 ± 0.1 | 4.0 ± 0.5 | <0.001 |
| Hsp70 | 2.2 ± 0.2 | 2.1 ± 0.3 | 12.2 ± 1.4 | <0.001 |
| ULBP-1 | 1.5 ± 0.3 | 1.4 ± 0.5 | 1.3 ± 0.2 | 0.792 |
| ULBP-2 | 1.6 ± 0.6 | 1.6 ± 0.3 | 1.7 ± 0.4 | 0.926 |
| ULBP-3 | 1.8 ± 0.6 | 1.8 ± 0.3 | 1.3 ± 0.1 | 0.236 |
| HLA class I | 9.9 ± 5.9 | 1.8 ± 0.3 | 1.0 ± 0.0 | 0.017 |
| HLA-E | 1.4 ± 0.4 | 1.4 ± 0.6 | 1.4 ± 0.4 | 0.995 |
| HLA-G | 1.6 ± 0.9 | 1.5 ± 0.6 | 1.1 ± 0.2 | 0.589 |

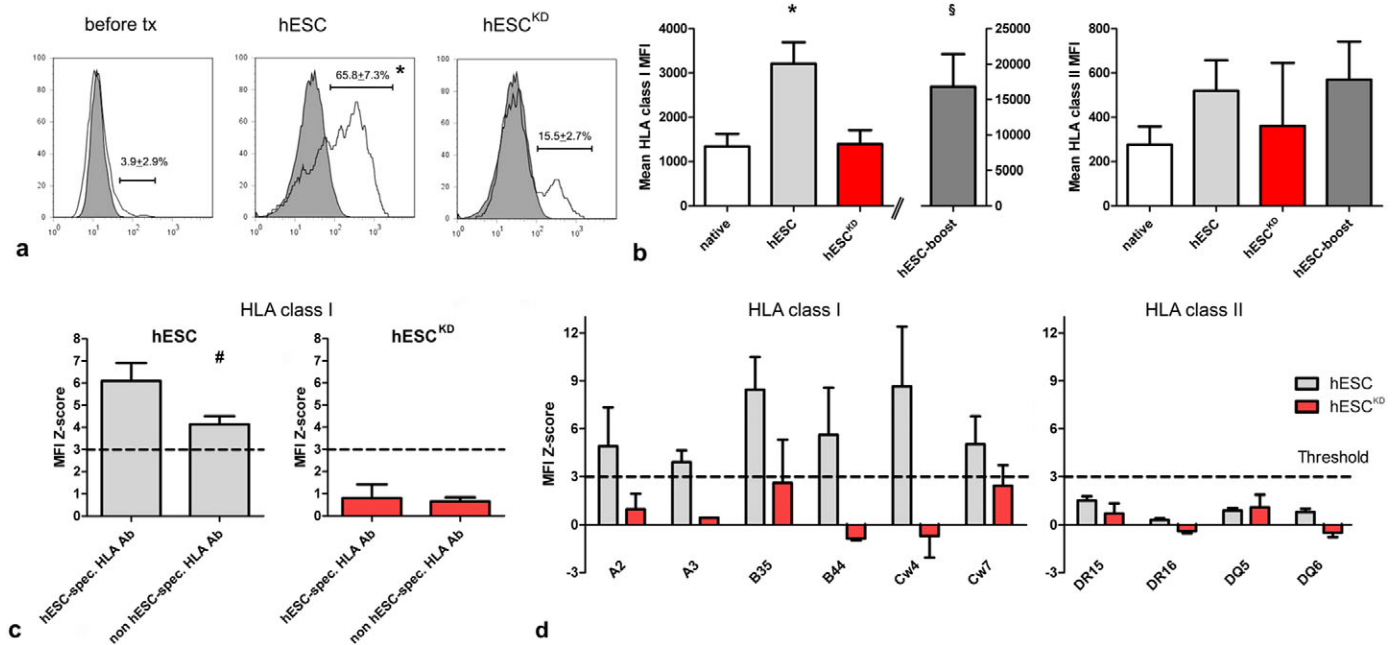


Fig. 4. Antibody response after hESC transplantation. (a) At 5 days after transplantation into Balb/c mice, flow cytometry showed a significantly stronger hESC-specific antibody production for hESCs compared with hESC^{KD}. * $P < 0.05$ compared with both before transplantation and with hESC^{KD} transplantation. (b) Luminex single-antigen assays revealed HLA class I-specific antibody induction by hESCs but not hESC^{KD}, which was massively boosted by hESC re-injection. * $P < 0.05$ compared with native Balb/c; § $P < 0.05$ compared with hESCs. HLA class II antibody induction was not observed. (c,d) In recipients of hESC grafts, the mean Z-score of hESC-specific class I antibodies was significantly higher than that of non-hESC-specific antibodies and all of the six hESC-specific HLA-A, -B and -C antibody Z-scores were above a threshold of 3 s.d. # $P < 0.05$. The recipients of hESC^{KD} did not significantly induce hESC-specific class I antibody production, and recipients of both groups did not develop relevant hESC-specific class II antibodies.

Although T cells are crucial for hESC recognition (the afferent limb of immune activation), other effector cells might participate in the killing. In a study with allogeneic leukemia cells, the blocking of both perforin- and FasL-dependent killing, two major cytotoxic effector mechanisms of T cells, did not prevent cell rejection. Macrophages had been identified as the effector cell population (Nomi et al., 2007). It has been further demonstrated that T cells can mediate rejection of allogeneic marrow progenitor cells through alternative effector pathways independent of perforin-, FasL-, TNF-like weak inducer of apoptosis (TWEAK)-, and TNF-related apoptosis-inducing ligand (TRAIL)-dependent cytotoxicity (Komatsu et al., 2003; Zimmerman et al., 2005). Other cytolytic mechanisms involving antibodies (Drukker and Benvenisty, 2004) and complement (Koch et al., 2006) have also been suggested to contribute to the killing of hESCs in vivo.

The importance of antibody-mediated rejection after cell transplantation is gaining increasing awareness and has already been reported for hematopoietic (Spellman et al., 2010) and mesenchymal stem cell (MSC) transplantation (Beggs et al., 2006; Cho et al., 2008) and for islet transplantation (Mohanakumar et al., 2006). FACS-based DSA quantification using living cells identifies all bound antibodies both against HLA and non-HLA epitopes. In our murine model, we did not find naturally occurring anti-hESC antibodies, but cell transplantation induced a rapid surge of DSAs. Antibody production after hESC transplantation was restricted to the HLA class I and was mostly specific for hESC HLA I. HLA II was absent on hESCs and could not be induced by stimulation.

Consequently, there was no significant antibody production against HLA II. hESC re-injection induced a boost in HLA I IgG antibodies, as has been reported after MSC transplantation in swine (Cho et al., 2008). Even non-cytotoxic alloantibodies detected by flow cross-match, which are negative in conventional complement-dependent lymphocytotoxic cross-match, have been reported to be sufficient to cause immunologic damage of transplanted islets (Mohanakumar et al., 2006). The antibody surge in our study occurred rapidly (within 5 days) and accompanied the strong cellular immune activation. Reports that short-term T-cell-specific immunosuppression prevented the antibody response against transplanted MSCs support the hypothesis of a T-cell-driven humoral response against cellular grafts (Poncelet et al., 2008). Ongoing humoral rejection of islet grafts was successfully treated with an anti-CD20 monoclonal antibody (Kessler et al., 2009). Epitope spreading might have caused some concomitant increase of non-hESC-specific antibodies in our study and has also been recognized after clinical hematopoietic stem cell transplantation (Leffell et al., 2009; Papassavas et al., 2002). The antigenicity of hESC^{KD} was low enough to prevent the induction of hESC-specific antibody production.

The naturally low HLA I expression of hESCs could make them susceptible to NK killing. However, the histological sections of immunocompetent hESC-rejecting Balb/c mice revealed macrophages as the dominant cell population, followed by CD3+ lymphocytes and revealed only scattered NK cells. The early surge of hESC-specific antibodies and the direct correlation between the level of HLA I knockdown and the

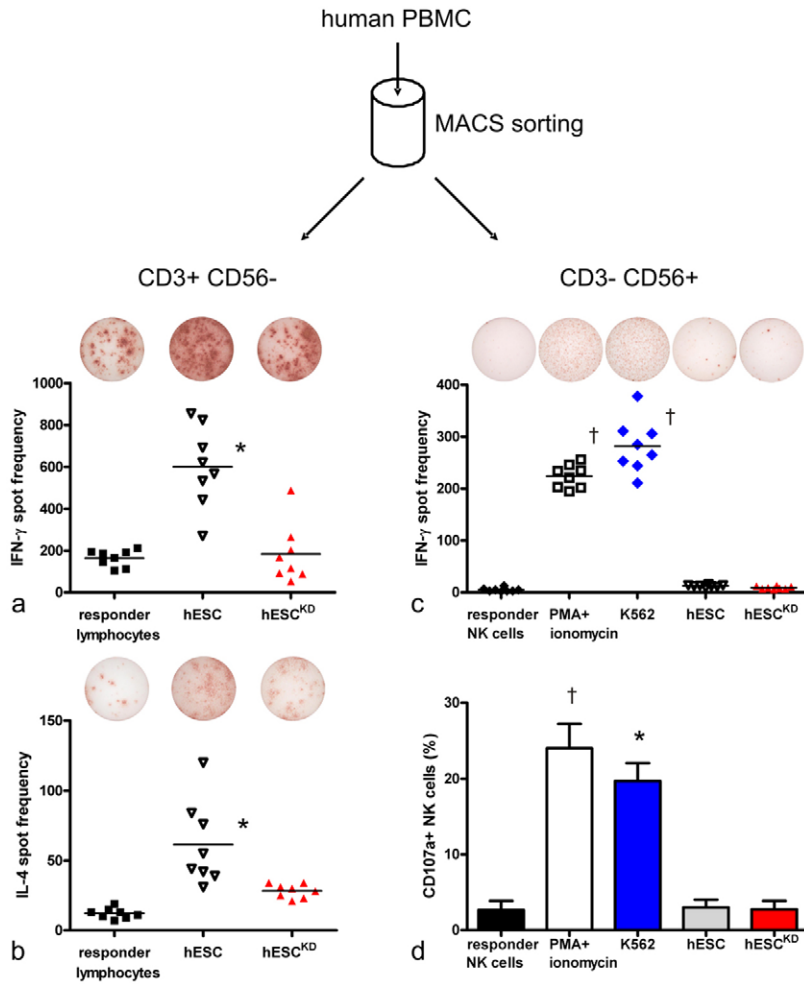


Fig. 5. Allogeneic cytotoxic killing of hESC. Human PBMCs were separated into lymphocytes (CD3+ CD56-) and NK cells (CD3- CD56+). IFN- γ (a) and IL-4 (b) Elispot assays revealed that only hESCs, and not hESC^{KD}, significantly induced allogeneic lymphocyte activation in vitro. * $P < 0.05$ compared with responder lymphocytes. NK cell activation (c) and CD107a surface expression (d) was provoked by either PMA plus ionomycin stimulation or K562 incubation. * $P < 0.05$ and † $P < 0.001$ compared with responder NK cells. Both hESCs and hESC^{KD} did not induce significant NK cell activation.

strength of the T cell response, as well as the pace of cell rejection, are further proof of an adaptive T-cell-directed immune response. There are reports of substantial (Dressel et al., 2010; Dressel et al., 2008) and negligible (Bonde and Zavazava, 2006; Koch et al., 2008; Mammolenti et al., 2004) in vitro NK responses against murine ESCs, presumably depending on the experimental conditions. Although even syngeneic NK cells have been reported to kill murine ESCs after adequate stimulation in vitro (Dressel et al., 2010), murine ESCs have uniformly been reported to form teratomas in syngeneic (Dressel et al., 2008; Koch et al., 2006; Kolossov et al., 2006) but not allogeneic (Dressel et al., 2008; Koch et al., 2006) or xenogeneic recipients (Dressel et al., 2008). Because the cytotoxic activity of mouse NK cells in vitro strongly depended on sufficient activation, SCID mice, deficient in T and B cells but with functional NK cells, were treated with poly(I:C) and were used as recipients for murine ESCs. The in vivo NK activity was found to be increased and the frequency of teratoma formation significantly reduced (Dressel et al., 2010). In vivo rejection of murine ESC derivatives by NK cells has also been reported in *Rag2*^{-/-} mice (Tabayoyong et al., 2009). Both mouse models lack functional lymphocytes and contain greatly increased numbers of NK cells (Tabayoyong et al., 2009). The impact of NK cells in immunocompetent hosts might, however, be less important. hESCs have been shown not to be effectively recognized by human NK cells in vitro (Drukker

et al., 2002) but only after additional in vitro NK stimulation (Tseng et al., 2010). Besides the lack of MHC I on target cells, the activation of additional stimulatory NK receptors is necessary to trigger NK killing (Bryceson et al., 2006), and the expression of stimulating NK ligands can lead to lysis even in the presence of MHC I (Cerwenka et al., 2001). Murine ESCs have been shown to express high levels of the NKG2D ligands REA-1, H60, MULT-1 (Bonde and Zavazava, 2006; Dressel et al., 2008; Frenzel et al., 2009) and ICAM-1 (Frenzel et al., 2009), and blocking of these receptors prevents cell lysis (Frenzel et al., 2009; Preynat-Seauve et al., 2009). Murine ESC-derived cardiomyocytes, however, which are negative for MHC I but also negative for NKG2D ligands, were spared by NK cells (Frenzel et al., 2009). Human equivalents for NKG2D ligands are MICA and MICB and ULBP1, 2 and 3. Here, we have shown that hESCs and hESC^{KD} express NKG2D ligands at negligible levels and might therefore be less susceptible to human and murine NK killing (Drukker et al., 2006) than their murine counterparts. Furthermore, hESC and hESC^{KD} express Hsp70 at much lower levels than the HLA-I-negative and NK-susceptible erythroleukemia cell line K562. Hsp70-blocking experiments with K562 cells strongly reduced NK cytotoxicity (Stangl et al., 2008), demonstrating the important activating role of Hsp70. Because of the 94.5% homology between human and mouse Hsp70, murine NK cells have been previously shown to kill

Hsp70-expressing MICA-positive human tumors (Elsner et al., 2007). NK depletion in nude mice has been demonstrated to facilitate tumor growth of K562 xenografts and the development of metastases (Yoshimura et al., 1996). hESCs have been shown previously to only very weakly express ligands for the natural cytotoxicity receptor (NCR) NKp44, and ligands for NKp30, NKp46 and CD16 were not found (Drukker et al., 2002). Blocking experiments with NCR antibodies did not inhibit *in vitro* NK killing of hESC derivatives and made NCR appear less important for NK activation of hESCs (Preynat-Seauve et al., 2009). The low levels of HLA-E and HLA-G on hESCs and hESC^{KD} do not support an NK-protective role in these cell populations. However, HLA-G is upregulated in hESC-derived mesenchymal progenitor cells and has been shown to contribute to the immunosuppressive properties of the mesenchymal stem cell phenotype (Yen et al., 2009).

Conclusions

We demonstrate a central role for HLA I in the recognition of hESCs by xenogeneic or allogeneic T cells. The HLA-I-knockdown hESC^{KD} experience strongly diminished cellular and antibody responses. Despite HLA-I-knockdown, hESC^{KD} do not trigger substantial NK activity, which might be related to their negligible expression of stimulating NK ligands. We believe the generation of hypoantigenic cell sources is a requisite for future *ex vivo* generation of hypoantigenic tissues for cell replacement therapies.

Materials and Methods

Animals

Male Balb/c ($n=72$) and SCID-beige (CB17.Cg-Prkdc^{scid}Lyst^{bg}/CrI; $n=8$) mice were purchased from Charles River Laboratories (Sulzfeld, Germany) and received humane care in compliance with the Guide for the Principles of Laboratory Animals.

hESCs

H9 hESCs (Wicell, Madison, WI) were maintained on inactivated murine embryonic fibroblast (MEF) feeder layers (Millipore, Billerica, MA) in hESC medium. hESC colonies were separated from MEF feeders by incubation with dispase (Invitrogen) and subcultured on feeder-free Matrigel-coated plates (Matrigel from BD Biosciences) before use. The hESC and iPS cell characterization kit (Applied StemCell, Sunnyvale, USA) was used to demonstrate the expression of Oct-4, Sox-2, SSEA-3 and TRA-1-60. HLA immunotyping was performed by using LiPA HLA-DRB1, -DQB1, -A, -B and -C kits according to the manufacturer's protocol (Innogenetics, Alpharetta, GA).

HLA I knockdown

Gene silencing both at the post-transcriptional level using small interfering RNA (siRNA) (Caplen et al., 2001) and at the post-translational level with intrabody (IB) technology (Beyer et al., 2004) were used to generate HLA-I-knockdown hESCs (hESC^{KD}).

siRNA technique

HLA class I siRNA (Ambion, Darmstadt, Germany), a target-specific 20–25 nucleotide siRNA, was used at a concentration of 20 μ M. A total of 10 μ l of 20 μ M siRNA solution was incubated with 200 μ l OptiMEM (Invitrogen) containing 0.3 μ l DharmaFECT 1 (Thermo Scientific). Then, 1.2 ml of prepared siRNA in OptiMEM was added into each hESC well and incubated for 24 hours. To assess the efficiency of siRNA delivery into cells, the localization of the siGLO green transfection indicator (Thermo Scientific), which localizes to the nucleus, was checked. hESC were transfected with siGLO green (20 nM), complexed with DharmaFECT 1 transfection reagent (0.1 μ l/well), fixed with 3.7% formaldehyde solution and stained with phalloidin–Alexa-Fluor-546.

Intrabody technique

E1-deleted human Ad5 recombinant adenovirus containing the anti-human-HLA-I single-chain intrabody fragment (AdScFv), driven by the cytomegalovirus (CMV) promoter, was constructed, purified and assayed for plaque forming units (pfu) per ml, as described previously (Kolls et al., 1994). The intrabodies recognize a non-

polymorphic HLA I epitope. Transduction of cells was performed with a multiplicity of infection (MOI) of 150 pfu. To assess transduction efficiency, E1-deleted, human Ad5 recombinant adenovirus encoding for the enhanced green fluorescent protein (AdvGFP), as a reporter construct, was generated and served as the control construct. The AdvGFP transduction dilutions were prepared at a MOI of 150 pfu.

hESC surface molecule expression

hESCs were dissociated by trypsinization, and 5×10^5 cells were stained for 45 minutes at 4°C in 100 μ l of 0.1% BSA in PBS containing an appropriate dilution of a desired phycoerythrin (PE)-conjugated antibody. Primary antibodies used were against: human-SSEA-1 (clone MC-480), SSEA-4 (clone MC813-70), IgG3 isotype control from R&D Systems (Minneapolis, MN), HLA DR/DP/DQ (clone WR18), IgG2a isotype control from Abcam (Cambridge, MA), β 2-microglobulin (clone TÛ99), HLA -A, -B and -C (clone DX17), CD80 (clone L307.4), CD40 (clone 5C3), CD86 [clone 2331(FUN-1)] and IgG1 (clone MOPC-21) from BD Biosciences. Sample measurement was performed on a FACSCalibur system (Becton Dickinson, Heidelberg, Germany) and analysis was performed using FlowJo (Tree Star, Ashland, OR). In the histograms, the isotype controls are represented by solid gray areas and the antigens of interest by black lines. To quantify surface molecule expression, mean fluorescence intensities (MFI) of the above molecules were compared to those of the associated negative isotype controls. Normalized expression was calculated as (MFI of molecule) divided by (MFI of isotype control). Therefore, a normalized expression of 1 corresponds to no molecule expression.

Cell transplantation

Before transplantation, hESCs were trypsinated and resuspended in sterile PBS at 1×10^6 cells per 50 μ l. Previous studies have shown that injections of 1×10^6 hESCs provide reliable signals for *in vivo* imaging and are sufficient to form stable grafts in immunocompromised recipients (Lee et al., 2009). hESCs viability was ~95% as determined by Trypan Blue staining. hESC transplantation was performed by direct injection into the right gastrocnemius muscle of recipient mice using a 27-gauge syringe. For histology, gastrocnemius muscle or teratomas were formalin-fixed and paraffin-embedded. Hematoxylin and eosin (H&E) or periodic acid Schiff (PAS) stained slides were interpreted by an expert pathologist (J.V.) blinded to the study. The density of MAC2+ macrophages, CD3+ lymphocytes and KLRA1+ NK cells was quantified in eight animals receiving hESC or hESC^{KD}, respectively using Image J (NIH, Bethesda, MD).

Bioluminescence imaging (BLI)

hESCs were transduced with pLenti CMV/TO V5-LUC Puro reporter gene at a multiplicity of infection (MOI) of 10 to stably express firefly luciferase (Fluc). Viral aliquots were kindly provided by Eric Campeau (Campeau et al., 2009). The Fluc-tagged hESC line is resistant to puromycin and cells were purified using a concentration of 0.2 μ g/ml puromycin for 5 days followed by plating on feeder layer cells for culturing. BLI was performed using the Xenogen *in vivo* imaging system (Caliper Life Sciences, Hopkinton, MA) as reported earlier (Cao et al., 2006). This imaging modality allows for quantitative, longitudinal and non-invasive studies of cell viability and location within the same animals (Sun et al., 2009; Swijnenburg et al., 2008b). Mice were anesthetized with 2% isoflurane and D-luciferin (Caliper Life Sciences) was administered intraperitoneally at a dose of 375 mg per kg of body weight. At the time of imaging, animals were placed in a light-tight chamber, and photons emitted from Fluc-expressing hESCs were counted. The recipient mice were scanned repetitively on days 0, 1, 3, 5, 7, 14, 21, 28, 35 and 42, or until the signal dropped to background levels. BLI signals were quantified in units of photons per second (total flux) and are presented on a logarithmic scale.

Immune response assays (xenogeneic *in vivo* immune response)

Elispot assays

The spleen of recipient animals was harvested 5 days after hESC transplantation, to isolate recipient splenocytes. Elispot assays using 1×10^5 mitomycin-treated hESC as stimulator cells and 1×10^6 recipient splenocytes as responder cells were performed according to the manufacturer's protocol (BD Biosciences) using IFN- γ and IL-4-coated plates. Spots were automatically enumerated using an Elispot plate reader (CTL, Ohio, USA) for scanning and analyzing.

Tregs

Inguinal lymph nodes were harvested from untreated Balb/c control mice and from recipients of hESC or hESC^{KD} transplants after 5, 14 and 42 days. The percentage of CD25+ Foxp3+ cells among the CD4+ population was assessed by FACS analysis using the FoxP3 Staining Kit (BD Biosciences).

Donor-specific antibodies (DSAs)

hESC-specific mouse xenoantibodies were detected by FACS analysis. The serum of Balb/c mice before and 5 days after transplantation of hESCs or hESC^{KD} was

incubated with graft cells and the binding of graft-specific antibodies was quantified. Only IgM antibodies were analysed because of their known rapid surge within 5 days upon allogeneic stimulation. Sera from 6 recipient mice per group were decomplexed and equal amounts of sera and hESC suspensions (1×10^6 cells per ml) were incubated. IgM antibodies were stained by incubation of the cells with a PE-conjugated goat antibody specific for the Fc portion of mouse IgM (BD Biosciences). Cells were washed and then analyzed on a FACSCalibur system (BD Biosciences). Fluorescence data were expressed as MFI.

Single antigen bead technology

Sera from untreated native Balb/c mice or Balb/c recipients of hESC or hESC^{KD} 5 days after cell transplantation were centrifuged (8,000–10,000g) for 10 min. Then, 20 μ l of undiluted serum supernatant per test well was incubated with 5 μ l of LABScreen single antigen beads (HLA Class I, LS1A04 Lot 006 and HLA Class II, LS2A01 Lot 008, One Lambda, Canoga Park, CA) for 30 minutes in the dark at 20–25°C. The specimens were then washed before being incubated with PE-conjugated anti-mouse IgG for a further 30 minutes at room temperature. Beads were washed again and re-suspended by adding 80 μ l of PBS to each well. Fluorescence was measured with the Luminex100 flow analyzer (Luminex, Austin, TX) in six animals per group and the data were expressed as MFI. A MFI Z-score, indicating how many standard deviations a specific antibody was above or below the mean of native mice was introduced to describe the humoral response.

Allogeneic in vitro immune response (Elispot assays)

For allogeneic in vitro Elispot assays, human peripheral blood mononuclear cells (PBMCs) were separated from 50 ml peripheral blood drawn from healthy blood donors and CD3⁺ CD56[–] lymphocytes and CD3[–] CD56⁺ NK cells were purified by MACS sorting (Miltenyi, Auburn, CA). Elispot assays were performed with 5×10^5 hESCs and 5×10^5 human CD3⁺ CD56[–] lymphocytes or CD3[–] CD56⁺ NK cells.

Degranulation assay with NK cells

The cell-mediated cytotoxicity of sorted CD3[–] CD56⁺ human NK cells was evaluated in a CD107a degranulation assay. This is a sensitive assay for the surface expression of CD107a as a result of activation-induced degranulation and secretion of the lytic granule contents. NK cells were incubated for 6 hours with FITC-labeled anti-CD107a monoclonal antibody (BD Biosciences), K562, hESCs or hESC^{KD} at ratios of 1:10, or PMA-ionomycin was added and the surface expression of CD107a was determined by FACS.

Statistical analysis

Data are presented as means \pm s.d. unless stated otherwise. Comparisons between groups were performed by independent sample Student's *t*-tests or ANOVA with Bonferroni post-hoc tests, where appropriate. Differences were considered significant for $P < 0.05$. Statistical analysis was performed using SPSS statistical software for Windows (SPSS, Chicago, IL, USA).

Supplementary material available online at

<http://jcs.biologists.org/lookup/suppl/doi:10.1242/jcs.087718/-DC1>

References

- Anderson, D., Self, T., Mellor, I. R., Goh, G., Hill, S. J. and Denning, C. (2007). Transgenic enrichment of cardiomyocytes from human embryonic stem cells. *Mol. Ther.* **15**, 2027–2036.
- Beggs, K. J., Lyubimov, A., Borneman, J. N., Bartholomew, A., Moseley, A., Dodds, R., Archambault, M. P., Smith, A. K. and McIntosh, K. R. (2006). Immunologic consequences of multiple, high-dose administration of allogeneic mesenchymal stem cells to baboons. *Cell Transplant.* **15**, 711–721.
- Beyer, F., Doebis, C., Busch, A., Ritter, T., Mhashilkar, A., Marasco, W. M., Laube, H., Volk, H. D. and Seifert, M. (2004). Decline of surface MHC I by adenoviral gene transfer of anti-MHC I intrabodies in human endothelial cells—new perspectives for the generation of universal donor cells for tissue transplantation. *J. Gene Med.* **6**, 616–623.
- Bonde, S. and Zavazava, N. (2006). Immunogenicity and engraftment of mouse embryonic stem cells in allogeneic recipients. *Stem Cells* **24**, 2192–2201.
- Bryceson, Y. T., March, M. E., Ljunggren, H. G. and Long, E. O. (2006). Activation, coactivation, and costimulation of resting human natural killer cells. *Immunol. Rev.* **214**, 73–91.
- Burridge, P. W., Anderson, D., Priddle, H., Barbado Munoz, M. D., Chamberlain, S., Allegrucci, C., Young, L. E. and Denning, C. (2007). Improved human embryonic stem cell embryoid body homogeneity and cardiomyocyte differentiation from a novel V-96 plate aggregation system highlights interline variability. *Stem Cells* **25**, 929–938.
- Busch, A., Marasco, W. A., Doebis, C., Volk, H. D. and Seifert, M. (2004). MHC class I manipulation on cell surfaces by gene transfer of anti-MHC class I intrabodies—a tool for decreased immunogenicity of allogeneic tissue and cell transplants. *Methods* **34**, 240–249.
- Campeau, E., Ruhl, V. E., Rodier, F., Smith, C. L., Rahmberg, B. L., Fuss, J. O., Campisi, J., Yaswen, P., Cooper, P. K. and Kaufman, P. D. (2009). A versatile viral system for expression and depletion of proteins in mammalian cells. *PLoS ONE* **4**, e6529.
- Cao, F., Lin, S., Xie, X., Ray, P., Patel, M., Zhang, X., Drukker, M., Dylla, S. J., Connolly, A. J., Chen, X. et al. (2006). In vivo visualization of embryonic stem cell survival, proliferation, and migration after cardiac delivery. *Circulation* **113**, 1005–1014.
- Caplen, N. J., Parrish, S., Imani, F., Fire, A. and Morgan, R. A. (2001). Specific inhibition of gene expression by small double-stranded RNAs in invertebrate and vertebrate systems. *Proc. Natl. Acad. Sci. USA* **98**, 9742–9747.
- Caspi, O., Huber, I., Kehat, I., Habib, M., Arbel, G., Gepstein, A., Yankelson, L., Aronson, D., Beyar, R. and Gepstein, L. (2007). Transplantation of human embryonic stem cell-derived cardiomyocytes improves myocardial performance in infarcted rat hearts. *J. Am. College Cardiol.* **50**, 1884–1893.
- Cerwenka, A., Baron, J. L. and Lanier, L. L. (2001). Ectopic expression of retinoic acid early inducible-1 gene (RAE-1) permits natural killer cell-mediated rejection of a MHC class I-bearing tumor in vivo. *Proc. Natl. Acad. Sci. USA* **98**, 11521–11526.
- Chidgey, A. P., Layton, D., Trounson, A. and Boyd, R. L. (2008). Tolerance strategies for stem-cell-based therapies. *Nature* **453**, 330–337.
- Cho, P. S., Messina, D. J., Hirsh, E. L., Chi, N., Goldman, S. N., Lo, D. P., Harris, I. R., Popma, S. H., Sachs, D. H. and Huang, C. A. (2008). Immunogenicity of umbilical cord tissue derived cells. *Blood* **111**, 430–438.
- Daley, G. Q. and Scadden, D. T. (2008). Prospects for stem cell-based therapy. *Cell* **132**, 544–548.
- Domian, I. J., Chiravuri, M., van der Meer, P., Feinberg, A. W., Shi, X., Shao, Y., Wu, S. M., Parker, K. K. and Chien, K. R. (2009). Generation of functional ventricular heart muscle from mouse ventricular progenitor cells. *Science* **326**, 426–429.
- Dressel, R., Schindehutte, J., Kuhlmann, T., Elsner, L., Novota, P., Baier, P. C., Schillert, A., Bickeboller, H., Herrmann, T., Trenkwalder, C. et al. (2008). The tumorigenicity of mouse embryonic stem cells and in vitro differentiated neuronal cells is controlled by the recipients' immune response. *PLoS ONE* **3**, e2622.
- Dressel, R., Nolte, J., Elsner, L., Novota, P., Guan, K., Streckfuss-Bomeke, K., Hasenfuss, G., Jaenisch, R. and Engel, W. (2010). Pluripotent stem cells are highly susceptible targets for syngeneic, allogeneic, and xenogeneic natural killer cells. *FASEB J.* **24**, 2164–2177.
- Drukker, M. and Benvenisty, N. (2004). The immunogenicity of human embryonic stem-derived cells. *Trends Biotechnol.* **22**, 136–141.
- Drukker, M., Katz, G., Urbach, A., Schuldiner, M., Markel, G., Itskovitz-Eldor, J., Reubinoff, B., Mandelboim, O. and Benvenisty, N. (2002). Characterization of the expression of MHC proteins in human embryonic stem cells. *Proc. Natl. Acad. Sci. USA* **99**, 9864–9869.
- Drukker, M., Katchman, H., Katz, G., Friedman, S., Shezen, E., Hornstein, E., Mandelboim, O., Reisner, Y. and Benvenisty, N. (2006). Human embryonic stem cells and their differentiated derivatives are less susceptible to immune rejection than adult cells. *Stem Cells* **24**, 221–229.
- Elsner, L., Muppala, V., Gehrmann, M., Lozano, J., Malzahn, D., Bickeboller, H., Brunner, E., Zientkowska, M., Herrmann, T., Walter, L. et al. (2007). The heat shock protein HSP70 promotes mouse NK cell activity against tumors that express inducible NKG2D ligands. *J. Immunol.* **179**, 5523–5533.
- Frenzel, L. P., Abdullah, Z., Kriegeskorte, A. K., Dieterich, R., Lange, N., Busch, D. H., Kronke, M., Utermohlen, O., Hescheler, J. and Saric, T. (2009). Role of natural-killer group 2 member D ligands and intercellular adhesion molecule 1 in natural killer cell-mediated lysis of murine embryonic stem cells and embryonic stem cell-derived cardiomyocytes. *Stem Cells* **27**, 307–316.
- Gonzalez, S., Castanotto, D., Li, H., Olivares, S., Jensen, M. C., Forman, S. J., Rossi, J. J. and Cooper, L. J. (2005). Amplification of RNAi-targeting HLA mRNAs. *Mol. Ther.* **11**, 811–818.
- Grinnemo, K. H., Genead, R., Kumagai-Braesch, M., Andersson, A., Danielsson, C., Mansson-Broberg, A., Dellgren, G., Stromberg, A. M., Ekberg, H., Hovatta, O. et al. (2008). Costimulation blockade induces tolerance to HESC transplanted to the testis and induces regulatory T-cells to HESC transplanted into the heart. *Stem Cells* **26**, 1850–1857.
- Hattori, F., Chen, H., Yamashita, H., Tohyama, S., Satoh, Y. S., Yuasa, S., Li, W., Yamakawa, H., Tanaka, T., Onitsuka, T. et al. (2010). Nongenetic method for purifying stem cell-derived cardiomyocytes. *Nat. Methods* **7**, 61–66.
- Kessler, L., Parisiadis, A., Bayle, F., Moreau, F., Pinget, M., Froelich, N., Cazenave, J. P., Berney, T., Benhamou, P. Y. and Hanau, D. (2009). Evidence for humoral rejection of a pancreatic islet graft and rescue with rituximab and IV immunoglobulin therapy. *Am. J. Transplant.* **9**, 1961–1966.
- Koch, C. A., Jordan, C. E. and Platt, J. L. (2006). Complement-dependent control of teratoma formation by embryonic stem cells. *J. Immunol.* **177**, 4803–4809.
- Koch, C. A., Galdes, P. and Platt, J. L. (2008). Immunosuppression by embryonic stem cells. *Stem Cells* **26**, 89–98.
- Kolls, J., Peppel, K., Silva, M. and Beutler, B. (1994). Prolonged and effective blockade of tumor necrosis factor activity through adenovirus-mediated gene transfer. *Proc. Natl. Acad. Sci. USA* **91**, 215–219.
- Kolossov, E., Bostani, T., Roell, W., Breibach, M., Pillekamp, F., Nygren, J. M., Sasse, P., Rubenchik, O., Fries, J. W., Wenzel, D. et al. (2006). Engraftment of engineered ES cell-derived cardiomyocytes but not BM cells restores contractile function to the infarcted myocardium. *J. Exp. Med.* **203**, 2315–2327.

- Komatsu, M., Mammolenti, M., Jones, M., Jurecic, R., Sayers, T. J. and Levy, R. B. (2003). Antigen-primed CD8⁺ T cells can mediate resistance, preventing allogeneic marrow engraftment in the simultaneous absence of perforin-, CD95L-, TNFR1-, and TRAIL-dependent killing. *Blood* **101**, 3991-3999.
- Lafamme, M. A., Chen, K. Y., Naumova, A. V., Muskheli, V., Fugate, J. A., Dupras, S. K., Reinecke, H., Xu, C., Hassanipour, M., Police, S. et al. (2007). Cardiomyocytes derived from human embryonic stem cells in pro-survival factors enhance function of infarcted rat hearts. *Nat. Biotechnol.* **25**, 1015-1024.
- Lee, A. S., Tang, C., Cao, F., Xie, X., van der Bogt, K., Hwang, A., Connolly, A. J., Robbins, R. C. and Wu, J. C. (2009). Effects of cell number on teratoma formation by human embryonic stem cells. *Cell Cycle* **8**, 2608-2612.
- Leffell, M. S., Cao, K., Coppage, M., Hansen, J. A., Hart, J. M., Pereira, N., Pereira, S., Reinsmoen, N. L., Senitzer, D., Smith, A. et al. (2009). Incidence of humoral sensitization in HLA partially mismatched hematopoietic stem cell transplantation. *Tissue Antigens* **74**, 494-498.
- Lin, G., Xie, Y., Ouyang, Q., Qian, X., Xie, P., Zhou, X., Xiong, B., Tan, Y., Li, W., Deng, L. et al. (2009). HLA-matching potential of an established human embryonic stem cell bank in China. *Cell Stem Cell* **5**, 461-465.
- Lui, K., Waldmann, H. and Fairchild, P. (2009). Embryonic stem cells: overcoming the immunological barriers to cell replacement therapy. *Curr. Stem Cell Res. Ther.* **4**, 70-80.
- Mammolenti, M., Gajavelli, S., Tsoulfas, P. and Levy, R. (2004). Absence of major histocompatibility complex class I on neural stem cells does not permit natural killer cell killing and prevents recognition by alloreactive cytotoxic T lymphocytes in vitro. *Stem Cells* **22**, 1101-1110.
- Mohanakumar, T., Narayanan, K., Desai, N., Ramachandran, S., Shenoy, S., Jendrisak, M., Susskind, B. M., Olack, B., Benschoff, N., Phelan, D. L. et al. (2006). A significant role for histocompatibility in human islet transplantation. *Transplantation* **82**, 180-187.
- Muller, Y. D., Mai, G., Morel, P., Serre-Beinier, V., Gonelle-Gispert, C., Yung, G. P., Ehrichtou, D., Wyss, J. C., Bigenzahn, S., Irla, M. et al. (2010). Anti-CD154 mAb and rapamycin induce T regulatory cell mediated tolerance in rat-to-mouse islet transplantation. *PLoS ONE* **5**, e10352.
- Mummery, C. (2010). Sorting cardiomyocytes: a simple solution after all? *Nat. Methods* **7**, 40-42.
- Nomi, H., Tashiro-Yamaji, J., Yamamoto, Y., Miura-Takeda, S., Miyoshi-Higashino, M., Takahashi, T., Azuma, H., Ueda, H., Katsuoka, Y., Kubota, T. et al. (2007). Acute rejection of allografted CTL-susceptible leukemia cells from perforin/Fas ligand double-deficient mice. *J. Immunol.* **179**, 2180-2186.
- Papassavas, A. C., Barnardo, M. C., Bunce, M. and Welsh, K. I. (2002). Is there MHC Class II restriction of the response to MHC Class I in transplant patients? *Transplantation* **73**, 642-651.
- Passier, R., Oostwaard, D., Snapper, J., Kloots, J., Hassink, R., Kuijk, E., Roelen, B., de la Riviere, A. and Mummery, C. (2005). Increased cardiomyocyte differentiation from human embryonic stem cells in serum-free cultures. *Stem Cells* **23**, 772-780.
- Pearl, J. I., Lee, A. S., Leveson-Gower, D. B., Sun, N., Ghosh, Z., Lan, F., Ransohoff, J., Negrin, R. S., Davis, M. M. and Wu, J. C. (2011). Short-term immunosuppression promotes engraftment of embryonic and induced pluripotent stem cells. *Cell Stem Cell* **8**, 309-317.
- Poncelet, A. J., Nizet, Y., Vercauysse, J., Hiel, A. L., Saliez, A. and Gianello, P. (2008). Inhibition of humoral response to allogeneic porcine mesenchymal stem cell with 12 days of tacrolimus. *Transplantation* **86**, 1586-1595.
- Preynat-Seauve, O., de Rham, C., Tirefort, D., Ferrari-Lacraz, S., Krause, K. H. and Villard, J. (2009). Neural progenitors derived from human embryonic stem cells are targeted by allogeneic T and natural killer cells. *J. Cell. Mol. Med.* **13**, 3556-3569.
- Robertson, N. J., Brook, F. A., Gardner, R. L., Cobbold, S. P., Waldmann, H. and Fairchild, P. J. (2007). Embryonic stem cell-derived tissues are immunogenic but their inherent immune privilege promotes the induction of tolerance. *Proc. Natl. Acad. Sci. USA* **104**, 20920-20925.
- Spellman, S., Bray, R., Rosen-Bronson, S., Haagenon, M., Klein, J., Flesch, S., Vierra-Green, C. and Anasetti, C. (2010). The detection of donor-directed, HLA-specific alloantibodies in recipients of unrelated hematopoietic cell transplantation is predictive of graft failure. *Blood* **115**, 2704-2708.
- Stangl, S., Gross, C., Pockley, A. G., Asea, A. A. and Multhoff, G. (2008). Influence of Hsp70 and HLA-E on the killing of leukemic blasts by cytokine/Hsp70 peptide-activated human natural killer (NK) cells. *Cell Stress Chaperones* **13**, 221-230.
- Sun, N., Lee, A. and Wu, J. C. (2009). Long term non-invasive imaging of embryonic stem cells using reporter genes. *Nat. Protoc* **4**, 1192-1201.
- Swijnenburg, R.-J., Schrepfer, S., Govaert, J., Cao, F., Ransohoff, K., Sheikh, A., Haddad, M., Connolly, A., Davis, M., Robbins, R. et al. (2008a). Immunosuppressive therapy mitigates immunological rejection of human embryonic stem cell xenografts. *Proc. Natl. Acad. Sci. USA* **105**, 12991-12996.
- Swijnenburg, R. J., Schrepfer, S., Cao, F., Pearl, J. I., Xie, X., Connolly, A. J., Robbins, R. C. and Wu, J. C. (2008b). In vivo imaging of embryonic stem cells reveals patterns of survival and immune rejection following transplantation. *Stem Cells Dev.* **17**, 1023-1029.
- Tabayoyong, W. B., Salas, J. G., Bonde, S. and Zavazava, N. (2009). HOXB4-transduced embryonic stem cell-derived Lin-c-kit⁺ and Lin-Sca-1⁺ hematopoietic progenitors express H60 and are targeted by NK cells. *J. Immunol.* **183**, 5449-5457.
- Tamaoki, N., Takahashi, K., Tanaka, T., Ichisaka, T., Aoki, H., Takeda-Kawaguchi, T., Iida, K., Kunisada, T., Shibata, T., Yamanaka, S. et al. (2010). Dental pulp cells for induced pluripotent stem cell banking. *J. Dent. Res.* **89**, 773-778.
- Tseng, H. C., Arasteh, A., Paranjpe, A., Teruel, A., Yang, W., Behel, A., Alva, J. A., Walter, G., Head, C., Ishikawa, T. O. et al. (2010). Increased lysis of stem cells but not their differentiated cells by natural killer cells; de-differentiation or reprogramming activates NK cells. *PLoS ONE* **5**, e11590.
- van Laake, L., Passier, R., Monshouer-Kloots, J., Verkleij, A., Lips, D., Freund, C., den Ouden, K., Oostwaard, D., Korving, J., Tertoolen, L. et al. (2007). Human embryonic stem cell-derived cardiomyocytes survive and mature in the mouse heart and transiently improve function after myocardial infarction. *Stem Cell Res.* **1**, 9-24.
- Xue, T., Cho, H. C., Akar, F. G., Tsang, S. Y., Jones, S. P., Marban, E., Tomaselli, G. F. and Li, R. A. (2005). Functional integration of electrically active cardiac derivatives from genetically engineered human embryonic stem cells with quiescent recipient ventricular cardiomyocytes: insights into the development of cell-based pacemakers. *Circulation* **111**, 11-20.
- Yen, B. L., Chang, C. J., Liu, K. J., Chen, Y. C., Hu, H. I., Bai, C. H. and Yen, M. L. (2009). Brief report-human embryonic stem cell-derived mesenchymal progenitors possess strong immunosuppressive effects toward natural killer cells as well as T lymphocytes. *Stem Cells* **27**, 451-456.
- Yoshimura, M., Ihara, Y., Ohnishi, A., Ijuhin, N., Nishiura, T., Kanakura, Y., Matsuzawa, Y. and Taniguchi, N. (1996). Bisecting N-acetylglucosamine on K562 cells suppresses natural killer cytotoxicity and promotes spleen colonization. *Cancer Res.* **56**, 412-418.
- Zimmerman, Z., Shatry, A., Deyev, V., Podack, E., Mammolenti, M., Blazar, B. R., Yagita, H. and Levy, R. B. (2005). Effector cells derived from host CD8 memory T cells mediate rapid resistance against minor histocompatibility antigen-mismatched allogeneic marrow grafts without participation of perforin, Fas ligand, and the simultaneous inhibition of 3 tumor necrosis factor family effector pathways. *Biol. Blood Marrow Transplant.* **11**, 576-586.